

**NOVEL INHIBITORS OF 17 β -HYDROXYSTEROID
DEHYDROGENASE TYPE 1
(17 β -HSD1) AND STEROID SULFATASE (STS) WITH
UNIQUE DUAL MODE OF ACTION:
POTENTIAL DRUGS FOR THE TREATMENT OF
NON-SMALL CELL LUNG CANCER
(NSCLC) AND ENDOMETRIOSIS**

Dissertation

zur Erlangung des Grades

des Doktors der Naturwissenschaften

der Naturwissenschaftlich-Technischen Fakultät

der Universität des Saarlandes

von

M.Sc.

Abdelrahman Mohamed Mahmoud Mohamed

Saarbrücken 2023

Tag des Kolloquiums: **07. März 2023**

Dekan: **Prof. Dr. Ludger Santen**

Berichterstatter: **Priv.-Doz. Dr. Martin Frotscher**
Prof. Dr. Anna K.H. Hirsch

Akad. Mitarbeiter: **Dr. Michael Kohr**

Vorsitz: **Prof. Dr. Alexandra K. Kiemer**

Die vorliegende Arbeit wurde von April 2017 unter Anleitung von PD Dr. Martin Frotscher in der Fachrichtung 8.2 Pharmazeutische und Medizinische Chemie der Naturwissenschaftlich-Technischen Fakultät III der Universität des Saarlandes.

In memory of my father

To my mother

To my brothers and sisters

To my lovely wife Ayat

To my angels Masarrah, Mohamed and Moemen

With love and eternal appreciation

بِسْمِ اللَّهِ الرَّحْمَنِ الرَّحِيمِ

”إِنَّمَا يَخْشَى اللَّهَ مِنْ عِبَادِهِ الْعُلَمَاءُ ۗ إِنَّ اللَّهَ عَزِيزٌ غَفُورٌ“

جزء من الآية 28 من سورة فاطر - القرآن الكريم

"Allah fürchten von Seinem Dienern eben nur die Gelehrten"

Sure 35:28-Fater-Der Heilige Quran

Acknowledgements

First and foremost, I would like praise and thank Allah the almighty, the Most Merciful, and the Most Gracious for the blessings, strength and patience He has bestowed upon me during my study, allowing me to finally complete the thesis. Allah's blessings be upon Allah's last Prophet Muhammad (peace be upon him), his family, and companions.

I would like to thank my dedicated supervisor, PD Dr. Martin Frotscher for fruitful discussions, writing of scientific papers, financial support after the end of my scholarship and encouragement during my doctoral research, which has been a fulfilling, rewarding journey and a true privilege.

I am grateful for the opportunity to collaborate with Dr. Ahmed Saad, Dr. Mohamed Salah, Dr. Mustafa Hamed and Mariam Tahoun. Throughout my career, they have always been a source of research assistance and inspiration.

I would like to express my gratitude to Prof. Dr. Christian Ducho for allowing me to do all synthetic schemes in his lab at the Department of Pharmacy, Pharmaceutical and Medicinal Chemistry, Saarland University. I would like to thank all members from Prof. Dr. Christian Ducho research group for their fruitful and enjoyable cooperation.

I would like to thank Nathalie Gladys Kagerah, Marie Grötschla, and Martina Jankowski for performing the metabolic stability and cytotoxicity tests, Manuel Hawner for undergoing the ER affinity tests, Dr. Joseph Zapp for help with NMR measurements, Dr. Stefan Boettcher for running and interpretation of the mass measurements and Lothar Jager for his sympathy and technical support. It was my great honor to be given the opportunity by Prof. Dr. Rolf W. Hartmann and Prof. Dr. Anna Hirsch for the opportunity to perform the biological work in the Department of Drug Design and Optimization, Helmholtz Institute for Pharmaceutical Research Saarland (HIPS).

I would like to thank the Deutscher Akademischer Austauschdienst (DAAD) and the Egyptian Ministry of Higher Education and Scientific Research (MHESR) as part of German-Egyptian Research Long Term Scholarship Program (GERLS) for the financial support.

Finally, I would like to express my gratitude to my beloved father (God forgive him), my mother, my brothers (Ibrahim, Mahmoud and Ali), my sisters (Fawzya and Samah) and my children (Masarrah, Mohamed and Moemen) for their help and unconditional support.

II

Above all, I would like to thank my wife, Ayat Ali, for her unequivocal support and great patience at all times, as always, for which my mere expression of thanks likewise does not suffice.

This thesis is dedicated to the memory of my father, Mohamed Mahmoud. I miss him every day, but I am sure that he is now happy to achieve his dream, which he always encouraged me to ensure its success.

Papers included in the thesis

I. 17 β -Hydroxysteroid Dehydrogenase Type 1 Inhibition: A Potential Treatment Option for Non-Small Cell Lung Cancer

Abdelrahman Mohamed, Emanuele M. Gargano, Ahmed S. Abdelsamie, Giuseppe F. Mangiatordi, Hanna Drzewiecka, Paweł P. Jagodziński, Arcangela Mazzini, Chris J. van Koppen, Matthias W. Laschke, Orazio Nicolotti, Angelo Carotti, Sandrine Marchais-Oberwinkler, Rolf W. Hartmann, and Martin Frotscher

Med. Chem. Lett. 2021, 12 (12), 1920–1924. doi:10.1021/acsmchemlett.1c00462.

II. Dual Targeting of Steroid Sulfatase and 17 β -Hydroxysteroid Dehydrogenase Type 1 by a Novel Drug-Prodrug Approach: A Potential Therapeutic Option for the Treatment of Endometriosis

Abdelrahman Mohamed, Mohamed Salah, Mariam Tahoun, Manuel Hawner, Ahmed S Abdelsamie, Martin Frotscher

J. Med. Chem. 2022, 65 (17):11726-11744. doi:10.1021/acs.jmedchem.2c00589.

III. A Hybrid In Silico/In Vitro Target Fishing Study to Mine Novel Targets of Urolithin A and B: A Step Towards a Better Comprehension of Their Estrogenicity

Luca Dellafiora, Marco Milioli, Angela Falco, Margherita Interlandi, Abdelrahman Mohamed, Martin Frotscher, Benedetta Riccardi, Paola Puccini, Daniele Del Rio, Gianni Galaverna, and Chiara Dall'Asta

Mol. Nutr. Food Res. 2020, 64 (16), 2000289. doi:10.1002/mnfr.202000289

Contribution Report

The author would like to explain his contributions to the papers **I-III** in the thesis:

- I. The author contributed to the design, synthesis and characterization of all the compounds. He performed the *in vitro* cell-free inhibition assays. Moreover, He conceived and wrote the manuscript.
- II. The author contributed to the design concept. He planned and performed the synthesis and characterization of all the compounds, the *in vitro* cell-free and cellular inhibition assays. He conceived and wrote the manuscript.
- III. The author performed and interpreted the radiolabeled *in vitro* biological assays.

Co-authors Agreement to Include an Article in a Doctoral Thesis

1. Student Identification

Student Name: Abdelrahman Mohamed
Student ID (Matriculation number): 2567087

2. Article Identification

17 β -Hydroxysteroid Dehydrogenase Type 1 Inhibition: A Potential Treatment Option for Non-Small Cell Lung Cancer

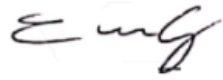
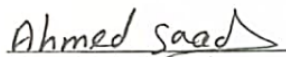
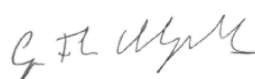







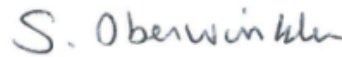


Emanuele M. Gargano, Abdelrahman Mohamed, Ahmed S. Abdelsamie, Giuseppe F. Mangiatordi, Hanna Drzewiecka, Paweł P. Jagodziński, Arcangela Mazzini, Chris J. van Koppen, Matthias W. Laschke, Orazio Nicolotti, Angelo Carotti, Sandrine Marchais-Oberwinkler, Rolf W. Hartmann, and Martin Frotscher
Med. Chem. Lett. 2021, 12 (12), 1920–1924. doi:10.1021/acsmchemlett.1c00462.

3. Contribution Report

Emanuele M. Gargano and Abdelrahman Mohamed contributed equally to this work (co-first authors). They contributed to the design, synthesis and characterization of the compounds. They further contributed in the biological assays and the interpretation of the results. They conceived and wrote the manuscript. Hanna Drzewiecka and Paweł P. Jagodziński performed xCELLigence experiments. Arcangela Mazzini conducted the estrogen receptor assay. Giuseppe F. Mangiatordi, Orazio Nicolotti, and Angelo Carotti planned and conducted all *in silico* studies. Ahmed S. Abdelsamie, Chris J. van Koppen, Matthias W. Laschke, Sandrine Marchais-Oberwinkler, Rolf W. Hartmann, and Martin Frotscher managed, directed and supervised the project.

4. Declaration of All Co-Authors Other than Student

As the co-author of the article identified above, I accept the above contribution report and authorize Abdelrahman Mohamed to include this article in his PhD dissertation entitled: “Novel Inhibitors of 17 β -Hydroxysteroid Dehydrogenase Type 1 (17 β -HSD1) and Steroid Sulfatase (STS) with Unique Dual Mode of Action: Potential Drugs for the Treatment of Non-Small Cell Lung Cancer (NSCLC) and Endometriosis”

Name of Co-Author	Date	Signature
Emanuele M. Gargano	12.12.2022	
Ahmed S. Abdelsamie	05.12.2022	
Giuseppe F. Mangiatordi	05/12/2022	
Hanna Drzewiecka	7.12.2022	
Paweł P. Jagodziński	7.12.2022	
Arcangela Mazzini	02.01.2023	
Chris J. van Koppen	07.12.2022	
Matthias W. Laschke	<u>12/07/2022</u>	
Orazio Nicolotti	06/12/2022	
Angelo Carotti	7 DEC. 2022	
Sandrine Marchais-Oberwinkler	11.12.2022	
Rolf W. Hartmann	15.12.2022	
Martin Frotscher	02.01.2023	

Co-authors Agreement to Include an Article in a Doctoral Thesis

1. Student Identification

Student Name: Abdelrahman Mohamed

Student ID (Matriculation number): 2567087

2. Article Identification

Dual Targeting of Steroid Sulfatase and 17 β -Hydroxysteroid Dehydrogenase Type 1 by a Novel Drug-Prodrug Approach: A Potential Therapeutic Option for the Treatment of Endometriosis

Abdelrahman Mohamed, Mohamed Salah, Mariam Tahoun, Manuel Hawner, Ahmed S Abdelsamie, Martin Frotscher

J. Med. Chem. 2022, 65 (17):11726-11744. doi:10.1021/acs.jmedchem.2c00589.

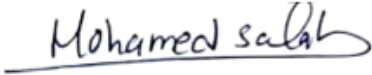



3. Contribution Report

Abdelrahman Mohamed contributed to the design concept. He planned and performed the synthesis and characterization of all the compounds, the *in vitro* cell-free and cellular inhibition assays. He conceived and wrote the manuscript. Mohamed Salah contributed to the design concept and had the idea of conducting an experimental validation of the prodrug-drug concept, and the interpretation of the results. Mariam Tahoun quantified the percentage conversion of **13** and **16** to their phenolic parent compounds using LC-MS/MS and contributed to the evaluation of HSD1 inhibition parallel to phenol formation. Manuel Hawner performed the ER affinity tests. Ahmed S Abdelsamie contributed to the design concept, experimental validation of the prodrug-drug concept and the interpretation of the results. Martin Frotscher directed and supervised the project.

4. Declaration of All Co-Authors Other than Student

As the co-author of the article identified above, I accept the above contribution report and authorize Abdelrahman Mohamed to include this article in his PhD dissertation entitled: "Novel Inhibitors of 17 β -Hydroxysteroid Dehydrogenase Type 1 (17 β -HSD1) and Steroid Sulfatase (STS) with Unique Dual Mode of Action: Potential Drugs for the Treatment of Non-Small Cell Lung Cancer (NSCLC) and Endometriosis"

VIII

Name of Co-Author	Date	Signature
Mohamed Salah	04. Dec. 2022	
Mariam Tahoun	06.12.2022	Mariam Tahoun
Manuel Hawner	09.12.2022	
Ahmed S Abdelsamie	05.12.2022	
Martin Frotscher	02.01.2023	

Co-authors Agreement to Include an Article in a Doctoral Thesis

1. Student Identification

Student Name: Abdelrahman Mohamed
Student ID (Matriculation number): 2567087

2. Article Identification

A Hybrid In Silico/In Vitro Target Fishing Study to Mine Novel Targets of Urolithin A and B: A Step Towards a Better Comprehension of Their Estrogenicity

Luca Dellafiora, Marco Milioli, Angela Falco, Margherita Interlandi, Abdelrahman Mohamed, Martin Frotscher, Benedetta Riccardi, Paola Puccini, Daniele Del Rio, Gianni Galaverna, and Chiara Dall'Asta

Mol. Nutr. Food Res. 2020, 64 (16), 2000289. doi:10.1002/mnfr.202000289

3. Contribution Report

Luca Dellafiora and Marco Milioli contributed equally to this work. Luca Dellafiora, Chiara Dall'Asta, Gianni Galaverna, and Daniele Del Rio conceptualization, writing-original draft preparation, data discussion; Marco Milioli, Angela Falco, Margherita Interlandi, Benedetta Riccardi, and Paola Puccini supervision of cell-based experiments and data discussion; Martin Frotscher and Abdelrahman Mohamed supervision of cell-free experiments.

4. Declaration of All Co-Authors Other than Student

As the first author/co-author of the article identified above, I accept the above contribution report and authorize Abdelrahman Mohamed to include this article in his PhD dissertation entitled:

“Novel Inhibitors of 17 β -Hydroxysteroid Dehydrogenase Type 1 (17 β -HSD1) and Steroid Sulfatase (STS) with Unique Dual Mode of Action: Potential Drugs for the Treatment of Non-Small Cell Lung Cancer (NSCLC) and Endometriosis”

Name of Co-Author	Date	Signature
Luca Dellafiora	10/12/2022	
Marco Milioli	21/12/2022	
Angela Falco	21/12/2022	
Margherita Interlandi	21/12/2022	
Martin Frotscher	02.01.2023	
Benedetta Riccardi	21/12/2022	
Paola Puccini	21/12/2022	
Daniele Del Rio	09/12/2022	
Gianni Galaverna	09/12/2022	
Chiara Dall'Asta	09.12.2022	

Abbreviations

17 β -HSD	17 β -hydroxysteroid dehydrogenase
3 β -diol	5 α -androstane-3 β ,17 β -diol
3 β -HSD2	3 β -hydroxysteroid dehydrogenase/ δ 5 \rightarrow 4-isomerase type 2
A4	Androstenedione
Adiol(-S)	Androstenediol(-Sulfate)
AIs	Aromatase inhibitors
AKR	Aldo-keto reductase
ARS	Aryl sulfatase
BSHs	Bicyclic substituted hydroxyphenylmethanones
Cl _{int}	Intrinsic clearance
COX-2	Cyclooxygenase type 2
CYP	Cytochrome P450
CYP17A1	Bifunctional 17 α -hydroxylase/17,20 lyase
CYP19A1	Aromatase enzyme
DASIs	Dual aromatase and STS inhibitors
DCC	N,N-Dicyclohexylcarbodiimide
DCM	Dichloromethane
DFT	Density functional theory
DHEA(-S)	Dehydroepiandrosterone(-Sulfate)
DHT	Dihydrotestosterone
DIPEA	N,N-Diisopropylethylamine
DMA	Dimethyl acetamide
DMAP	4-Dimethylaminopyridine
DME	Dimethyl ether
DMEM	Dulbecco's modified eagle medium
DMSO	Dimethyl sulfoxide
DMF	Dimethyl formamide
DPH	Diphenhydramine
DSHIs	Dual STS and 17 β -HSD1 inhibitors
E1(-S)	Estrone(-Sulfate)

XII

E2(-S)	Estradiol(-Sulfate)
E2MATE	Estradiol-3-O-sulfamate
E3	Estriol
EDDs	Estrogen dependent diseases
EDSP	Endocrine disruptor screening program
EGF	Epidermal growth
EMATE	Estrone-3-O-sulfamate
EPA	Environmental protection agency
ER	Estrogen receptor
EREs	Estrogen-responsive elements
ESI	Electrospray interface
FCS	Fetal calf serum
FSH	Follicle-stimulating hormone
G6S	Glucosamine (N-acetyl)-6-sulfatase
GALNS	Galactosamine (N-acetyl)-6-sulfatase
GnRH	Gonadotropin-releasing hormone
GPOR	G protein-coupled ER
HPLC	High performance liquid chromatography
<i>hS9</i>	Human liver S9 fraction
IDS	Iduronate-2-sulfatase
LC	Lung cancer
LH	Luteinizing hormone
MEP	Molecular electrostatic potential
MgSO ₄	Magnesium sulfate
<i>mS9</i>	Mouse liver S9 fraction
NAD ⁺	Nicotinamide adenine dinucleotide
NADPH	Dihyronicotinamide adenine dinucleotide phosphate
NSAIDs	Non-steroidal anti-inflammatory drugs
NSCLC	Non-small cell lung cancer
PAPS	3'-phosphoadenosine-5'-phosphosulfate
PBS	Phosphate-buffered saline

XIII

PDB	Protein data bank
PGE ₂	Prostaglandin type 2
RBA	Relative binding affinity
RESP	Restrained electrostatic potential
RMSD	Root mean square deviation
SCC	Side-chain cleavage enzyme
SCLC	Small cell lung cancer
SD	Standard deviation
SDR	Short chain dehydrogenase/reductase
SDS	Sodium dodecyl sulphate
SERMs	Selective estrogen receptor modulators
SF	Selectivity factor
SGSH	N-sulfoglucosamine sulfohydroloase
StAR	Steroid acute regulatory
STS	Steroid sulfatase
Sulf 1	Endo sulfatase 1
Sulf 2	Endo sulfatase 2
SULT	Sulfotransferase
T	Testosterone
THF	Tetrahydrofuran
TsCl	4-Toluenesulfonyl chloride
UDPGA	Uridine diphosphate glucuronic acid
VEGF	Vascular-endothelial growth factor

Summary

Estrogens, in particular estradiol (E2) play an important role in estrogen-dependent diseases (EDDs), such as non-small-cell lung cancer (NSCLC) and endometriosis. 17 β -Hydroxysteroid dehydrogenase type 1 (17 β -HSD1) is frequently expressed in NSCLC tissues, leading to cancer development and progression. Thus, the first objective of this study (chapter **3.1**) is the development of a novel series of highly potent non-steroidal, selective 17 β -HSD1 inhibitors in order to enhance the treatment of NSCLC. This section of the study showed that 17 β -HSD1 is a promising therapeutic target for NSCLC, providing new avenues for the treatment of this lethal cancer. Steroid sulfatase (STS) and 17 β -HSD1 are promising targets for the treatment of endometriosis because they limit estrogen formation mainly in the target cells, leading to fewer side effects. Thus, the second part of the study (chapter **3.2**) aims at developing dual inhibitors of STS and 17 β -HSD1, which provide a novel treatment option. The synthesized sulfamates should be drugs for inhibition of STS, and prodrugs for 17 β -HSD1 inhibition. The most active compounds of this part showed nanomolar IC₅₀ values for STS in cellular assays and their corresponding phenols displayed potent 17 β -HSD1 inhibition in cell-free and cellular assays as well as high selectivity over 17 β -HSD2. These findings suggest that the “drug-prodrug concept” has been applied successfully (chapter **3.2**).

Zusammenfassung

Estrogene, insbesondere Estradiol (E2), spielen eine zentrale Rolle bei Estrogen-abhängigen Erkrankungen (estrogen-dependent diseases, EDD) wie nicht-kleinzellige Bronchialkarzinome (non-small-cell lung cancer, NSCLC) und Endometriose. 17 β -Hydroxysteroid Dehydrogenase Typ 1 (17 β -HSD1) ist in NSCLC-Gewebe häufig überexprimiert und trägt zu Tumorentstehung und-wachstum bei. Das erste Ziel dieser Arbeit war daher die Entwicklung von neuartigen und hochpotenten, nicht-steroidalen 17 β -HSD1 Inhibitoren als potenzielle NSCLC-Therapeutika (Kapitel 3.1). Die Daten zeigen, dass 17 β -HSD1 ein vielversprechendes Target darstellt, das neue Möglichkeiten in der NSCLC-Therapie eröffnen kann. Steroid Sulfatase (STS) und 17 β -HSD1 sind vielversprechende Wirkstofftargets zur Behandlung der Endometriose, da sie die E2-Produktion lokal im erkrankten Gewebe reduzieren, was im Vergleich zu systemischen Therapien zu weniger Nebenwirkungen führen sollte. Gegenstand des zweiten Teils der Arbeit (Kapitel 3.2) war die Entwicklung von dualen Inhibitoren von STS und 17 β -HSD1. Die so synthetisierten Sulfamate sollten Drugs für die Hemmung von STS und gleichzeitig Prodrugs für die Hemmung von 17 β -HSD1 darstellen. Die aktivsten Verbindungen dieses Teils zeigten nanomolare IC₅₀-Werte für STS in zellulären Assays und ihre entsprechenden Phenole zeigten eine starke 17 β -HSD1-Hemmung in zellfreien und zellulären Assays sowie eine hohe Selektivität gegenüber 17 β -HSD2. Die Daten belegen, dass das verfolgte "Drug-Prodrug-Konzept" der dualen Hemmstoffwirkung erfolgreich umgesetzt wurde (Kapitel 3.2).

Table of content

Acknowledgements	I
Papers included in the thesis	III
Contribution Report.....	IV
Abbreviations	XI
Summary.....	XIV
Zusammenfassung	XV
Table of content.....	XVI
1. Introduction	1
1.1 Steroid sex hormones	1
1.2 Estrogens, the female sex hormones	1
1.2.1 General	1
1.2.2 Biosynthesis of estrogens.....	2
1.2.3 Regulation of production	5
1.2.4 Estrogen receptors and mode of action.....	5
1.2.5 Actions of estrogens.....	6
1.3 Estrogen-dependent diseases.....	6
1.3.1 General	6
1.3.2 Non-small cell lung cancer (NSCLC).....	7
1.3.3 Endometriosis.....	8
1.3.3.1 General.....	8
1.3.3.2 Etiology and pathogenesis of endometriosis	8
1.3.3.3 Treatment options of endometriosis	9
1.3.4 Local estrogen biosynthesis in endometriosis	10
1.3.4.1 General.....	10
1.3.4.2 Aromatase pathway.....	11
1.3.4.3 Sulfatase pathway	12
1.4 Sulfatases.....	12
1.4.1 General	12
1.4.2 Steroid sulfatase (STS).....	13

XVII

1.4.2.1 Structural characteristics	13
1.4.2.2 Biological characteristics	14
1.4.2.3 STS and EDDs	15
1.5 17 β -HSDs	15
1.5.1 General	15
1.5.2 17 β -HSD1	17
1.5.2.1 Structural characteristics	17
1.5.2.2 Biological characteristics	18
1.5.2.3 17 β -HSD1 and EDDs.....	19
1.6 Novel treatment approaches for endometriosis.....	20
1.6.1 STS inhibitors.....	20
1.6.2 17 β -HSD1 inhibitors	21
1.6.3 Dual inhibition of STS and 17 β -HSD1	23
2. Aim of the thesis	26
3. Results	29
3.1 17 β -Hydroxysteroid Dehydrogenase Type 1 Inhibition: A Potential Treatment Option for Non-Small Cell Lung Cancer (Publication A).....	29
3.2 Dual Targeting of Steroid Sulfatase and 17 β -Hydroxysteroid Dehydrogenase Type 1 by a Novel Drug-Prodrug Approach: A Potential Therapeutic Option for the Treatment of Endometriosis (Publication B)	35
3.3 A Hybrid In Silico/In Vitro Target Fishing Study to Mine Novel Targets of Urolithin A and B: A Step Towards a Better Comprehension of Their Estrogenicity.....	55
4. Discussion and conclusions.....	67
4.1 Synthesis of inhibitors of 17 β -HSD1 for treatment non-small cell lung cancer (NSCLC).....	67
4.2 Dual inhibition of STS and 17 β -HSD1: a novel drug-prodrug approach for the treatment of endometriosis	68
5. Supporting information	72
5.1 Supporting Information for Publication A.....	72
5.1.1 Chemical Methods	72
5.1.2 Biological Methods	81

XVIII

5.1.3 Computational Details.....	83
5.1.4 Representative ¹ H-NMR and ¹³ C-NMR spectra	86
5.1.5 Representative MS spectra.....	91
5.1.6 Overview on molecular formulas and MS data	97
5.1.7 References	98
5.2 Supporting Information for Publication B.....	100
5.2.1 Synthesis of compounds 1a, 5a-12a, 25a-27a, 32a-34a, 1b, 9b, 10b- 12b,25b, 26b, 31b-34b, 10c, 31c, 32c, 1-12, 25-27 and 31-34.....	100
5.2.2 Representative ¹ H-NMR, ¹³ C-NMR and MS spectra of compounds 13, 17, 19, 33 and 37	113
5.2.3 Validation of drug-prodrug concept (compounds 16, 19, and 37)	120
5.2.4 Validation of drug-prodrug concept for compound 13 at different starting concentrations	125
5.2.5 HEK-293 cell growth inhibition assay and cytotoxicity data.....	127
6. References	128

1. Introduction

1.1 Steroid sex hormones

Steroid hormones are lipophilic, cholesterol-derived molecules. Cholesterol has the cyclopentanoperhydrophenanthrene nucleus (steroid core) as the basic structure with three rings of cyclohexane (A, B and C) and a ring of cyclopentane (D) as shown in Figure 1.

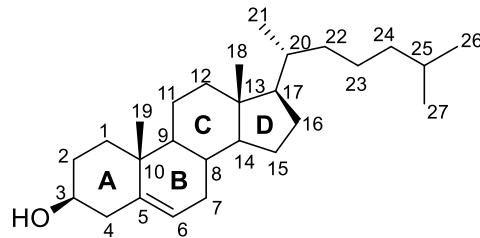


Figure 1: Structure of cholesterol showing ring identification system (A–D) and standard carbon numbering system (1–27).

Steroid hormones can be classified into two categories: corticosteroids (synthesized in adrenal cortex) and sex steroids (synthesized in gonads or placenta). According to the receptors to which they bind, they can be subcategorized into five classes: glucocorticoids, mineralocorticoids (both corticosteroids), androgens, estrogens and progestogens (sex steroids)^{1, 2}. Androgens (male sex hormones) including androstenedione (A4) and testosterone (T) are produced predominantly in the testes, while dihydrotestosterone (DHT) is mostly formed in the prostate. Estrogens (female sex hormones) including estradiol (E2) and estrone (E1) are mainly formed in the placenta and ovaries. Sex steroids are important hormones for the proper growth and function of the body; they control sexual differentiation, and patterns of sexual activity. The potency of these hormones is facilitated by the action of different enzymes. Sex hormones are secreted through two mechanisms: firstly, an endocrine mechanism, which generates the active hormones in certain glands and transfers them through blood circulation to the target tissues to exert their effects; and secondly, by an intracrine mode of action, which requires certain hormones to be secreted within target cells without releasing them into the pericellular compartment³⁻⁶.

1.2 Estrogens, the female sex hormones

1.2.1 General

Estrogens are females' main sex steroid hormones. In 1929, Edward Doisy and coworkers successfully crystallized estrone from urine extracts of pregnant women ⁷. This was followed in 1936 by the discovery of estradiol. These two discoveries had a significant effect on the area of endocrinology. Estrone (E1), 17 β -estradiol (E2) and estriol (E3) are the three estrogens present in the body and the most potent and effective one in women of reproductive age is E2. E3, which evolved from E1 by 16 α -hydroxylation, is the least potent estrogen, but is formed in high concentrations by the placenta during pregnancy, where it plays a greater role. In postmenopausal women, E1 is the most relevant estrogen and produced from dehydroepiandrosterone (DHEA) in the adipose tissue ⁸. Figure 2 displays the structures of E1, E2, and E3.

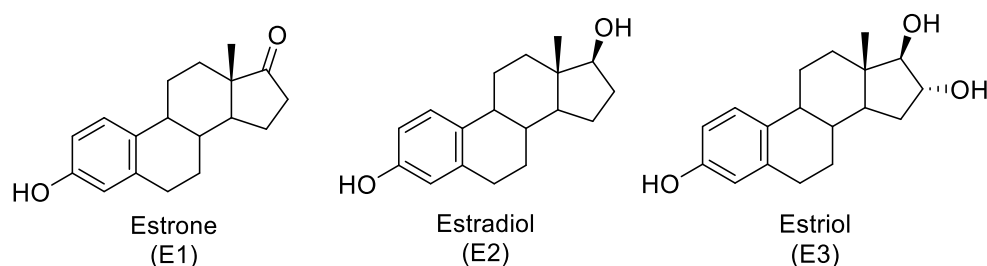


Figure 2: Structures of the estrogens in the body ⁹.

1.2.2 Biosynthesis of estrogens

The pathways involved in the biosynthesis of estrogens from cholesterol are illustrated in Figure 3 ^{10, 11}. The first step is the production of pregnenolone from cholesterol through the action of the side-chain cleavage enzyme (SCC), CYP11A1, which takes place in the mitochondria ¹². So, cholesterol has to be transferred by a cholesterol carrier protein, StAR (steroidogenic acute regulatory protein), into the mitochondria before the first step occurs. 3 β -hydroxysteroid dehydrogenase type 2 (3 β -HSD2) activates the conversion of pregnenolone to progesterone by the dehydrogenation of the hydroxyl group at C-3 of pregnenolone, giving a keto group, and the migration of the double bond from C-5–C-6 to C-4–C-5 (product, progesterone) ¹³. The bifunctional 17 α -hydroxylase/17,20 lyase (CYP17A1) transforms pregnenolone into dehydroepiandrosterone (DHEA) or progesterone into androstenedione (A4) ¹³. DHEA can be transformed quickly by 3 β -HSD2 to androstenedione (A4) or by (17 β -HSD 1 and 5) to androstenediol (Adiol).

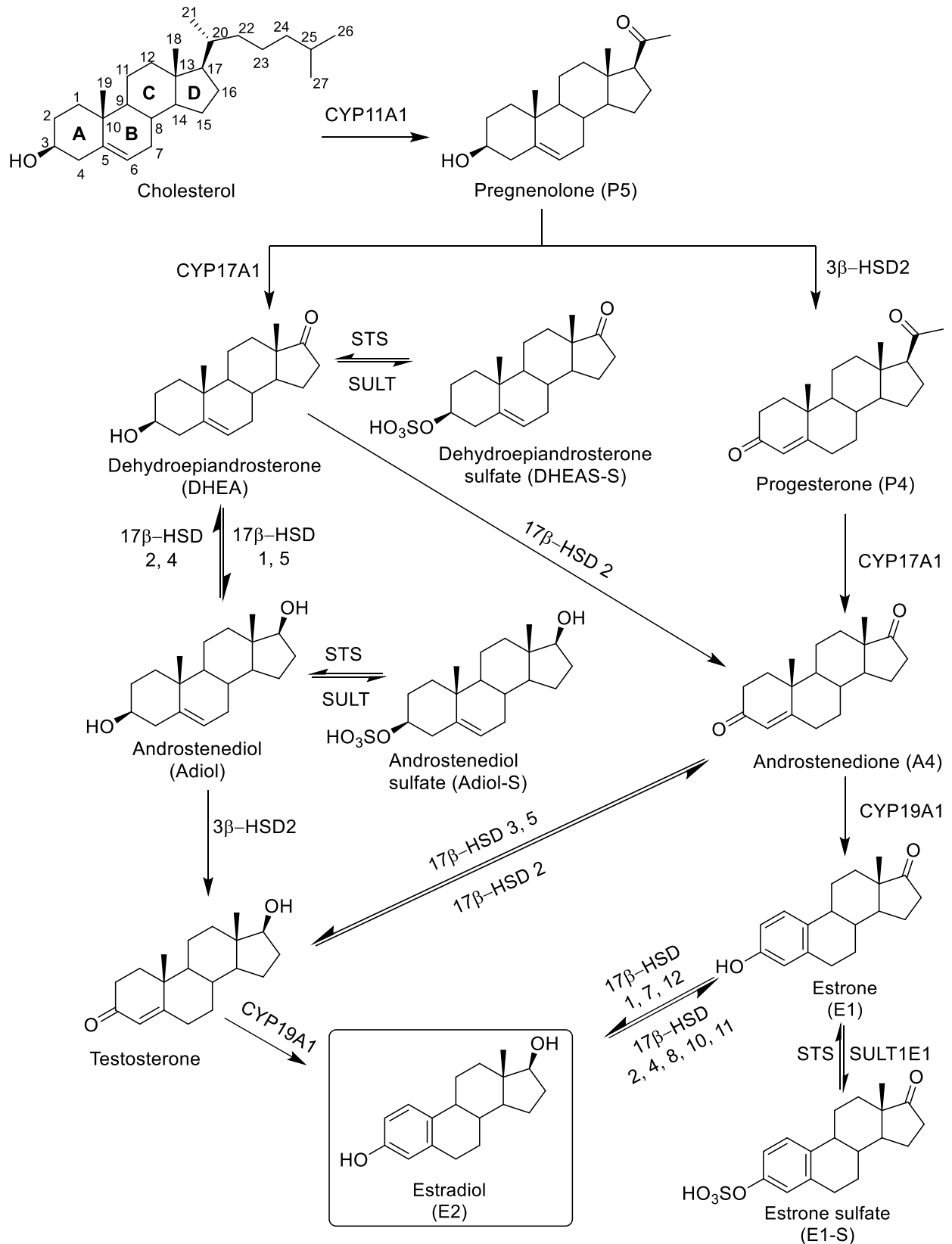


Figure 3: Pathway for estrogen biosynthesis from cholesterol¹⁴.

Both A4 and Adiol are further converted to testosterone by 17β -HSD 3 and 5 and 3β -HSD2, respectively ¹⁵⁻²¹. Testosterone is then transformed by the aromatase enzyme (CYP19A1) into estradiol (E2). Furthermore, A4 is formed in the ovarian theca cells that surround the developing follicles and then transferred to the granulosa cells in the follicles, where it is converted to the weakly active estrogen, estrone (E1) by aromatase (CYP19A1), and then 17β -HSD1 mediates the catalysis of E1 to the most potent estrogen, estradiol (E2) ^{11, 16}. In premenopausal women, circulating E2 is produced primarily by the ovaries ²² and moved to the target organs such as the mammary glands through circulation. The pregnenolone to estrogen pathway can be divided into two specific steps, each occurring in specialized ovarian follicle cells: the synthesis of androgens in the theca cells and the transformation of androgens into estrogen in the granulosa cells, as shown in Figure 4 ^{8, 23}.

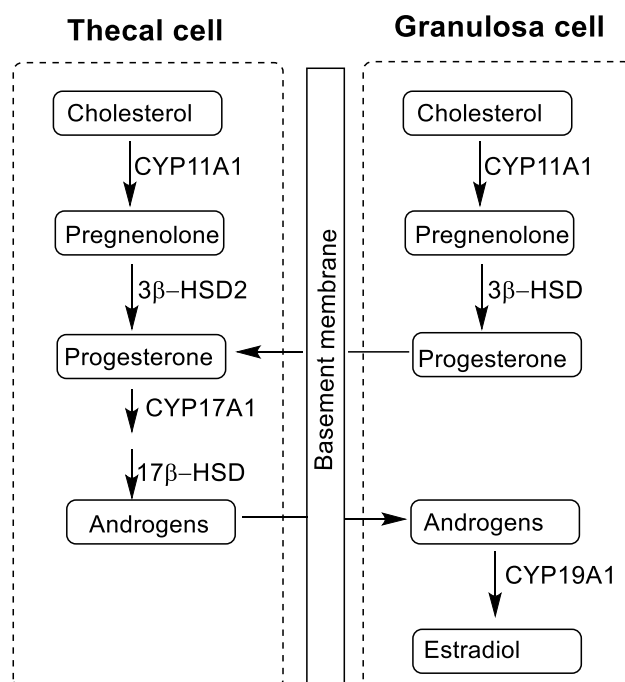


Figure 4: Cell-specific estrogen synthesis in the ovary ⁸.

After menopause, the ovaries become atrophied and fail to work and estrogens are mainly produced by peripheral tissues e.g., endometrium, placenta, adipose tissue, brain, liver, and skin ^{8, 22}. These tissues convert the inactive sulfated forms E1-S, DHEA-S and Adiol-S to their free parents by the action of the steroid sulfatase enzyme (STS).

1.2.3 Regulation of production

Estrogen production is regulated by gonadotropins, luteinizing hormones (LH) and follicle stimulating hormone (FSH)²⁴. For premenopausal women, estrogen production is accompanied by monthly periods during which an ovum is released. Each cycle consists of follicular and luteal phases corresponding to the pre- and postovulatory phases²⁵. The gonadotropin-release hormone (GnRH) secretion from the hypothalamus triggers LH and FSH release during the follicular process, which, in turn, stimulates ovarian output of estrogen and induces endometrial proliferation.

As the estrogen level peaks, FSH secretions are blocked and a beneficial feedback loop is activated where estrogen stimulates the anterior pituitary gland to release LH. This contributes to a rise in LH that induces ovulation and marked the transition into the period luteal level. The developed empty follicles mature into what is known as the corpus luteum, which secretes E2 and progesterone. The secretion of LH and FSH is disrupted by negative feedback as the amount of both hormones increases. The corpus luteum regresses without continued stimulation by LH, and the secretion of progesterone and E2 decreases. Consequently, this triggers the release of LH and FSH and the start of a new cycle.

1.2.4 Estrogen receptors and mode of action

Two receptors of estrogens, ER α and ER β , are known as nuclear transcription factors activated by estrogens²⁶⁻³⁰. ER α is the most common subtype, and usually expressed in cervix, breasts, vagina, and several various extra destined organs, whereas ER β exhibited more restricted patterns of expression, and detected mainly in ovaries, prostates, testis, spleen, endometrium, and lung³¹. The ER is the main mediator of estrogen action in these target organs and tissues, which normally influences target cell growth and differentiation³². When an estrogen binds, it creates a conformational shift within the ER that enables the receptor monomers to be dimerized³³. The homodimer then binds the estrogen response elements (EREs) in DNA binding sites. The DNA binding receptor stimulates (up-regulation) or represses (down-regulation) the expression of the gene of interest. This mechanism is called the ERs genomic signaling pathway²⁹. Figure 5 provides a graphical depiction of these steps.

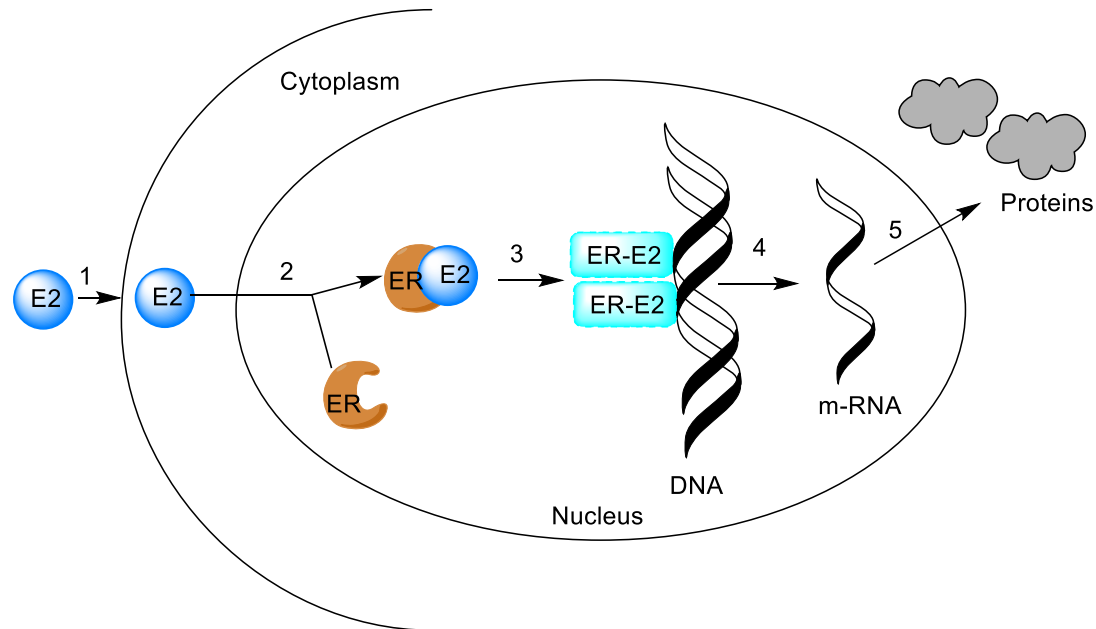


Figure 5: Genomic signaling pathways of estrogen and its mode of action: (1) cell membrane diffusion of E2; (2) development of the ER-steroid complex (ER-E2); (3) conformational changes and complex dimerization; (4) regulatory gene transcription; (5) the synthesis of regulatory proteins (Figure revised from ³⁴).

1.2.5 Actions of estrogens

Estrogens are associated with the natural production and growth of the female reproductive system, breast development and the conventional female form of the body. E2 promotes granulosa cell proliferation and follicle growth in the ovary ³⁵⁻³⁷. In the uterus, E2 controls the cyclic development of the endometrium in conjunction with progesterone³⁸ and promotes the development of breast epithelium ^{39, 40}. Moreover, estrogen and progesterone are essential for sustaining pregnancy and fetal growth ^{41, 42}. Estrogens also have an effect on a variety of other physiological processes: for example, in the skeleton, estrogens are essential for adult women to sustain bone mass by balancing osteoblasts and osteoclasts ^{34, 43}. Furthermore, several studies have demonstrated the role of estrogen in the cardiovascular ⁴⁴, central nervous ⁴⁵⁻⁴⁹, and immune systems ⁵⁰.

1.3 Estrogen-dependent diseases

1.3.1 General

The different vital physiological functions of estrogens are closely linked with the initiation and development of many diseases once a misbalance in the estrogen levels occurs ⁵¹. These diseases

are known as estrogen dependent diseases (EDDs), that include various kinds of female cancers⁵²: breast^{53, 54}, endometrial^{55, 56} and ovarian^{57, 58} cancers. Endometriosis^{59, 60}, non-small cell lung cancer (NSCLC)⁶¹⁻⁶⁵ and osteoporosis⁶⁶⁻⁶⁸ are general diseases that are closely associated with females' estrogen.

1.3.2 Non-small cell lung cancer (NSCLC)

Lung cancer (LC) is the world's largest cause of cancer death⁶⁹. The two most common types of lung cancer are small cell lung cancer (SCLC) and non-small cell lung cancer (NSCLC). The latter is the major type of LC in women, and is responsible for 85% of all LC cases. It is one of the most fatal human cancers, despite comprehensive research efforts for new treatments. While smoking is still the leading cause of LC and the lung is historically not considered to be an objective tissue for sex hormones, many studies have found variations in LC pathogenesis between the sexes^{70, 71}. These findings indicate that estrogens may play an important role in the development of LC. According to some studies, women are more vulnerable to the adverse effects of smoking⁷²⁻⁷⁴, since smoking has been shown to increase the expression and function of cytochrome P450 family 1 subfamily B member 1 (CYP1B1) in the lungs⁷⁵, potentially leading to the development of 2- and 4-catechol estrogens, which can be transformed to toxic metabolites and mediates DNA damage^{76, 77}. Furthermore, E2 can increase *in vitro* and *in vivo* development of lung cancer cells^{78, 79}. *In vitro*, E2 can stimulate the secretion of growth factors such as vascular-endothelial growth factor (VEGF) and epidermal growth factor (EGF) in both lung cancer cells and normal lung fibroblasts^{79, 80}. In addition, estrogen receptors (ERs), as well as a membrane G protein-coupled ER (GPER) were found in NSCLC tumors in several studies, regardless of sex^{61, 79, 81-85}. Estrogen can act through these receptors and contribute to cancer development and progression⁶¹⁻⁶⁵. Niikawa *et al* found high levels of E2 in LC tissues in patients with NSCLC, suggesting local biosynthesis of estrogens during LC development⁸⁶. Also, it was shown that increased E2 levels in LC tissues are associated with enhanced expression of aromatase, which transforms A4 into estrone (E1) and testosterone to E2^{86, 87}. Exemestane, an aromatase inhibitor, has been tested in preclinical experiments, and the results have been promising⁸⁸. According to recent research⁸⁹⁻⁹¹, 17 β -HSD1 and 17 β -HSD2 are overexpressed in NSCLC which contribute to the tumor growth and development: the first is by catalyzing E1 into E2 and the second is by triggering the reverse reaction, which protects against an excess of E2. Also, the expression of 17 β -HSD1 in NSCLC tissues was higher compared with matched, histopathologically unaltered specimens^{90, 91}. Because E2 is so important in the progression of NSCLC, interfering with E2 synthesis intratumorally has been

proposed as a treatment option and recently, 17 β -HSD1 became a new drug target for NSCLC treatment.

1.3.3 Endometriosis

1.3.3.1 General

Endometriosis is a gynecological condition caused by the existence of endometrial tissue outside the uterus, usually on the ovaries (ovarian endometriosis), pelvic peritoneum (peritoneal endometriosis), and uterosacral ligaments, and in vesico-uterine fold and the rectovaginal septum⁹²⁻⁹⁴. It is a serious disease, sometimes correlated with pelvic pain and infertility⁹², and can contribute to deformation of the pelvic anatomy and extensive pelvic adhesions which negatively impacts the quality of life and productivity at work⁹⁵. Initially, endometriosis was largely considered as a benign disease⁹⁵⁻⁹⁷. Nowadays, it is considered to be a neoplastic disease that may grow into a specific type of invasive ovarian cancer^{98,99}. It is believed that 6 to 10 percent of the endometriotic cases are in premenopausal women, while occurrence increases up to 50 percent in cases of women with infertility⁹². Estrogens have been found to play a key role in the development and maintenance of endometriosis¹⁰⁰. In the development of E2 related endometriosis, regulation of sex hormones producing enzymes has an important role. Over-expressions of aromatase, STS, 17 β -HSD1, and deficiency of 17 β -HSD2 are found in endometriotic tissues, which may contribute to an accumulation of E2¹⁰¹.

1.3.3.2 Etiology and pathogenesis of endometriosis

Many hypotheses have been proposed to clarify the pathogenesis of endometriosis. To date, however, none of these hypotheses can integrate all phenomena related to the development and evolution of this disease. Rather, the pathology of endometriosis appears to be a complex interaction of the factors described in the various theories. The one with the widest acceptance is the transplantation theory of Sampson¹⁰² which states that the condition arises from the movement of endometrial tissue into the peritoneal cavity through fallopian tubes (retrograde theory)^{103,104}. There is also another hypothesis called coelomic metaplasia theory, which assumes that disease is thought to develop as a result the metaplasia of cells lining the abdominal peritoneum under the influence of hormones, growth factors, inflammatory and stimuli from undifferentiated celomic epithelial cells¹⁰⁵. The discovery of endometrioma in a woman with Rokitansky–Küster–Hauser syndrome who lacked a uterus, supports the coelomic metaplasia theory^{105,106}. Following the implantation of the endometrial lesion in the surface of the peritoneum or the ovaries, an inflammatory reaction is triggered, and is followed by adhesion to tissues, fibrosis, neuronal infiltration and anatomical distortion resulting in pain and

infertility^{92, 96}. Also, there are positive feedback loops in endometrial tissue for E2 and prostaglandin synthesis¹⁰⁷, as shown in Figure 6.

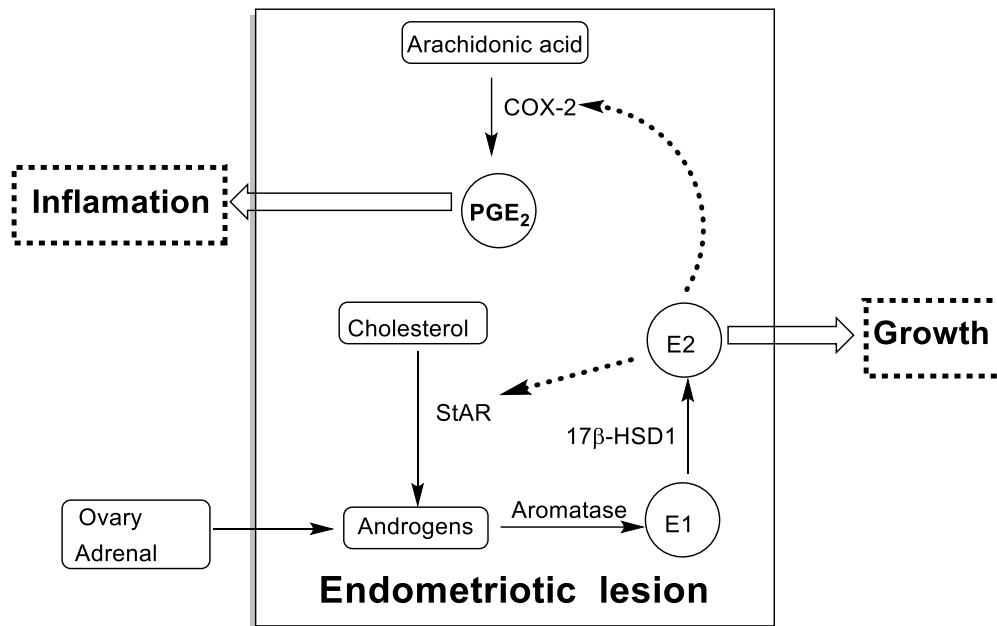


Figure 6: The positive feedback loop for the formation of estrogen and prostaglandin in endometriotic lesions. StAR, steroidogenic acute regulatory protein; COX-2, cyclooxygenase-2; PGE₂, prostaglandin E₂. (Figure revised from¹⁰⁷).

High levels of E2 in the endometriotic lesions promote cell proliferation and growth of endometriotic tissue and, on the other hand, induce type 2 cyclooxygenase (COX-2)¹⁰⁸. COX-2 activation results in increased prostaglandin (PGE₂) biosynthesis, which mediates both pain (inflammation) and infertility¹⁰⁸. In endometriotic lesions, PGE₂ is a strong stimulator of StAR and aromatase and also increases 3β-HSD2, CYP11A1, and CYP17A1 expressions^{101, 109}. This offers a positive feedback loop for the continued formation of estrogen and prostaglandin in endometriosis¹⁰⁸.

1.3.3.3 Treatment options of endometriosis

Endometriosis is diagnosed during pelvic exams, like gynecological examinations, laparoscopy, CT and MRI scans¹¹⁰. Present treatment choices include surgical removal of endometrial lesions and/or pharmacological therapy. Both give only a temporary pain relief, and recurrence happens in most cases after treatment is interrupted. Medical therapy includes analgesics, hormonal contraceptives, progestogens, anti-progestogens, and endocrine therapy (GnRH receptor agonists and aromatase inhibitors)^{92, 96, 111-113}. The first line of pharmacological treatments for this disease are non-steroidal anti-inflammatory drugs (NSAIDs) because they

relieve dysmenorrhea, but their use is limited to those who have extreme endometriosis because of the potential adverse effects which may appear ^{114, 115}. Progestogens, antiprogestogens, and hormonal contraceptives act by regulating the amount of menstrual secretions and relieving menstrual pain, but they have no effect on the progression of the disease. The goal of endocrine therapy is to suppress biosynthesis of E₂, but its use is limited to 6-9 months due to the developed side effects associated with low systemic levels of estrogen ^{92, 116}. Aromatase inhibitors could decrease local biosynthesis of estrogens in endometriosis. However, they block the negative feedback mechanisms of estrogen on the hypothalamic pituitary axis, leading to dangerous side effects such as a reduced bone mineral mass, so that the hormonal contraception or GnRH agonists are often paired with them ¹¹⁶. When all other choices are unsuccessful, Danazol, an anterior pituitary suppressant that suppresses the production of gonadotropins, is added to the protocol but its use is restricted due to extreme hyper-androgenic side effects ⁹². In conclusion, the current treatment options have significant side effects related to the lowering of systemic estrogen levels and do not stop the progression of the disease. Therefore, novel drugs that could repress endometriosis, without impacting the levels of circulating E₂, are required. These therapies are anticipated to exhibit fewer side effects, a better safety profile and a longer treatment window than the current treatment options. The local biosynthesis of estrogen in endometriosis and the key enzymes involved will be addressed in detail in the section below.

1.3.4 Local estrogen biosynthesis in endometriosis

1.3.4.1 General

As described before, estrogens are also synthesized in extragonadal sites, such as the kidney, adipose tissue, skin and brain and the synthesized estrogens remain locally at the site of production and maintain vital tissue actions by performing paracrine or intracrine functions ⁸. The local production of estrogens in extragonadal sites occurs by one of two pathways: the “aromatase pathway” and the “sulfatase pathway”, in which the precursors of estrogens are androgens or estrogen sulfates, respectively ^{4, 117}. Figure 7 provides a description of the 2 pathways.

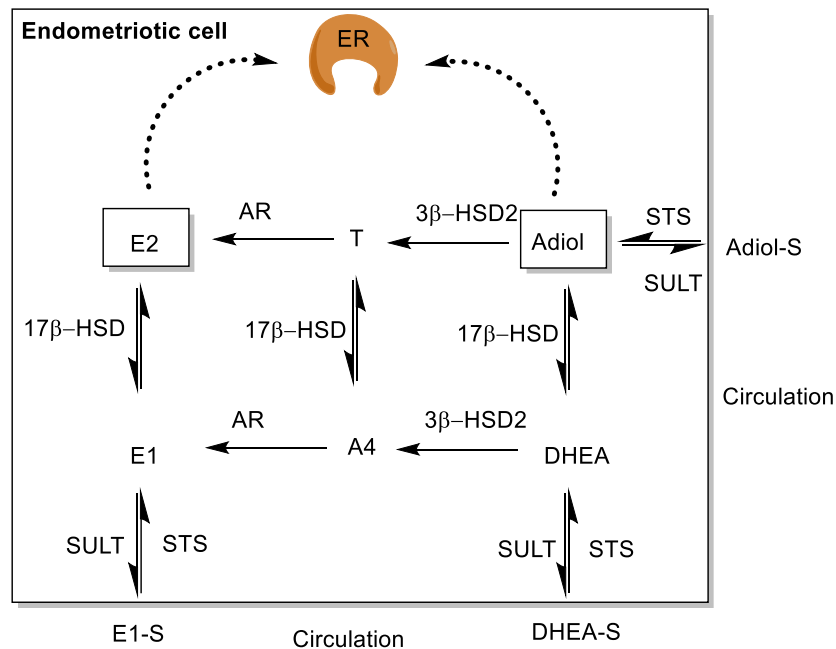


Figure 7: Schematic of the aromatase and sulfatase pathways for local estrogen biosynthesis¹¹⁷. E1-S, estrone-3-sulfate; DHEA(-S), dehydroepiandrosterone (sulfate); Adiol(-S) androstenediol (sulfate); STS, steroid sulfatase; SULT, sulfotransferase; E1, estrone; E2, 17 β -estradiol; 17 β -HSD, 17 β -hydroxysteroid dehydrogenases; 3 β -HSD2, 3 β -hydroxysteroid dehydrogenase type 2; A4, androstenedione; T, testosterone, AR, aromatase; ER, estrogen receptor.

1.3.4.2 Aromatase pathway

The enzyme responsible for this pathway is aromatase cytochrome P450 (P450arom), a member of the cytochrome P450 superfamily, particularly the CYP19 family, located in the endoplasmic reticulum of estrogen-producing cells¹¹⁸. Aromatase activates the aromatization of 19-carbon androgenic steroids to 18-carbon estrogens¹¹⁹. Dehydroepiandrosterone sulfate (DHEA-S) and androstenediol sulfate (Adiol-S) are the inactive hormonal precursors that supply the aromatase pathway. They are carried into the bloodstream and picked up by target cells where they are hydrolyzed to DHEA and Adiol by steroid sulfatase (STS) through the hydrolysis of sulfate group.¹²⁰ DHEA is a precursor to androgens: testosterone (T) and androstenedione (A4), which are aromatase enzyme substrates¹²¹. Adiol is structurally an androgen, but functions as an agonist of the estrogen receptor and hence exerts an estrogenic effect. In addition, it was proposed that Adiol was the major estrogen present after menopause¹²²⁻¹²⁴ and able to boost breast cancer cell development *in vitro*¹²⁵ and promoting mammary tumors *in vivo*¹²⁶. While its receptor affinity is weak, high Adiol levels can have an estrogenic effect compared to that of E2¹²⁷. As demonstrated in Figure 7, DHEA and Adiol are transformed to A4 and T,

respectively, by the action of 3β -HSD2¹²⁸. A4 can either be transformed to E1 by aromatase, from which 17β -HSD1 can form E2, or it can be converted to T by 17β -HSD3, which will be converted directly into E2 by aromatase^{117, 129}. It was observed that levels of aromatase expression were highest in ovarian endometriosis^{130, 131}.

1.3.4.3 Sulfatase pathway

The bulk of synthesized estrogens are transferred by sulfotransferase (SULT) to their physiologically inert, hydrophilic 3-sulfates and transported to their target tissues in the form of estrone-3-sulfate (E1S)^{132, 133}. E1-S has a longer half-life than E2, and hence considered to be the storage form of estrogens. In the sulfatase pathway, E1S is the most essential precursor of E2, since it is the most abundant estrogen in women of all ages and men¹¹⁷. In this pathway, two enzymes synthesize estrogens from the highly available precursor E1S: steroid sulfatase (STS) that hydrolyses E1-S into E1, and 17β -HSD1 which reduces E1 into E2 using NADPH as a cofactor (Figure 7). Therefore, STS and 17β -HSD1, the two enzymes responsible for transforming E1S into the strong estrogen E2, are important therapeutic targets for estrogen depletion strategies. 17β -hydroxysteroid dehydrogenase type 2 (17β -HSD2) deactivates E2 to E1 through oxidation of the 17β -hydroxyl group to a ketone group, and is therefore the physiological counterpart of 17β -HSD1¹³⁴. Also, when comparing the activity of aromatase and STS at various stages of the disease, the activity of STS was higher at advanced stages, while the activity levels of aromatase did not vary significantly¹³¹. Furthermore, both STS and 17β -HSD1, have been shown to be over-expressed in endometriosis relative to normal endometriotic tissue¹³⁵. This showed that the sulfatase pathway is more significant in local estrogen biosynthesis and in the progression of endometriosis than the aromatase pathway^{131, 136}.

1.4 Sulfatases

1.4.1 General

Sulfatases are esterases that act in the reverse direction of sulfotransferases and catalyze the sulfate ester hydrolysis in various substrates, such as proteoglycans, conjugated steroids, and aromatic compounds¹³⁷. Seventeen sulfatases have been characterized in humans, (Table 1)¹³⁷⁻¹³⁹. Sulfatases are now considered to have functions in various processes such as hormone regulation, cellular degradation, development of bone and cartilage, intracellular communication, and signaling pathways^{140, 141}.

Table 1. Human sulfatases: their substrates and cellular locations (taken from ¹⁴⁰)

Sulfatase Name	Abbreviation	Location	Substrate	Ref.
Aryl sulfatase A	ARSA	Lysosome	Cerebroside sulfate	142
Aryl sulfatase A	ARSA	Lysosome	Dermatan sulfate	143
Aryl sulfatase C (Steroid sulfatase)	ARSC (STS)	ER	Steroid sulfates	142
Aryl sulfatase D	ARSD	ER	Unknown	144
Aryl sulfatase E	ARSE	Golgi App.	Unknown	144
Aryl sulfatase F	ARSF	ER	Unknown	145
Aryl sulfatase G	ARSG	ER	Unknown	146
Aryl sulfatase H	ARSH	Unknown	Unknown	139
Aryl sulfatase I	ARSI	Unknown	Unknown	139
Aryl sulfatase J	ARSJ	Unknown	Unknown	139
Aryl sulfatase K	ARSK	Lysosome	Glycosaminoglycans	147
Galactosamine (N-acetyl)-6-sulfatase	GALNS	Lysosome	Keratin and Chondroitin sulfate	148
Glucosamine (N-acetyl)-6-sulfatase	G6S	Lysosome	Heparan and Keratan sulfate	149
N-sulfoglucosamine sulfohydroloase	SGSH	Lysosome	Heparan sulfate	150
Iduronate-2-sulfatase	IDS	Lysosome	Dermatan and Heparan sulfate	151
Endo sulfatase 1	Sulf 1	ECM	Heparan sulfate	152
Endo sulfatase 2	Sulf 2	ECM	Heparan sulfate	152

1.4.2 Steroid sulfatase (STS)

1.4.2.1 Structural characteristics

Human steroid sulfatase (E.C.3.1.6.2) is found in almost all mammalian tissues, but often located in placenta (the richest source of STS), breasts, fallopian tubes, endometrium, ovary, testis, adrenal glands, brain, kidney, skin, fetal lung, and bone ^{153, 154}. STS is expressed as a monomeric protein of 63-73 kDA composed of residues of 583 amino acids. The difference in molecular weight is attributed to the change in glycosylation states on the enzyme at four potential N-glycosylation sites ¹⁴². Dr. Debashis Ghosh, New York, reported the crystal structure of STS in 2003 (Figure 8) ¹⁵⁵.

STS assumes a tertiary structure consisting of a polar globular domain (the head of the mushroom) and a hydrophobic stem domain (two antiparallel α -helices 8 and 9) resembling a mushroom's shape. The mushroom (hydrophobic domain) stem is thought to anchor STS into the endoplasmic reticulum membrane. The active site is located at the base of the polar domain, close to the top of the two hydrophobic α -helices ¹⁵⁵.

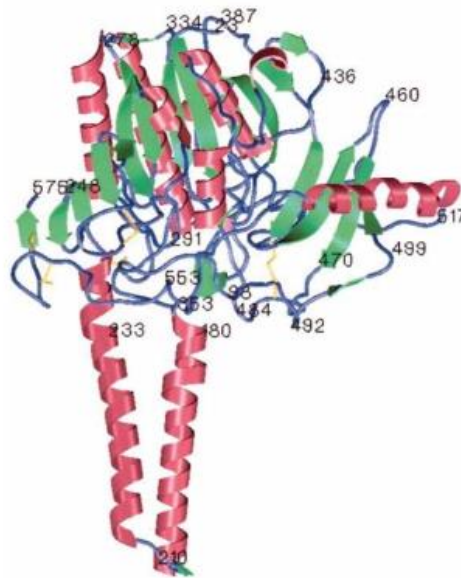


Figure 8: STS crystal structure revealing the tertiary mushroom-shape structure ¹⁵⁵.

1.4.2.2 Biological characteristics

Steroid sulfatase catalyzes the desulfation of steroidal sulfates to produce unconjugated steroids by hydrolysis of the sulfate group of 3β -hydroxysteroid sulfates, including estrone sulfate (E1-S), estradiol sulfate (E2-S), and dehydroepiandrosterone sulfate (DHEA-S) (Figure 9) ¹⁵⁶. Sulfated steroid substrates are biosynthesized using 3'-phosphoadenosine-5'-phosphosulfate (PAPS), which acts as a sulfate donor, through the action of sulfotransferase (SULT) (Figure 9). Sulfated steroids are biologically inert and are not capable of binding to steroid hormone receptors until the sulfate group is removed by STS. Sulfated steroids have been proposed as a water soluble and transportable storage reservoir of steroids and thus, serve as the source of bioactive steroid hormones after their activation with STS. This is confirmed by the observation that sulfated steroids such as E1-S and DHEA-S are considerably higher in circulating plasma concentrations than their non-sulfated counterparts, E1 and DHEA ¹⁵⁷. In comparison, the plasma half-life of E1-S and DHEA-S is about 10-12 hours, which is slightly longer than the E1 and DHEA-S half-life of 30-40 minutes ¹⁵⁸.

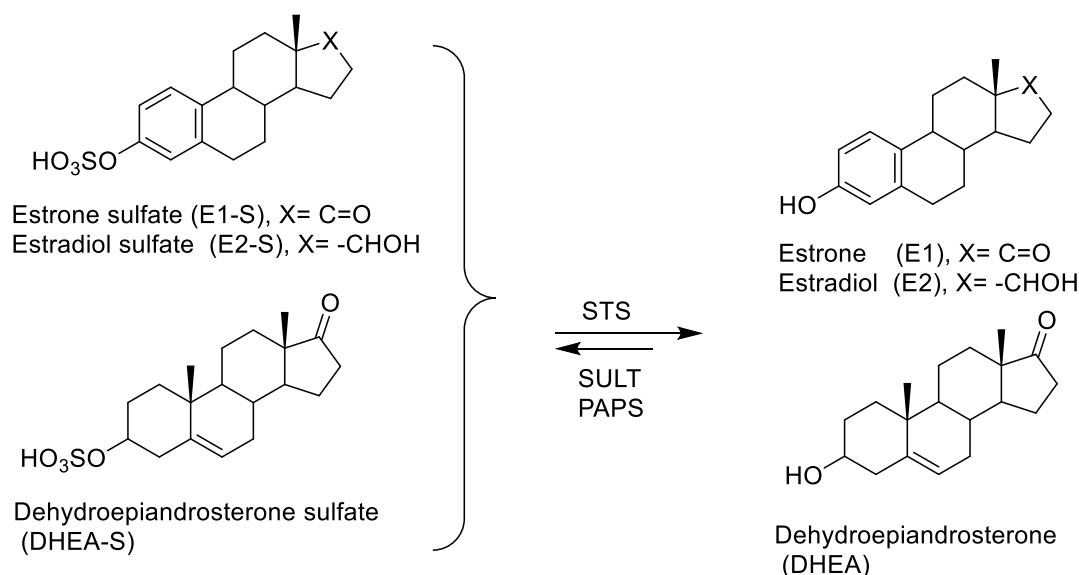


Figure 9: Reactions catalyzed by STS ¹⁵⁶.

1.4.2.3 STS and EDDs

STS expression in breast tissue is significantly higher than normal one ^{136, 157, 159, 160}, and STS expression is now used as a prognostic factor in human breast carcinoma ¹⁶¹. STS activity is around 50 to 200 times greater in malignant breast tissue than aromatase activity. Furthermore, in endometriotic lesions, the STS enzyme was found to be overexpressed ^{162, 163}, and the levels of STS expression were correlated to the severity of the disease ¹⁶⁴⁻¹⁶⁶. In ovarian endometriosis, STS mRNA expression was observed to be five times greater than normal endometrium and in peritoneal endometriosis, STS activity was higher than aromatase activity ^{131, 162}. Also, STS is upregulated in endometrial carcinoma ^{167, 168}. Moreover, STS inhibitors were shown to slow the development of endometriotic lesions in a mouse model while keeping E2 levels in the plasma unchanged ¹⁶⁹.

1.5 17 β -HSDs

1.5.1 General

17 β -HSDs are oxidoreductive enzymes that depend on NADPH/NAD⁺ for their activity, interconverting ketones and the respective secondary alcohols. The principal substrates are steroid hormones, but certain HSDs are active in the synthesis of various non-steroidal compounds ¹⁷⁰⁻¹⁷². It is reported that there are 15 known types of 17 β -HSDs ¹⁷³⁻¹⁷⁵, but only thirteen have been characterized in human (17 β -HSD6 and 17 β -HSD9 have only been identified in rodents). The 17 β -HSDs belong to two superfamilies of proteins: the protein superfamily of short-chain dehydrogenase/reductase (SDR) ¹⁷⁶ and the protein superfamily of aldo-

ketoreductase (AKR) ¹⁷⁷. Except for 17 β -HSD5, all 17 β -HSDs belong to the SDR protein superfamily. They can be divided into two categories: (a) reductive enzymes (17 β -HSD1, 3, 5, 7, 12 and 15) that catalyze NADP(H)-dependent reduction of active steroid hormones *in vivo* and b) oxidative enzymes (17 β -HSD2, 4, 6, 8, 9, 10, 11, 13 and 14), which catalyze the NADP⁺-dependent oxidation *in vivo* and hence the inactivation of steroids ¹⁷⁸. 17 β -HSDs play an essential role in the final stages of estrogen and androgen biosynthesis and are expressed exclusively in the tissues. They've also attracted a lot of attention in recent years as possible therapeutic targets for steroid-related sex-hormone disorders. Table 2 gives an overview of the various functions and disease associations for the fifteen 17 β -HSDs. The various 17 β -HSDs are numbered in the order of their discovery.

Table 2. Oxidative and reductive 17 β -HSDs (modified and updated from ¹⁷⁸⁻¹⁸¹)

Enzyme	SDR nomenclature	Cofactor preference	Subcellular localization	Expression pattern	Substrate	Function	Disease or Pathology	Ref.
17 β -HSD1	SDR28C1	NADP(H)	Soluble in cytosol	Breast, ovary, endometrium, placenta, lung	Estrogens, in a minor extent androgens	E2 production	Breast cancer, prostate cancer, endometriosis	182-184
17 β -HSD2	SDR9C2	NAD(H)	Membrane bound on ER	Liver, GI tract breast, prostate, bones, lungs, kidney, placenta, endometrium	Estrogens, androgens	E2, T inactivation	Breast cancer, prostate cancer, endometriosis, osteoporosis	180, 182, 183
17 β -HSD3	SDR12C2	NADP(H)	Membrane bound on ER	mainly testis	Androgens	T production	Pseudohermaphroditism and prostate cancer Prostate cancer, D-specific	185
17 β -HSD4	SDR8C1	NAD(H)	Peroxisomes	Breast, liver, lung, placenta	Estrogens, androgens, bile acids, fatty acids	E2 inactivation, β -oxidation of Fatty acids	Bifunctional Protein-deficiency,	186
17 β -HSD5	AKR1C3	NADP(H)	Soluble in cytosol	Liver, prostate	Androgens and estrogens	T and E2 production	Breast, prostate cancer	187-189
17 β -HSD6	SDR9C6	NAD(H)	Endosomes	Not characterized in human	-	Retinoid metabolism	-	190
17 β -HSD7	SDR37C1	NADP(H)	Membrane bound on ER	Liver, ovary, breast, lung, placenta, thymus	Estrogens, cholesterol	Cholesterol synthesis and E2 production	Breast cancer, malformation as CHILD syndrome	191-194

17 β -HSD8	SDR30C1	NAD(H)	Mitochondria	Kidney, placenta, liver	Estrogens, androgens	E2 and androgen inactivation, fatty acid elongation	Polycystic kidney disease	195, 196
17 β -HSD9	SDR	NAD(H)	Membrane bound on ER	Not characterized in human	-	Retinoid metabolism	-	197
17 β -HSD10	SDR5C1	NAD(H)	Mitochondria	CNS, brain	Estrogens, androgens, bile acids, progestogens	β -oxidation of fatty acids, estrogen and androgen inactivation, bile acid isomerization	Alzheimer's disease, isoleucine degradation deficiency	198-200
17 β -HSD11	SDR6C2	NAD(H)	Membrane bound on ER	Kidney, placenta, lung, liver	androgens	Steroid inactivation, fatty acid metabolism	-	201, 202
17 β -HSD12	SDR12C1	NADP(H)	Membrane bound on ER	Liver, breast, placenta, kidney, uterus, ovary	Estrogens, (long chain fatty acids)	formation E2, regulator of lipid biosynthesis	Breast cancer	191, 203, 204
17 β -HSD13	SDR16C3	NAD(H)	Membrane bound on ER	liver		Activity not known	-	205
17 β -HSD14	SDR47C1	NAD(H)	Soluble in cytosol	Placenta, brain, liver	Androgens estrogens	β -oxidation, E2, T inactivation,	Breast cancer (prognostic marker)	206-208
17 β -HSD15	-	NADP(H)	Membrane bound on ER	Retina, prostate, brain, testis	Retinoids, androgens	-	Prostate cancer, retinitis pigmentosa	209

1.5.2 17 β -HSD1

1.5.2.1 Structural characteristics

Human 17 β -hydroxysteroid dehydrogenase type 1 (EC 1.1.1.62) has a molecular weight of 34.9 kDa and it contains 327 amino acid residues²¹⁰. The enzyme is commonly expressed in endometrium, breast, ovaries, placenta, breast tissues, skin, and adipose tissues. The first crystallization of human estrogenic 17 β -HSD1 was published by Zhu and co-workers in 1993²¹¹. In 1995, the first three-dimensional X-ray structure of 17 β -HSD1 was reported²¹². Since then, 22 17 β -HSD1 structures have been added to the protein data bank (PDB)^{213,214} as crystal structures with estrogenic²¹⁵⁻²¹⁸, androgenic²¹⁹⁻²²¹ ligands or with steroid-based inhibitors^{222,223}. This led to a description of the enzyme's substrate and cofactor binding cavities at the atomic level and a thorough explanation of its mode of action^{217,220,224}. Human 17 β -HSD1 is a part of the SDR family and is a soluble cytosolic homodimer. 17 β -HSD1 has a core structure made up of a seven-stranded parallel β -sheet (β A to β G) surrounded by six parallel α -helices (α B to α G),

three on either side of the β -sheet (Figure 10). The protein structure typically forms into two segments: the first segment, β A to β F, is a classic Rossmann fold, responsible for cofactor binding; the second segment, β D to β G, is partially in the Rossmann fold, regulating the binding of the steroid substrate^{212, 216, 225}.

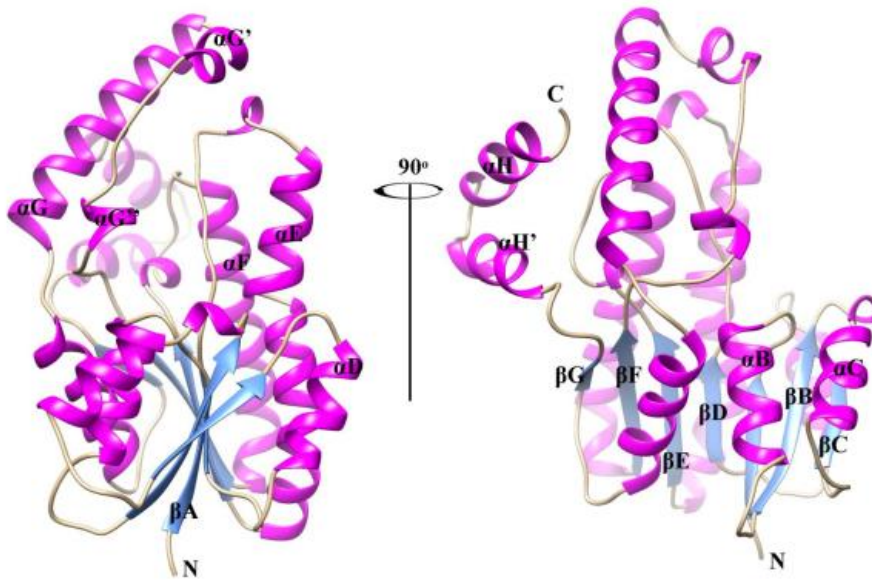


Figure 10: Stereo ribbon presentation of human 17 β -HSD1 structure. The alpha-helices are represented as magenta coils, β -strands are blue arrows, and loops and turns are drawn as gray ropes. The N- and C-termini of the protein molecule are both shown in the figure²¹².

1.5.2.2 Biological characteristics

17 β -HSD1 converts the weakly active estrogen, estrone (E1), into the active estrogen, E2 (Figure 11)^{226, 227}. In addition, it can reduce dehydroepiandrosterone (DHEA) into 5-androstene-3 β ,17 β -diol (Adiol) and dihydrotestosterone (DHT) into 5 α -androstane-3 β ,17 β -diol (3 β -diol)^{228, 229}. Adiol has been indicated to be the major estrogen present after menopause^{122, 123}, while 3 β -diol has been able to activate and proliferate α estrogen receptor (ER α)²³⁰. It requires the involvement of a cofactor of dinucleotides (NADP⁺/NADPH or NAD⁺/NADH) during estrogen conversion. *In vitro*, both NAD(H) and NADP(H) are used as cofactors²³¹, but only NADPH has been identified as a cofactor in cells and *in vivo*²³².

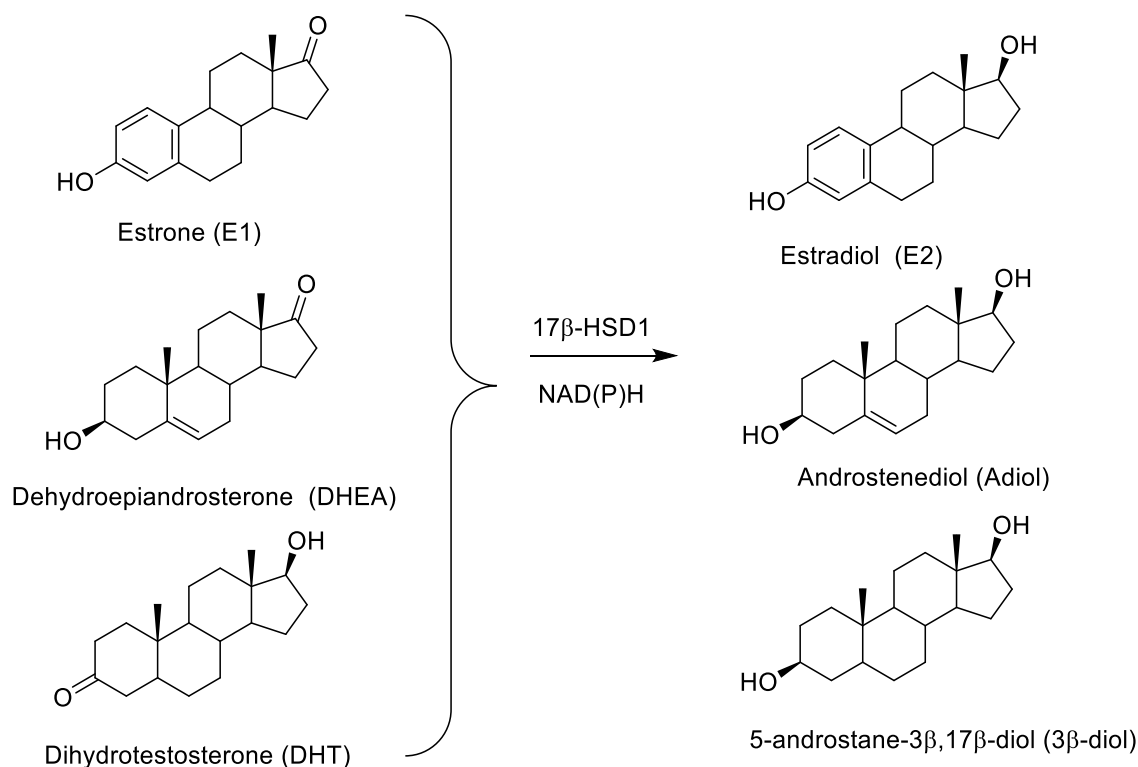


Figure 11: Human 17β-HSD1 catalyze the conversion of E1 to E2, DHEA to Adiol, and DHT to 3β-diol ^{227, 229}.

1.5.2.3 17β-HSD1 and EDDs

In comparison to the expression of aromatase and sulfatase mRNA, 17β-HSD1 mRNA expression levels are substantially higher in tumors from postmenopausal women than from those who are premenopausal and that indicates the significance of 17β-HSD1 upregulation in maintaining high intratumoral E2 levels in postmenopausal patients ²³³. Compared to normal endometrium, 17β-HSD1 upregulation and downregulation of 17β-HSD2 mRNA were found in lesions of endometrial patients ^{108, 135, 162, 165, 234}. Also, breast cancer ^{233, 235}, endometrial cancer ^{236, 237}, ovarian cancer ²³⁸, and NSCLC ^{90, 91} are characterized by the over-expression of 17β-HSD1. As a result, 17β-HSD1 inhibition is being considered as a potential therapeutic approach for treating these diseases ¹⁸⁰.

1.6 Novel treatment approaches for endometriosis

1.6.1 STS inhibitors

For over 30 years, studies have been conducted focused on the discovery of STS inhibitors with minimal side effects as drug candidates. At that time, several scientific papers were written explaining the synthesis, and biological evaluation of steroidal or non-steroidal compounds^{156, 239-248}. In general, STS inhibitors are divided into two categories: irreversible aryl sulfamate inhibitors and reversible non-sulfamate inhibitors^{241, 249} and the majority of STS inhibitors identified to date are irreversible aryl sulfamate inhibitors.

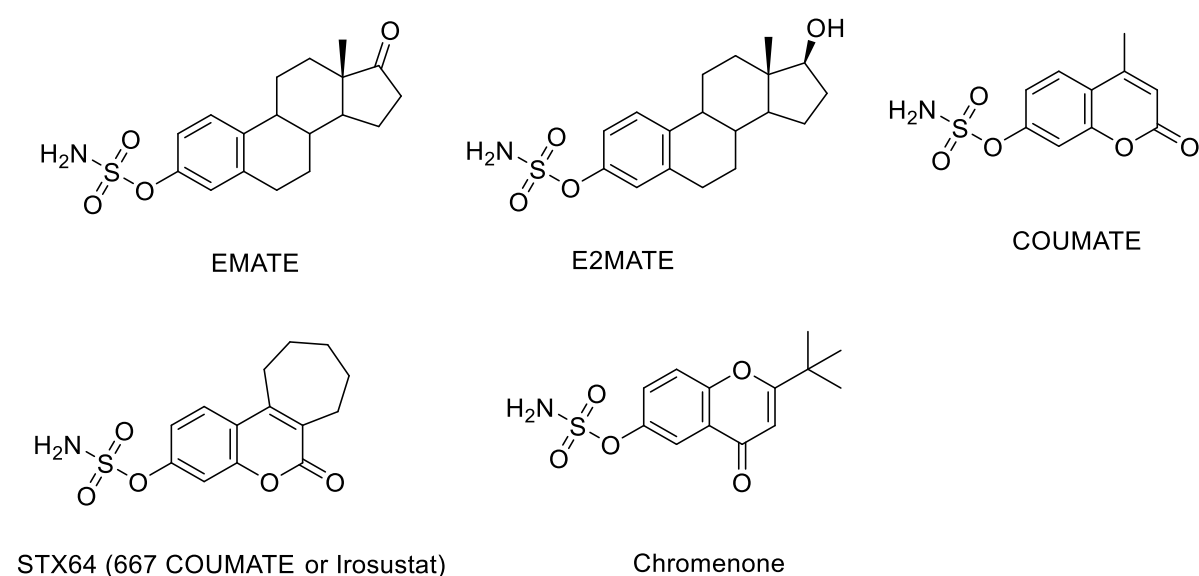


Figure 12: Structures of selected sulfamate inhibitors.

EMATE, estrone-3-O-sulfamate^{250, 251}, and E2MATE, estradiol-3-O-sulfamate^{250, 252}, highly active and irreversible STS inhibitors, are the earliest examples of this class and are used as a reference for evaluating the effectiveness of other STS inhibitors *in vitro* (Figure 12). Unfortunately, they are estrogenic, so they are not acceptable candidates for the further development of drugs²⁵³. However, several studies have successfully addressed the estrogenicity problem, and a number of highly effective non-estrogenic STS inhibitors based on aryl sulfamate have also been developed, such as COUMATE²⁵⁴, STX64 (also known as 667-COUMATE or Irosustat)²⁵⁵ and chromenone²⁵⁶ (Figure 12). In cellular assays, all these compounds are also very powerful STS inhibitors. While STX64 has passed the phase I clinical trials with success in breast cancer therapy²⁵⁷, concerns have been raised about the poor stability of its aqueous solution and the possible adverse effects of the long-term application²⁴⁹.

1.6.2 17 β -HSD1 inhibitors

In recent years, a variety of 17 β -HSD1 inhibitors have been developed, and there are various review articles published several steroidal and non-steroidal 17 β -HSD1 inhibitors^{180, 225, 258-263}. The majority of 17 β -HSD1 inhibitors are based on the steroid core by modification of the substrate E1 or the product E2²⁶⁴⁻²⁶⁶. Variations have been performed on the steroid backbone by substitution at different positions (C2, C6, C15, and C16²⁶⁷⁻²⁷³). Two patents from Solvay Pharmaceuticals include examples of E1 derivatives replaced at position 15²⁷¹ and in a recombinant 17 β -HSD1 assay, compound A demonstrated an IC₅₀ value of 4 nM (Figure 13). Compound B, EM-1745, with an IC₅₀ value of 52 nM is an example of C16 substitution which could interact with E1 (substrate) and NADPH (co-factor) binding sites, thereby producing dual site inhibitors^{223, 274}. The drug candidate STX1040 (Figure 13, compound C) produced at Bath University is another example of C16 substitution with cellular IC₅₀ of 27 nM and blocked the proliferation of E1-stimulated T-47D cells *in vitro* and significantly reduced the volume of tumor and plasma levels of E2 *in vivo*²⁷⁵. The development of non-steroidal 17 β -HSD1 inhibitors is of rising concern as they have many benefits over steroidal inhibitors, such as selectivity, non-estrogenicity, ease of synthesis and drug-likeness. Most of the synthesized compounds maintain certain essential characteristics which include a phenol moiety and a hydrophobic scaffold that mimics the steroid center. Benzothienopyrimidones, phenylnaphthalenes and derivatives of coumarin are the scaffolds used. One of the most active benzothienopyrimidones is compound D, with IC₅₀ value of 5 nM, selective for 17 β -HSD1 over 17 β -HSD2 and doesn't show undesired estrogenicity in the ER- α or ER- β binding assay²⁷⁶⁻²⁷⁸, (Figure 13). To date, four different highly active classes of non-steroidal inhibitors have been developed in our group, all of which showed good selectivities towards 17 β -HSD2. The first class were bis(hydroxyphenyl) substituted arenes and the most active one in this series was compound E, with a cell-free IC₅₀ = 8 nM²⁷⁹⁻²⁸². Extensive SAR studies have been performed to this class leading to identification of further classes, for example, (hydroxyphenyl) naphthalenes²⁸³⁻²⁸⁵, among which compound F was the most potent one with a cell-free IC₅₀ value of 15 nM. Compound G was an example of the bicyclic substituted hydroxyphenyl-methanones (BSHs)^{286, 287} and showed strong inhibitory activity toward the 17 β -HSD1 enzyme (cell-free IC₅₀ = 0.5 nM) as well as high selectivity towards 17 β -HSD2²⁶¹, and estrogen receptors²⁸⁸, rendering it a promising candidate for further development as a therapeutic agent. It was shown that a 17 β -HSD1 inhibitor was effective at lowering elevated E2 levels in human endometriosis samples²⁸⁹. Recently, a novel 17 β -HSD1 inhibitor, FOR-6219, developed primarily by Forendo Pharma for the treatment of endometriosis was studied in a phase I clinical

trial and it was found to be safe and well tolerated (NCT03709420)^{290, 291}. In addition, its developers reported no side effects associated with systemic estrogen deficiency. It is now entering phase II clinical development with endometriosis patients in the US to assess its efficacy as a long-term treatment option for endometriosis. A second 17 β -HSD1 inhibitor that has reached the stage of *in vivo* testing (in murine and monkey models) is a covalent inhibitor of 17 β -HSD1 (called PBRM), whose biopharmaceutical attributes and pharmacodynamics are conducive to further development^{123, 292, 293}. It is likely that these drugs will be coupled with other ovarian function inhibitors (progestins, GnRH-agonists).

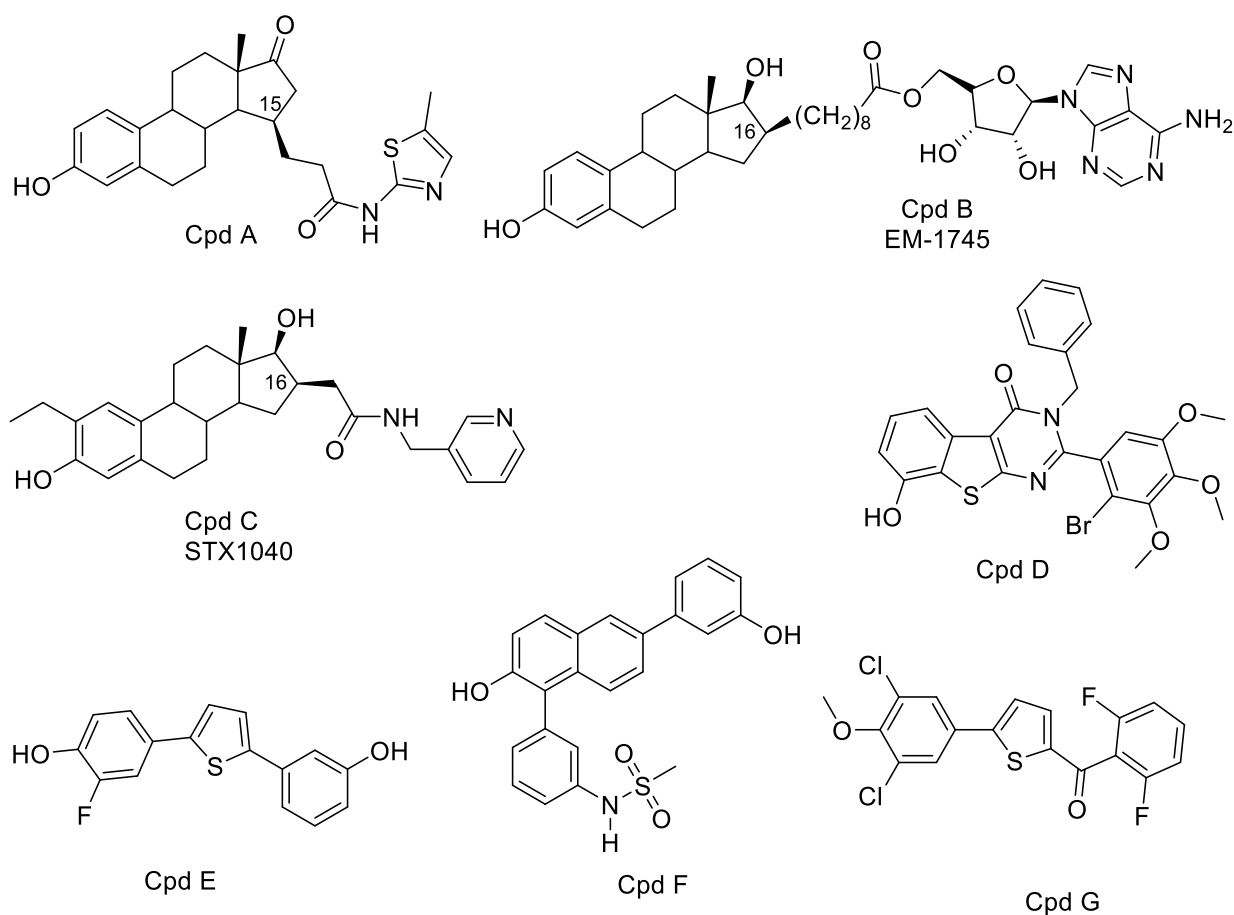


Figure 13: Structures of selected 17 β -HSD1 inhibitors.

1.6.3 Dual inhibition of STS and 17 β -HSD1

Targeting multiple biological targets by single agents is an attractive and emerging approach in the design and discovery of new medications and may enhance the efficacy of novel treatment methods^{169, 294-303}. Using a single agent could prevent drug-drug interactions, as well as overcome resistance that may arise from single targeted drugs. One of the drawbacks of aromatase inhibitors is that the affected tissues seek to compensate for decreased levels of estrogen by increasing the expression of enzymes associated with other biosynthetic pathways of estrogen, for example, over-expression of STS and 17 β -HSD1 in breast cancer tissue³⁰⁴. Also, the synthesis of E2 derived from the aromatase pathway is not prevented by selective STS inhibitors, and selective 17 β -HSD1 inhibitors do not preclude the synthesis of E1 from E1-S via the sulfatase pathway. Yet, it can be imagined that a more effective decrease in estrogen levels could be accomplished by the use of (a) a combination of two distinct inhibitors or (b) an inhibitor and an antagonist of the ER. In the literature, there are some examples of dual acting-agents which affect estrogen production or the action of it at the ER. In 1996, the synthesis and biological evaluation of 17 β -HSD1 inhibitors having antiestrogenic activity were reported by Tremblay et al. The most potent example was compound H, (Figure 14) which inhibited 17 β -HSD1 activity with an IC₅₀ of 14 μ M while being antiestrogenic at 1 μ M²⁷⁴. Several flavonoids were found to inhibit the action of both 17 β -HSD1 and aromatase, as shown by Apigenin (compound I, Figure 14), which inhibited the activity of these enzymes by 78% and 95%, respectively in placental microsomes^{305, 306}. Multitargeting drugs that inhibit both aromatase and STS have been termed dual aromatase-sulphatase inhibitors (DASIs). Woo et al.^{254, 307, 308} published the first examples of DASIs with high potency. The first dual aromatase-STs inhibitors (DASIs) have been synthesized by Woo *et al*³⁰⁹ and compound J (Figure 14) was active *in vivo* against both enzymes. Many new DASIs have been developed in recent years, including sulfamoylated letrozoles³¹⁰⁻³¹² and anastrozole derivatives³¹³. Both the aromatase and sulfatase pathways are blocked by DASIs, resulting in severe hypo-estrogenic side effects that may hinder their therapeutic application.

The development of molecules which inhibit STS and modulate estrogen receptors has been pursued by several groups³¹⁴⁻³¹⁶. In particular, EO-33 (compound K, Figure 14)³¹⁵⁻³¹⁷, was one of the most promising candidates, which is a sulfamate derivative based on tetrahydroisoquinoline that acts as an STS inhibitor and selective estrogen receptor modulator at the same time. The compound exerted strong activity against STS (IC₅₀ = 3.9 nM) in HEK-293 cells. In addition, it displayed a SERM effect in ovariectomized mice, blocked changes in

uterine weight induced by E1S, and had no toxic effects (based on body weight, liver weight, and liver appearance)³¹⁵⁻³¹⁷.

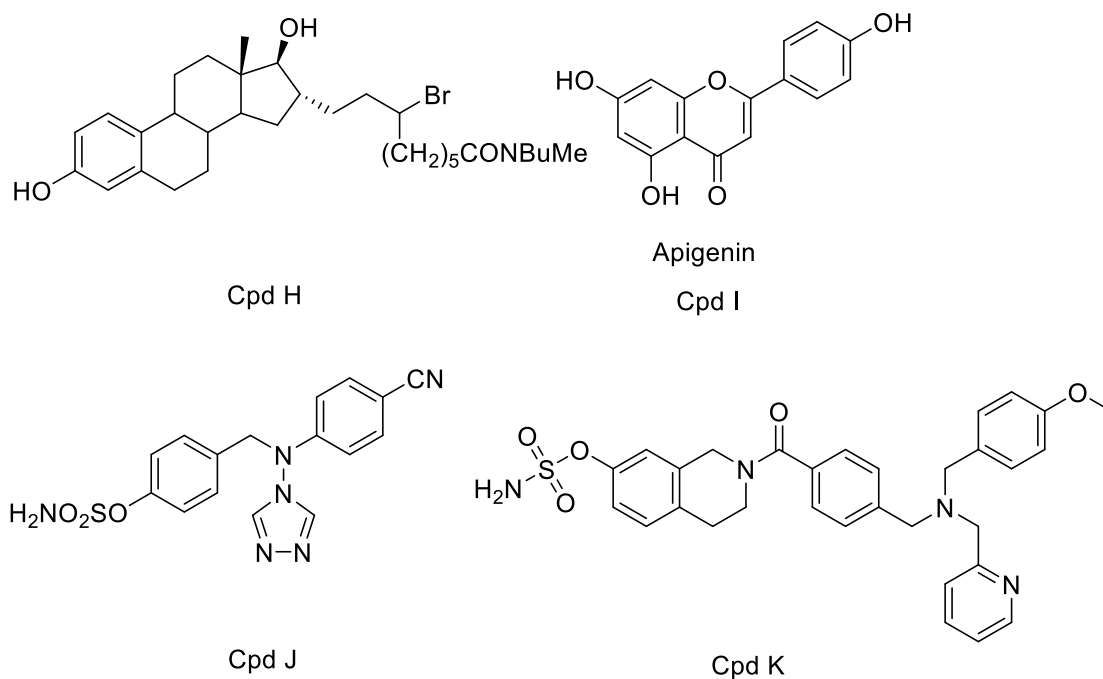


Figure 14: Structure of dual-acting agents: combined 17β -HSD1 inhibitor and antiestrogen (compound H), dual 17β -HSD1 and aromatase inhibitor (Apigenin, compound I), dual STS and aromatase inhibitor, DASI (compound J), combined STS inhibitor and selective estrogen receptor modulator (compound K).

These findings prompted our group to determine whether a similar concept could be applied to the dual inhibition of 17β -HSD1 and STS. Simultaneous inhibition of both enzymes is a new strategy for the reduction of local E2 biosynthesis and a potential therapeutic strategy for endometriosis and has the following advantages compared to known endocrine approaches: (a) STS is the key enzyme in local estrogen biosynthesis and according to literature plays a more important role than aromatase in the progression of the disease; (b) Also, STS inhibition causes the suppression of androstenediol (Adiol) production, which has estrogenic activity; (c) The conversion of E1 to E2 is blocked when 17β -HSD1 is inhibited, regardless of whether the source of E1 is from the sulfatase or aromatase pathway, and finally; (d) It is expected that systemic estrogen levels will remain relatively unaltered, resulting in less side effects³¹⁸, since inhibition of STS and 17β -HSD1 is an intracrine concept aimed at preventing local estrogen biosynthesis in diseased tissues, where enzymes are overexpressed. Bacsa et al.³¹⁹, discovered a non-sulfamate steroidal derivative that inhibits both STS and 17β -HSD1 with IC_{50} values of 230 and 360 nM, respectively. Recently our workgroup published the first dual inhibitors of STS and

17 β -HSD1 (DSHIs) as promising therapeutics for estrogen-dependent diseases¹⁶⁹. The design of DSHIs was facilitated by the introduction of a sulfamate aryl pharmacophore which is important for STS inhibitory activity, for example, STS-64, into an established 17 β -HSD1 inhibitor (compound L), Figure 15. Among 12 synthesized compounds, compound L was the most potent derivative, and it was active against both enzymes (cellular IC₅₀ (STS) = 15.6 nM and cellular IC₅₀ (17 β -HSD1) = 22.2 nM), Figure 15¹⁶⁹. It is also an irreversible inhibitor of STS, has a high selectivity over 17 β -HSD2 and effectively reversed proliferation of T47D breast cancer cell lines stimulated by E1-S and E1 without cytotoxicity or interference with ERs¹⁶⁹.

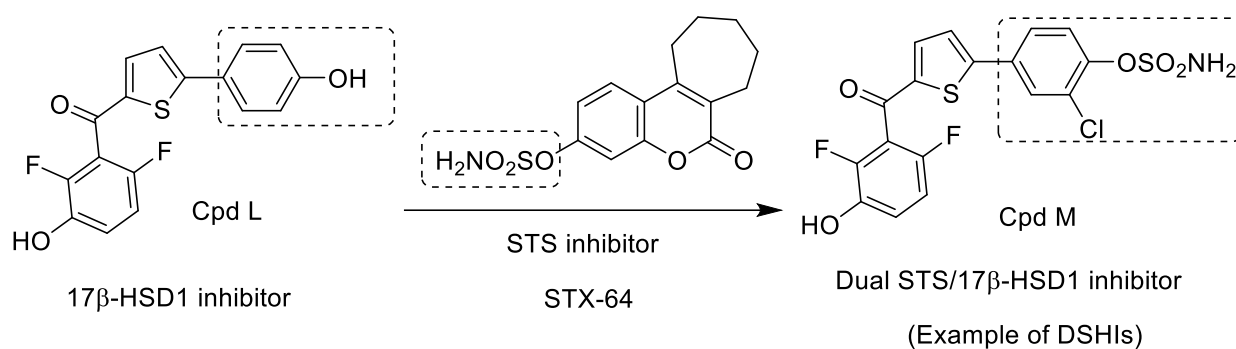


Figure 15: Structures of compound L (17 β -HSD1 inhibitor), STS inhibitor and compound M (dual STS and 17 β -HSD1 inhibitor, DSHI).

2. Aim of the thesis

In the treatment of EDDS, for example non-small cell lung cancer (NSCLC) and endometriosis, drugs which antagonize the ER or inhibit estrogen biosynthesis play a central role. Although the effects of using endocrine agents such as antiestrogens and aromatase inhibitors are important, but yet there is a clear need to find alternative treatments for patients that may not respond or become resistant to these therapies. Inhibition of peripheral E2 production is now thought to be a safer therapeutic approach for treating EDDs than conventional endocrine treatments, with the potential for less adverse effects since systemic estrogen levels may not be influenced. Such a clinical approach (intracrine concept) is currently being followed by using 5 α -reductase inhibitors in the treatment of benign prostate hyperplasia. Two pathways can produce E2 locally: the first is the aromatase pathway, in which aromatase and reductive 17 β -hydroxysteroid dehydrogenases catalyze the process of converting androstenedione or testosterone into estradiol (E2), the potent estrogen. The other pathway is the sulfatase pathway which is mediated by the actions of steroid sulfatase (STS), which converts estrone-sulfate (E1-S) into estrone (E1), and 17 β -hydroxysteroid dehydrogenase type 1 (17 β -HSD1), which activates E1 into E2. In addition, STS and 17 β -HSD1 are also involved in the synthesis of additional steroids such as Adiol, produced by the STS action on dehydroepiandrosterone sulfate (DHEA-Sulfate), which is then reduced to androst-5-ene-3 β (Adiol) by the action of 17 β -HSD1. Furthermore, aromatase inhibitors will not impair Adiol biosynthesis. Adiol has been proposed as the main estrogen after menopause and can stimulate *in vivo* mammalian tumors and induce breast cancer cell growth *in vitro*. The sulfatase pathway has been found to be more important in local estrogen biosynthesis than the aromatase pathway.

As mentioned before, many studies have shown that E2 can contribute to the progression of non-small cell lung cancer (NSCLC) and both estrogen receptors (ERs) α and β are also expressed in NSCLC tissues. In addition, both 17 β -HSD1 and 17 β -HSD2 have recently been discovered to be expressed in NSCLC, with the first catalyzing the intratumoral E1 to E2 and the second activating the reversible reaction, thereby protecting against an excess of E2. As a result, the first part of this study aimed to discover novel, potent and selective non-steroidal inhibitors of 17 β -HSD1 capable of improving therapeutic response in estrogen-dependent NSCLC patients and for achieving this aim, novel 17 β -HSD1 inhibitors have been designed and synthesized. This section presents the first proof that a highly selective 17 β -HSD1 inhibitor can be used to inhibit NSCLC cell proliferation. After evaluation of the inhibitory activities of

the compounds towards 17 β -HSD1 in a cell-free assay, the selectivity of the compounds towards 17 β -HSD2 was also measured. Further biological investigations were done on the most potent compound including, the efficacy of this compound in cellular experiments using human NSCLC Calu-1 cell lines, its toxic effect on HEK293 cells, a preliminary pharmacokinetic study using Sprague-Dawley rats inoculated with human cancer cells as a preclinical proof of principle and finally the metabolic half-life of it in rat liver S9 fraction. This work is presented in paper I chapter **3.1**.

The steroidogenic enzymes STS and 17 β -HSD1 have recently emerged as potential therapeutic targets for the treatment of endometriosis, since their inhibition can potentially achieve an efficient depletion of peripheral and local estrogen levels. 17 β -HSD2 catalyzes the conversion of potent estrogen, estradiol E2 to estrone E1 and thereby plays a protective role and should not be inhibited. The pharmacophore for STS inhibition has long been identified as an aryl-O-sulfamate moiety and its incorporation into an established non-steroidal 17 β -HSD1 inhibitor (*in-house* compound library), by masking the OH group with the sulfamate moiety, gave rise to a new design concept for inhibition of the two target enzymes (drug-prodrug approach). Phenolic derivatives (17 β -HSD1 inhibitors) are anticipated to be released from their sulfamate compounds through inactivation of STS and/or chemical hydrolysis, as it was known that the OH group plays an essential role in the inhibition and selectivity profiles towards 17 β -HSD1. Accordingly, the aim of the second part of the thesis was to develop a range of non-steroidal molecules which could be used as drugs for STS inhibition and prodrugs for 17 β -HSD1 inhibition, provided that the sulfamate group is cleaved to the phenolic hydroxyl group in a biological system, and thus is a “drug-prodrug approach”. One of the most potential advantages of this drug-prodrug strategy is the improvement of metabolic stability achieved by masking the OH group as a sulfamate moiety, as it was previously known that the existence of a free OH group would result in potentially poor metabolic stability (phase II metabolism). These inhibitors could be used as lead compounds for a novel endometriotic therapy choice, as well as scientific tools in proof-of-concept experiments to study the impact of dual inhibition of STS and 17 β -HSD1 on local biosynthesis of E2. The synthesized sulfamates were tested against STS in a cellular assay (T47D tumor cells), and their corresponding phenols were evaluated towards 17 β -HSD1 in both cell-free and cellular assays. The selectivity of the compounds towards 17 β -HSD2 (cell-free assay) and their binding to estrogen receptor ER α (binding affinity test) were also assessed. Moreover, the most promising inhibitors were screened for their metabolic stability using human and mouse liver microsomes. An assay that quantifies and time-

independently monitors the formation of the phenolic compound from the parent sulfamate should be developed and at the same time, this assay should facilitate measuring the percentage of 17 β -HSD1 inhibition as a function of time. The findings of the second part of this study are summarized in paper II chapter 3.2. The structural outline of the compounds in chapter 3 is given in Figure 16.

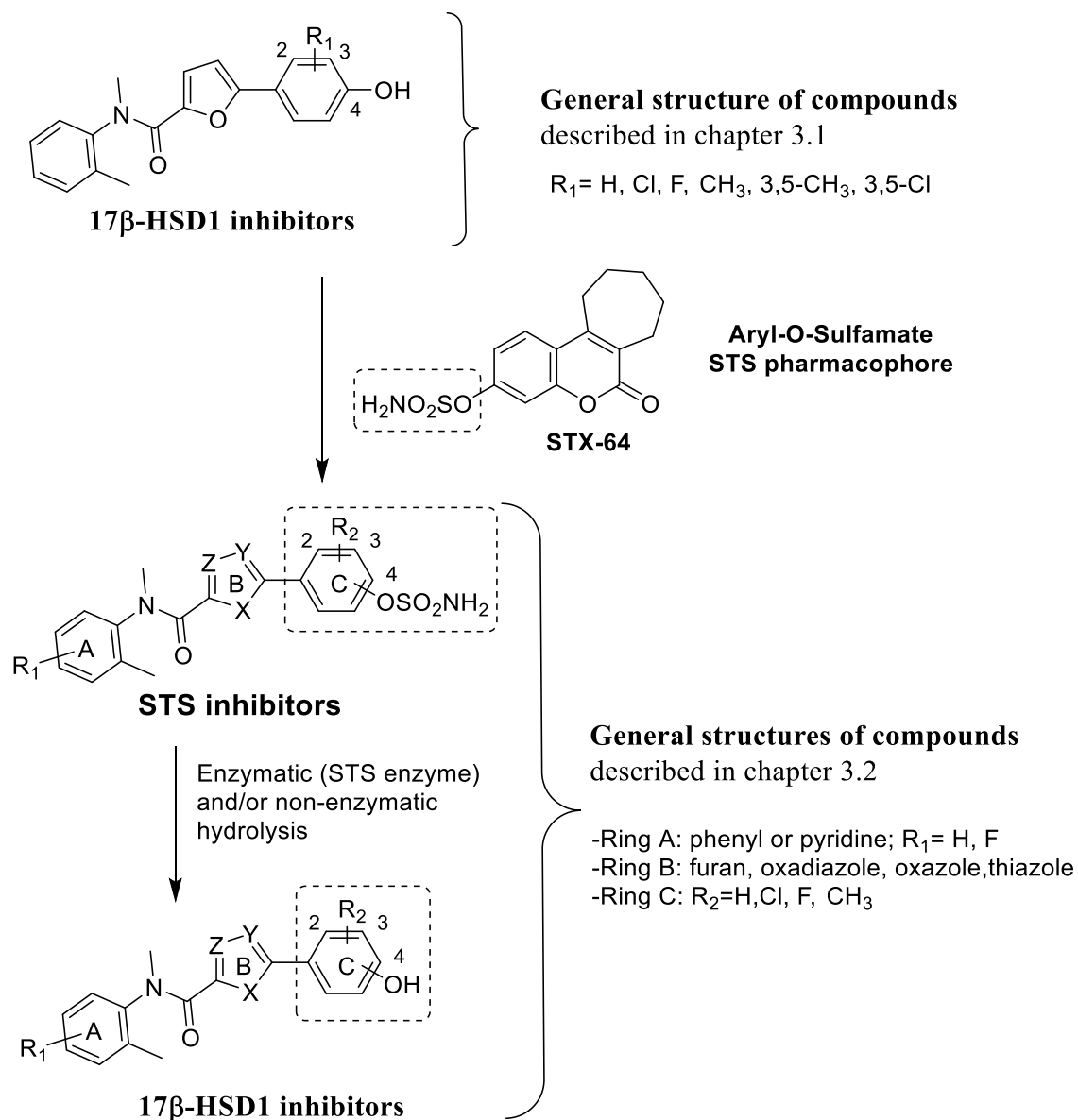


Figure 16: Proposed design and a general overview of the compounds mentioned in this thesis.

3. Results

3.1 17 β -Hydroxysteroid Dehydrogenase Type 1 Inhibition: A Potential Treatment Option for Non-Small Cell Lung Cancer (Publication A)

Abdelrahman Mohamed*, Emanuele M. Gargano*, Ahmed S. Abdelsamie, Giuseppe F. Mangiatordi, Hanna Drzewiecka, Arcangela Mazzini, Chris Van Koppen, Mathias W. Laschke, Orazio Nicolotti, Angelo Carotti, Sandrine-Marchais-Oberwinkler, Rolf W. Hartmann, and Martin Frotscher.

Reprinted with permission *Med. Chem. Lett.* 2021, 12 (12), 1920–1924.

DOI:10.1021/acsmchemlett.1c00462.

Copyright (2021) American Chemical Society

* These authors contributed equally

Publication A

Contribution Report

The author contributed to the design, synthesis and characterization of all the compounds. He performed the in vitro cell-free inhibition assays. Moreover, He conceived and wrote the manuscript.

17 β -Hydroxysteroid Dehydrogenase Type 1 Inhibition: A Potential Treatment Option for Non-Small Cell Lung Cancer

Emanuele M. Gargano,[△] Abdelrahman Mohamed,[△] Ahmed S. Abdelsamie, Giuseppe F. Mangiatordi, Hanna Drzewiecka, Paweł P. Jagodziński, Arcangela Mazzini, Chris J. van Koppen, Matthias W. Laschke, Orazio Nicolotti, Angelo Carotti, Sandrine Marchais-Oberwinkler, Rolf W. Hartmann, and Martin Frotscher^{*}



Cite This: *ACS Med. Chem. Lett.* 2021, 12, 1920–1924



Read Online

ACCESS |



Metrics & More



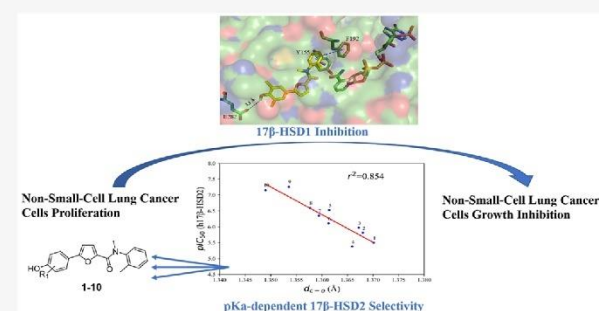
Article Recommendations



Supporting Information

ABSTRACT: In the face of the clinical challenge posed by non-small cell lung cancer (NSCLC), the present need for new therapeutic approaches is genuine. Up to now, no proof existed that 17 β -hydroxysteroid dehydrogenase type 1 (17 β -HSD1) is a viable target for treating this disease. Synthesis of a rationally designed library of 2,5-disubstituted furan derivatives followed by biological screening led to the discovery of 17 β -HSD1 inhibitor **1**, capable of fully inhibiting human NSCLC Calu-1 cell proliferation. Its pharmacological profile renders it eligible for further *in vivo* studies. The very high selectivity of **1** over 17 β -HSD2 was investigated, revealing a rational approach for the design of selective inhibitors. 17 β -HSD1 and **1** hold promise in fighting NSCLC.

KEYWORDS: 17 β -hydroxysteroid dehydrogenase type 1 (17 β -HSD1), non-small cell lung cancer (NSCLC), steroidogenic enzyme inhibition, drug design, structure–activity relationship (SAR), molecular docking



Lung cancer is the leading cause of death from cancer worldwide,¹ and in particular, non-small cell lung cancer (NSCLC), which accounts for more than 85% of the cases, shows only 15.9% and 49% five-year predicted survival rate for all and early stages of lung cancer, respectively.² Thus, finding more efficient drugs with novel modes of action is an urgent necessity.

The recognition of the great heterogeneity of lung cancer constitutes the most important advance in the field made in recent years,³ suggesting the need for exploring different therapeutic targets and leading today to the discovery of a few novel targets and therapies.⁴ We disclose in this report that compound **1**, a highly selective inhibitor of 17 β -hydroxysteroid dehydrogenase type 1 (17 β -HSD1), inhibits NSCLC cell proliferation at low nanomolar concentrations, providing the first proof of principle of 17 β -HSD1 as a target for NSCLC treatment. We document that **1** presents suitable *in vitro* properties and shows an acceptable bioavailability and toxicological profile. Finally, we provide a rationale for its very high selectivity over 17 β -hydroxysteroid dehydrogenase type 2 (17 β -HSD2).

Over the last 20 years, increasing evidence has demonstrated the pivotal role of estrogens in lung tumorigenesis, both in women and men.^{5–7} Different strategies to target the estrogen signaling pathway, such as the use of the down-regulator of

estrogen receptors (ERs) function. Fulvestrant⁸ and aromatase inhibitors such as Anastrozole⁹ and Exemestane¹⁰ have shown promising results in preclinical studies. However, 17 β -HSD1 and 17 β -HSD2, which are key local regulators of the estradiol/estrone (E2/E1) ratio,¹¹ have remained unexplored targets for the treatment of NSCLC. 17 β -HSD1 catalyzes the conversion of the weakly active E1 to the potent E2, and 17 β -HSD2 is its biological counterpart. The expression levels of these enzymes were found to be altered in NSCLC cells compared to healthy tissue, providing a significant prognostic factor and contributing to tumor progression in a stimulatory fashion, probably by increasing the E2/E1 ratio.^{12–15} Selective inhibition of 17 β -HSD1 seems therefore a potential approach for the treatment of NSCLC and might be superior to aromatase inhibition in terms of potential side effects: 17 β -HSD1 inhibition would result in only a local, intracellular drop in estradiol levels in the

Received: August 27, 2021

Accepted: November 11, 2021

Published: November 18, 2021



ACS Publications

© 2021 American Chemical Society

1920

<https://doi.org/10.1021/acsmmedchemlett.1c00462>
ACS Med. Chem. Lett. 2021, 12, 1920–1924

target cells while aromatase inhibition would decrease systemic circulating estradiol levels.

We have reported on the synthesis of different classes of 17 β -HSD1 inhibitors for the treatment of breast cancer and have demonstrated their antitumor activity *in vitro*.^{16,17} In light of the higher expression of 17 β -HSD2 mRNA in NSCLC cells than in breast carcinoma cells and given the positive correlation between 17 β -HSD2 expression and NSCLC survival rate,¹² we reasoned that a 17 β -HSD1 inhibitor should display very high selectivity over 17 β -HSD2 to be effective in NSCLC.

Applying our experience in the SARs of 17 β -HSD1 and 17 β -HSD2 inhibitors, we synthesized around 50 furan analogues of compound **A**¹⁸ and screened them for inhibitory activity toward 17 β -HSD1 and 17 β -HSD2, affinity for the estrogen receptors α and β (ERs), metabolic stability, and cytotoxicity.

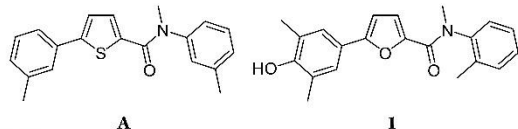


Table 1 shows the inhibitory data of the ten most interesting compounds which resulted. Inhibitor **1** emerged from this

Table 1. Inhibition of 17 β -HSD1 and 17 β -HSD2 by 2,5-Disubstituted Furans 1–10

compound	R ₁ ^b	IC ₅₀ (nM) ^{a,c}		s.f. ^e
		17 β -HSD1 ^c	17 β -HSD2 ^d	
1	3,5-Me	5.6	3155	563
2	3-Me	8.1	1171	145
3	2-Me	31.0	1077	35
4	H	55.2	2786	50
5	2-Cl	31.5	426	14
6	2-F	22.4	928	41
7	3-F	11.6	927	80
8	3-Cl	2.7	203	75
9	3,5-F	18.0	56	3
10	3,5-Cl	2.9	71	25

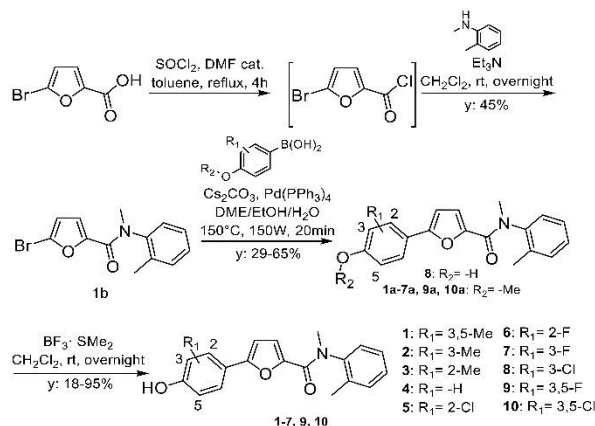
^aMean value of at least two determinations, standard deviation less than 20%. ^bcf. Scheme 1. ^cHuman placental, cytosolic fraction, substrate E1 [500 nM], cofactor NADH [500 μ M]. ^dHuman placental, microsomal fraction, substrate E2 [500 nM], cofactor NAD⁺ [1500 μ M]. ^es.f.: selectivity factor = IC₅₀ (17 β -HSD2)/IC₅₀ (17 β -HSD1).

study with the desired attributes, including very high selectivity over 17 β -HSD2.

Compounds **1–10** were synthesized as depicted in Scheme 1. The intermediate 5-bromofuran-2-carboxylic acid chloride was obtained from the corresponding carboxylic acid by reaction with SOCl₂. Subsequent reaction with *N*,2-dimethylaniline afforded the amide **1b**. The latter was subjected to a Suzuki coupling reaction with the appropriate boronic acid, under microwave irradiation (150 $^{\circ}$ C, 150 W, 20 min), providing the desired 2,5-disubstituted furans. The cleavage of the methoxy group was performed using a boron trifluoride dimethyl-sulfide complex.

Compound **1** displayed a half-life of 50 min in human liver preparation (S9 fraction; phase I and II metabolism), a relative binding affinity (RBA) toward ERs lower than 0.1%, and no detectable toxic effect on HEK293 cells at a concentration 1000-fold higher than the human 17 β -HSD1 IC₅₀ value (for

Scheme 1. Synthesis of the 2,5-Disubstituted Furans 1–10



details, see Supporting Information). Human NSCLC Calu-1 cells convert E1 to E2, which in turn promotes Calu-1 cell proliferation.¹⁴ We investigated the effect of inhibitor **1** on this stimulation (Figure 1).

The proliferation of Calu-1 cells was monitored in real-time (Figure 1A). After seeding (phase 1), Calu-1 cells were preincubated with medium, 50 nM compound **1**, 500 nM compound **1** or DMSO (vehicle control) for 48 h (phase 2). There was no effect of 50 or 500 nM compound **1** on cell proliferation (see Figure 1 legend for details). Then, cells were exposed to the compounds: 0.5 μ M E1 (green curve), 0.5 μ M E1 + 50 nM compound **1** (dark blue curve), 0.5 μ M E1 + 500 nM compound **1** (red curve), or DMSO alone (purple curve) as a vehicle control (phase 3). Addition of E1 to the incubation medium during a total of 75 h strongly increased cell proliferation compared to vehicle control (Figure 1). Coincubation of E1 with 50 nM of compound **1** reduced the cell proliferation to the vehicle control level at all time points (Figure 1B). There was no statistical difference in cell proliferation between coincubation between either 50 or 500 nM compound **1** (together with E1) and vehicle control, as measured at 12, 24, 36, 48, 60, and 72 h after initiation of phase 3 (Tukey HSD test, $P > 0.05$).

Preclinical proof of principle is to be demonstrated *in vivo* in an animal model of cancer, usually nude mouse or rat xenograft models inoculated with human cancer cells. We therefore performed a preliminary pharmacokinetic study with inhibitor **1** administered subcutaneously in Sprague–Dawley rats at a dose of 200 μ mol/kg (67.0 mg/kg). Successive administration at 0, 24, 48, and 72 h resulted in plasma concentrations more than sufficient to block human 17 β -HSD1 (i.e., 51, 82, 119, and 156 nM at 23.5, 47.5, 71.5, and 95.5 h, respectively). Half-life of **1** was determined in rat liver S9 fraction to be 19 min.

Among known nonsteroidal 17 β -HSD1 inhibitors, compound **1** displays the highest selectivity over 17 β -HSD2, whose crystal structure, contrary to 17 β -HSD1, is not yet available. To provide a structure-based hypothesis for this remarkable selectivity, docking simulations of **1** were performed by GLIDE v6.8¹⁹ on the 17 β -HSD1 crystal structure (PDB 3HBS).²⁰ The top score pose is shown in Figure 2. As displayed, the phenolic hydroxy group engages an H-bond interaction with the carboxylate group of E282, while the benzamide moiety establishes π – π interactions with two close aromatic side chains, namely Y155 and F192.

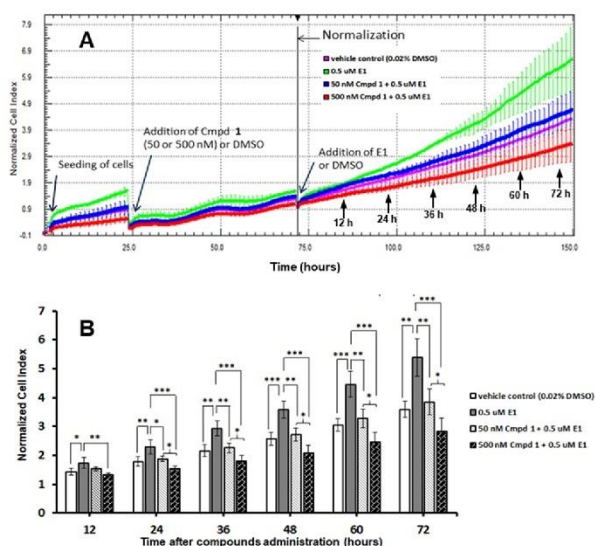


Figure 1. Effect of compound **1** on Calu-1 cell proliferation in the presence of E1 in real-time conditions. (A) Proliferation of Calu-1 cells was monitored in real-time by the xCELLigence RTCA DP System. Cells were seeded and incubated overnight in phenol red-free RPMI 1640 medium, supplemented with 10% charcoal-dextran-stripped FBS (Phase 1). After 24 h, cells were cultured for 48 h (phase 2) in the following experimental groups: control group—cells cultured in phenol red-free RPMI 1640 alone (green curve), cells cultured in phenol red-free RPMI 1640 plus 50 nM compound **1** (dark blue curve), cells cultured in phenol red-free RPMI 1640 plus 500 nM compound **1** (red curve), and vehicle control group—cells cultured in phenol red-free RPMI 1640 plus DMSO (final conc. 0.02%) (purple curve). At 72 h, media were changed once again, and cells were cultured further in the presence of following compounds (Phase 3): 0.5 μM E1 (green curve), 0.5 μM E1 + 50 nM compound **1** (dark blue curve), 0.5 μM E1 + 500 nM compound **1** (red curve), and DMSO (0.02%) as a vehicle control (purple curve). Cell index values were normalized to the starting time point of phase 3 (black vertical line). Four replicates at each investigated time point were used, and the mean normalized cell index values with standard deviation for each time point for each group are shown. The electrical impedance was measured at 15 min intervals throughout the cultivation period (total time: 150 h). There was no statistical significance between the data groups at 4, 12, and 20 h after seeding (phase 1) or between the data groups after 12, 24, 36, and 45 h of phase 2 treatment as assessed by ANOVA analysis. (B) Statistical analysis of Phase 3. Effect of inhibitor **1** treatment on Calu-1 cell proliferation in the presence of 0.5 μM E1. Mean values of normalized cell index \pm SD for each group after 12, 24, 36, 48, 60, and 72 h of treatment (see Figure 1, A) are shown. All experiments were performed in four replicates. Data groups were assessed by ANOVA to evaluate whether there was significance ($p < 0.05$) between the groups. Individual comparisons were made by post hoc Tukey's HSD (honestly significant difference) test. Statistical significance: * $p < 0.05$; ** $p < 0.01$; *** $p < 0.001$. For more details, see the Supporting Information.

Comparison between the primary sequences of binding sites of the two 17β -HSD enzymes, although appearing highly conserved, revealed an interesting difference: 17β -HSD2 shows an arginine (R364) in place of the glutamate (E282) of 17β -HSD1. Therefore, these two residues may play a pivotal role in addressing ligand protein interactions and even in explaining the molecular selectivity. In fact, the side chains of arginine and glutamate are very much diverse, with the result that

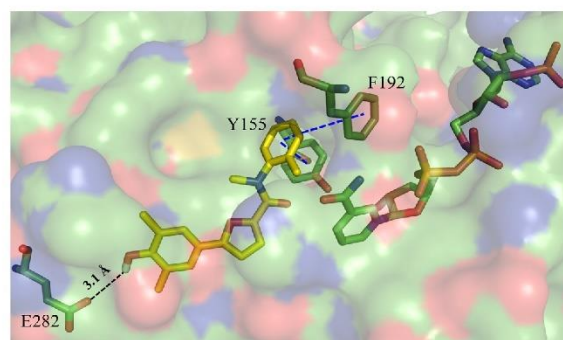


Figure 2. Top-scored docking pose of **1**. Important amino acid residues of 17β -HSD1, cofactor NADPH, and compound **1** are rendered as sticks, while the protein is shown as a surface. For the sake of clarity, the nonpolar hydrogen atoms of the ligand are not displayed. H-bond interaction is depicted with a black dotted line; π - π interactions are depicted with a blue dotted line.

replacement of the negative charge of E282 in 17β -HSD1 by the positively charged R364 in 17β -HSD2 should lead to a stronger binding of negatively ionized species to 17β -HSD2.

To prove the validity of this interaction model, we synthesized and tested a series of derivatives of compound **1**. The methyl groups next to the hydroxy function were exchanged by different substituents, leading to inhibitors **2**–**10** (Table 1), with diverse hydroxy-associated pK_a values. The new molecules were obtained using the same synthetic strategy as applied for **1** (Scheme 1).

It is acknowledged that the C–O bond distance ($d_{\text{C-O}}$) is an appropriate measure to explain the electronic effects of substituents on physicochemical properties like pK_a of phenols and it has been successfully correlated with the empirical Hammett constant.^{21,22} Consequently, the relationship between the $d_{\text{C-O}}$ values, measured using density functional theory (DFT) optimized structures, and the pIC_{50} s observed for 17β -HSD2 inhibition was investigated for **1**–**10**. As shown in Figure 3, a very good linear correlation was found: the lower the $d_{\text{C-O}}$ value (thus, lower pK_a), the higher is 17β -HSD2 inhibition. On the contrary, such correlation is not found with pIC_{50} values observed for 17β -HSD1 inhibition.

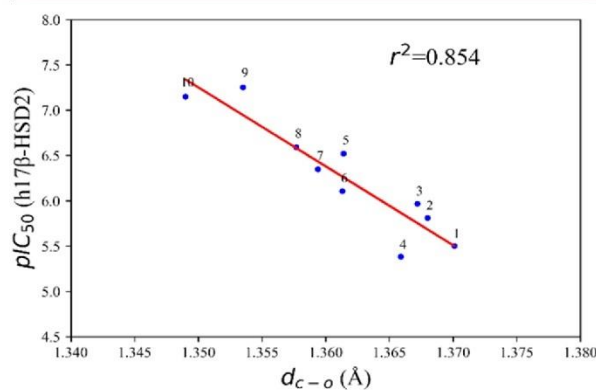


Figure 3. Relationship between pIC_{50} values toward 17β -HSD2 and $d_{\text{C-O}}$ distance calculated with the DFT optimized structures.

The robustness of this relationship was further challenged performing an intensive γ -randomization analysis to avoid the risk of chance correlations.²³

In this respect, we performed 1 million γ -scrambling runs to assess the reliability and goodness of the correlations (Figure S2), and satisfactorily, all the scrambled r^2 values were far from that reported in Figure 3.

The obtained correlation supports the hypothesis whereby the electronic structure of the phenolic ring is a key element for addressing molecular selectivity.

The discovery that the inhibitory activity on 17 β -HSD2 is dependent on the pK_a of the phenolic group is an important finding which can be further exploited for the rational development of additional selective 17 β -HSD1 inhibitors.

In summary, we validated 17 β -HSD1 as new therapeutic target for the treatment of NSCLC. Compound **1** fully inhibits the E1-dependent Calu-1 cell proliferation at low nanomolar concentrations. In addition, its pharmacological profile renders it a highly suitable candidate for further *in vivo* studies in animal models to establish a novel strategy for the treatment of NSCLC, which is urgently needed.

■ ASSOCIATED CONTENT

SI Supporting Information

The Supporting Information is available free of charge at <https://pubs.acs.org/doi/10.1021/acsmchemlett.1c00462>.

Biological experimental details, detailed synthesis, molecules spectral data, docking simulations, density functional theory calculations, and model validation (PDF)

■ AUTHOR INFORMATION

Corresponding Author

Martin Frotscher – Department of Pharmacy, Pharmaceutical and Medicinal Chemistry, Saarland University, D-66123 Saarbrücken, Germany; orcid.org/0000-0003-1777-8890; Email: m.frotscher@mx.uni-saarland.de

Authors

Emanuele M. Gargano – Department of Pharmacy, Pharmaceutical and Medicinal Chemistry, Saarland University, D-66123 Saarbrücken, Germany; Present Address: Drug Discovery Sciences, Boehringer Ingelheim Pharma GmbH & Co. KG, 88397 Biberach an der Riss, Germany

Abdelrahman Mohamed – Department of Pharmacy, Pharmaceutical and Medicinal Chemistry, Saarland University, D-66123 Saarbrücken, Germany; Pharmaceutical Organic Chemistry Department, Assiut University, Assiut 71526, Egypt

Ahmed S. Abdelsamie – Department of Drug Design and Optimization, Helmholtz Institute for Pharmaceutical Research Saarland (HIPS), D-66123 Saarbrücken, Germany; Chemistry of Natural and Microbial Products Department, National Research Centre, Dokki, Cairo 12311, Egypt

Giuseppe F. Mangiatordi – Dipartimento di Farmacia Scienze del Farmaco, Università degli Studi di Bari, I-70125 Bari, Italy; Present Address: Institute of Crystallography, National Research Council (CNR), Via Amendola 122/o, I-70126 Bari, Italy; orcid.org/0000-0003-4042-2841

Hanna Drzewiecka – Department of Biochemistry and Molecular Biology, Poznan University of Medical Sciences, 60-781 Poznan, Poland

Pawel P. Jagodziński – Department of Biochemistry and Molecular Biology, Poznan University of Medical Sciences, 60-781 Poznan, Poland

Arcangela Mazzini – Department of Pharmacy, Pharmaceutical and Medicinal Chemistry, Saarland University, D-66123 Saarbrücken, Germany

Chris J. van Koppen – ElexoPharm GmbH, D-66123 Saarbrücken, Germany; orcid.org/0000-0003-2799-6728

Matthias W. Laschke – Institute for Clinical and Experimental Surgery, Saarland University, D-66421 Homburg, Saar, Germany

Orazio Nicolotti – Dipartimento di Farmacia Scienze del Farmaco, Università degli Studi di Bari, I-70125 Bari, Italy; Present Address: Institute of Crystallography, National Research Council (CNR), Via Amendola 122/o, I-70126 Bari, Italy; orcid.org/0000-0001-6533-5539

Angelo Carotti – Dipartimento di Farmacia Scienze del Farmaco, Università degli Studi di Bari, I-70125 Bari, Italy; Present Address: Institute of Crystallography, National Research Council (CNR), Via Amendola 122/o, I-70126 Bari, Italy

Sandrine Marchais-Oberwinkler – Department of Pharmacy, Pharmaceutical and Medicinal Chemistry, Saarland University, D-66123 Saarbrücken, Germany

Rolf W. Hartmann – Department of Pharmacy, Pharmaceutical and Medicinal Chemistry, Saarland University, D-66123 Saarbrücken, Germany; Department of Drug Design and Optimization, Helmholtz Institute for Pharmaceutical Research Saarland (HIPS), D-66123 Saarbrücken, Germany; orcid.org/0000-0002-5871-5231

Complete contact information is available at: <https://pubs.acs.org/doi/10.1021/acsmchemlett.1c00462>

Author Contributions

Δ E.M.G. and A.M. contributed equally to this work.

Notes

The authors declare the following competing financial interest(s): A.S.A., C.J.v.K., S.M.-O., R.W.H., and M.F. are inventors of a US patent covering compounds 1-10 (US9884839(B2)).

■ ACKNOWLEDGMENTS

We would like to thank the Deutsche Forschungsgemeinschaft (DFG) (Grants HA1315/12-1 and FR3002/1-1) for financial support. We would like also to thank the Deutscher Akademischer Austauschdienst DAAD for funding this publication as part of the German-Egyptian Research Long Term Scholarship Program (GERLS) 2016 (S7222240) and Short-Term Scholarships for Foreign Students (STIBET), Saarland University 2020/2021. Help with the biological testing from Martina Jankowski is also highly appreciated.

■ ABBREVIATIONS

17 β -HSD1, 17 β -hydroxysteroid dehydrogenase type 1; 17 β -HSD2, 17 β -hydroxysteroid dehydrogenase type 2; NSCLC, non-small cell lung cancer; E1, estrone; E2, 17 β -estradiol; ER, estrogen receptor; s.f., selectivity factor; IC₅₀, inhibitor concentration resulting in 50% enzyme inhibition; pIC₅₀, negative logarithm of IC₅₀; RBA, relative binding affinity

(relative to the binding affinity of E2 which was set at 100%); DFT, density functional theory

REFERENCES

- (1) American Cancer Society. *Global Cancer Facts & Figures*, 3rd ed.; American Cancer Society: Atlanta; 2015.
- (2) Ettinger, D. S.; Akerley, W.; Borghaei, H.; Chang, A. C.; Cheney, R. T.; Chirieac, L. R.; D'Amico, T. A.; Demmy, T. L.; Govindan, R.; Grannis, F. W. Non-small cell lung cancer, version 2.2013. *J. Natl. Compr. Canc. Netw.* **2013**, *11* (6), 645–653.
- (3) Chen, Z.; Fillmore, C. M.; Hammerman, P. S.; Kim, C. F.; Wong, K. K. *Nat. Rev. Cancer* **2014**, *14*, 535. Chen, Z.; Fillmore, C. M.; Hammerman, P. S.; Kim, C. F.; Wong, K.-K. Non-small-cell lung cancers: a heterogeneous set of diseases. *Nat. Rev. Cancer* **2014**, *14* (8), 535–546.
- (4) Johnson, D.; Schiller, J.; Bunn Jr, P. Recent clinical advances in lung cancer management. *J. Clin. Oncol.* **2014**, *32* (10), 973–982.
- (5) Pietras, R. J.; Márquez, D. C.; Chen, H.-W.; Tsai, E.; Weinberg, O.; Fishbein, M. Estrogen and growth factor receptor interactions in human breast and non-small cell lung cancer cells. *Steroids* **2005**, *70* (5–7), 372–381.
- (6) Stabile, L. P.; Davis, A. L. G.; Gubish, C. T.; Hopkins, T. M.; Luketich, J. D.; Christie, N.; Finkelstein, S.; Siegfried, J. M. Human non-small cell lung tumors and cells derived from normal lung express both estrogen receptor α and β and show biological responses to estrogen. *Cancer Res.* **2002**, *62* (7), 2141–2150.
- (7) Márquez-Garbán, D. C.; Chen, H.-W.; Fishbein, M. C.; Good-Glick, L.; Pietras, R. J. Estrogen receptor signaling pathways in human non-small cell lung cancer. *Steroids* **2007**, *72* (2), 135–143.
- (8) Stabile, L. P.; Lyker, J. S.; Gubish, C. T.; Zhang, W.; Grandis, J. R.; Siegfried, J. M. Combined targeting of the estrogen receptor and the epidermal growth factor receptor in non-small cell lung cancer shows enhanced antiproliferative effects. *Cancer Res.* **2005**, *65* (4), 1459–1470.
- (9) Weinberg, O. K.; Marquez-Garban, D. C.; Fishbein, M. C.; Goodglick, L.; Garban, H. J.; Dubinett, S. M.; Pietras, R. J. Aromatase inhibitors in human lung cancer therapy. *Cancer Res.* **2005**, *65* (24), 11287–11291.
- (10) Coombes, R. C.; Hall, E.; Gibson, L. J.; Paridaens, R.; Jassem, J.; Delozier, T.; Jones, S. E.; Alvarez, I.; Bertelli, G.; Ortmann, O. A randomized trial of exemestane after two to three years of tamoxifen therapy in postmenopausal women with primary breast cancer. *N. Engl. J. Med.* **2004**, *350* (11), 1081–1092.
- (11) Vihko, P.; Isomaa, V.; Ghosh, D. Structure and function of 17 β -hydroxysteroid dehydrogenase type 1 and type 2. *Mol. Cell. Endocrinol.* **2001**, *171* (1–2), 71–76.
- (12) Verma, M. K.; Miki, Y.; Abe, K.; Suzuki, T.; Niikawa, H.; Suzuki, S.; Kondo, T.; Sasano, H. Intratumoral localization and activity of 17 β -hydroxysteroid dehydrogenase type 1 in non-small cell lung cancer: a potent prognostic factor. *J. Transl. Med.* **2013**, *11* (1), 1–11.
- (13) Drzewiecka, H.; Jagodzinski, P. P. Conversion of estrone to 17-beta-estradiol in human non-small-cell lung cancer cells in vitro. *Biomed. Pharmacother.* **2012**, *66* (7), 530–534.
- (14) Drzewiecka, H.; Gałęcki, B.; Jarmolowska-Jurczyszyn, D.; Kluk, A.; Dyszkiewicz, W.; Jagodziński, P. P. Increased expression of 17-beta-hydroxysteroid dehydrogenase type 1 in non-small cell lung cancer. *Lung Cancer* **2015**, *87* (2), 107–116.
- (15) Drzewiecka, H.; Jarmolowska-Jurczyszyn, D.; Kluk, A.; Gałęcki, B.; Dyszkiewicz, W.; Jagodziński, P. P. Altered expression of 17 β -hydroxysteroid dehydrogenase type 2 and its prognostic significance in non-small cell lung cancer. *Int. J. Oncol.* **2020**, *56* (6), 1352–1372.
- (16) Marchais-Oberwinkler, S.; Kruchten, P.; Frotscher, M.; Ziegler, E.; Neugebauer, A.; Bhoga, U.; Bey, E.; Müller-Vieira, U.; Messinger, J.; Thole, H. Substituted 6-phenyl-2-naphthols. Potent and selective nonsteroidal inhibitors of 17 β -hydroxysteroid dehydrogenase type 1 (17 β -HSD1): design, synthesis, biological evaluation, and pharmacokinetics. *J. Med. Chem.* **2008**, *51* (15), 4685–4698.
- (17) Abdelsamie, A. S.; Salah, M.; Siebenbürger, L.; Hamed, M. M.; Börger, C.; van Koppen, C. J.; Frotscher, M.; Hartmann, R. W. Development of potential preclinical candidates with promising in vitro ADME profile for the inhibition of type 1 and type 2 17 β -hydroxysteroid dehydrogenases: design, synthesis, and biological evaluation. *Eur. J. Med. Chem.* **2019**, *178*, 93–107.
- (18) Salah, M.; Abdelsamie, A. S.; Frotscher, M. Inhibitors of 17 β -hydroxysteroid dehydrogenase type 1, 2 and 14: Structures, biological activities and future challenges. *Mol. Cell. Endocrinol.* **2019**, *489*, 66–81.
- (19) *Schrödinger Suite 2015-3*; Schrödinger, LLC: New York, NY, 2015.
- (20) Mazumdar, M.; Fournier, D.; Zhu, D.-W.; Cadot, C.; Poirier, D.; Lin, S.-X. Binary and ternary crystal structure analyses of a novel inhibitor with 17 β -HSD type 1: a lead compound for breast cancer therapy. *Biochem. J.* **2009**, *424* (3), 357–366.
- (21) Amunugama, R.; Rodgers, M. The influence of substituents on cation- π interactions. 4. Absolute binding energies of alkali metal cation-phenol complexes determined by threshold collision-induced dissociation and theoretical studies. *J. Phys. Chem. A* **2002**, *106* (42), 9718–9728.
- (22) Gross, K. C.; Seybold, P. G. Substituent effects on the physical properties and pKa of phenol. *Int. J. Quantum Chem.* **2001**, *85* (4–5), 569–579.
- (23) Nicolotti, O.; Carotti, A. QSAR and QSPR studies of a highly structured physicochemical domain. *J. Chem. Inf. Model.* **2006**, *46* (1), 264–276.

3.2 Dual Targeting of Steroid Sulfatase and 17 β -Hydroxysteroid Dehydrogenase Type 1 by a Novel Drug-Prodrug Approach: A Potential Therapeutic Option for the Treatment of Endometriosis (Publication B)

Abdelrahman Mohamed, Mohamed Salah, Mariam Tahoun, Manuel Hawner, Ahmed S Abdelsamie, Martin Frotscher

Reprinted with permission *J. Med. Chem.* 2022, 65 (17):11726-11744.
DOI:10.1021/acs.jmedchem.2c00589.

Copyright (2022) American Chemical Society

Publication B

Contribution Report

The author contributed to the design concept. He planned and performed the synthesis and characterization of all the compounds, the *in vitro* cell-free and cellular inhibition assays. He conceived and wrote the manuscript.

Dual Targeting of Steroid Sulfatase and 17 β -Hydroxysteroid Dehydrogenase Type 1 by a Novel Drug-Prodrug Approach: A Potential Therapeutic Option for the Treatment of Endometriosis

Abdelrahman Mohamed, Mohamed Salah, Mariam Tahoun, Manuel Hawner, Ahmed S. Abdelsamie, and Martin Frotscher*

Cite This: *J. Med. Chem.* 2022, 65, 11726–11744

Read Online

ACCESS |

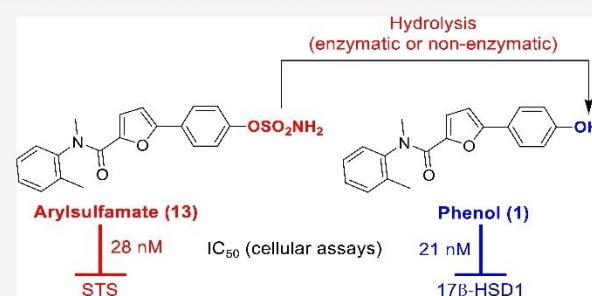
Metrics & More

Article Recommendations

Supporting Information

ABSTRACT: A novel approach for the dual inhibition of steroid sulfatase (STS) and 17 β -hydroxysteroid dehydrogenase type 1 (17 β -HSD1) by a single drug was explored, starting from in-house 17 β -HSD1 inhibitors via masking their phenolic OH group with a sulfamate ester. The sulfamates were intentionally designed as drugs for the inhibition of STS and, at the same time, prodrugs for 17 β -HSD1 inhibition (“drug-prodrug approach”). The most promising sulfamates 13, 16, 18–20, 22–24, 36, and 37 showed nanomolar IC₅₀ values for STS inhibition in a cellular assay and their corresponding phenols displayed potent 17 β -HSD1 inhibition in cell-free and cellular assays, high selectivity over 17 β -HSD2, reasonable metabolic stability, and low estrogen receptor α affinity.

A close relationship was found between the liberation of the phenolic compound by sulfamate hydrolysis and 17 β -HSD1 inactivation. These results showed that the envisaged drug-prodrug concept was successfully implemented. The novel compounds constitute a promising class of therapeutics for the treatment of endometriosis and other estrogen-dependent diseases.



INTRODUCTION

17 β -estradiol (E2) plays a vital role in the progression of several estrogen-dependent diseases (EDDs), such as endometriosis,^{1–3} breast cancer,^{4,5} endometrial cancer,^{6,7} and ovarian cancer.⁸ Endometriosis is an estrogen-activated gynecological, frequently chronic, inflammatory disease in women where endometriotic glands and stroma are located at sites outside the uterus. Endometriotic lesions can be located in various areas; mostly in the pelvic area including the ovaries, ligaments, peritoneal surfaces, and at the vesico-uterine fold.^{9,10} The disease can lead to the deformation of the pelvic anatomy and is often accompanied by pelvic pain and infertility.^{9,11} It affects ~5–10% of women in their reproductive age (~176 million women worldwide), whereas the percentage increases up to 50% of women with infertility.^{11,12} Current treatment options for endometriosis involve the surgical removal of endometriotic lesions and/or medical therapy. Surgical excision of endometriosis significantly decreases pain symptoms.¹³ However, the recurrence rate of pain symptoms after surgery is high.¹⁴ Available medical treatment does not eradicate the disease and the pharmaceutical possibilities of intervention suffer from the same main drawbacks, in that they must be stopped before the side effects get more severe than the symptoms being treated, and the symptoms reappear after the treatment has been terminated.^{15,16} Analgesics, such as NSAIDs, are the first line but only relieve symptoms such as dysmenorrhea.¹⁷ Current

hormonal therapies are aimed either at minimizing estrogen biosynthesis [by use of gonadotropin-releasing hormone (GnRH) analogues or aromatase inhibitors (AIs)] or at blocking the estrogen action at the receptor level [with antiestrogens or selective estrogen receptor modulators (SERMs)].¹⁸ However, these therapies can cause systemic estrogen deprivation, leading to unwanted adverse effects.^{19–22} Therefore, their use is restricted to a period of 3–6 months. There is thus a substantial demand for novel drug treatment options which effectively suppress the progression of endometriosis over a prolonged period of time and have fewer side effects.

Reducing estrogen levels in the target tissues is a rather new strategy for the treatment of endometriosis and could be linked to less adverse effects. In the diseased tissues, E2 can be biosynthesized mainly through the sulfatase pathway by the actions of steroid sulfatase (STS),^{23–26} which hydrolyzes inactive estrone-sulfate (E1-S), the main transport- and storage form of estrogens, into estrone (E1), and 17 β -hydroxysteroid

Received: April 13, 2022
Published: August 22, 2022



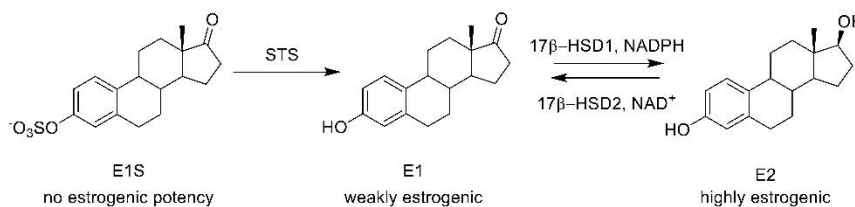
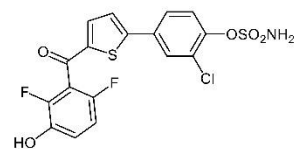


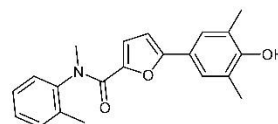
Figure 1. Sulfatase pathway of local estrogen biosynthesis.

Chart 1. First Dual STS/ 17β -HSD1 Inhibitor (A)⁷⁴ and 17β -HSD1 Inhibitor (B),⁹¹ Reported by Our Group^a



Compound A

Cellular STS IC_{50} = 15 nM
 Cellular (*h*17 β -HSD1) = 22.2 nM
 Cell-free (*h*17 β -HSD1) = 1.1 nM
 Cell-free (*h*17 β -HSD2) = 36.1 nM
 Selectivity Factor (SF) = 33
 Metabolic stab. $t_{1/2}$ (*h*S9) <5 min
 Metabolic stab. $t_{1/2}$ (*m*S9) <5 min



Lead compound B

Cellular STS = n.i
 Cellular (*h*17 β -HSD1) = 2.9 nM
 Cell-free (*h*17 β -HSD1) = 5.6 nM
 Cell-free (*h*17 β -HSD2) = 3155 nM
 Selectivity Factor (SF) = 563
 Metabolic stab. $t_{1/2}$ (*h*S9) = 38.1 min
 Metabolic stab. $t_{1/2}$ (*m*S9) = 19.1 min

^aExperimental data are derived from previous publications of the authors.^{74,91} *H*17 β -HSD1: human 17 β -HSD1, *h*S9 and *m*S9: human and mouse liver S9 fraction, S.F.: selectivity factor = cell-free $hIC_{50}(17\beta\text{-HSD2})/hIC_{50}(17\beta\text{-HSD1})$, n.i: no inhibition (<10% inhibition at 1 μ M).

dehydrogenase type 1 (17 β -HSD1),^{27,28} which catalyzes the conversion of the weakly active estrogen E1 into the highly active E2 (Figure 1).

For local estrogen production, the sulfatase pathway was found to play an even more important role than the aromatase pathway.^{29–31} Additionally, STS has been found to be overexpressed in endometriotic lesions,^{2,32} and the levels of STS expression were correlated to the severity of the disease.³⁰ Furthermore, 17 β -HSD1 is overexpressed in endometriosis;^{2,22,33} and at the same time, 17 β -HSD2 is downregulated which impairs E2 deactivation to E1.^{22,34,35} Also, STS and 17 β -HSD1 are involved in the synthesis of other steroids such as androst-5-ene-3 β ,17 β -diol (A-diol), which is produced by the action of STS on dehydroepiandrosterone sulfate (DHEA-sulfate) to give dehydroepiandrosterone (DHEA), which is then reduced by 17 β -HSD1 to A-diol.^{5,36} A-diol was suggested to be the major estrogen present after menopause.^{37–39} It is known to induce the growth of breast cancer cells *in vitro*⁴⁰ and to stimulate mammary tumors *in vivo*.⁴¹ A-diol biosynthesis is unaffected by aromatase inhibitors. STS and 17 β -HSD1 thus represent promising drug targets for treating endometriosis. 17 β -HSD2 catalyzes the inactivation of E2 to E1 (Figure 1). Thus, it plays a protective role and should therefore not be inhibited. A variety of steroidal and non-steroidal 17 β -HSD1 inhibitors have been developed, and there are several review articles giving a good overview.^{42–49} Recently, a novel 17 β -HSD1 inhibitor, FOR-6219, developed primarily by Forendo Pharma for the treatment of endometriosis was studied in a phase I clinical trial and it was found to be safe and well tolerated (NCT03709420). In addition, no side effects associated with systemic estrogen deficiency are reported. The compound is now entering phase II of clinical development with endome-

triosis patients in the US to assess its efficacy as a long-term treatment option for endometriosis. A second 17 β -HSD1 inhibitor that has reached the stage of *in vivo* testing (in murine and monkey models) is a covalent inhibitor of 17 β -HSD1 (called PBRM), whose biopharmaceutical attributes and pharmacodynamics are conducive to further development.^{38,50–52}

It is likely that these drugs will be coupled with other ovarian function inhibitors (progestins, GnRH-agonists). Also, for STS, a number of steroidal and non-steroidal inhibitors are described.^{25,53–62}

Targeting multiple biological targets by single agents is an attractive and emerging approach in the design and discovery of new medications and may enhance the efficacy of novel treatment methods.^{63–74} Using a single agent could prevent drug–drug interactions, as well as overcome resistance that may arise from single targeted drugs. In the literature, there are some examples of dual acting-agents which affect estrogen production or estrogenic effects. In 1996, the synthesis and biological evaluation of 17 β -HSD1 inhibitors having antiestrogenic activity were reported by Tremblay et al. The most potent derivative inhibited 17 β -HSD1 activity with an IC_{50} of 14 μ M while being antiestrogenic at 1 μ M.⁷⁵ Several flavonoids were found to inhibit the action of both 17 β -HSD1 and aromatase. An example is apigenin, which inhibited the activity of these enzymes by 78 and 95%, respectively, in placental microsomes.^{76,77} Multi-targeting drugs that inhibit both aromatase and STS have been termed dual aromatase-sulfatase inhibitors (DASIs). Woo et al.^{78–80} published the first examples of DASIs with high potency. For instance, in a cellular assay (JEG-3 cells), STX1983 inhibited STS and aromatase activities with IC_{50} values of 5.5 and 0.5 nM, respectively, and it was non-estrogenic. Many new

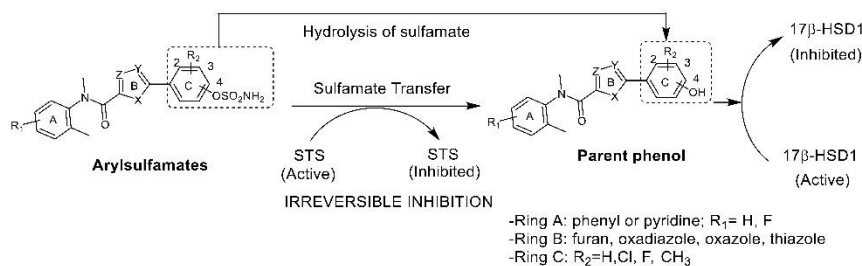
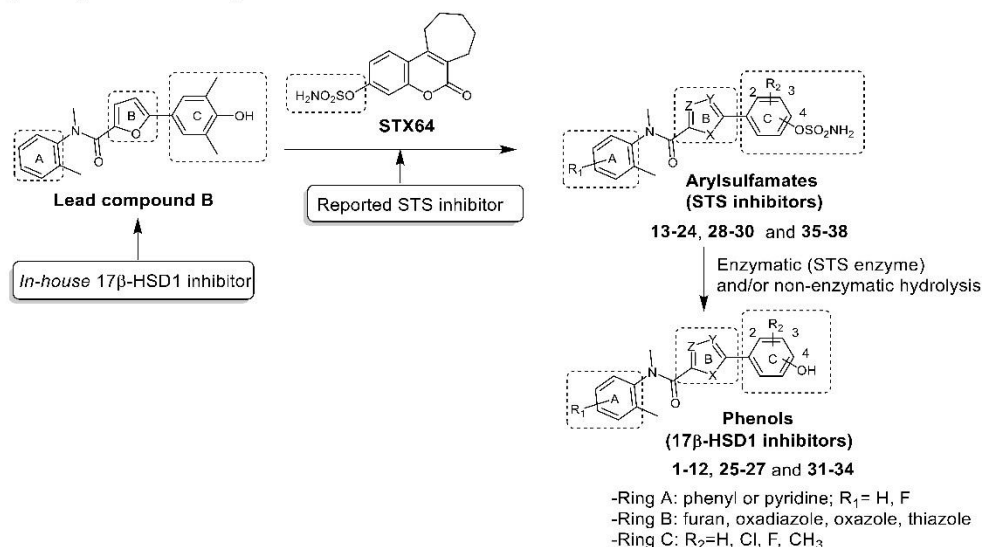


Figure 2. Proposed mechanism of action for aryl sulfamate compounds.

Chart 2. Design Rationale and General Structures of Drug-Prodrug STS/17β-HSD1 Inhibitors (13–24, 28–30, and 35–38) and Their Corresponding Phenolic Compounds (1–12, 25–27, and 31–34)



DASIs have been developed in recent years, including sulfamoylated letrozoles^{81–83} and anastrozole derivatives.⁸⁴ Both the aromatase and sulfatase pathways are blocked by DASIs, resulting in severe hypo-estrogenic side effects that may hinder their therapeutic application. The development of molecules which inhibit STS and modulate estrogen receptors has been pursued by several groups.^{85–87} In particular, EO-33,^{86–88} was one of the most promising candidates, which is a sulfamate derivative based on tetrahydroisoquinoline that acts as an STS inhibitor and selective estrogen receptor modulator at the same time. The compound exerted strong activity against STS ($IC_{50} = 3.9$ nM) in HEK-293 cells. In addition, it displayed a SERM effect in ovariectomized mice, blocked changes in uterine weight induced by E1S, and had no toxic effects (based on body weight, liver weight, and liver appearance).^{86–88}

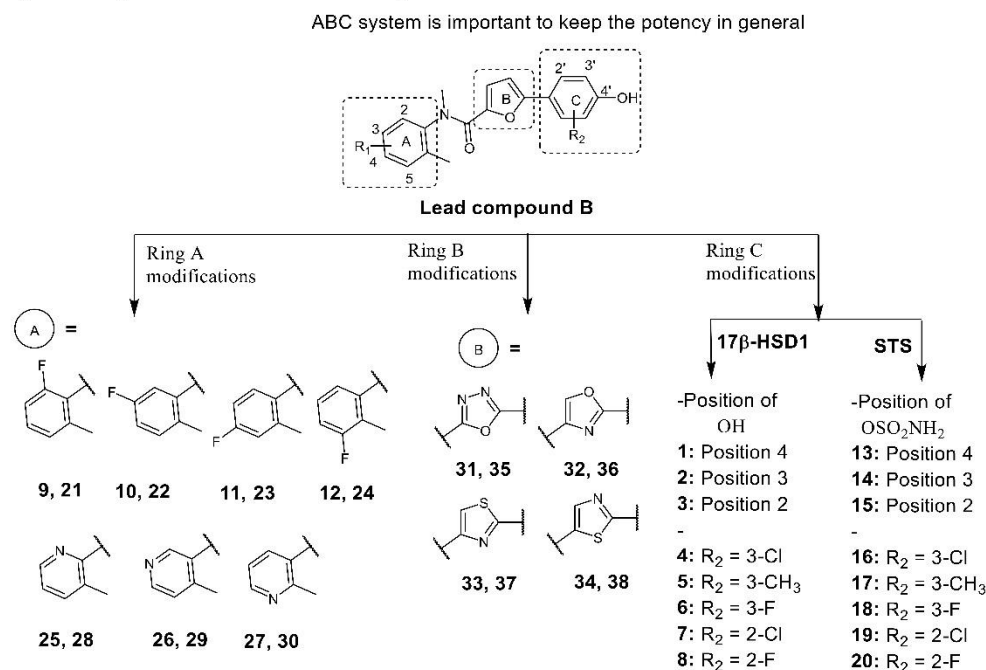
The simultaneous inhibition of both STS and 17β-HSD1 with a dual-acting drug may result in a better therapeutic option for patients with endometriosis, with the prospect of fewer adverse effects compared to the current treatments, and it may be more effective than selectively inhibiting either STS or 17β-HSD1 alone.⁸⁹ Systemic estrogen levels should remain rather unaltered, resulting in less side effects because the inhibition of STS and 17β-HSD1 primarily interferes with intracrine estrogen modulation, preventing the local biosynthesis of active estrogen from the inactive precursor E1-S in diseased tissues where the enzymes are overexpressed. Bacsa et al.,⁹⁰ discovered

a non-sulfamate steroidal derivative that inhibits both STS and 17β-HSD1 with IC_{50} values of 230 and 360 nM, respectively. Recently, our workgroup published the first dual inhibitors of STS and 17β-HSD1 (DSHIs) as promising therapeutics for estrogen-dependent diseases.⁷⁴

RESULTS AND DISCUSSION

Design. Dual inhibitors of STS and 17β-HSD1 recently published by our group showed strong inhibition of both target enzymes.⁷⁴ The most interesting compound was compound A (Chart 1), bearing a thiophene moiety. It showed IC_{50} values in the low nanomolar range. Unfortunately, the thiophene scaffold was found to suffer from some drawbacks. Compound A and related thiophene-based inhibitors showed fast biotransformation when tested using human and mouse liver S9 fractions. In addition, they displayed low to moderate selectivity over 17β-HSD2, see Chart 1.⁷⁴ Therefore, the lead for the present was a hydroxyphenylfurancarboxamide scaffold recently reported by our group (compound B, Chart 1)⁹¹ that showed better selectivity (SF = 563 for B vs 33 for A) and higher metabolic stability than A (half-life in human liver S9 fraction 38 min for B vs less than 5 min for A).

Design Rationale (Drug-Prodrug Approach). The novel inhibitors of STS and 17β-HSD1 were rationally designed based upon two considerations: First, most literature-known STS inhibitors bear an *N*-unsubstituted aryl sulfamate group as a

Chart 3. Design of Compounds Based on Lead Compound B^a

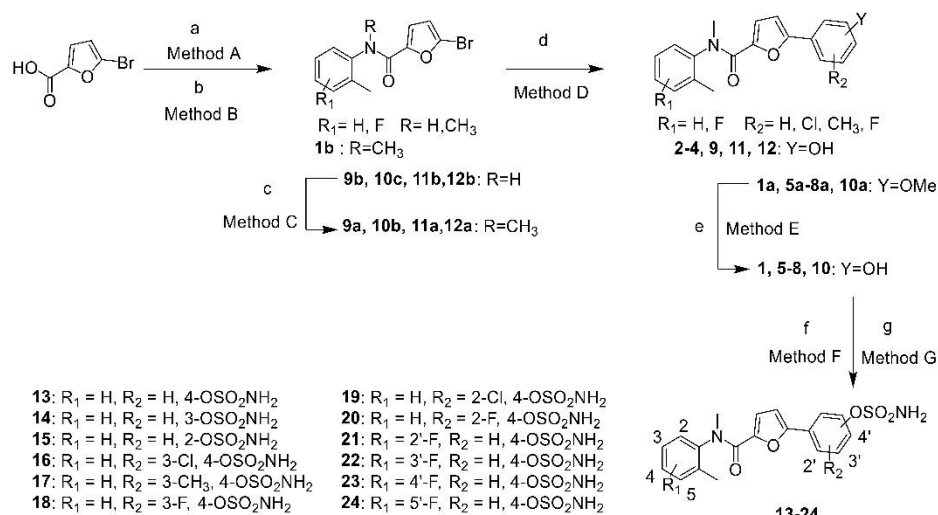
^aRing A was modified by introducing a fluorine atom as an electron-withdrawing group (compounds 9–12 and 21–24). Moreover, ring A was exchanged by the more hydrophilic pyridine system (compounds 25–30). The furan ring B was replaced with different heterocyclic rings, namely, oxadiazole (compounds 31 and 35), oxazole (compounds 32 and 36), and thiazole (compounds 33, 34, 37 and 38) in order to modulate the lipophilicity of the compounds. The substitution pattern of ring C was optimized. On the one hand, this involved the search for the optimal position of the hydroxyl or sulfamate group, respectively (compounds 1–3 and 13–15). On the other hand, the influence of additional electron-donating or -withdrawing groups added to ring C on the biological properties was investigated (compounds 4–8 and 16–20).

common feature that acts as the main pharmacophore for (irreversible) STS inhibition. A prominent example is STX-64 which was the first STS inhibitor to be used in clinical trials.⁹² Therefore, the aryl sulfamate group was implemented also in the newly designed compounds. The second consideration was that the sulfamate group is cleaved by STS (and/or non-enzymatically)—as shown for literature described STS inhibitors—releasing the free phenolic parent compound.^{93–100} These two considerations give rise to an intriguing concept for sequential inhibition of the two target enzymes. We aimed at synthesizing compounds in which a phenolic OH group of a 17β-HSD1 inhibitor, that is, a main pharmacophoric feature for 17β-HSD1 inhibition, is masked by a sulfamate group (Figure 2).

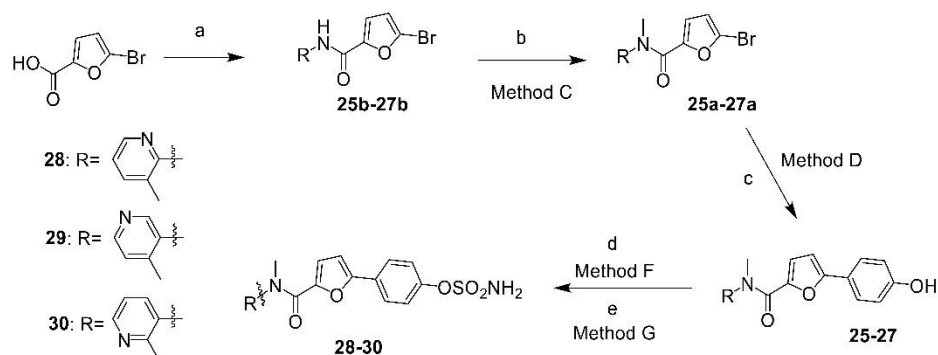
On the one hand, this approach should be advantageous in terms of pharmacokinetics as free phenolic OH-groups often give rise to fast biotransformation and elimination. On the other hand—and more fascinating: it may be anticipated that the thus modified compounds are inhibitors of STS, but probably not of 17β-HSD1 because from earlier studies, the central role of a free phenolic OH-group for strong 17β-HSD1 inhibition is known.^{42,45,46} However, after application to a biological system, the free OH-group should be released again from the sulfamate compound in a time-dependent manner (enzymatically by concomitant STS-inhibition or non-enzymatically), transforming an STS inhibitor into an inhibitor of 17β-HSD1. Thus, the designed aryl sulfamates should be drugs for inhibition of STS and at the same time prodrugs for inhibition of 17β-HSD1. Therefore, the underlying concept may be called a “drug-prodrug approach”. Properly selecting the substitution pattern

of the aromatic ring bearing the sulfamate group should facilitate the discovery of compounds releasing the phenolic product in an appropriate time frame, enabling STS-inhibition before the 17β-HSD1 inhibiting molecular species are formed. As mentioned before, STS is inactivated by transferring the sulfamoyl group from aryl sulfamates to the active site of the enzyme, releasing the phenolic component of the inhibitor. In addition to this, the activation of the prodrug (sulfamate) to the drug (phenol) of 17β-HSD1 inhibition can also occur non-enzymatically through chemical hydrolysis. As known from the literature—and as demonstrated also in this study—there is an irreversible inhibition of STS by aryl sulfamates. Consequently, chemical hydrolysis is another route of forming the drug for 17β-HSD1 inhibition if cleavage by STS is prevented, for example, in the case of advanced irreversible inactivation of the enzyme. Preliminary experiments using compound 13 (Chart 3) as a probe compound suggested the feasibility of this approach (data not shown). The general structure of potential drug-prodrug STS/17β-HSD1 inhibitors (compounds 13–24, 28–30, and 35–38) is given in Chart 2.

Due to its favorable properties, compound B (Chart 1) was chosen as a starting point for inhibitor design. Previous investigations revealed that the presence of both the three rings (rings A, B, and C) and of the methyl group on ring A is important for biological activity (data not shown). Consequently, these structural properties were maintained. In order to find a substitution pattern that leads to strong inhibition of the target enzymes (STS and 17β-HSD1) and at the same time establishes selectivity toward 17β-HSD2, three

Scheme 1. Synthetic Route to Compounds 1–24^a

^a(a) SOCl₂, DMF cat, toluene, reflux 4 h (method A); (b) corresponding amine, Et₃N, DCM, rt, overnight (method B); (c) NaH, DMF, CH₃I, 0 °C to rt, 2 h (method C); (d) corresponding phenyl boronic acid, Cs₂CO₃, Pd(PPh₃)₄, DME/water (1:1), 110 °C, 4 h (method D); (e) (CH₃)₂S·BF₃, DCM, reflux 40 °C, overnight (method E); (f) ClSO₂NCO, Formic acid 99% (1 equiv), 0 °C to rt, 15 min, (sulfamoyl chloride prepared *in situ*) (method F); and (g) DMA, sulfamoyl chloride, 0 °C to rt, overnight (method G).

Scheme 2. Synthetic Route to Compounds 25–30^a

^a(a) Corresponding aminopyridine, DCC, DMAP, rt, overnight; (b) NaH, DMF, CH₃I, 0 °C to rt, 2 h (method C); (c) 4-hydroxyphenyl boronic acid, Cs₂CO₃, Pd(PPh₃)₄, DME/water (1:1), 110 °C, 4 h (method D); (d) ClSO₂NCO, formic acid 99% (1 equiv), 0 °C to rt, 15 min, (sulfamoyl chloride prepared *in situ*) (method F); and (e) DMA, sulfamoyl chloride, 0 °C to rt, overnight (method G).

types of modifications have been applied to compound B (Chart 3).

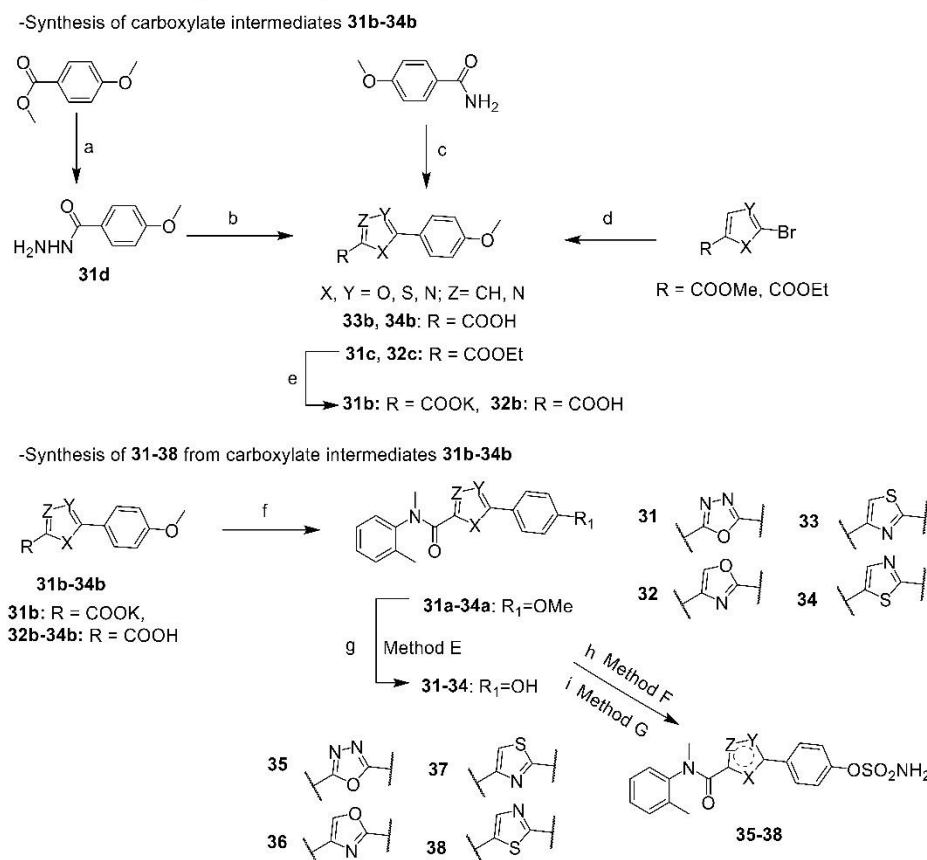
Chemistry. Compounds 1–24 were synthesized according to Scheme 1. 5-Bromofuran-2-carboxamides were obtained from 5-bromofuran-2-carboxylic acid by reaction with SOCl₂ and the corresponding aniline according to methods A and B yielding the intermediates 1b, 9b, 10c, 11b, and 12b. N-methylation for intermediates 9b, 10c, 11b, and 12b was attained by the reaction with methyl iodide according to method C affording intermediates 9a, 10b, 11a, and 12a.

Phenolic derivatives 1–12 were obtained either directly by Suzuki coupling reaction (method D) with the corresponding hydroxyphenylboronic acids or—when methoxyphenylboronic acids were used—by additional ether cleavage (method E) using BF₃·S(CH₃)₂ after the coupling reaction. Sulfamoylation (method G) was achieved by the reaction of phenolic derivatives 1–12 with freshly prepared sulfamoyl chloride (method F) in

dimethylacetamide (DMA) to obtain the final compounds 13–24 (Scheme 1). The starting point for the synthesis of compounds 25–30 (Scheme 2) was amide formation by the reaction of 5-bromofuran-2-carboxylic acid with the corresponding aminopyridine derivatives in the presence of DCC and DMAP to yield the intermediates 25b–27b.

Subsequent Suzuki coupling reaction (method D) with (4-hydroxyphenyl)boronic acid yielded the phenolic derivatives 25–27. The latter were reacted with freshly prepared sulfamoyl chloride in DMA (method G), giving the final compounds 28–30.

The synthesis of compounds 31 and 35 (Scheme 3) started with refluxing of methyl 4-methoxybenzoate with hydrazine hydrate in MeOH for 6 h to afford 4-methoxybenzohydrazide 31d. The latter was stirred with DIPEA, DMAP, ethyl 2-chloro-2-oxoacetate, Et₃N, and TsCl in DCM yielding the 1,3,4-oxadiazole carboxylic acid ethyl ester 31c which was converted

Scheme 3. Synthetic Route to Compounds 31–38^a

^a(a) $\text{NH}_2\text{NH}_2\cdot\text{H}_2\text{O}$, MeOH, reflux, 6 h; (b) ethyl 2-chloro-2-oxoacetate, DIPEA, DMAP, DCM, 0 °C to rt, overnight, then TsCl, NEt_3 , rt, overnight; (c) ethyl bromopyruvate, ethanol reflux, 5 h; (d) 4-methoxyphenyl boronic acid, Cs_2CO_3 , $\text{Pd}(\text{PPh}_3)_4$, toluene/ethanol(1:1), Na_2CO_3 , 120 °C, 4 h; (e) for **31b**: THF/ethanol (2:1), KOH, 0 °C 2h; for **32b**: THF/EtOH (2:1), KOH, 0 °C, 2 h, acidify with 2 M HCl to pH 2; (f) For **31b**: (i) oxalyl chloride, DMF cat., CH_3CN , 0 °C to rt, 2 h. (ii) *N*,2-dimethylaniline, DIPEA, DCM, 0 °C to rt, overnight; for **32b–34b**: (i) SOCl_2 , DMF cat., toluene, reflux 4 h. (ii) *N*,2-dimethylaniline, Et_3N , DCM, rt, overnight; (g) $(\text{CH}_3)_2\text{S}\cdot\text{BF}_3$, DCM, reflux, 40 °C overnight (method E); (h) ClSO_2NCO , formic acid 99% (1 equiv), 0 °C to rt, 15 min, (sulfamoyl chloride prepared *in situ*) (method F); and (i) DMA, sulfamoyl chloride, 0 °C to rt, overnight (method G).

into the corresponding carboxylic acid potassium salt **31b** by hydrolysis using THF/EtOH in an aqueous solution of KOH. The potassium salt was reacted with oxalyl chloride and a catalytic amount of DMF in acetonitrile to give the acyl chloride. Subsequent amide formation using *N*,2-dimethylaniline in the presence of DIPEA yielded the ether derivative **31a**. Ether cleavage (method E) of the latter afforded the phenolic derivative **31** which was reacted with sulfamoyl chloride (method G) to give the sulfamate derivative **35**.

For the synthesis of compounds **32** and **36**, 4-methoxybenzamide and ethyl bromopyruvate were refluxed in ethanol for 5 h to give the ethyl ester of oxazole **32c**, which was then converted into carboxylic acid **32b** (Scheme 3). Subsequent amide formation using methods A and B gave the intermediate **32a**. Demethylation (method E) of the latter afforded the phenolic derivative **32**, which in turn was sulfamoylated to the sulfamate **36**. The thiazoles **33**, **34**, **37**, and **38** were synthesized according to Scheme 3 by Suzuki coupling of 2-bromothiazole-carboxylate esters with (4-methoxyphenyl)boronic acid to give the carboxylic acids **33b** and **34b** which were converted into the

amides **33a** and **34a** according to methods A and B. The phenolic derivatives **33** and **34** were obtained by subsequent ether cleavage (method E). Finally, sulfamoylation of the phenols **33** and **34** gave the sulfamates derivatives **37** and **38**, respectively.

IN VITRO BIOLOGICAL RESULTS AND DISCUSSION

Cellular Inhibition of Human STS. Sulfamates **13–24**, **28–30**, and **35–38** were incubated with intact T47D human breast cancer cells followed by the addition of radiolabeled substrate E1-S⁷⁴. After 24 h incubation, the radiolabeled steroids were isolated and quantified with HPLC coupled to a radio detector, and IC_{50} values are used to express the inhibitory activities, compared to STX-64 (Irosustat) (Table 1). The optimal position of the sulfamate moiety for strong activity toward STS is the para position of ring C; moving it to the meta position decreased the inhibitory activity and the ortho position is unfavorable (compare compounds **13–15**). Furthermore, the presence of an electron-withdrawing group at ring C (compounds **16**, **18–20**) increased STS inhibition, while the

Table 1. Inhibitory Activities of Compounds 13–24, 28–30, and 35–38 toward *h*STS in Cellular Assays and Metabolic Stability in Human and Mouse Hepatic S9 Fractions

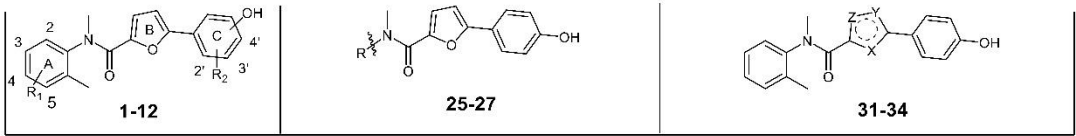
Cpd	-OSO ₂ NH ₂ Position	R ₁	R ₂	Cellular IC ₅₀ (nM) ^a		Cell-free % inhibition at 1 μM ^b	<i>t</i> _{1/2} [min] ^{c,d}		Cl _{int} [μL/min/mg protein] ^e	
				<i>h</i> STS ^e	<i>h</i> STS ^e irreversible		human ^e	mouse ^b	human ^e	mouse ^b
13	4'	H	H	28	31	15	47	25	15	31
14	3'	H	H	690	nd	nd	nd	nd	nd	nd
15	2'	H	H	ni	nd	nd	nd	nd	nd	nd
16	4'	H	3'-Cl	25	27	25	48	31	15	24
17	4'	H	3'-CH ₃	570	nd	nd	nd	nd	nd	nd
18	4'	H	3'-F	17	17	18	43	6.1	16	140
19	4'	H	2'-Cl	27	29	13	39	20	18	39
20	4'	H	2'-F	12	16	19	51	23	14	38
21	4'	2-F	H	150	nd	nd	nd	nd	nd	nd
22	4'	3-F	H	40	nd	ni	34	3.9	21	180
23	4'	4-F	H	14	15	13	44	4.6	16	150
24	4'	5-F	H	27	25	nd	24	4.8	29	150
28			R	1100	nd	nd	nd	nd	nd	nd
29			R	820	nd	nd	nd	nd	nd	nd
30			R	270	nd	nd	nd	nd	nd	nd
35			R	1100	nd	nd	nd	nd	nd	nd
36			R	60	68	nd	180	47	3.9	15
37			R	63	60	17	50	15	14	46
38			R	130	nd	nd	nd	nd	nd	nd
7-Hydroxy-coumarin ⁱ				nd	nd	nd	5.0	3.0	140	280
STX-64 (Irosustat)				2.7	2.6	nd	nd	nd	nd	nd

^aMean value of at least two independent experiments each conducted in triplicates using intact T47D cells, standard deviation less than 15%.

^bMean value of at least two independent experiments each conducted in duplicates, standard deviation less than 20%. ^cMean value of three independent experiments, standard deviation less than 15%. ^d*t*_{1/2}: half-life. ^eSubstrate [³H]-E1S + E1S [5 nM]. ^fHuman placenta, cytosolic fraction, substrate [³H]-E1 + E1 [500 nM], and cofactor NADH [0.5 mM]. ^gHuman liver S9 fraction. ^hMouse liver S9 fraction. ⁱReference compound for the metabolic stability assay; ni: no inhibition (<10% inhibition at 1 μM); and nd: not determined.

methyl group as an electron-donor decreased it (compound 17). This is in agreement with the hypothesis for how aryl sulfamates inactivate STS by transferring the sulfamoyl group to the active site of the enzyme, releasing the phenolic part of the inhibitor.^{25,101,102} Indeed, the inactivation of STS is more facilitated, as the sulfamate group is more easily transferred to the STS (sulfamoyl transfer potential). Enhancement of the STS inhibitory activity of the halogenated sulfamates can thus be attributed to the increased leaving group ability of the phenolate

moiety by electronic effects.^{78,103–105} The lower potency observed for the compound methylated 17 is consistent with previous observations which showed that the presence of alkyl substituents on the ring bearing the sulfamate group lead to a decrease of STS inhibition.^{104,106,107} A fluoro-substitution of ring A in positions 3, 4, or 5 (compounds 22–24) kept STS inhibitory activity in the low nanomolar range, while a fluorine atom in position 2 (compound 21) was unfavorable. A 10- to 40-fold reduction in STS inhibitory activity compared to compound

Table 2. Inhibitory Activities of Compounds 1–12, 25–27, and 31–34 toward *h*17 β -HSD1 and 2 in Cellular and Cell-Free Assays and the Corresponding Selectivity Factors


Cpd	-OH Position	R ₁	R ₂	Cellular IC ₅₀ (nM) ^a		Cell-free IC ₅₀ (nM) ^a		SF ^e
				<i>h</i> 17 β -HSD1 ^b	<i>h</i> 17 β -HSD1 ^c	<i>h</i> 17 β -HSD1 ^c	<i>h</i> 17 β -HSD2 ^d	
1	4'	H	H	21	55	2800	51	
2	3'	H	H	29	150	2800	19	
3	2'	H	H	1900	1900	>10000	>5.2	
4	4'	H	3'-Cl	5.2	2.7	200	74	
5	4'	H	3'-CH ₃	8.6	8.1	1200	150	
6	4'	H	3'-F	10.0	11	930	85	
7	4'	II	2'-Cl	14	32	430	13	
8	4'	II	2'-F	10.0	22	930	42	
9	4'	2-F	H	120	310	3200	10	
10	4'	3-F	H	12	41	2200	54	
11	4'	4-F	H	7.6	23	1700	74	
12	4'	5-F	II	50	170	3900	23	
25				1100	3300	>10000	>3	
26				64	260	>20000	>77	
27				43	160	>30000	>190	
31				320	490	6200	13	
32				110	250	>10000	>40	
33				12	34	3900	115	
34				340	600	4500	7.5	

^aMean value of at least two independent experiments each conducted in duplicates, standard deviation less than 15%. ^bUsing intact T47D cells, substrate [³H]-E1 + E1 [50 nM]. ^cHuman placenta, cytosolic fraction, substrate [H]-E1 + E1 [500 nM], and cofactor NADH [0.5 mM]. ^dHuman placenta, microsomal fraction, substrate [³H]-E2 + E2 [500 nM], and cofactor NAD⁺ [1.5 mM]. ^eSF (selectivity factor): IC₅₀(17 β -HSD2)/IC₅₀(17 β -HSD1).

13 was observed when the phenyl moiety of ring A was replaced by pyridine (compounds 28–30). Replacement of the furan ring (B) of 13 with oxazole (compound 36) or thiazole (compounds 37 and 38) resulted in a low to moderate decrease in STS inhibition, while oxadiazole (compound 35) proved to be an even less suitable substitute for the furan ring. As a conclusion, the furan derivatives 13, 16, 18–20, and 22–24, the oxazole 36, and the 2,4-disubstituted thiazole 37 demonstrated potent inhibition of STS with nanomolar IC₅₀ values (albeit not quite reaching the inhibitory potency of the reference compound Irostatat), suggesting high activity and good cell penetration.

Irreversible Inhibition of Human STS. An important part of the present investigation was to obtain further information about the nature of the STS inhibition induced by sulfamate derivatives. T47D cells were pretreated with the most potent sulfamates (compounds 13, 16, 18–20, 23, 24, 36, and 37) and the reference STX64, respectively. After thorough washing with phosphate-buffered saline (PBS) in order to remove the compounds, the radiolabeled substrate E1-S was added to the cells. After an incubation time of 24 h, STS activity was evaluated. The compounds effectively inhibited STS, and the obtained IC₅₀ values were close to those obtained from the

standard intracellular STS inhibition assay (Table 1), implying an irreversible mode of STS inhibition. These findings are in agreement with an irreversible inhibition of the STS enzyme as shown for other sulfamate-containing STS inhibitors, for example, for STX64.¹⁰⁷

Cellular and Cell-Free Inhibition of Human 17 β -HSD1.

The immediate product released by a sulfamate-based STS inhibitor after STS inactivation and/or hydrolytic cleavage is its corresponding phenol.^{78,104,105,108} Therefore, the phenols 1–12, 25–27, and 31–34 were anticipated to be released from their sulfamate congeners and act as 17 β -HSD1 inhibitors because of the formation of the important pharmacophore for 17 β -HSD1 inhibition, the phenolic moiety. The 17 β -HSD1 cellular assay was carried out in the same manner as the STS assay, except that tritiated E1 was used as the substrate, and the incubation time was reduced to 40 min. In the case of the cell-free 17 β -HSD1 assay, the human placental enzyme was purified following a previously described protocol¹⁰⁹ and incubated with tritiated E1, NADH, and inhibitor for 10 min at 37 °C. HPLC was used to separate the steroidal substrate and product. The importance of a phenolic hydroxyl group for 17 β -HSD1 inhibition was shown in previous studies.^{45,110} In accordance to this, all STS inhibitors of the present study which have been tested for 17 β -HSD1 inhibition in the cell-free assay (compounds 13, 16, 18–20, 22, and 23—all of them lacking a free phenolic OH group) only showed marginal activities (Table 1), which can be reasonably attributed to partial hydrolysis of the inactive sulfamates to their corresponding highly active phenols during incubation. Strong 17 β -HSD1 inhibition, however, was exerted by the phenols 1–12, 25–27, and 31–34 (Table 2). All phenolic compounds which were expected to be released from the hydrolysis of the most interesting sulfamate compounds showed good to potent inhibition of 17 β -HSD1. The best position of the hydroxyl group in the ring C is the para position (compound 1). For drug design, this is advantageous because the position coincides with the optimal position of the sulfamate group for STS inhibition (Table 1). Interestingly, the presence of both electronegative atoms (F and Cl) or an electron-donating group (CH₃) increased the inhibitory activity (see compounds 4–8). Fluorination of ring A in positions 3 and 4 (compounds 10 and 11) led to an increase in activity compared to the unsubstituted furan 1 in both cellular and cell-free assays. The 2,4-disubstituted thiazole 33 showed stronger inhibitory activity compared to the furan 1 while inhibitory potency decreased when furan was replaced with oxadiazole (31), oxazole (32), and 2,5-disubstituted thiazole (34).

Selectivity: Cell-Free Inhibition of Human 17 β -HSD2 and Affinities to the Estrogen Receptor α . Inhibition of human 17 β -HSD2 was determined under cell-free conditions using tritiated E2 and NAD⁺ as a co-substrate. IC₅₀ values for phenolic derivatives 1–12, 25–27, and 31–34 and selectivity factors (SF) [SF = IC₅₀(17 β -HSD2)/IC₅₀(17 β -HSD1)] are shown in Table 2. Regarding the different phenyl ring (C)-modified compounds, compounds with substituents in position 3 (ortho to OH) are more selective over 17 β -HSD2 than compounds with substituents in position 2 (meta to OH), compared to the unsubstituted compound 1 (see compounds 4–6). Fluorination of ring A in positions 3 and 4 (compounds 10 and 11) maintained or increased selectivity over 17 β -HSD2, while in positions 2 and 5 (compounds 9 and 12) selectivity decreased compared to the unsubstituted compound 1. Pyridine derivatives 26 and 27 showed high selectivity. The nature of the

five-membered middle ring also affected selectivity: the 2,4-disubstituted thiazole (33) showed a strong increase in selectivity (compared to compound 1) and oxazole (32) gave the same selectivity factor as 1, while substitution of furan with oxadiazole (31) and 2,5-disubstituted thiazole (34) provided compounds with decreased selectivity over 17 β -HSD2.

Interaction with ER is another critical parameter for the potential applicability of the compounds as drugs. Agonistic effects will of course conflict with the therapeutic approach of STS/17 β -HSD1 inhibition, while antagonistic effects will lead to undesired systemic antiestrogenic or SERM like-effects. Consequently, an ER affinity as low as possible should be aimed at. The relative binding affinities (RBA) of the 10 most active compounds (sulfamates 13, 16, 19, 23, and 37 and their corresponding phenols 1, 4, 7, 11, and 33) were determined using the fluorescence-based PolarScreen ER Alpha Competitor Assay, Green (Thermo Fisher Scientific). RBA of E2 was set to 100%. Most of the compounds showed low RBA values in the range of 0.28–1.5% (Table 3). Although the values are rather low, they still reveal some residual receptor affinities which might be relevant. Further compound optimizations will address this issue.

Table 3. Binding Affinities of Selected Compounds for the Human Estrogen Receptor α

Cpd	RBA (%) ^a
	ER α ^b
1	0.51
4	1.05
7	4.98
11	0.45
33	0.73
13	0.55
16	0.28
19	1.47
23	1.51
37	0.38

^aRBA (relative binding affinity), mean value of at least two independent experiments, standard deviations less than 20%.

^bIncubation of human recombinant receptor ER α , with 10 μ M FITC-E2 and inhibitor for 1 h at 25 °C.

In Vitro Metabolic Stability and Cytotoxicity. The most interesting sulfamates (13, 16, 18–20, 22–24, 36, and 37) were tested for their metabolic stability using human and mouse hepatic S9 fractions. The half-lives and intrinsic body clearances are shown in Table 1. Oxazole 36 proved to be the most stable compound in both human and mouse hepatic S9 fractions. The furan containing compounds 13, 16, 18–20, and 22–24 showed good metabolic stability in human hepatic S9 fraction and low intrinsic clearance Clint (<30 μ L/min/mg protein). Concerning mouse liver microsomes, compounds (13, 16, 19, and 20) showed moderate half-lives, while compounds (18 and 22–24) showed low half-lives and high intrinsic clearance which indicate low metabolic stability. In all cases, the newly synthesized compounds have higher metabolic stability than the previously discovered thiophene compounds such as compound A (Chart 1).

The most promising sulfamates 13, 16, 19, and 37 as well as their conjugate phenols 1, 4, 7, and 33 were analyzed for potential cytotoxicity in an MTT assay using HEK-293 cells. At a concentration of 20 μ M, cell growth was inhibited by 11.7%

(13) to 30.0% (19), indicating a low cytotoxicity. Only for compounds 4 and 16, slightly higher values of approximately 55% were detected. The assay conditions and a table with the data of all eight compounds are given in the Supporting Information (page S36, Table S1).

Validation of the Drug-Prodrug Approach. Based upon its beneficial biological properties, compound 13 was considered a suitable candidate for the validation of the drug-prodrug approach. For this purpose, the development of a new assay was required, which allowed to monitor the transformation of the STS inhibitor 13 (prodrug for 17 β -HSD1 inhibition) to the 17 β -HSD1 inhibitor 1 both in buffer and in a cell-based setup quantitatively and in a time-dependent manner. In parallel, the assay should facilitate the quantification of the increase in 17 β -HSD1 inhibition. Thus, a possible correlation of phenol formation and 17 β -HSD1 inhibition could be derived. Compound 13 was incubated at 37 °C either in phosphate buffer or in the presence of T47D cells in DMEM. These two assay variants were established to be able to compare the results with those of the respective 17 β -HSD1 inhibition assays described above. At different time points, samples were taken and analyzed to quantify the percentage of conversion of compound 13 to its phenolic counterpart 1 using LC–MS/MS. Simultaneously, the percentage of 17 β -HSD1 inhibition exerted by the released drug at the same time points was evaluated. The starting concentration of compound 13 in the assay variant used (cell-free or cellular) was chosen based on the respective IC₅₀; see the Experimental Section for more details.

The data showed that compound 13 remained within detection limits after 24 h of incubation and that it was more stable in phosphate buffer than in T47D/DMEM (40% vs 94% conversion after 24 h). In the cell-free setup (phosphate buffer), the starting concentration of 13 was set to 250 nM. The experiment revealed a clear correlation between the formation of compound 1 and 17 β -HSD1 inhibition (Figure 3). Moreover, a

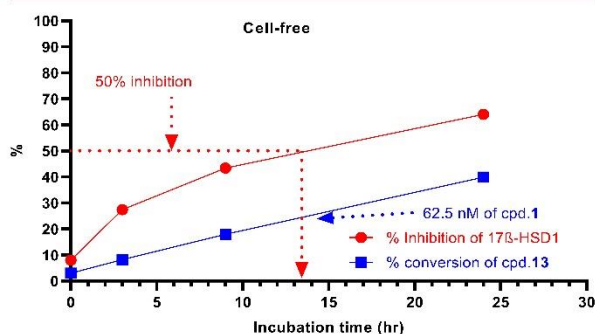


Figure 3. Plots of percentage conversion (blue) of 13 to 1 and percentage inhibition of 17 β -HSD1 (red) at a starting concentration of 13 of 250 nM in a cell-free system. Each data point in the figure represents the mean value of two independent experiments each conducted in duplicates, standard deviation less than 20%.

closer data analysis showed that when 50% inhibition of 17 β -HSD1 was reached (after 13.5 h), 25% of 13 had been converted into 1, which corresponds to a concentration of 62.5 nM of 1. This is in very good agreement to the previously determined cell-free IC₅₀ value for 17 β -HSD1 inhibition of 1 (55 nM).

In the cellular setup, compound 13 was applied in a starting concentration of 50 nM in the presence of T47D cells in DMEM. After 6.5 h, 50% inhibition of 17 β -HSD1 was achieved

when 47% of 13 had been transformed to 1 which is equivalent to a concentration of 23.6 nM of 1 (Figure 4). Again, this value

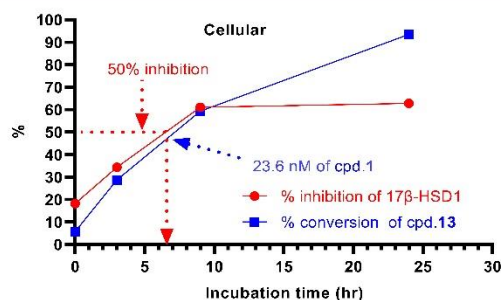


Figure 4. Plots of percentage conversion of 13 into 1 and the percentage inhibition of 17 β -HSD1 at a starting concentration of 50 nM of 13 in a cellular system. Each point in the figure represents the mean value of two independent experiments each conducted in duplicates, standard deviation less than 20%.

matches well the previously determined IC₅₀ for 17 β -HSD1 inhibition exerted by 1 in the cellular assay (21 nM). It is worth mentioning that even after 24 h of incubation, 17 β -HSD1 inhibition does not increase much above 60%. This can be attributed to the fact that 13 was applied in a low starting concentration of 50 nM, which is consequently the maximum concentration of 1 after complete conversion of 13. A full inhibition was achieved at higher starting concentrations of 13 (see Supporting Information, page S34).

In summary, the experiments demonstrate—both in the cell-free and in the cellular setup—that the 17 β -HSD1 inhibitor 1 is released time-dependently from the sulfamate prodrug 13 and that 17 β -HSD1 inhibition is exerted by the released phenol-based drug 1 exclusively. Thus, the envisaged drug-prodrug concept was successfully implemented.

In addition to compound 13, three of the most active sulfamates (16, 19, and 37) were subjected to the assay. The results are provided in the Supporting Information (page S29). In all cases, the validity of the drug-prodrug concept was confirmed. Moreover, the data indicate that the rate of conversion from sulfamate to phenol is delicately dependent on additional substituents present at the aryl sulfamate moiety.

CONCLUSIONS

Inhibition of STS and 17 β -HSD1 with dual acting drugs is a promising strategy for the treatment of endometriosis and other estrogen-dependent diseases. Pursuing the novel idea to design compounds which are drugs for STS inhibition and prodrugs for 17 β -HSD1 inhibition was facilitated by the fact that in-house 17 β -HSD1 inhibitors possessed the structural requirements to be modified for the implementation of this “drug-prodrug approach”. Nineteen new aryl sulfamates have been synthesized. Many of them were highly potent STS inhibitors, and their respective phenols showed strong and selective inhibition of 17 β -HSD1. Due to their beneficial biological properties, among them good metabolic stabilities, 4 of the 19 aryl sulfamates (compounds 13, 16, 19, and 37) were selected for the successful validation of the novel approach. To the best of our knowledge, this is the first time that compounds have been intentionally and successfully designed as drugs for one target and prodrugs for a second target, both of which are involved in the pathogenesis of the same disease. Highly interesting, though not unexpected,

was the finding that the rate of transformation from aryl sulfamate to phenol was strongly dependent on the substitution at the aryl moiety bearing the sulfamate group. This fact opens up the exciting possibility to modulate the transformation rate according to the demands—which may differ, for instance, depending on the application route of the compound—by selecting an appropriate substitution.

EXPERIMENTAL SECTION

Chemical Methods. Chemical names follow IUPAC nomenclature [PerkinElmer ChemDraw Professional 16.0.1.4 (77)]. Starting materials were purchased from Acros Organics, Alfa Aesar, Combi-Blocks, Fluorochem, and Sigma-Aldrich. Column chromatography was performed on silica gel (0.04–0.063 mm, Macherey–Nagel) and reaction progress was monitored by TLC on aluminum sheets (Silicagel 60 F254, Merck). Visualization was accomplished with UV light at 254 nm. ^1H and ^{13}C NMR spectra were measured on a Bruker-500 (at 500 and 126 MHz, respectively) or Bruker-300 (at 300 MHz). Chemical shifts are reported in δ (parts per million: ppm) using residual peaks of the deuterated solvents as an internal standard: $(\text{CD}_3)_2\text{SO}$ (DMSO- d_6): 2.50 ppm (^1H NMR), 39.52 ppm (^{13}C NMR); $(\text{CD}_3)_2\text{CO}$ (acetone- d_6): 2.05 ppm (^1H NMR), 29.84, and 206.26 ppm (^{13}C NMR); CDCl_3 (chloroform- d): 2.05 ppm (^1H NMR), 29.84, and 206.26 ppm (^{13}C NMR). Signals are described as s, d, t, dd, ddd, dt, td, and m for singlet, doublet, triplet, doublet of doublets, doublet of doublets, doublet of triplets, triplets of doublets, and multiplet, respectively. All coupling constants (J) are given in Hertz (Hz). All tested compounds have $\geq 95\%$ chemical purity as evaluated by LC/MS. The Surveyor-LC-system consisted of a pump, an autosampler, and a PDA detector. Mass spectrometry was performed by a TSQ Quantum (ThermoFisher, Dreieich, Germany). The triple quadrupole mass spectrometer was equipped with an electrospray interface (ESI). The system was operated by the standard software Xcalibur. A RP C18 NUCLEODUR 100–5 (3 mm) column (Macherey–Nagel GmbH, Düren, Germany) was used as a stationary phase. All solvents were of HPLC grade. In a gradient run, the percentage of acetonitrile (containing 0.1% trifluoroacetic acid) was increased from an initial concentration of 30% at 0 min to 100% at 12 min and kept at 100% for 3 min. The injection volume was 25 μL and the flow rate was set to 700 $\mu\text{L}/\text{min}$. MS analysis was carried out at a needle voltage of 3000 V and a capillary temperature of 350 $^\circ\text{C}$. Mass spectra were recorded in the positive mode from 100 to 1000 m/z , and UV spectra were recorded at the wavelength of 254 nm. The melting points were measured using Stuart melting point apparatus SMP3.

Method A, General Procedure for Acyl Chloride Formation.^{111,112} A mixture of 5-bromofuran-2-carboxylic acid (2 mmol), thionyl chloride (4 mmol), and DMF (5 drops) in toluene (10 mL) was refluxed at 110 $^\circ\text{C}$ for 4 h. The reaction mixture was cooled to room temperature; the solvent and the excess of thionyl chloride were removed under reduced pressure. The crude product was used in the next step without any further purification.

Method B, General Procedure for Amide Formation.^{111,112} The corresponding aniline (2 mmol) and Et_3N (2 mmol) in DCM (10 mL) were added at 0 $^\circ\text{C}$ to the acyl chloride. After 30 min at 0 $^\circ\text{C}$, the ice bath was removed and the solution was warmed up and stirred at room temperature overnight. The reaction mixture was extracted twice with ethyl acetate (2×15 mL); the organic layer was dried over MgSO_4 , filtered, and the solution was concentrated under reduced pressure. The residue was purified by silica gel column chromatography.

Method C, General Procedure for the *N*-Methylation.¹¹³ A mixture of furan-2-carboxamide (1 equiv) and NaH (2 equiv) in DMF (20 mL) was stirred for 30 min at room temperature, and then, iodomethane (1 equiv) was added. After 2 h, the reaction mixture was poured into water. The resulting precipitate was collected, washed with water, dried, and purified by silica gel column chromatography.

Method D, General Procedure for Suzuki Coupling.¹¹⁰ Aryl bromide (1 equiv), boronic acid derivative (1.5 equiv), cesium carbonate (4 equiv) or sodium carbonate (5 equiv), and tetrakis(triphenylphosphine) palladium (0.05 equiv) were added to an oxygen-

free DME/water (1:1) or toluene/ethanol (1:1) and refluxed under a nitrogen atmosphere for 4 h. The reaction mixture was cooled to room temperature. The aqueous layer was extracted with ethyl acetate (acidify with 2 M HCl to pH 2 if the product is acid before extraction). The organic layers were combined, dried over MgSO_4 , and concentrated to dryness under reduced pressure. The product was purified by column chromatography.

Method E, General Procedure for Ether Cleavage.¹¹² To a solution of methoxy heteroaryl derivative (1 equiv) in DCM (30 mL) at 0 $^\circ\text{C}$ boron trifluoride methyl sulfide complex (10 equiv per methoxy group) was added. The reaction mixture was warmed up to room temperature and stirred overnight. Methanol was added to quench the reaction at 0 $^\circ\text{C}$. After warming up to room temperature for 1 h, the solvent was carefully removed under reduced pressure (temperature of bath was 25 $^\circ\text{C}$). Cold water was added to the residue and the aqueous layer was extracted with DCM (3×15 mL). The organic layer was washed once with water, dried over MgSO_4 , filtered, and evaporated to dryness under reduced pressure. The product was purified by column chromatography.

Method F, Preparation of Sulfamoyl Chloride.⁷⁴ A fresh solution was prepared for each reaction. Chlorosulfonyl isocyanate (1 equiv) was cooled to 0 $^\circ\text{C}$. Then, formic acid 99% (1 equiv) was then added dropwise to the isocyanate slowly over 10 min. Slow, steady evolution of CO_2 was observed; eventually a white solid was formed. After 15 min, the ice bath was removed and the reaction mixture was warmed to room temperature and then used in the next reaction without further workup.

Method G, General Procedure for Sulfamoylation.⁷⁴ A solution of phenol derivative (1 equiv) in DMA was cooled to 0 $^\circ\text{C}$. A freshly prepared sulfamoyl chloride (5 equiv) was subsequently added over 5 min and the reaction mixture was warmed to room temperature and stirred overnight. The reaction was quenched with water, and then, the aqueous layer was extracted with ethyl acetate. The organic layers were combined, dried over MgSO_4 , and concentrated to dryness under reduced pressure. The product was purified by column chromatography.

4-[5-[Methyl(*o*-tolyl)carbamoyl]furan-2-yl]phenyl Sulfamate (13). The title compound was prepared according to method G by the reaction of **1** (0.2 g, 0.65 mmol, 1 equiv) and sulfamoyl chloride (0.375 g, 3.25 mmol, 5 equiv) in DMA (5 mL). The product was purified by column chromatography (dichloromethane/methanol 98:2) to give 0.175 g (0.45 mmol/70%) of the analytically pure compound (purity: 98.22%). $\text{C}_{19}\text{H}_{18}\text{N}_2\text{O}_5\text{S}$; MW 386.42; mp 194–196 $^\circ\text{C}$; ^1H NMR (500 MHz, DMSO- d_6): δ 8.05 (s, 2H), 7.43–7.36 (m, 2H), 7.36–7.29 (m, 4H), 7.27–7.21 (m, 2H), 6.91 (d, $J = 3.6$ Hz, 1H), 6.46 (d, $J = 3.6$ Hz, 1H), 3.25 (s, 3H), 2.17 (s, 3H); ^{13}C NMR (126 MHz, DMSO- d_6): δ 157.79, 153.39, 150.00, 146.80, 142.70, 135.27, 131.17, 128.29, 128.12, 127.45, 127.41, 125.31, 122.58, 118.37, 107.45, 36.98, 16.97; MS (ESI): 387.02 ($M + H$) $^+$.

3-[5-[Methyl(*o*-tolyl)carbamoyl]furan-2-yl]phenyl Sulfamate (14). The title compound was prepared according to method G by the reaction of **2** (0.2 g, 0.65 mmol, 1 equiv) and sulfamoyl chloride (0.375 g, 3.25 mmol, 5 equiv) in DMA (5 mL). The product was purified by column chromatography (petroleum ether/ethyl acetate 1:1) to give 0.175 g (0.452 mmol/70%) of the analytically pure compound (purity: 96.37%). $\text{C}_{19}\text{H}_{18}\text{N}_2\text{O}_5\text{S}$; MW 386.42; mp 191–193 $^\circ\text{C}$; ^1H NMR (500 MHz, DMSO- d_6): δ 8.05 (s, 2H), 7.47–7.38 (m, 2H), 7.40–7.31 (m, 1H), 7.35–7.25 (m, 2H), 7.30–7.23 (m, 1H), 7.24–7.17 (m, 2H), 6.95 (d, $J = 3.6$ Hz, 1H), 6.40 (d, $J = 3.7$ Hz, 1H), 3.26 (s, 3H), 2.17 (s, 3H); ^{13}C NMR (126 MHz, DMSO- d_6): δ 157.77, 153.01, 150.57, 146.87, 142.52, 135.21, 131.20, 130.65, 130.25, 128.43, 128.05, 127.43, 122.08, 121.98, 118.14, 117.66, 108.04, 36.90, 16.92; MS (ESI): 387.08 ($M + H$) $^+$.

2-[5-[Methyl(*o*-tolyl)carbamoyl]furan-2-yl]phenyl Sulfamate (15). The title compound was prepared according to method G by the reaction of **3** (0.157 g, 0.51 mmol, 1 equiv) and sulfamoyl chloride (0.295 g, 2.25 mmol, 5 equiv) in DMA (5 mL). The product was purified by column chromatography (petroleum ether/ethyl acetate 2:1) to give 0.148 g (0.38 mmol/75%) of the analytically pure compound (purity: 96.32%). $\text{C}_{19}\text{H}_{18}\text{N}_2\text{O}_5\text{S}$; MW 386.42; mp 188–190

$^{\circ}\text{C}$; ^1H NMR (500 MHz, DMSO- d_6): δ 8.32 (s, 2H), 7.46–7.42 (m, 2H), 7.41–7.30 (m, 4H), 7.25 (td, J = 7.6, 1.3 Hz, 1H), 7.02 (dd, J = 8.0, 1.7 Hz, 1H), 6.90 (d, J = 3.6 Hz, 1H), 6.34 (d, J = 3.6 Hz, 1H), 3.27 (s, 3H), 2.17 (s, 3H); ^{13}C NMR (126 MHz, DMSO- d_6): δ 157.79, 149.69, 146.24, 146.12, 142.52, 135.26, 131.28, 129.53, 128.42, 128.16, 127.56, 126.43, 126.29, 122.05, 121.90, 118.24, 111.57, 37.04, 16.95; MS (ESI): 387.00 (M + H) $^+$.

2-Chloro-4-[5-[Methyl(o-tolyl)carbamoyl]furan-2-yl]phenyl Sulfamate (16). The title compound was prepared according to method G by the reaction of **4** (0.130 g, 0.38 mmol, 1 equiv) and sulfamoyl chloride (0.219 g, 1.9 mmol, 5 equiv) in DMA (5 mL). The product was purified by column chromatography (petroleum ether/ethyl acetate 1:1) to give 0.092 g (0.21 mmol/57%) of the analytically pure compound (purity: 99%). $\text{C}_{19}\text{H}_{17}\text{ClN}_2\text{O}_5\text{S}$; MW 420.86; mp 176–178 $^{\circ}\text{C}$; ^1H NMR (500 MHz, DMSO- d_6): δ 8.32 (s, 2H), 7.45–7.39 (m, 2H), 7.40–7.30 (m, 4H), 7.224 (d, J = 2.1 Hz, 1H), 7.04 (d, J = 3.6 Hz, 1H), 6.68 (d, J = 3.6 Hz, 1H), 3.26 (s, 3H), 2.16 (s, 3H); ^{13}C NMR (126 MHz, DMSO- d_6): δ 157.57, 151.88, 151.87, 147.33, 145.69, 142.68, 135.22, 131.12, 128.44, 128.08, 127.41, 127.17, 125.24, 124.15, 123.69, 118.67, 108.57, 37.05, 16.98; MS (ESI): 421.00, 423.01 (M + H) $^+$.

2-Fluoro-4-[5-[Methyl(o-tolyl)carbamoyl]furan-2-yl]phenyl Sulfamate (17). The title compound was prepared according to method G by the reaction of **5** (0.130 g, 0.39 mmol, 1 equiv) and sulfamoyl chloride (0.230 g, 1.9 mmol, 5 equiv) in DMA (5 mL). The product was purified by column chromatography (dichloromethane/methanol 99:1) to give 0.1 g (0.24 mmol/62%) of the analytically pure compound (purity: 99.99%). $\text{C}_{19}\text{H}_{17}\text{FN}_2\text{O}_5\text{S}$; MW 404.41; mp 188–190 $^{\circ}\text{C}$; ^1H NMR (500 MHz, DMSO- d_6): δ 8.29 (s, 2H), 7.43–7.37 (m, 3H), 7.36–7.30 (m, 2H), 7.21–7.11 (m, 2H), 7.02 (d, J = 3.6 Hz, 1H), 6.60 (d, J = 3.6 Hz, 1H), 3.26 (s, 3H), 2.16 (s, 3H); ^{13}C NMR (126 MHz, DMSO- d_6): δ 157.62, 154.42 (d, J = 249.8 Hz), 152.18, 147.27, 142.70, 136.97 (d, J = 12.6 Hz), 135.26, 131.15, 128.86 (d, J = 7.3 Hz), 128.23 (d, J = 27.1 Hz), 127.45, 125.24, 120.29 (d, J = 3.5 Hz), 118.56, 112.29 (d, J = 21.4 Hz), 108.61, 105.81, 37.05, 16.98; MS (ESI): 404.90 (M + H) $^+$.

2-Methyl-4-[5-[Methyl(o-tolyl)carbamoyl]furan-2-yl]phenyl Sulfamate (18). The title compound was prepared according to method G by the reaction of **6** (0.196 g, 0.60 mmol, 1 equiv) and sulfamoyl chloride (0.35 g, 3.04 mmol, 5 equiv) in DMA (5 mL). The product was purified by column chromatography (dichloromethane/methanol 98:2) to give 0.180 g (0.44 mmol/75%) of the analytically pure compound (purity: 99.99%). $\text{C}_{20}\text{H}_{20}\text{N}_2\text{O}_5\text{S}$; MW 400.45; mp 190–192 $^{\circ}\text{C}$; ^1H NMR (500 MHz, DMSO- d_6): δ 8.08 (s, 2H), 7.45–7.28 (m, 4H), 7.24 (t, J = 1.4 Hz, 2H), 7.03 (s, 1H), 6.89 (d, J = 3.6 Hz, 1H), 6.60 (d, J = 3.6 Hz, 1H), 3.25 (s, 3H), 2.26 (s, 3H), 2.16 (s, 3H); ^{13}C NMR (126 MHz, DMSO- d_6): δ 157.77, 153.55, 148.62, 146.81, 142.82, 135.26, 131.77, 131.18, 128.31, 128.10, 127.45, 127.24, 126.44, 122.80, 122.58, 118.60, 107.30, 37.08, 17.01, 16.04; MS (ESI): 401.05 (M + H) $^+$.

3-Chloro-4-[5-[Methyl(o-tolyl)carbamoyl]furan-2-yl]phenyl Sulfamate (19). The title compound was prepared according to method G by the reaction of **7** (0.174 g, 0.509 mmol, 1 equiv) and sulfamoyl chloride (0.294 g, 2.54 mmol, 5 equiv) in DMA (5 mL). The product was purified by column chromatography (petroleum ether/ethyl acetate 2:1) to give 0.185 g (0.43 mmol/86%) of the analytically pure compound (purity: 99.99%). $\text{C}_{19}\text{H}_{17}\text{ClN}_2\text{O}_5\text{S}$; MW 420.86; mp 193–195 $^{\circ}\text{C}$; ^1H NMR (500 MHz, DMSO- d_6): δ 8.20 (s, 2H), 7.45–7.36 (m, 3H), 7.35–7.29 (m, 2H), 7.23 (dd, J = 8.8, 2.4 Hz, 1H), 7.07 (d, J = 3.7 Hz, 1H), 7.00 (d, J = 8.8 Hz, 1H), 6.47 (d, J = 3.7 Hz, 1H), 3.26 (s, 3H), 2.17 (s, 3H); ^{13}C NMR (126 MHz, DMSO- d_6): δ 157.64, 149.79, 149.54, 146.84, 142.55, 135.24, 131.28, 129.87, 128.82, 128.38, 128.14, 127.54, 125.61, 124.17, 121.33, 117.94, 112.19, 37.04, 16.97; MS (ESI): 421.00, 422.99 (M + H) $^+$.

3-Fluoro-4-[5-[Methyl(o-tolyl)carbamoyl]furan-2-yl]phenyl Sulfamate (20). The title compound was prepared according to method G by the reaction of **8** (0.2 g, 0.614 mmol, 1 equiv) and sulfamoyl chloride (0.355 g, 3.07 mmol, 5 equiv) in DMA (5 mL). The product was purified by column chromatography (petroleum ether/ethyl acetate 2:1) to give 0.182 g (0.45 mmol/73%) of the analytically

pure compound (purity: 99.99%). $\text{C}_{19}\text{H}_{17}\text{FN}_2\text{O}_5\text{S}$; MW 404.41; mp 199–201 $^{\circ}\text{C}$; ^1H NMR (500 MHz, DMSO- d_6): δ 8.19 (s, 2H), 7.45–7.39 (m, 1H), 7.42–7.35 (m, 1H), 7.37–7.29 (m, 2H), 7.25 (dd, J = 11.8, 2.3 Hz, 1H), 7.12 (dd, J = 8.7, 2.3 Hz, 1H), 7.01 (t, J = 8.7 Hz, 1H), 6.76 (t, J = 3.7 Hz, 1H), 6.47 (d, J = 3.6 Hz, 1H), 3.26 (s, 3H), 2.17 (s, 3H); ^{13}C NMR (126 MHz, DMSO- d_6): δ 158.28 (d, J = 220.3 Hz), 156.94, 150.35 (d, J = 11.2 Hz), 147.49 (d, J = 3.0 Hz), 146.78, 142.54, 135.25, 131.21, 128.25 (d, J = 31.2 Hz), 127.49, 126.52 (d, J = 4.0 Hz), 118.62 (d, J = 3.3 Hz), 118.26, 115.48 (d, J = 11.8 Hz), 111.32, 111.23, 110.71 (d, J = 24.2 Hz), 36.99, 16.94; MS (ESI): 404.90 (M + H) $^+$.

4-[5-[(2-Fluoro-6-methylphenyl)(methyl)carbamoyl]furan-2-yl]phenyl Sulfamate (21). The title compound was prepared according to method G by the reaction of **9** (0.085 g, 0.261 mmol, 1 equiv) and sulfamoyl chloride (0.15 g, 1.30 mmol, 5 equiv) in DMA (5 mL). The product was purified by column chromatography (petroleum ether/ethyl acetate 2:1) to give 0.055 g (0.52 mmol/52%) of the analytically pure compound (purity: 99.99%). $\text{C}_{19}\text{H}_{17}\text{FN}_2\text{O}_5\text{S}$; MW 404.41; mp 180–182 $^{\circ}\text{C}$; ^1H NMR (300 MHz, Acetone- d_6): δ 7.46–7.36 (m, 2H), 7.36–7.32 (m, 1H), 7.31–7.25 (m, 2H), 7.24–7.11 (m, 3H), 6.88–6.74 (m, 2H), 6.63 (dd, J = 22.5, 3.6 Hz, 1H), 3.29 (s, 3H), 2.29 (s, 3H); ^{13}C NMR (126 MHz, DMSO- d_6): δ 160.31 (d, J = 240.6 Hz), 156.85, 152.42, 149.01, 145.69, 138.01 (d, J = 2.3 Hz), 137.23 (d, J = 8.6 Hz), 129.10 (d, J = 10.3 Hz), 126.43, 124.22, 121.64, 117.53, 116.48 (d, J = 25.4 Hz), 112.99 (d, J = 23.7 Hz), 106.54, 35.98, 16.05; MS (ESI): 404.94 (M + H) $^+$.

4-[5-[(5-Fluoro-2-methylphenyl)(methyl)carbamoyl]furan-2-yl]phenyl Sulfamate (22). The title compound was prepared according to method G by the reaction of **10** (0.275 g, 0.845 mmol, 1 equiv) and sulfamoyl chloride (0.488 g, 4.22 mmol, 5 equiv) in DMA (5 mL). The product was purified by column chromatography (petroleum ether/ethyl acetate 1:1) to give 0.238 g (0.58 mmol/69%) of the analytically pure compound (purity: 97.54%). $\text{C}_{19}\text{H}_{17}\text{FN}_2\text{O}_5\text{S}$; MW 404.41; mp 193–195 $^{\circ}\text{C}$; ^1H NMR (500 MHz, DMSO- d_6): δ 8.07 (s, 2H), 7.44 (t, J = 7.5 Hz, 1H), 7.38–7.29 (m, 3H), 7.28–7.22 (m, 3H), 6.96 (d, J = 3.6 Hz, 1H), 6.62 (d, J = 3.6 Hz, 1H), 3.25 (s, 3H), 2.13 (s, 3H); ^{13}C NMR (126 MHz, DMSO- d_6): δ 160.79 (d, J = 243.8 Hz), 157.62, 153.49, 150.05, 146.63, 143.76 (d, J = 10.8 Hz), 132.28 (d, J = 8.4 Hz), 131.55 (d, J = 4.6 Hz), 127.39, 125.22, 122.62, 118.67, 115.24 (d, J = 20.1 Hz), 115.07 (d, J = 18.1 Hz), 107.58, 36.80, 16.27; MS (ESI): 404.88 (M + H) $^+$.

4-[5-[(4-Fluoro-2-methylphenyl)(methyl)carbamoyl]furan-2-yl]phenyl Sulfamate (23). The title compound was prepared according to method G by the reaction of **11** (0.227 g, 0.697 mmol, 1 equiv) and sulfamoyl chloride (0.403 g, 3.48 mmol, 5 equiv) in DMA (5 mL). The product was purified by column chromatography (petroleum ether/ethyl acetate 1:1) to give 0.190 g (0.46 mmol/67%) of the analytically pure compound (purity: 97.03%). $\text{C}_{19}\text{H}_{17}\text{FN}_2\text{O}_5\text{S}$; MW 404.41; mp 200–202 $^{\circ}\text{C}$; ^1H NMR (500 MHz, DMSO- d_6): δ 8.07 (d, J = 3.5 Hz, 2H), 7.43–7.34 (m, 3H), 7.31 (dd, J = 9.7, 3.0 Hz, 1H), 7.28–7.23 (m, 2H), 7.16 (td, J = 8.5, 3.1 Hz, 1H), 6.94 (d, J = 3.6 Hz, 1H), 6.52 (d, J = 3.6 Hz, 1H), 3.24 (s, 3H), 2.17 (s, 3H); ^{13}C NMR (126 MHz, DMSO- d_6): δ 161.32 (d, J = 245.2 Hz), 157.86, 153.43, 150.01, 146.69, 139.02 (d, J = 2.1 Hz), 138.24 (d, J = 8.2 Hz), 130.11 (d, J = 9.2 Hz), 127.43, 125.23, 122.64, 118.54, 117.49 (d, J = 22.4 Hz), 114.00 (d, J = 22.5 Hz), 107.54, 36.99, 17.05; MS (ESI): 404.96 (M + H) $^+$.

4-[5-[(3-Fluoro-2-methylphenyl)(methyl)carbamoyl]furan-2-yl]phenyl Sulfamate (24). The title compound was prepared according to method G by the reaction of **12** (0.2 g, 0.614 mmol, 1 equiv) and sulfamoyl chloride (0.355 g, 3.07 mmol, 5 equiv) in DMA (5 mL). The product was purified by column chromatography (petroleum ether/ethyl acetate 1:1) to give 0.150 g (0.37 mmol/60%) of the analytically pure compound (purity: 99.99%). $\text{C}_{19}\text{H}_{17}\text{FN}_2\text{O}_5\text{S}$; MW 404.41; mp 196–198 $^{\circ}\text{C}$; ^1H NMR (500 MHz, DMSO- d_6): δ 8.07 (s, 2H), 7.44–7.28 (m, 4H), 7.28–7.21 (m, 2H), 7.21 (d, J = 7.4 Hz, 1H), 6.95 (d, J = 3.6 Hz, 1H), 6.63 (d, J = 3.6 Hz, 1H), 3.26 (s, 3H), 2.09 (s, 3H); ^{13}C NMR (126 MHz, DMSO- d_6): δ 161.09 (d, J = 243.2 Hz), 157.27 (d, J = 9.5 Hz), 155.21, 145.30, 144.55 (d, J = 8.9 Hz), 127.89 (d, J = 10.0 Hz), 125.54, 124.23, 122.85 (d, J = 16.9 Hz), 122.59, 120.34, 118.80, 115.53, 114.70 (d, J = 21.8 Hz), 104.72, 37.02, 9.29; MS (ESI): 404.94 (M + H) $^+$.

4-[5-[Methyl(3-methylpyridin-2-yl)carbamoyl]furan-2-yl]phenyl Sulfamate (28). The title compound was prepared according to method G by the reaction of **25** (0.3 g, 0.972 mmol, 1 equiv) and sulfamoyl chloride (0.562 g, 4.86 mmol, 5 equiv) in DMA (5 mL). The product was purified by column chromatography (petroleum ether/ethyl acetate 2:1) to give 0.273 g (0.704 mmol/72%) of the analytically pure compound (purity: 99.99%). $C_{18}H_{17}N_3O_5S$; MW 387.41; mp 197–199 °C; 1H NMR (500 MHz, DMSO- d_6): δ 8.36 (ddd, $J = 4.8, 1.9, 0.7$ Hz, 1H), 8.06 (s, 2H), 7.89 (ddd, $J = 7.6, 1.9, 0.8$ Hz, 1H), 7.41 (dd, $J = 7.6, 4.7$ Hz, 1H), 7.34–7.19 (m, 4H), 6.97 (d, $J = 3.6$ Hz, 1H), 6.78 (s, 1H), 3.26 (s, 3H), 2.23 (s, 3H); ^{13}C NMR (126 MHz, DMSO- d_6): δ 158.22, 154.91, 153.44, 150.00, 146.95, 146.90, 140.29, 130.25, 127.27, 125.17, 123.82, 122.62, 118.49, 107.63, 35.10, 16.68; MS (ESI): 387.94 (M + H) $^+$.

4-[5-[Methyl(4-methylpyridin-3-yl)carbamoyl]furan-2-yl]phenyl Sulfamate (29). The title compound was prepared according to method G by the reaction of **26** (0.21 g, 0.681 mmol, 1 equiv) and sulfamoyl chloride (0.393 g, 3.4 mmol, 5 equiv) in DMA (5 mL). The product was purified by column chromatography (petroleum ether/ethyl acetate 2:1) to give 0.15 g (0.38 mmol/57%) of the analytically pure compound (purity: 96.79%). $C_{18}H_{17}N_3O_5S$; MW 387.41; mp 180–182 °C; 1H NMR (500 MHz, Acetone- d_6): δ 8.80 (s, 1H), 8.73 (d, $J = 5.4$ Hz, 1H), 7.84 (d, $J = 5.4$ Hz, 1H), 7.33–7.28 (m, 4H), 7.20 (s, 2H), 6.96 (s, 1H), 6.90 (s, 1H), 3.43 (s, 3H), 2.47 (s, 3H); ^{13}C NMR (126 MHz, Acetone- d_6): δ 161.23, 157.71, 156.46, 155.76, 138.43, 138.16, 136.80, 135.93, 133.38, 130.10, 129.75, 125.18, 117.85, 104.01, 37.62, 27.40; MS (ESI): 387.84 (M + H) $^+$.

4-[5-[Methyl(2-methylpyridin-3-yl)carbamoyl]furan-2-yl]phenyl Sulfamate (30). The title compound was prepared according to method G by the reaction of **27** (0.246 g, 0.797 mmol, 1 equiv) and sulfamoyl chloride (0.46 g, 3.98 mmol, 5 equiv) in DMA (5 mL). The product was purified by column chromatography (petroleum ether/ethyl acetate 2:1) to give 0.177 g (0.45 mmol/57%) of the analytically pure compound (purity: 98.89%). $C_{18}H_{17}N_3O_5S$; MW 387.41; mp 194–196 °C; 1H NMR (500 MHz, Acetone- d_6): δ 8.88 (dd, $J = 5.5, 1.5$ Hz, 1H), 8.46 (d, $J = 8.0$ Hz, 1H), 7.97 (dd, $J = 8.1, 5.5$ Hz, 1H), 7.33 (d, $J = 6.6$ Hz, 4H), 7.22 (s, 2H), 7.06 (s, 1H), 6.93 (s, 1H), 3.48 (s, 3H), 2.73 (s, 3H); ^{13}C NMR (126 MHz, Acetone- d_6): δ 160.12, 159.82, 155.67, 155.35, 151.66, 147.71, 128.59, 126.28, 126.00, 123.71, 120.91, 117.83, 115.54, 108.28, 37.35, 17.50; MS (ESI): 387.93 (M + H) $^+$.

4-[5-[Methyl(o-tolyl)carbamoyl]-1,3,4-oxadiazol-2-yl]phenyl Sulfamate (35). The title compound was prepared according to method G by the reaction of **31** (0.25 g, 0.808 mmol, 1 equiv) and sulfamoyl chloride (0.466 g, 4.04 mmol, 5 equiv) in DMA (5 mL). The product was purified by column chromatography (dichloromethane/methanol 95:5) to give 0.24 g (0.62 mmol/76%) of the analytically pure compound (purity: 99.55%). $C_{17}H_{16}N_4O_5S$; MW 388.40; mp 206–208 °C; 1H NMR (500 MHz, Acetone- d_6): δ 7.98–7.92 (m, 2H), 7.53–7.47 (m, 2H), 7.40–7.31 (m, 3H), 7.34–7.26 (m, 2H), 7.26–7.19 (m, 1H), 3.41 (s, 3H), 2.36 (s, 3H); ^{13}C NMR (126 MHz, Acetone- d_6): δ 165.23, 162.03, 158.64, 156.14, 142.39, 136.92, 132.07, 129.82, 129.73, 129.09, 128.01, 117.05, 115.35, 37.11, 17.64; MS (ESI): 388.91 (M + H) $^+$.

4-[4-[Methyl(o-tolyl)carbamoyl]oxazol-2-yl]phenyl Sulfamate (36). The title compound was prepared according to method G by the reaction of **32** (0.2 g, 0.648 mmol, 1 equiv) and sulfamoyl chloride (0.374 g, 3.24 mmol, 5 equiv) in DMA (5 mL). The product was purified by column chromatography (dichloromethane/methanol 97:3) to give 0.175 g (0.45 mmol/69%) of the analytically pure compound (purity: 99.15%). $C_{18}H_{17}N_3O_5S$; MW 387.41; mp 186–188 °C; 1H NMR (500 MHz, DMSO- d_6): δ 8.13 (s, 2H), 7.84–7.78 (m, 2H), 7.62 (s, 1H), 7.40–7.35 (m, 2H), 7.33 (d, $J = 7.3$ Hz, 1H), 7.30 (dt, $J = 12.1, 4.3$ Hz, 1H), 7.25 (d, $J = 4.0$ Hz, 2H), 3.26 (s, 3H), 2.19 (s, 3H); ^{13}C NMR (126 MHz, DMSO- d_6): δ 160.70, 158.76, 151.91, 142.32, 141.68, 136.49, 135.54, 130.94, 128.38, 128.35, 127.65, 127.12, 124.26, 122.85, 36.52, 17.11; MS (ESI): 387.97 (M + H) $^+$.

4-[4-[Methyl(o-tolyl)carbamoyl]thiazol-2-yl]phenyl Sulfamate (37). The title compound was prepared according to method G by the reaction of **33** (0.2 g, 0.616 mmol, 1 equiv) and sulfamoyl chloride (0.355 g, 3.08 mmol, 5 equiv) in DMA (5 mL). The product was

purified by column chromatography (petroleum ether/ethyl acetate 2:1) to give 0.156 g (0.386 mmol/62%) of the analytically pure compound (purity: 99.99%). $C_{18}H_{17}N_3O_4S_2$; MW 403.47; mp 186–188 °C; 1H NMR (500 MHz, DMSO- d_6): δ 8.11 (s, 2H), 8.02 (s, 1H), 7.61 (d, $J = 8.2$ Hz, 2H), 7.29 (t, $J = 7.4$ Hz, 3H), 7.19 (tt, $J = 7.9, 3.9$ Hz, 1H), 7.15 (d, $J = 4.2$ Hz, 2H), 3.27 (s, 3H), 2.23 (s, 3H); ^{13}C NMR (126 MHz, DMSO): δ 164.18, 162.56, 151.43, 150.71, 143.35, 135.30, 130.73, 130.55, 128.04, 127.66, 127.54, 126.71, 125.04, 122.78, 36.85, 17.39; MS (ESI): 403.92 (M + H) $^+$.

4-[5-[Methyl(o-tolyl)carbamoyl]thiazol-2-yl]phenyl Sulfamate (38). The title compound was prepared according to method G by the reaction of **34** (0.25 g, 0.771 mmol, 1 equiv) and sulfamoyl chloride (0.445 g, 3.85 mmol, 5 equiv) in DMA (5 mL). The product was purified by column chromatography (petroleum ether/ethyl acetate 2:1) to give 0.21 g (0.52 mmol/67%) of the analytically pure compound (purity: 98.12%). $C_{18}H_{17}N_3O_4S_2$; MW 403.47; mp 203–205 °C; 1H NMR (500 MHz, DMSO- d_6): δ 8.13 (s, 2H), 7.91–7.84 (m, 2H), 7.46–7.41 (m, 2H), 7.40–7.34 (m, 4H), 7.17 (s, 1H), 3.29 (s, 3H), 2.18 (s, 3H); ^{13}C NMR (126 MHz, DMSO- d_6): δ 169.31, 159.83, 151.96, 146.51, 141.44, 135.98, 133.44, 131.72, 130.41, 129.53, 129.00, 127.95, 127.88, 123.00, 37.00, 16.87; MS (ESI): 403.90 (M + H) $^+$.

Biochemical Assays. *h17 β -HSD1* and *h17 β -HSD2* Cell-Free Inhibition Assays. The human enzymes were partially purified from human placental tissue according to previously described procedures.¹⁰⁹ Fresh human placenta was provided by the Department of Obstetrics and Gynecology, Saarland University, Homburg/Saar, Germany. After birth, the placenta was kept at 0 °C and was immediately processed. After homogenization, the cytosolic and microsomal fractions were separated by fractional centrifugation. In the case of the *h17 β -HSD1* assay, the cytosolic fraction was incubated with NADH (500 μ M), while in the case of the *h17 β -HSD2* assay, the microsomal fraction was incubated with NAD $^+$ (1500 μ M) at 37 °C in a phosphate buffer (50 mM) with 20% of glycerol and EDTA (1 mM) in the presence of potential inhibitors which were prepared in DMSO (final DMSO concentration in the assay was 1%). The enzymatic reaction was started by the addition of a mixture of unlabeled and radiolabeled substrate (final concentration: 500 nM), [3H]-E1 for 10 min in the case of *h17 β -HSD1* assay or with [3H]-E2 for 20 min in the case of *h17 β -HSD2* assay.¹⁰⁹ HgCl $_2$ (10 mM in case of *h17 β -HSD1* or 1mM in case of *h17 β -HSD2*) was used to stop the enzymatic reactions and the steroids were extracted with diethyl ether. After evaporation, they were dissolved in acetonitrile/water (45:55). E1 and E2 were separated on a C18 reverse phase chromatography column (Nucleodur C $_{18}$ Isis, Macherey-Nagel) connected to an Agilent 1200 Series (Agilent Technologies) HPLC-system using acetonitrile/water (45:55) as the mobile phase. A radio flow detector (Ramona, raytest) was coupled to the HPLC-system for the detection and quantification of the steroids. After the analysis of the resulting chromatograms, the conversion rates were calculated according to the following equation

$$\%conversion = \left[\frac{\%product}{\%product + \%substrate} \right] \times 100$$

Each value was calculated from at least two independent experiments.

Then, the percentage inhibition corresponding to each inhibitor concentration was calculated according to the following equation:

$$\%inhibition = \left[1 - \left(\frac{\%conversion \text{ of the inhibitor}}{\%conversion \text{ of the control (DMSO)}} \right) \right] \times 100$$

At least three different concentrations of each inhibitor leading to inhibitions ranging from 30 to 80% were chosen to deduce the IC $_{50}$ of each inhibitor. The IC $_{50}$ of each inhibitor was calculated from at least two independent experiments.

Cell Culture. The T47D human mammary cancer cell line was purchased from ECACC, Salisbury. The cells were routinely cultivated in Dulbecco's modified Eagle medium (DMEM, Sigma) (supplemented with 10% FCS (Sigma) and 100 IU/mL penicillin–

streptomycin) and incubated at 37 °C under a humidified atmosphere of 5% CO₂. The medium was changed every 2–3 days, and the cells were passed every 9–10 days. The T47D cells were seeded into a 24-well flat-bottom plate at 5 × 10⁵ cells/well in DMEM supplemented with 10% FCS and 100 IU/mL penicillin–streptomycin according to previously described procedures.^{114,115} After incubation for 24 h at 37 °C, the medium was exchanged by 445 μL of a fresh FCS-free DMEM, and 5 μL of the test compound dissolved in DMSO was added (final concentration of DMSO was adjusted to 1% in all samples). Followed by the incubation of T47D cells for 1 h (in case of *h*STS and *h*17β-HSD1 cellular inhibition assays) or different pre-incubation time points (in case of validation of drug-prodrug model).

***h*STS and *h*17β-HSD1 Cellular Inhibition Assays.** After 1 h, the incubation period was started by the addition of a mixture of unlabeled and radioactive substrate ([³H]-E1-S for 24 h in case of STS or with [³H]-E1 (50 nM, 50 μL) for 40 min in the case of *h*17β-HSD1 assay) at 37 °C. The reaction was stopped by the removal of the supernatant (200 μL in the case of STS or 450 μL in the case of the *h*17β-HSD1 assay). In the case of STS, the supernatant was centrifuged at 12,500 rpm for 15 min at 4 °C to precipitate any suspended cells or proteins and then was injected directly, but in the case of the *h*17β-HSD1 assay, the supernatant was added to 500 μL of ethyl acetate in Eppendorf tubes and then the tubes were shaken for 10 min and evaporated to dryness in a speed-vac operating at vacuum and 37 °C for 30 min. The injection was done into the same radio-HPLC system mentioned above for cell-free inhibition assays and the IC₅₀s are calculated as described.

Nature of Inhibition of STS Activity. In order to investigate the mode of inhibition of STS activity, T47D cells were cultivated as mentioned above but with some changes described by Purohit et al.¹⁰³ The cells were pre-incubated with the inhibitors for 2 h at 37 °C, and then, the medium was removed and the cells were washed 3–4 times with PBS. The remaining STS activity was performed as described in the recent procedure by incubating the cells using [³H]-E1S for 24 h at 37 °C, then subsequent quantification of the steroids in the supernatant was determined using HPLC coupled to a radio detector. IC₅₀ values were calculated as described for the cell-free inhibition assay.

Estrogen Receptor Affinity (ERα) in a Cell-free Assay. Compounds were tested for ERα affinity using the PolarScreen ER Alpha Competitor Assay Green (Thermo Fisher Scientific) according to the manufacturer's protocol with the only exception that fourfold instead of twofold concentrated Fluormone ES2 Red (fluorescent probe) was used to obtain a sufficient signal-to-noise ratio. Serial dilutions of each compound were prepared from a 200 μM stock solution in binding buffer containing 4% DMSO resulting in nine concentrations ranging from 50 μM to 1 nM in a final working volume of 20 μL. The ERα and Fluormone ES2 Red stock solutions were diluted to 288 and 72 nM, respectively, and preincubated in an ice bath for at least 30 min (master mix). A 10 μM solution of E2 was chosen as the positive control and bare master mix as the negative control. 5 μL of binding buffer (4% DMSO) along with 5 μL of each dilution of the positive control were pipetted in a 384-well plate in quadruplicates and brought to the final volume of 20 μL by the addition of 10 μL of the freshly preincubated master mix. The negative control consisted of 10 μL of binding buffer and 10 μL of master mix. The freshly prepared well plate was placed in an opaque box together with a moistened piece of pulp to avoid evaporation. After 1 h of incubation at 25 °C, the parallel and perpendicular polarization values of each well were measured using a plate reader (BMG Labtech POLARstar Omega, 384-well plate format, top-optics) equipped with a 485 nm excitation filter and a 520 nm emission filter (both with 20 nm bandwidth, BMG Labtech) and a preset gain adjustment of 2800. The plate was shaken prior to the measurement (double-orbital, 10 s, 500 rpm). The polarization values were converted into percentage displacement (*D* %) with respect to the controls using the equation $D \% = (P_{\text{neg}} - P_x) / (P_{\text{neg}} - P_{\text{pos}})$, where *P*_{neg} and *P*_{pos} are the polarization values for the negative (0% displacement) and positive (100% displacement) controls, respectively, and *P*_x is the observed polarization value in each well. The obtained values for displacement were plotted against the concentrations of the compounds using OriginPro 2020 (PerkinElmer) and were analyzed using a four-parameter log-logistic function ("dose–response") to

obtain relative IC₅₀ values (the concentration needed to displace half of the fluorescent probe) without restrictions to any parameter. The relative IC₅₀ values were transformed to relative binding affinities (RBA's) for the purpose of comparison via the equation $RBA [\%] = [IC_{50} \times 10^2 / IC_{50} (\text{compound})] \times 100$. The performance of the assay was checked by the *Z*-factor introduced by Zhang et al.¹¹⁶ It is a dimensionless parameter which takes the replicated controls (positive and negative) into account to assess information about the separation band and the dynamic range of the assay and to make the assays comparable made within and between days. *Z* is expressed in the following equation

$$Z = 1 - \frac{3(\sigma_+ + \sigma_-)}{|\mu_+ - \mu_-|}$$

where σ_+ and σ_- are the standard deviations of the means of the positive resp. negative control and μ_+ and μ_- are the means of the replicated controls. Assays with values in the range of 1.0 > *Z* > 0.5 are declared as excellent assays.¹¹⁷

Metabolic Stability. Compounds were tested according to established method.^{111,118–120} For the evaluation of phases I and II metabolic stability, 1 μM compound was incubated with 1 mg/mL pooled mammalian (human or mouse) liver S9 fraction (BD Gentest, Heidelberg, Germany), 2 mM NADPH regenerating system, 1 mM UDPGA, 10 mM MgCl₂, and 0.1 mM PAPS at 37 °C for 0, 5, 15, and 60 min at a final volume of 100 μL of 100 mM Potassium hydrogen phosphate buffer pH = 7.4. The incubation was stopped by the precipitation of S9 enzymes with 2 volumes of cold acetonitrile containing internal standard and then centrifuged for 10 min at 4 °C and 12,500 rpm. For quantification, a calibration curve was developed for each compound assayed by LC–MS/MS (Accucore RP-MS, TSQ Quantum triple quadrupole mass spectrometer, ESI interface) using a serial dilution of 6 standards in the range 10–500 nM. Then, LC–MS/MS was used to analyze the remaining concentration of the test compound at different time points. The half-life (*t*_{1/2}) was determined using the following equation

$$t_{1/2} = \frac{\ln(2)}{-K}$$

where *K* (decay rate) is the slope of the linear regression from log [test compound] versus time:

$$K = \frac{\ln(\text{Concentration})}{\text{Time}}$$

Then, the intrinsic clearance (Cl_{int}) [μL/min/mg protein] estimates of the compounds were determined using the following equation

$$Cl_{\text{int}} = K \times V \times f_u$$

where: *V* = incubation volume [μL]/microsomal protein [mg] = 1000 [μL/mg protein]. *f*_u = unbound fraction of the tested compounds (unknown) = 1

Validation of the Drug-Prodrug Concept. Our drug-prodrug model was validated using a new assay, and the principle of the assay had been discussed earlier. For cell-free assays, the test compounds (13, 16, 19, and 37) dissolved in DMSO were pre-incubated at different time points in Eppendorf tubes at 37 °C in 345 μL of phosphate buffer (50 mM) with 20% of glycerol and EDTA (1 mM). The tubes were divided into two identical groups: the first group (group A) is for measuring the percentage of inhibition of 17β-HSD1 as a function of time, and the second one (group B) is for quantifying the percentage conversion of R–OSO₂NH₂ into R–OH. The time points measurements were performed in duplicates. At the end of the incubation periods, 50 μL of cytosolic fraction of *h*17β-HSD1, 50 μL of NADH (500 μM), and 50 μL of a mixture of unlabeled and radioactive substrate [³H]-E1 (50 nM) were added to all tubes in group A. Tubes were incubated for 10 min at 37 °C. Then, the workup and measuring percentages of inhibition of 17β-HSD1 were done as described for the *h*17β-HSD1 cell-free inhibition assay. For group B, the reaction was stopped by the addition of 500 μL of diethylether, the tubes were

shaken, centrifuged for 10 min, and the organic layers were evaporated to dryness. 25 μL of 2 μM diphenhydramine (DPH) solution in ACN was used for re-dispensing and then transferred to an HPLC vial with micro-insert. 2 μL was injected onto the analytical column and the samples were measured using LC–MS/MS. The following equation was used to calculate the percentage conversion of R–OSO₂NH₂ into R–OH for each biological duplicate:

$$\% \text{conversion} = \left[\frac{\text{Quantity of ROH}}{\text{Quantity of ROSO}_2\text{NH}_2 + \text{Quantity of ROH}} \right] \times 100$$

For cellular assays, the test compounds dissolved in DMSO were pre-incubated at different time points at 37 °C with T47D cells seeded into a 24-well flat-bottom plate as mentioned above in cell culture preparation. The plate was divided into two groups, A and B as above. The time points were performed in duplicates. At the end of the incubation periods, a mixture of unlabeled and radioactive substrate [³H]-E1 (50 nM, 50 μL) was added to all wells in group A and cells were incubated for 40 min at 37 °C and then the workup and measuring percentages of inhibition of 17 β -HSD1 were done as mentioned in 17 β -HSD1 cellular inhibition assays. For group B, the reaction was stopped by the removal of 450 μL of supernatant, added to 500 μL of ethyl acetate, tubes were shaken then centrifuged for 10 min, and the organic layers were evaporated to dryness. Re-dispensing, injection in LC–MS/MS, and calculation of percentage conversion were done as mentioned above.

■ ASSOCIATED CONTENT

Supporting Information

The Supporting Information is available free of charge at <https://pubs.acs.org/doi/10.1021/acs.jmedchem.2c00589>.

Additional information on the synthesis of compounds 1a, 5a–12a, 25a–27a, 32a–34a, 1b, 9b, 10b–12b, 25b, 26b, 31b–34b, 10c, 31c, 32c, 1–12, 25–27, and 31–34; representative ¹H NMR, ¹³C NMR, and MS spectra of compounds 13, 17, 19, 33, and 37; validation of the drug-prodrug concept (compounds 16, 19, and 37); validation of the drug-prodrug concept for compound 13 at different starting concentrations; HEK-293 cell growth inhibition assay; and cytotoxicity data (PDF)

Molecular formula strings (CSV)

■ AUTHOR INFORMATION

Corresponding Author

Martin Frotscher – Department of Pharmacy, Pharmaceutical and Medicinal Chemistry, Saarland University, Saarbrücken D-66123, Germany; orcid.org/0000-0003-1777-8890; Phone: +49 681 / 302-70330; Email: m.frotscher@mx.uni-saarland.de

Authors

Abdelrahman Mohamed – Department of Pharmacy, Pharmaceutical and Medicinal Chemistry, Saarland University, Saarbrücken D-66123, Germany; Pharmaceutical Organic Chemistry Department, Assiut University, Assiut 71526, Egypt

Mohamed Salah – Department of Pharmacy, Pharmaceutical and Medicinal Chemistry, Saarland University, Saarbrücken D-66123, Germany; Department of Pharmaceutical Chemistry, Faculty of Pharmacy, October University for Modern Sciences and Arts, Cairo 12451, Egypt

Mariam Tahoun – Department of Pharmacy, Pharmaceutical and Medicinal Chemistry, Saarland University, Saarbrücken D-66123, Germany; Present Address: PharmaCenter Bonn,

Pharmaceutical Institute, Pharmaceutical & Medicinal Chemistry, University of Bonn, An der Immenburg 4, D-53121 Bonn, Germany; orcid.org/0000-0001-8787-0399

Manuel Hawner – Department of Pharmacy, Pharmaceutical and Medicinal Chemistry, Saarland University, Saarbrücken D-66123, Germany

Ahmed S. Abdelsamie – Department of Chemistry of Natural and Microbial Products, Institute of Pharmaceutical and Drug Industries Research, National Research Centre, Cairo 12451, Egypt; Department of Drug Design and Optimization, Helmholtz Institute for Pharmaceutical Research Saarland (HIPS) - Helmholtz Centre for Infection Research (HZI), Saarbrücken 66123, Germany; orcid.org/0000-0002-5326-4400

Complete contact information is available at: <https://pubs.acs.org/10.1021/acs.jmedchem.2c00589>

Notes

The authors declare no competing financial interest.

■ ACKNOWLEDGMENTS

We are grateful to the Deutsche Forschungsgemeinschaft (DFG) for financial support (Grants HA1315/12–1 and FR3002/1–1). We would like also to thank the Deutscher Akademischer Austauschdienst (DAAD) for funding this publication as part of the German-Egyptian Research Long Term Scholarship Program (GERLS) 2016 (57222240) and Short-Term Scholarships for Foreign Students (STIBET) 2020/2021. Thanks are due to Dr. Stefan Boettcher and Martina Jankowski for their help in performing the metabolic stability tests and to Dr. Matthias Engel, Nathalie Gladys Kagerah, and Marie Grötschla for performing the cytotoxicity test.

■ ABBREVIATIONS

17 β -HSD, 17 β -hydroxysteroid dehydrogenase; ADDs, androgen-dependent diseases; A-diol, androst-5-ene-3 β ,17 β -diol; AIs, aromatase inhibitors; DCC, *N,N'*-dicyclohexylcarbodiimide; DCM, dichloromethane; DHEA, dehydroepiandrosterone; DIPEA, *N,N*-diisopropylethylamine; DMA, dimethylacetamide; DMAP, 4-dimethylaminopyridine; DME, dimethyl ether; DMEM, Dulbecco's modified Eagle medium; DMF, dimethyl formamide; DPH, diphenhydramine; DSHIs, dual STS and 17 β -HSD1 inhibitors; E1(-S), estrone(-sulfate); E2, estradiol; EDDs, estrogen-dependent diseases; ER, estrogen receptor; FCS, fetal calf serum; GnRH, gonadotropin releasing hormone analogues; *h*, human; HPLC, high-performance liquid chromatography; MgSO₄, magnesium sulfate; *m*, mouse; MTT, 3-(4,5-dimethylthiazol-2-yl)-2,5-diphenyltetrazolium bromide; NAD⁺, nicotinamide adenine dinucleotide; NADPH, dihydronicotinamide adenine dinucleotide phosphate; NSAIDs, nonsteroidal anti-inflammatory drugs; PAPS, 3'-phosphoadenosine-5'-phosphosulfate; PBS, phosphate-buffered saline; RB, relative binding affinity; SERMs, relative binding affinity; SERMs selective estrogen receptor modulators; SF, selectivity factor; STS, steroid sulfatase; THF, tetrahydrofuran; TsCl, 4-toluenesulfonyl chloride; UDPGA, uridine-diphosphate-glucuronic acid

■ REFERENCES

(1) Delvoux, B.; D'Hooghe, T.; Kyama, C.; Koskimies, P.; Hermans, R. J.; Dunselman, G. A.; Romano, A. Inhibition of type 1 17 β -

- hydroxysteroid dehydrogenase impairs the synthesis of 17 β -estradiol in endometriosis lesions. *J. Clin. Endocrinol. Metab.* **2014**, *99*, 276–284.
- (2) Šmuc, T.; Pucelj, M. R.; Sinkovec, J.; Husen, B.; Thole, H.; Rižner, T. L. Expression analysis of the genes involved in estradiol and progesterone action in human ovarian endometriosis. *Gynecol. Endocrinol.* **2007**, *23*, 105–111.
- (3) Mori, T.; Ito, F.; Matsushima, H.; Takaoka, O.; Koshihara, A.; Tanaka, Y.; Kusuki, I.; Kitawaki, J. Dienogest reduces HSD17b1 expression and activity in endometriosis. *J. Endocrinol.* **2015**, *225*, 69–76.
- (4) Miyoshi, Y.; Ando, A.; Shiba, E.; Taguchi, T.; Tamaki, Y.; Noguchi, S. Involvement of up-regulation of 17 β -hydroxysteroid dehydrogenase type 1 in maintenance of intratumoral high estradiol levels in postmenopausal breast cancers. *Int. J. Cancer* **2001**, *94*, 685–689.
- (5) Lin, S.-X.; Chen, J.; Mazumdar, M.; Poirier, D.; Wang, C.; Azzi, A.; Zhou, M. Molecular therapy of breast cancer: progress and future directions. *Nat. Rev. Endocrinol.* **2010**, *6*, 485–493.
- (6) Konings, G. F.; Cornel, K. M.; Xanthoulea, S.; Delvoux, B.; Skowron, M. A.; Kooreman, L.; Koskimies, P.; Krakstad, C.; Salvesen, H. B.; van Kuijk, K.; Schrooders, Y. J.; Vooijs, M.; Groot, A. J.; Bongers, M. Y.; Kruitwagen, R. F.; Romano, A. Blocking 17 β -hydroxysteroid dehydrogenase type 1 in endometrial cancer: a potential novel endocrine therapeutic approach. *J. Pathol.* **2018**, *244*, 203–214.
- (7) Cornel, K. M.; Kruitwagen, R. F.; Delvoux, B.; Viscinti, L.; Van de Vijver, K. K.; Day, J. M.; Van Gorp, T.; Hermans, R. J.; Dunselman, G. A.; Romano, A. Overexpression of 17 β -hydroxysteroid dehydrogenase type 1 increases the exposure of endometrial cancer to 17 β -estradiol. *J. Clin. Endocrinol. Metab.* **2012**, *97*, E591–E601.
- (8) Blomquist, C. H.; Bonenfant, M.; McGinley, D. M.; Posalaky, Z.; Lakatua, D. J.; Tuli-Puri, S.; Bealka, D. G.; Tremblay, Y. Androgenic and estrogenic 17 β -hydroxysteroid dehydrogenase/17-ketosteroid reductase in human ovarian epithelial tumors: evidence for the type 1, 2 and 5 isoforms. *J. Steroid Biochem. Mol. Biol.* **2002**, *81*, 343–351.
- (9) Giudice, L. Clinical Practice. Endometriosis. *N. Engl. J. Med.* **2010**, *362*, 2389–2398.
- (10) Kiesel, L.; Sourouni, M. Diagnosis of endometriosis in the 21st century. *Climacteric* **2019**, *22*, 296–302.
- (11) Zondervan, K. T.; Becker, C. M.; Missmer, S. A. Endometriosis. *N. Engl. J. Med.* **2020**, *382*, 1244–1256.
- (12) Bulun, S. E. Endometriosis. *N. Engl. J. Med.* **2009**, *360*, 268–279.
- (13) Duffy, J. M.; Arambage, K.; Correa, F. J. S.; Olive, D.; Farquhar, C.; Garry, R.; Barlow, D. H.; Jacobson, T. Z. Laparoscopic surgery for endometriosis. *Cochrane Database Syst. Rev.* **2014**, *4*, CD011031.
- (14) Shakiba, K.; Bena, J. F.; McGill, K. M.; Minger, J.; Falcone, T. Surgical treatment of endometriosis: a 7-year follow-up on the requirement for further surgery. *Obstet. Gynecol.* **2008**, *111*, 1285–1292.
- (15) Vercellini, P.; Viganò, P.; Somigliana, E.; Fedele, L. Endometriosis: pathogenesis and treatment. *Nat. Rev. Endocrinol.* **2014**, *10*, 261–275.
- (16) Fedele, L.; Bianchi, S.; Zanconato, G.; Tozzi, L.; Raffaelli, R. Gonadotropin-releasing hormone agonist treatment for endometriosis of the rectovaginal septum. *Am. J. Obstet. Gynecol.* **2000**, *183*, 1462–1467.
- (17) Brown, J.; Crawford, T. J.; Allen, C.; Hopewell, S.; Prentice, A. Nonsteroidal anti-inflammatory drugs for pain in women with endometriosis. *Cochrane Database Syst. Rev.* **2017**, *1*, CD004753.
- (18) Barra, F.; Grandi, G.; Tantari, M.; Scala, C.; Facchinetti, F.; Ferrero, S. A comprehensive review of hormonal and biological therapies for endometriosis: latest developments. *Expert Opin. Biol. Ther.* **2019**, *19*, 343–360.
- (19) Bush, N. J. Advances in hormonal therapy for breast cancer. *Semin. Oncol. Nurs.* **2007**, *23*, 46–54.
- (20) Dunselman, G.; Vermeulen, N.; Becker, C.; Calhaz-Jorge, C.; D'Hooghe, T.; De Bie, B.; Heikinheimo, O.; Horne, A.; Kiesel, L.; Nap, A.; Prentice, A.; Saridogan, E.; Soriano, D.; Nelen, W. ESHRE guideline: management of women with endometriosis. *Hum. Reprod.* **2014**, *29*, 400–412.
- (21) Giudice, L. C. Clinical Practice. Endometriosis. *N. Engl. J. Med.* **2010**, *362*, 2389–2398.
- (22) Miller, W. R.; Bartlett, J.; Canney, P.; Verrill, M. Hormonal therapy for postmenopausal breast cancer: the science of sequencing. *Breast Cancer Res. Treat.* **2007**, *103*, 149–160.
- (23) Boon, W. C.; Chow, J. D.; Simpson, E. R. The multiple roles of estrogens and the enzyme aromatase. *Prog. Brain Res.* **2010**, *181*, 209–232.
- (24) Miller, W. R. Aromatase inhibitors: mechanism of action and role in the treatment of breast cancer. *Semin. Oncol.* **2003**, *30*, 3–11.
- (25) Reed, M. J.; Purohit, A.; Woo, L. W.; Newman, S. P.; Potter, B. V. Steroid sulfatase: molecular biology, regulation, and inhibition. *Endocr. Rev.* **2005**, *26*, 171–202.
- (26) Sinreih, M.; Knific, T.; Anko, M.; Hevir, N.; Vouk, K.; Jerin, A.; Frković Grazio, S.; Rižner, T. L. The significance of the sulfatase pathway for local estrogen formation in endometrial cancer. *Front. Pharmacol.* **2017**, *8*, 368.
- (27) Dumont, M.; Luu-The, V.; de Launoit, Y.; Labrie, F. Expression of human 17 β -hydroxysteroid dehydrogenase in mammalian cells. *J. Steroid Biochem. Mol. Biol.* **1992**, *41*, 605–608.
- (28) The, V. L.; Labrie, C.; Zhao, H. F.; Couët, J.; Lachance, Y.; Simard, J.; Leblanc, G.; Côté, J.; Bérubé, D.; Gagné, R.; Labrie, F. Characterization of cDNAs for human estradiol 17 β -dehydrogenase and assignment of the gene to chromosome 17: evidence of two mRNA species with distinct 5'-termini in human placenta. *Mol. Endocrinol.* **1989**, *3*, 1301–1309.
- (29) Santner, S.; Feil, P.; Santen, R. In situ estrogen production via the estrone sulfatase pathway in breast tumors: relative importance versus the aromatase pathway. *J. Clin. Endocrinol. Metab.* **1984**, *59*, 29–33.
- (30) Purohit, A.; Fusi, L.; Brosens, J.; Woo, L.; Potter, B.; Reed, M. Inhibition of steroid sulphatase activity in endometriotic implants by 667 COUMATE: a potential new therapy. *Hum. Reprod.* **2008**, *23*, 290.
- (31) Chetrite, G.; Cortes-Prieto, J.; Philippe, J.; Wright, F.; Pasqualini, J. Comparison of estrogen concentrations, estrone sulfatase and aromatase activities in normal, and in cancerous, human breast tissues. *J. Steroid Biochem. Mol. Biol.* **2000**, *72*, 23–27.
- (32) Adamson, G. D.; Pasta, D. J. Endometriosis fertility index: the new, validated endometriosis staging system. *Fertil. Steril.* **2010**, *94*, 1609–1615.
- (33) Borghese, B.; Mondon, F.; Noël, J.-C.; Fayt, I.; Mignot, T.-M.; Vaiman, D.; Chapron, C. Research resource: gene expression profile for ectopic versus eutopic endometrium provides new insights into endometriosis oncogenic potential. *Mol. Endocrinol.* **2008**, *22*, 2557–2562.
- (34) Zeitoun, K.; Takayama, K.; Sasano, H.; Suzuki, T.; Moghrabi, N.; Andersson, S.; Johns, A.; Meng, L.; Putman, M.; Carr, B.; Bulun, S. E. Deficient 17 β -hydroxysteroid dehydrogenase type 2 expression in endometriosis: failure to metabolize 17 β -estradiol. *J. Clin. Endocrinol. Metab.* **1998**, *83*, 4474–4480.
- (35) Bulun, S. E.; Cheng, Y.-H.; Pavone, M. E.; Yin, P.; Imir, G.; Utsunomiya, H.; Thung, S.; Xue, Q.; Marsh, E. E.; Tokunaga, H.; Ishikawa, H.; Kurita, T.; Su, E. J. 17 β -hydroxysteroid dehydrogenase-2 deficiency and progesterone resistance in endometriosis. *Semin. Reprod. Med.* **2010**, *28*, 44–50.
- (36) Aka, J. A.; Zerradi, M.; Houle, F.; Huot, J.; Lin, S.-X. 17 β -hydroxysteroid dehydrogenase type 1 modulates breast cancer protein profile and impacts cell migration. *Breast Cancer Res* **2012**, *14*, R92.
- (37) Simard, J.; Vincent, A.; Duchesne, R.; Labrie, F. Full oestrogenic activity of C19- Δ 5 adrenal steroids in rat pituitary lactotrophs and somatotrophs. *Mol. Cell. Endocrinol.* **1988**, *55*, 233–242.
- (38) Trottier, A.; Maltais, R.; Ayan, D.; Barbeau, X.; Roy, J.; Perreault, M.; Poulin, R.; Lagüe, P.; Poirier, D. Insight into the mode of action and selectivity of PBRM, a covalent steroidal inhibitor of 17 β -hydroxysteroid dehydrogenase type 1. *Biochem. Pharmacol.* **2017**, *144*, 149–161.
- (39) Apa, R.; Lanzone, A.; Miceli, F.; Mastrandrea, M.; Caruso, A.; Mancuso, S.; Canipari, R. Growth hormone induces in vitro maturation of follicle- and cumulus-enclosed rat oocytes. *Mol. Cell. Endocrinol.* **1994**, *106*, 207–212.

- (40) Poulin, R.; Labrie, F. Stimulation of cell proliferation and estrogenic response by adrenal C19- Δ 5-steroids in the ZR-75-1 human breast cancer cell line. *Cancer Res.* **1986**, *46*, 4933.
- (41) Dauvois, S.; Labrie, F. Androstenedione and androst-5-ene-3 β , 17 β -diol stimulate DMBA-induced rat mammary tumors-role of aromatase. *Breast Cancer Res. Treat.* **1989**, *13*, 61–69.
- (42) Poirier, D. Inhibitors of 17 β -hydroxysteroid dehydrogenases. *Curr. Med. Chem.* **2003**, *10*, 453–477.
- (43) Poirier, D. 17 β -Hydroxysteroid dehydrogenase inhibitors: a patent review. *Expert Opin. Ther. Pat.* **2010**, *20*, 1123–1145.
- (44) Deluca, D.; Krazeisen, A.; Breiting, R.; Prehn, C.; Möller, G.; Adamski, J. Inhibition of 17 β -hydroxysteroid dehydrogenases by phytoestrogens: Comparison with other steroid metabolizing enzymes. *J. Steroid Biochem. Mol. Biol.* **2005**, *93*, 285–292.
- (45) Salah, M.; Abdelsamie, A. S.; Frotscher, M. Inhibitors of 17 β -hydroxysteroid dehydrogenase type 1, 2 and 14: structures, biological activities and future challenges. *Mol. Cell. Endocrinol.* **2019**, *489*, 66–81.
- (46) Gobec, S.; Brozic, P.; Rizner, T. Inhibitors of 17 β -hydroxysteroid dehydrogenase type 1. *Curr. Med. Chem.* **2008**, *15*, 137–150.
- (47) Day, J. M.; Tutill, H. J.; Purohit, A.; Reed, M. J. Design and validation of specific inhibitors of 17 β -hydroxysteroid dehydrogenases for therapeutic application in breast and prostate cancer, and in endometriosis. *Endocr. Relat. Cancer* **2008**, *15*, 665–692.
- (48) Day, J. M.; Tutill, H. J.; Purohit, A. 17 β -hydroxysteroid dehydrogenase inhibitors. *Minerva Endocrinol* **2010**, *35*, 87–108.
- (49) Marchais-Oberwinkler, S.; Henn, C.; Möller, G.; Klein, T.; Negri, M.; Oster, A.; Spadaro, A.; Werth, R.; Wetzel, M.; Xu, K.; Frotscher, M.; Hartmann, R. W.; Adamski, J. 17 β -Hydroxysteroid dehydrogenases (17 β -HSDs) as therapeutic targets: Protein structures, functions, and recent progress in inhibitor development. *J. Steroid Biochem. Mol. Biol.* **2011**, *125*, 66–82.
- (50) Maltais, R.; Trottier, A.; Roy, J.; Ayan, D.; Bertrand, N.; Poirier, D. Pharmacokinetic profile of PBRM in rodents, a first selective covalent inhibitor of 17 β -HSD1 for breast cancer and endometriosis treatments. *J. Steroid Biochem. Mol. Biol.* **2018**, *178*, 167–176.
- (51) Poirier, D.; Roy, J.; Maltais, R. A Targeted-Covalent Inhibitor of 17 β -HSD1 Blocks Two Estrogen-Biosynthesis Pathways: In Vitro (Metabolism) and In Vivo (Xenograft) Studies in T-47D Breast Cancer Models. *Cancers* **2021**, *13*, 1841.
- (52) Poirier, D.; Nyachio, A.; Romano, A.; Roy, J.; Maltais, R.; Chai, D.; Delvoux, B.; Tomassetti, C.; Vanhie, A. An irreversible inhibitor of 17 β -hydroxysteroid dehydrogenase type 1 inhibits estradiol synthesis in human endometriosis lesions and induces regression of the non-human primate endometriosis. *J. Steroid Biochem. Mol. Biol.* **2022**, *222*, 106136.
- (53) Shah, R.; Singh, J.; Singh, D.; Jaggi, A. S.; Singh, N. Sulfatase inhibitors for recidivist breast cancer treatment: A chemical review. *Eur. J. Med. Chem.* **2016**, *114*, 170–190.
- (54) Foster, P. A.; Reed, M. J.; Purohit, A. Recent developments of steroid sulfatase inhibitors as anti-cancer agents. *Anti Cancer Agents Med. Chem.* **2008**, *8*, 732–738.
- (55) Purohit, A.; Foster, P. A. Steroid sulfatase inhibitors for estrogen- and androgen-dependent cancers. *J. Endocrinol.* **2012**, *212*, 99–110.
- (56) Maltais, R.; Poirier, D. Steroid sulfatase inhibitors: a review covering the promising 2000–2010 decade. *Steroids* **2011**, *76*, 929–948.
- (57) Mostafa, Y. A.; Taylor, S. D. Steroid derivatives as inhibitors of steroid sulfatase. *J. Steroid Biochem. Mol. Biol.* **2013**, *137*, 183–198.
- (58) Woo, L. L.; Purohit, A.; Potter, B. V. L. Development of steroid sulfatase inhibitors. *Mol. Cell. Endocrinol.* **2011**, *340*, 175–185.
- (59) Geisler, J.; Sasano, H.; Chen, S.; Purohit, A. Steroid sulfatase inhibitors: promising new tools for breast cancer therapy? *J. Steroid Biochem. Mol. Biol.* **2011**, *125*, 39–45.
- (60) Daško, M.; Demkowicz, S.; Biernacki, K.; Ciupak, O.; Kozak, W.; Masyk, M.; Rachon, J. Recent progress in the development of steroid sulphatase inhibitors – examples of the novel and most promising compounds from the last decade. *J. Enzyme Inhib. Med. Chem.* **2020**, *35*, 1163–1184.
- (61) Foster, P. A. Steroid Sulphatase and Its Inhibitors: Past, Present, and Future. *Molecules* **2021**, *26*, 2852.
- (62) Anbar, H. S.; Isa, Z.; Elounais, J. J.; Jameel, M. A.; Zib, J.; Samer, A. M.; Jawad, A. F.; El-Gamal, M. I. Steroid sulfatase inhibitors: the current landscape. *Expert Opin. Ther. Pat.* **2021**, *31*, 453–472.
- (63) Morphy, R.; Rankovic, Z. The physicochemical challenges of designing multiple ligands. *J. Med. Chem.* **2006**, *49*, 4961–4970.
- (64) Morphy, R.; Rankovic, Z. Designed multiple ligands. An emerging drug discovery paradigm. *J. Med. Chem.* **2005**, *48*, 6523–6543.
- (65) Espinoza-Fonseca, L. M. The benefits of the multi-target approach in drug design and discovery. *Biorg. Med. Chem.* **2006**, *14*, 896–897.
- (66) Baraldi, P. G.; Preti, D.; Fruttarolo, F.; Tabrizi, M. A.; Romagnoli, R. Hybrid molecules between distamycin A and active moieties of antitumor agents. *Biorg. Med. Chem.* **2007**, *15*, 17–35.
- (67) Chen, L.; Wilson, D.; Jayaram, H. N.; Pankiewicz, K. W. Dual inhibitors of inosine monophosphate dehydrogenase and histone deacetylases for cancer treatment. *J. Med. Chem.* **2007**, *50*, 6685–6691.
- (68) Apsel, B.; Blair, J. A.; Gonzalez, B.; Nazif, T. M.; Feldman, M. E.; Aizenstein, B.; Hoffman, R.; Williams, R. L.; Shokat, K. M.; Knight, Z. A. Targeted polypharmacology: discovery of dual inhibitors of tyrosine and phosphoinositide kinases. *Nat. Chem. Biol.* **2008**, *4*, 691–699.
- (69) Meunier, B. Hybrid molecules with a dual mode of action: dream or reality? *Acc. Chem. Res.* **2008**, *41*, 69–77.
- (70) Wei, D.; Jiang, X.; Zhou, L.; Chen, J.; Chen, Z.; He, C.; Yang, K.; Liu, Y.; Pei, J.; Lai, L. Discovery of multitarget inhibitors by combining molecular docking with common pharmacophore matching. *J. Med. Chem.* **2008**, *51*, 7882–7888.
- (71) Gangjee, A.; Li, W.; Yang, J.; Kisliuk, R. L. Design, synthesis, and biological evaluation of classical and nonclassical 2-amino-4-oxo-5-substituted-6-methylpyrrolo [3, 2-d] pyrimidines as dual thymidylate synthase and dihydrofolate reductase inhibitors. *J. Med. Chem.* **2008**, *51*, 68–76.
- (72) Woo, L. L.; Bubert, C.; Purohit, A.; Potter, B. V. Hybrid dual aromatase-steroid sulfatase inhibitors with exquisite picomolar inhibitory activity. *ACS Med. Chem. Lett.* **2011**, *2*, 243–247.
- (73) Gediya, L. K.; Njar, V. C. Promise and challenges in drug discovery and development of hybrid anticancer drugs. *Expert Opin. Drug Discov* **2009**, *4*, 1099–1111.
- (74) Salah, M.; Abdelsamie, A. S.; Frotscher, M. First dual inhibitors of steroid sulfatase (STS) and 17 β -hydroxysteroid dehydrogenase type 1 (17 β -HSD1): designed multiple ligands as novel potential therapeutics for estrogen-dependent diseases. *J. Med. Chem.* **2017**, *60*, 4086–4092.
- (75) Pelletier, J. D.; Poirier, D. Synthesis and evaluation of estradiol derivatives with 16 α -(bromoalkylamide), 16 α -(bromoalkyl) or 16 α -(bromoalkynyl) side chain as inhibitors of 17 β -hydroxysteroid dehydrogenase type 1 without estrogenic activity. *Biorg. Med. Chem.* **1996**, *4*, 1617–1628.
- (76) Le Bail, J.; Laroche, T.; Marre-Fournier, F.; Habrioux, G. Aromatase and 17 β -hydroxysteroid dehydrogenase inhibition by flavonoids. *Cancer Lett* **1998**, *133*, 101–106.
- (77) Le Bail, J.-C.; Pouget, C.; Fagnere, C.; Basly, J.-P.; Chulia, A.-J.; Habrioux, G. Chalcones are potent inhibitors of aromatase and 17 β -hydroxysteroid dehydrogenase activities. *Life Sci.* **2001**, *68*, 751–761.
- (78) Woo, L. L.; Howarth, N. M.; Purohit, A.; Hejaz, H. A.; Reed, M. J.; Potter, B. V. Steroidal and nonsteroidal sulfamates as potent inhibitors of steroid sulfatase. *J. Med. Chem.* **1998**, *41*, 1068–1083.
- (79) Woo, L. L.; Sutcliffe, O. B.; Bubert, C.; Grasso, A.; Chander, S. K.; Purohit, A.; Reed, M. J.; Potter, B. V. First dual aromatase-steroid sulfatase inhibitors. *J. Med. Chem.* **2003**, *46*, 3193–3196.
- (80) Woo, L. L.; Wood, P. M.; Bubert, C.; Thomas, M. P.; Purohit, A.; Potter, B. V. Synthesis and structure–activity relationship studies of derivatives of the dual Aromatase–sulfatase inhibitor 4-[(4-Cyanophenyl)(4H-1, 2, 4-triazol-4-yl) amino] methyl} phenyl sulfamate. *ChemMedChem* **2013**, *8*, 779–799.
- (81) Wood, P. M.; Woo, L. L.; Labrosse, J.-R.; Trusselle, M. N.; Abbate, S.; Longhi, G.; Castiglioni, E.; Lebon, F.; Purohit, A.; Reed, M. J.; Potter, B. V. Chiral aromatase and dual aromatase–steroid sulfatase

inhibitors from the letrozole template: Synthesis, absolute configuration, and in vitro activity. *J. Med. Chem.* **2008**, *51*, 4226–4238.

(82) Wood, P. M.; Woo, L. L.; Labrosse, J. R.; Thomas, M. P.; Mahon, M. F.; Chander, S. K.; Purohit, A.; Reed, M. J.; Potter, B. V. Bicyclic derivatives of the potent dual aromatase–steroid sulfatase inhibitor 2-Bromo-4-[[[4-cyanophenyl](4H-1, 2, 4-triazol-4-yl) amino] methyl] phenylsulfamate: Synthesis, SAR, crystal structure, and in vitro and in vivo activities. *ChemMedChem* **2010**, *5*, 1577–1593.

(83) Wood, P. M.; Woo, L. L.; Thomas, M. P.; Mahon, M. F.; Purohit, A.; Potter, B. V. Aromatase and dual aromatase-steroid sulfatase inhibitors from the letrozole and vorozole templates. *ChemMedChem* **2011**, *6*, 1423–1438.

(84) Jackson, T.; Woo, L. L.; Trusselle, M. N.; Chander, S. K.; Purohit, A.; Reed, M. J.; Potter, B. V. Dual aromatase–sulfatase inhibitors based on the anastrozole template: synthesis, in vitro SAR, molecular modelling and in vivo activity. *Org. Biomol. Chem.* **2007**, *5*, 2940–2952.

(85) Rausch, L.; Green, C.; Steinmetz, K.; LeValley, S.; Catz, P.; Zaveri, N.; Schweikart, K.; Tomaszewski, J.; Mirsalis, J. Preclinical pharmacokinetic, toxicological and biomarker evaluation of SR16157, a novel dual-acting steroid sulfatase inhibitor and selective estrogen receptor modulator. *Cancer Chemother. Pharmacol.* **2011**, *67*, 1341–1352.

(86) Ouellet, C.; Ouellet, É.; Poirier, D. In vitro evaluation of a tetrahydroisoquinoline derivative as a steroid sulfatase inhibitor and a selective estrogen receptor modulator. *Invest. New Drugs* **2015**, *33*, 95–103.

(87) Ouellet, C.; Maltais, R.; Ouellet, É.; Barbeau, X.; Lagüe, P.; Poirier, D. Discovery of a sulfamate-based steroid sulfatase inhibitor with intrinsic selective estrogen receptor modulator properties. *Eur. J. Med. Chem.* **2016**, *119*, 169–182.

(88) Ouellet, E.; Maltais, R.; Ouellet, C.; Poirier, D. Investigation of a tetrahydroisoquinoline scaffold as dual-action steroid sulfatase inhibitors generated by parallel solid-phase synthesis. *MedChemComm* **2013**, *4*, 681–692.

(89) Lespérance, M.; Roy, J.; Ngueta, A. D.; Maltais, R.; Poirier, D. Synthesis of 16 β -derivatives of 3-(2-bromoethyl)-estra-1, 3, 5 (10)-trien-17 β -ol as inhibitors of 17 β -HSD1 and/or steroid sulfatase for the treatment of estrogen-dependent diseases. *Steroids* **2021**, *172*, 108856.

(90) Bacsa, I.; Herman, B. E.; Jójárt, R.; Herman, K. S.; Wölfling, J.; Schneider, G.; Varga, M.; Tömböly, C.; Rižner, T. L.; Szécsi, M.; Mernyák, E. Synthesis and structure–activity relationships of 2-and/or 4-halogenated 13 β - and 13 α -estrone derivatives as enzyme inhibitors of estrogen biosynthesis. *J. Enzyme Inhib. Med. Chem.* **2018**, *33*, 1271–1282.

(91) Gargano, E. M.; Mohamed, A.; Abdelsamie, A. S.; Mangiatordi, G. F.; Drzewiecka, H.; Jagodziński, P. P.; Mazzini, A.; van Koppen, C. J.; Laschke, M. W.; Nicolotti, O.; Carotti, A.; Marchais-Oberwinkler, S.; Hartmann, R. W.; Frotscher, M. 17 β -Hydroxysteroid dehydrogenase type 1 inhibition: A potential treatment option for non-small cell lung cancer. *ACS Med. Chem. Lett.* **2021**, *12*, 1920–1924.

(92) Stanway, S. J.; Purohit, A.; Woo, L. L.; Sufi, S.; Vigushin, D.; Ward, R.; Wilson, R. H.; Stanczyk, F. Z.; Dobbs, N.; Kulinskaya, E.; Elliott, M.; Potter, B. V. L.; Reed, M. J.; Coombes, R. C. Phase I study of STX 64 (667 Coumate) in breast cancer patients: the first study of a steroid sulfatase inhibitor. *Clin. Cancer Res.* **2006**, *12*, 1585–1592.

(93) Ahmed, S.; James, K.; Owen, C. P.; Patel, C. K.; Patel, M. Novel inhibitors of the enzyme estrone sulfatase (ES). *Bioorg. Med. Chem. Lett.* **2001**, *11*, 841–844.

(94) Ferriz, J. M.; Vinsova, J. Prodrug design of phenolic drugs. *Curr. Pharm. Des.* **2010**, *16*, 2033–2052.

(95) Williams, S. J.; Denehy, E.; Krenske, E. H. Experimental and theoretical insights into the mechanisms of sulfate and sulfamate ester hydrolysis and the end products of type I sulfatase inactivation by aryl sulfamates. *J. Org. Chem.* **2014**, *79*, 1995–2005.

(96) Spillane, W. J.; Malaubier, J.-B. Mechanism of the hydrolysis of the sulfamate EMATE—an irreversible steroid sulfatase inhibitor. *Tetrahedron Lett.* **2010**, *51*, 2059–2062.

(97) Spillane, W. J.; McCaw, C. J.; Maguire, N. P. Kinetic and mechanistic studies of the hydrolysis of sulfamate esters: a non-

elimination decomposition route. *Tetrahedron Lett.* **2008**, *49*, 1049–1052.

(98) Bojarová, P.; Williams, S. J. Sulfotransferases, sulfatases and formylglycine-generating enzymes: a sulfation fascination. *Curr. Opin. Chem. Biol.* **2008**, *12*, 573–581.

(99) Ahmed, V.; Liu, Y.; Silvestro, C.; Taylor, S. D. Boronic acids as inhibitors of steroid sulfatase. *Biorg. Med. Chem.* **2006**, *14*, 8564–8573.

(100) Woo, L. W. L.; Bubert, C.; Sutcliffe, O. B.; Smith, A.; Chander, S. K.; Mahon, M. F.; Purohit, A.; Reed, M. J.; Potter, B. V. L. Dual aromatase–steroid sulfatase inhibitors. *J. Med. Chem.* **2007**, *50*, 3540–3560.

(101) Nussbaumer, P.; Billich, A. Steroid sulfatase inhibitors. *Med. Res. Rev.* **2004**, *24*, 529–576.

(102) Potter, B. V. SULFATION PATHWAYS: steroid sulphatase inhibition via aryl sulphamates: clinical progress, mechanism and future prospects. *J. Mol. Endocrinol.* **2018**, *61*, T233–T252.

(103) Purohit, A.; Williams, G. J.; Howarth, N. M.; Potter, B. V.; Reed, M. J. Inactivation of steroid sulfatase by an active site-directed inhibitor, estrone-3-O-sulfamate. *Biochemistry* **1995**, *34*, 11508–11514.

(104) Reed, J. E.; Lawrence Woo, L. L.; Robinson, J. J.; Leblond, B.; Leese, M. P.; Purohit, A.; Reed, M. J.; Potter, B. V. L. 2-Difluoromethyloestrone 3-O-sulphamate, a highly potent steroid sulphatase inhibitor. *Biochem. Biophys. Res. Commun.* **2004**, *317*, 169–175.

(105) Woo, L. L.; Purohit, A.; Malini, B.; Reed, M. J.; Potter, B. V. Potent active site-directed inhibition of steroid sulphatase by tricyclic coumarin-based sulphamates. *Chem. Biol.* **2000**, *7*, 773–791.

(106) Purohit, A.; Vernon, K.; Wagenaar Hummelinck, A. W.; Woo, L.; Hejaz, H.; Potter, B.; Reed, M. The development of A-ring modified analogues of oestrone-3-O-sulphamate as potent steroid sulphatase inhibitors with reduced oestrogenicity. *J. Steroid Biochem. Mol. Biol.* **1998**, *64*, 269–275.

(107) Thomas, M. P.; Potter, B. V. Discovery and development of the aryl O-sulfamate pharmacophore for oncology and women's health. *J. Med. Chem.* **2015**, *58*, 7634–7658.

(108) Chander, S. K.; Purohit, A.; Woo, L. L.; Potter, B. V.; Reed, M. J. The role of steroid sulphatase in regulating the oestrogenicity of oestrogen sulphamates. *Biochem. Biophys. Res. Commun.* **2004**, *322*, 217–222.

(109) Kruchten, P.; Werth, R.; Marchais-Oberwinkler, S.; Frotscher, M.; Hartmann, R. W. Development of a biological screening system for the evaluation of highly active and selective 17 β -HSD1-inhibitors as potential therapeutic agents. *Mol. Cell. Endocrinol.* **2009**, *301*, 154–157.

(110) Abdelsamie, A. S.; van Koppen, C. J.; Bey, E.; Salah, M.; Börger, C.; Siebenbürger, L.; Laschke, M. W.; Menger, M. D.; Frotscher, M. Treatment of estrogen-dependent diseases: Design, synthesis and profiling of a selective 17 β -HSD1 inhibitor with sub-nanomolar IC50 for a proof-of-principle study. *Eur. J. Med. Chem.* **2017**, *127*, 944–957.

(111) Gargano, E. M.; Perspicace, E.; Hanke, N.; Carotti, A.; Marchais-Oberwinkler, S.; Hartmann, R. W. Metabolic stability optimization and metabolite identification of 2, 5-thiophene amide 17 β -hydroxysteroid dehydrogenase type 2 inhibitors. *Eur. J. Med. Chem.* **2014**, *87*, 203–219.

(112) Perspicace, E.; Cozzoli, L.; Gargano, E. M.; Hanke, N.; Carotti, A.; Hartmann, R. W.; Marchais-Oberwinkler, S. Novel, potent and selective 17 β -hydroxysteroid dehydrogenase type 2 inhibitors as potential therapeutics for osteoporosis with dual human and mouse activities. *Eur. J. Med. Chem.* **2014**, *83*, 317–337.

(113) Abdelsamie, A. S.; Bey, E.; Gargano, E. M.; van Koppen, C. J.; Empting, M.; Frotscher, M. Towards the evaluation in an animal disease model: Fluorinated 17 β -HSD1 inhibitors showing strong activity towards both the human and the rat enzyme. *Eur. J. Med. Chem.* **2015**, *103*, 56–68.

(114) Chetrite, G. S.; Ebert, C.; Wright, F.; Philippe, A.-C.; Pasqualini, J. R. Control of sulfatase and sulfotransferase activities by medrogestone in the hormone-dependent MCF-7 and T-47D human breast cancer cell lines. *J. Steroid Biochem. Mol. Biol.* **1999**, *70*, 39–45.

(115) Kruchten, P.; Werth, R.; Bey, E.; Oster, A.; Marchais-Oberwinkler, S.; Frotscher, M.; Hartmann, R. W. Selective inhibition

of 17 β -hydroxysteroid dehydrogenase type 1 (17 β HSD1) reduces estrogen responsive cell growth of T47-D breast cancer cells. *J. Steroid Biochem. Mol. Biol.* **2009**, *114*, 200–206.

(116) Zhang, J.-H.; Chung, T. D.; Oldenburg, K. R. Confirmation of primary active substances from high throughput screening of chemical and biological populations: a statistical approach and practical considerations. *J. Comb. Chem.* **2000**, *2*, 258–265.

(117) Zhang, J.-H.; Chung, T. D.; Oldenburg, K. R. A simple statistical parameter for use in evaluation and validation of high throughput screening assays. *J. Biomol. Screen.* **1999**, *4*, 67–73.

(118) Moreno-Farre, J.; Workman, P.; Raynaud, F. Analysis of potential drug-drug interactions for anticancer agents in human liver microsomes by high throughput liquid chromatography/mass spectrometry assay. *Aust.-Asian J. Cancer* **2007**, *6*, 55–69.

(119) Hui, J. P.; Stuart Grossert, J.; Cutler, M. J.; Melanson, J. E. Strategic identification of in vitro metabolites of 13-desmethyl spirolicide C using liquid chromatography/high-resolution mass spectrometry. *Rapid Commun. Mass Spectrom.* **2012**, *26*, 345–354.

(120) Di, L.; Kerns, E. H.; Hong, Y.; Kleintop, T. A.; Mc Connell, O. J.; Huryn, D. M. Optimization of a higher throughput microsomal stability screening assay for profiling drug discovery candidates. *J. Biomol. Screen.* **2003**, *8*, 453–462.

3.3 A Hybrid In Silico/In Vitro Target Fishing Study to Mine Novel Targets of Urolithin A and B: A Step Towards a Better Comprehension of Their Estrogenicity

Luca Dellafiora, Marco Milioli, Angela Falco, Margherita Interlandi, **Abdelrahman Mohamed**, Martin Frotscher, Benedetta Riccardi, Paola Puccini, Daniele Del Rio, Gianni Galaverna, and Chiara Dall'Asta

Reprinted with permission *Mol. Nutr. Food Res.* 2020, 64 (16), 2000289.

DOI: 10.1002/mnfr.202000289

Copyright (2020) Wiley Online Library

Publication C

Contribution Report

The author performed and interpreted the radiolabeled *in vitro* biological assays.

RESEARCH ARTICLE

A Hybrid In Silico/In Vitro Target Fishing Study to Mine Novel Targets of Urolithin A and B: A Step Towards a Better Comprehension of Their Estrogenicity

Luca Dellafiora,* Marco Milioli, Angela Falco, Margherita Interlandi, Abdelrahman Mohamed, Martin Frotscher, Benedetta Riccardi, Paola Puccini, Daniele Del Rio, Gianni Galaverna, and Chiara Dall'Asta

Scope: Urolithin A and B are gut metabolites of ellagic acid and ellagitannins associated with many beneficial effects. Evidence in vitro pointed to their potential as estrogenic modulators. However, both molecular mechanisms and biological targets involved in such activity are still poorly characterized, preventing a comprehensive understanding of their bioactivity in living organisms. This study aimed at rationally identifying novel biological targets underlying the estrogenic-modulatory activity of urolithins.

Methods and Results: The work relies on an in silico/in vitro target fishing study coupling molecular modeling with biochemical and cell-based assays.

Estrogen sulfotransferase and 17 β -hydroxysteroid dehydrogenase are identified as potentially subject to inhibition by the investigated urolithins.

The inhibition of the latter undergoes experimental confirmation either in a cell-free or cell-based assay, validating computational outcomes.

Conclusions: The work describes target fishing as an effective tool to identify unexpected targets of food bioactives detailing the interaction at a molecular level. Specifically, it described, for the first time, 17 β -hydroxysteroid dehydrogenase as a target of urolithins and highlighted the need of further investigations to widen the understanding of urolithins as estrogen modulators in living organisms.

1. Introduction

Urolithins are small molecules with a dibenzo- α -pyrone scaffold variously hydroxylated (Figure 1) produced by the human gut microbiota from ellagitannins and ellagic acid.^[1] Urolithin precursors can be prevalent in certain diets being abundant in many fruits (e.g., pomegranates and berries), nuts (e.g., walnuts and almonds), and some wines.^[2] Urolithins may have a prominent role in the health benefits associated to diets rich in ellagitannins and ellagic acid, as a consequence of their rapid gastrointestinal formation and to the higher bioavailability in comparison to their high molecular weight precursors.^[3] Indeed, unlike ellagitannins and ellagic acid, urolithins may reach relatively high plasma concentration (up to 40 μ M) with a prevalence of conjugated forms and with a significant age-dependent variability.^[4,5] Urolithin aglycones were shown to be abundant in feces^[6] and their release from glucuronides either upon

gastrointestinal fermentation or at tissues level was displayed in vitro.^[7,8] The accumulation of both urolithin aglycones and glucuronides was also described in several tissues and at a cellular level,^[3,9,10] pointing to their capability to get broadly distributed throughout the body, either in the conjugated or un-conjugated state.

The spectrum of health-promoting effects of urolithins includes anti-inflammatory, anti-carcinogenic, cardioprotective, and neuroprotective properties.^[11,12] From a molecular perspective, urolithin A and B (UroA and UroB) can bind and modulate estrogen receptors (ERs).^[13–15] Additionally, urolithins were shown to act as estrogen modulators by influencing the expression of estrogen-regulated genes via an ER α -dependent mechanism.^[16] This evidence suggests a possible protective role in the framework of the cardiovascular system and prevention against estrogen-dependent cancer, similarly to other phytoestrogens.^[17,18] However, the network of biological targets underlying their capability to affect estrogenic pathways is only partially elucidated, preventing a full comprehension of

Dr. L. Dellafiora, Prof. G. Galaverna, Prof. C. Dall'Asta
Department of Food and Drug
University of Parma
Parma 43124, Italy
E-mail: luca.dellafiora@unipr.it

Dr. M. Milioli, Dr. A. Falco, Dr. M. Interlandi, Dr. B. Riccardi, Dr. P. Puccini
Corporate Pre-Clinical R&D
Chiesi Farmaceutici Spa
Parma 43122, Italy

Dr. A. Mohamed, Prof. M. Frotscher
Pharmaceutical and Medicinal Chemistry
Saarland University
Campus C23, Saarbrücken D-66123, Germany

Prof. D. D. Rio
Department of Veterinary Science
University of Parma
Parma 43126, Italy

The ORCID identification number(s) for the author(s) of this article can be found under <https://doi.org/10.1002/mnfr.202000289>

DOI: 10.1002/mnfr.202000289

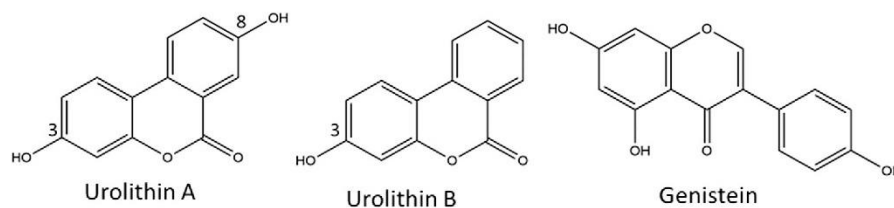


Figure 1. Structures of UroA, UroB, and genistein.

estrogen-related actions of urolithins *in vivo*. Contextually, the multi-target activity of food bioactives is increasingly gaining evidence. Therefore, additional targets beyond ERs are likely to be involved in urolithin estrogenicity and their identification has a primary importance for a more comprehensive understanding of urolithin bioactivity.

In this context, we applied an *in silico/in vitro* target fishing study to identify novel proteins possibly involved in the network of molecular events underlying the modulatory activity of urolithins on the estrogenic system. The workflow consisted in a ligand-based virtual screening followed by structure-based molecular modeling. All the ligands bound to proteins recorded in the Protein Data Bank (PDB; <https://www.rcsb.org>) were screened to find those most similar to UroA, taken as a reference. The chemical similarity between UroA and PDB ligands could be used as “bait” to identify proteins conceivably able to interact with urolithins. The interaction between the best protein candidates identified and UroA or UroB was then investigated with structure-based molecular modeling as previously shown.^[19] The interaction with the most promising candidate was checked experimentally.

2. Experimental Section

2.1. In Silico Study

2.1.1. Assembly of Ligands Database

The 3D structures of UroA and UroB were retrieved from PubChem (<https://pubchem.ncbi.nlm.nih.gov>; CID 5488186 and 5380406, respectively). The ligands database derived from the small molecules (26.868 structures; accessed on December 17, 2018) bound to proteins recorded in PDB (<https://www.rcsb.org>). The downloaded structures were processed using the FLAP software (<https://www.moldiscovery.com>)^[20] using default setting and choosing the descriptors (“probes”) H, DRY, N1, and O to describe ligands in terms of shape, hydrophobicity, and capability to donate or receive hydrogen bonds, respectively.

2.1.2. Ligand-Based Virtual Screening

The ligands database was screened using FLAP^[20] with default parameters selecting UroA as external template. The “quadruplet-based bit string mode” was used to speed up calculations. The outcome was ranked according to the “Global Sum” parameter.

2.1.3. Structure-Based Molecular Modeling

Docking simulations, pharmacophoric analysis, and molecular dynamic (MD) were applied on a selection of targets identified by the ligand-based virtual screening. The docking software GOLD was used to calculate binding architectures, as previously shown.^[21] The models for estrogen sulfotransferase (EST), fungal and human 17 β -hydroxysteroid dehydrogenase (17 β -HSD) were derived from PDB structures having code 1G3M, 4FJ1, and 3HB5, respectively. Software parameters, protocols, models, and ligands were set as previously reported.^[22] The GOLD scoring function PLPScore was used as it may reliably estimate the capability of ligands to satisfy pocket requirements (the higher the score, the better the fitting within pockets).^[19] For each protein target, the best-scored docking pose was considered as the most likely binding architecture, which served as input for MD.

MDs were run to investigate the permanence of urolithins within proteins binding site and to check the geometrical stability of complexes over the time. GROMACS version 5.1.4^[23] was used with CHARMM27 all-atom force field parameters support.^[24] Urolithins were processed with CHARMM27 all-atom force field using the SwissParam tool (<http://www.swissparam.ch>).^[25] Unresolved amino acid side chains were added using the “Composition” tool of “Biopolymer” module of Sybyl software (www.certara.com). A 50 nanoseconds simulation (300 K with a coupling time of 0.1 ps and 1 bar with a coupling time of 2.0 ps) for each complex was run as previously described.^[26]

2.2. In Vitro Assessment of Enzyme Inhibition

All non-radioactive chemicals were purchased with the highest grade available from Merck Sigma (St. Louis, MO, US) or Gibco—Thermo Fisher Scientific (Waltham, MA, US) unless stated otherwise. Radioactively labeled [2,4,6,7-³H]-E1 (50–100 Ci mmol⁻¹) was purchased from Perkin Elmer, Boston. Quick Safe Flow 2 Plus scintillator fluid was bought from Zinsser Analytic, Frankfurt.

2.2.1. Cell-Free 17 β -Hydroxysteroid Dehydrogenase Type 1 Inhibition Assay

The human enzyme was partially purified from human placental tissue as previously described.^[27] Fresh human placenta was homogenized, then cytosolic and microsomal fractions were separated by centrifugation. The cytosolic fraction was incubated with NADH (500 μ M) in phosphate buffer (50 mM, 37 °C pH = 7.4)

with 20% glycerol and EDTA (1 mM) in the presence of inhibitors in DMSO (the final DMSO concentration in the assay was 1%). The enzymatic reaction was started adding a mixture of unlabeled and radiolabeled substrate (total final concentration 500 nM). After 10 min, mercuric chloride (10 mM) was added to stop the reaction and steroids were extracted with diethylether. After evaporation, they were dissolved in acetonitrile/water (45:55). Estrone (E1) and 17 β -estradiol (E2) were separated on a C18 reversed phase chromatography column (Nucleodur C18 Gravity, Macherey–Nagel) connected to an Agilent 1200 Series (Agilent, Palo Alto, CA, USA) HPLC-system using acetonitrile/water (45:55) as mobile phase. A radioflow detector (Ramona, raytest) was coupled to the HPLC-system for the detection and quantification of steroids. After reviewing chromatograms (three independent experiments each), the conversion rates were calculated according to the following equation:

$$\% \text{conversion} = \left[\frac{\% E2}{\% E2 + \% E1} \right] \times 100 \quad (1)$$

Finally, the percentage of inhibition was calculated according to the following equation:

$$\% \text{inhibition} = \left[1 - \left(\frac{\% \text{conversion with inhibitor}}{\% \text{conversion of control (DMSO)}} \right) \right] \times 100 \quad (2)$$

Standard deviations were below 10%.

2.2.2. Cell-Based Assay

Cell Culture: Breast cancer cell line (MCF-7 cells) was obtained from the American Type Culture Collection and maintained in a 75 cm² culture flask at 37 °C in a humidified atmosphere at 5% CO₂. Cells were grown in DMEM/F12 (1:1) with 15 mM HEPES, without phenol red, supplemented with 10% fetal bovine serum (FBS), 1% L-glutamine and 1% penicillin/streptomycin. The medium was replaced every 2 days. Cells at 80% confluence were sub-cultured every 7 days by routine trypsinization. The assessment of enzymatic inhibition and proliferation assays were performed using cells from the same flask to minimize outcomes variability.

17 β -HSD Inhibition Assay: Cells were seeded in 24-well plates (65 × 10³ cells per well) in complete medium until they reached 80% confluence. Then they were placed in DMEM/F-12 (1:1) supplemented with 5% charcoal stripped and delipidated FBS for 2 days. To evaluate the inhibitory effect on 17- β -HSD, cells were treated with UroA or UroB at three different concentrations (10, 25, or 50 μ M). Each plate was pre-incubated for 30 min with enzyme inhibitors only (genistein, UroA, UroB, or HBSS buffer for control wells), as formerly mentioned,^[27] hence co-incubated with inhibitors plus the enzyme substrate E1 (50 nM). The well-known 17 β -HSD inhibitor genistein was taken as positive control (25 μ M), while the treatment with E1 50 nM alone was used to evaluate the baseline activity of the enzyme. Plates were incubated at 37 °C with 5% CO₂ for 3 and 6 h. At each time point (T0, 3 h, and 6 h) the supernatant was collected to evaluate the amount of E2 in all experimental conditions. Moreover, cell lysates were collected via osmotic lysis to measure inhibitors in-

take and growth medium was removed. Thus, cells were placed in lysis solution (250 μ L acetonitrile/water 75:25) and were shaken for 20 min. Three replicates of each treatment were run in each experiment and collected samples were analyzed using LC-ESI-MS/MS (see below).

Proliferation Assay: The effects of urolithins and genistein on MCF-7 viability were evaluated using the In Vitro toxicology assay kit-MTT based according to the manufacturer's instructions (Merk Sigma, St. Louis, MO, USA). Cells were seeded in 96-well microtiter plates at a density of 10.000 cells per well in maintenance medium. Absorbance was spectrophotometrically detected at a wavelength of 570 nm. Background absorbance of multiwell plates at 690 nm (blank containing complete medium without cells) was also measured and subtracted from the 570 nm measurement.

LC-ESI-MS/MS Analyses: An Agilent 1260 liquid chromatography system was used (Agilent, Palo Alto, CA, USA). Auto-sampler and column oven were kept at 8 °C and 35 °C, respectively. Chromatographic separation was achieved on a Gemini NX C18 (50 mm × 2.1 mm, 5 μ m, Phenomenex, Torrance, CA, USA) using ammonium hydroxide 0.5 mM in water (Solvent A) and ammonium hydroxide 0.5 mM in methanol (Solvent B) as mobile phases for E2. The gradient program was 0.0–0.5 min, 10% B; 0.5–2.0 min, gradient to 80% B; 2.0–3.5 min, gradient to 95% B; 3.5–3.7 min, gradient to 10% B; 3.7–6.0 min, 10% B. Regarding urolithins and genistein, ammonium formate (10 mM, pH = 4.6, Solvent A) and acetonitrile (Solvent B) were used. The gradient program was 0.0–0.5 min, 5% B; 0.5–2.0 min, gradient to 95% B; 2.0–3.0 min, 95% B; 3.0–3.5 min, gradient to 5% B; 3.5–6.0 min, 5% B. The flow rate and injection volume were set at 0.8 mL min⁻¹ and 10 μ L, respectively. The HPLC system was coupled with an AB SCIEX 4500 Q-TRAP triple quadrupole mass spectrometer (AB Sciex, Foster City, CA) equipped with an ESI Turbo ionspray source. The mass spectrometer was operated in negative ion mode. Ion spray voltage and temperature were set at -4500 V and 550 °C, respectively. Curtain and source gases were set at 30 and 35, respectively. Quantification was operated in multiple reaction monitoring (MRM) mode using the following m/z transitions: 271.011→144.950 for E2, 268.900→132.933 for genistein, 226.891→197.848 for UroA, 210.880→166.865 for UroB and 266.927→251.888 for formononetin (IS), respectively. Calibration curves were built from 3 to 125 nM for E2 (1/x² weighting, *r* = 0.995), from 6 to 1000 nM for urolithins (1/x weighting, *r* = 0.997) and from 6 to 500 nM for genistein (1/x weighting, *r* = 0.997). Data were acquired and processed using Analyst 1.6.2 software (AB Sciex, Foster City, CA).

Statistical Analysis: Data were expressed as means ± SEM. Statistical analyses were performed with GraphPad Prism 8.3.0 (GraphPad Software, San Diego, CA, USA) using two-way analysis of variance (ANOVA) and Tukey's post hoc test. Statistical significance was set at *p* < 0.05.

3. Results and Discussion

3.1. Target Fishing Study

Target fishing refers to the identification of novel biological targets for a given small molecule.^[28] It was applied here to identify

Table 1. List of top-ranked ligands from ligand-based virtual screening and respective proteins.

Ligand PDB code	Glob-Sum	Associated protein PDB code	Protein name	Organism
4HB	29.0	3ZV6	<i>cis</i> -biphenyl-2,3-dihydrodiol-2,3-dehydrogenase	<i>Comamonas testosteroni</i>
64I	27.7	4IGS/4ICC	Aldo-keto reductase	<i>Homo sapiens</i>
DDJ	27.6	3VLJ	KatG catalase-peroxidase	<i>Haloarcula marismortui</i>
7C3	26.1	5TN8	ER α	<i>H. sapiens</i>
7C2	21.0	5TN7	ER α	<i>H. sapiens</i>
PCQ	18.0	4MAS/2G5U	Transthyretin	<i>H. sapiens</i>
		1G3M	Estrogen sulfotransferase (EST) *	<i>H. sapiens</i>
REF	17.5	6RWD	Glutathione transferase	<i>Schistosoma japonicum</i>
		4YUA	Glycogen phosphorylase	<i>Oryctolagus cuniculus</i>
		2ZJW	Casein kinase 2 (CK2)	<i>H. sapiens</i>
HOM	16.6	1CJF	Profilin	<i>H. sapiens</i>
15Q	16.2	4IWF	ER α	<i>H. sapiens</i>
7EG	13.9	5TLG	ER α	<i>H. sapiens</i>
JSX	13.6	5QA8	Oxycillinase-48	<i>Klebsiella pneumoniae</i>
CHV	13.5	4ICF	Enoyl-acyl-carrier-protein reductase	<i>Plasmodium falciparum</i>
DV7	13.3	6BJZ	Antibody fragment	<i>H. sapiens</i>
		3CN2	Transthyretin	<i>H. sapiens</i>
3WJ	13.0	4 × 2F	Growth factor β receptor type 1 kinase domain	<i>H. sapiens</i>
6JM	12.9	5JCJ	Pteridine reductase 1	<i>Trypanosoma brucei brucei</i>
1HP	12.9	2QSE	ER α	<i>H. sapiens</i>
27N	12.9	4MGD	ER α	<i>H. sapiens</i>
TCT	12.8	1NNU	Enoyl-acyl-carrier-protein reductase	<i>Plasmodium falciparum</i>
CUE	12.7	5KR9	ER α	<i>Homo sapiens</i>
		4FIZ/3QWI	17 β -hydroxysteroid dehydrogenase (17 β -HSD) *	<i>Cochliolobus lunatus</i>
MYU	12.7	2O64	Pim-1 kinase	<i>H. sapiens</i>
		3V3V	c-jun NH2-terminal kinases	<i>H. sapiens</i>
BP7	12.7	4MMM	Pdx5	<i>H. sapiens</i>
		2EI0	1,2-dihydroxynaphthalene dioxygenase	<i>Pseudomonas sp.</i>
F95	12.6	4QAG/5HBM	HIV-1 Reverse Transcriptase	<i>Human immunodeficiency virus</i>
MRI	12.6	6AE3	GSK3 β -kinase	<i>H. sapiens</i>
		5AUY	Death-associated protein kinase 1	<i>H. sapiens</i>
4EV	12.6	4YKZ	HS protein 90	<i>H. sapiens</i>

*indicates proteins considered for molecular modeling.

novel targets likely involved in the capability of UroA and UroB to modulate the estrogenic system. As previously described,^[19] the target fishing study consisted in: i) ligand-based virtual screening to calculate chemical similarities between UroA and a wide set of molecules with known biological targets; ii) structure-based molecular modeling to study the interaction of urolithins with the targets identified (“fished”) in the ligand-based virtual screening.

3.1.1. Ligand-Based Virtual Screening

The ligands database was derived from all the ligands bound to proteins collected in PDB (26,036 ligands from the Ligands Repository; database accessed on December 17, 2018; <https://www.rcsb.org>). The FLAP software was used to screen 26,011 (25 ligands were excluded due to processing flaws) using UroA as template. Ligands were ranked according to the

“Glob-Sum” parameter, which estimates chemical similarities between molecules (the higher the score, the higher the ligands similarity), supporting a straightforward identification of ligands similar to UroA. The top 1% of ranked ligands was subsequently analyzed to track the respective biological targets to be considered for the next steps of analysis. The analysis was limited to the top 1%, focusing on proteins closely related to a ligand-dependent estrogenicity, to define a manageable set of proteins to carry forth the analysis. Three proteins directly related to a ligand-dependent estrogenic action were identified (Table 1): ER alpha, EST, and 17 β -HSD. UroA and UroB were previously depicted as ER ligands and their identification proved the fit-for-purpose effectiveness of methodology used. However, the presence of additional relevant targets among those listed in Table 1, either with indirect or ligand-independent roles on urolithins estrogenicity, cannot be excluded. For instance, CK2 is a kinase involved in the trans-activation and expression of ERs^[29] and assessing its inhibition,

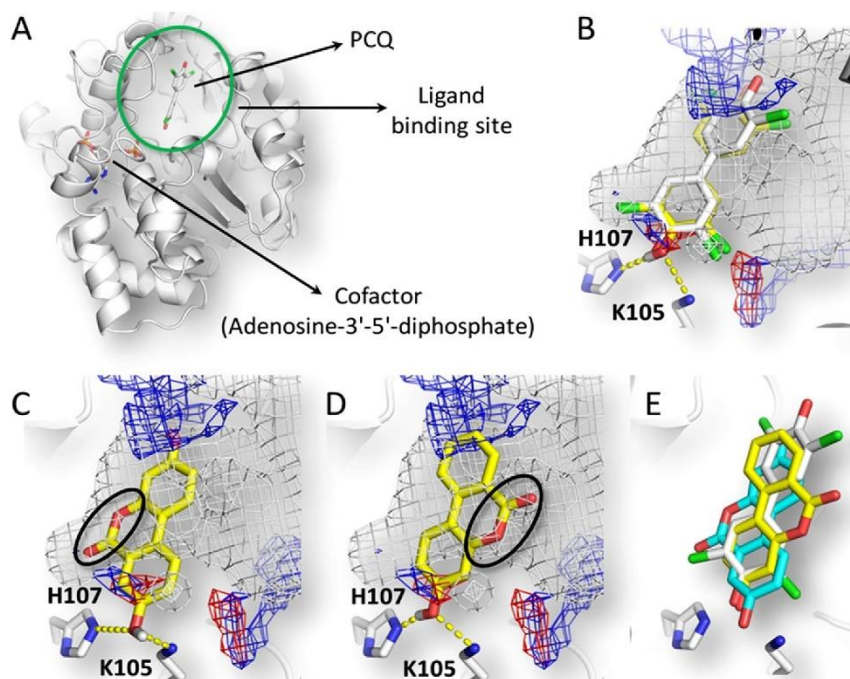


Figure 2. Docking simulations and pharmacophoric analysis of EST. The protein is represented in cartoon. Ligands and residues involved in polar interactions are represented in sticks. Yellow dotted lines indicate polar contacts. Black rings indicate the improper arrangement of polar groups within hydrophobic space. White, blue and red meshes indicate spaces suitable to receive hydrophobic, H-bond donor and H-bond acceptor groups, respectively. A) Graphical representation of EST (PDB code 1G3M). B) Superimposition of crystallographic and computed pose of PCQ (white and yellow, respectively) as in the structure with PDB code 1G3M. C) Calculated pose of UroA. D) Calculated pose of UroB. E) Superimposition of the crystallographic pose of PCQ (PDB code 1G3M; white) and the calculated pose of UroA and UroB (cyan and yellow, respectively).

which may have an indirect role on urolithins-dependent estrogenicity, might worth future dedicated investigations.

3.1.2. Structure-Based Modeling

EST and 17β -HSD underwent structure-based modeling, consisting in docking simulations to predict the binding mode of urolithins, coupled with pharmacophoric analysis and MD simulations to better estimate their capability to fit enzymes pocket and stably persist therein, as previously shown.^[26]

Estrogen sulfotransferase (EST). The enzyme may reduce estrogens activity transferring a sulfate group to free phenolic groups lowering estrogens amount at systemic or local level.^[30,31] The capability of UroA and UroB to interact with EST was assessed comparing their docking pose with the crystallographic architecture of the similar ligand identified by ligand-based virtual screening (PCQ; Table 1). Moreover, docking poses were analyzed in respect to the pocket pharmacophoric fingerprint to visually check the degree of urolithin-pocket complementarity. Furthermore, MD simulations were run to estimate the capability of UroA and UroB to persist within EST ligand binding site. Concerning docking simulations, the calculated pose of PCQ (43.4 score units) was in agreement with its crystallographic architecture (Figure 2B), pointing to the procedural efficacy to provide reliable binding ar-

chitectures, as previously discussed.^[26] The calculated poses of UroA and UroB (37.2 and 35.2 score units, respectively) were found well-fitting the ligand binding site with a good match between molecules arrangement and pocket pharmacophoric fingerprint (Figure 2C,D). However, the polar benzopyrone moiety of both urolithins occupied a hydrophobic region suggesting a degree of hydrophobic/polar interferences possibly resulting in a weaker interaction in comparison to PCQ (which better matched pocket hydrophobicity instead). This evidence was in line with the lower scores recorded for urolithins compared to PCQ. However, UroB was found mimicking the pocket occupancy of PCQ better than UroA (Figure 2E), potentially suggesting a more favored interaction. Concerning MD, the overall structure of EST in complex with both urolithins increased the RMSD (root-mean-square deviation) value during the first 20 ns, reaching a more stable geometry in the last part of simulations (Figure 3A). This result highlighted the non-optimal geometrical stability of starting conformations. Moreover, the analysis of geometrical stability of ligands and the network of polar interactions revealed important differences between the two urolithins (Figure 3B,C). UroA was found stably interacting within the pocket (with a low RMSD and a stable residence within the binding site over the time), while UroB was found less stable, as evidenced by the high RMSD value, with a trajectory outward the ligand binding site. Moreover, the analysis of hydrogen bonds described a

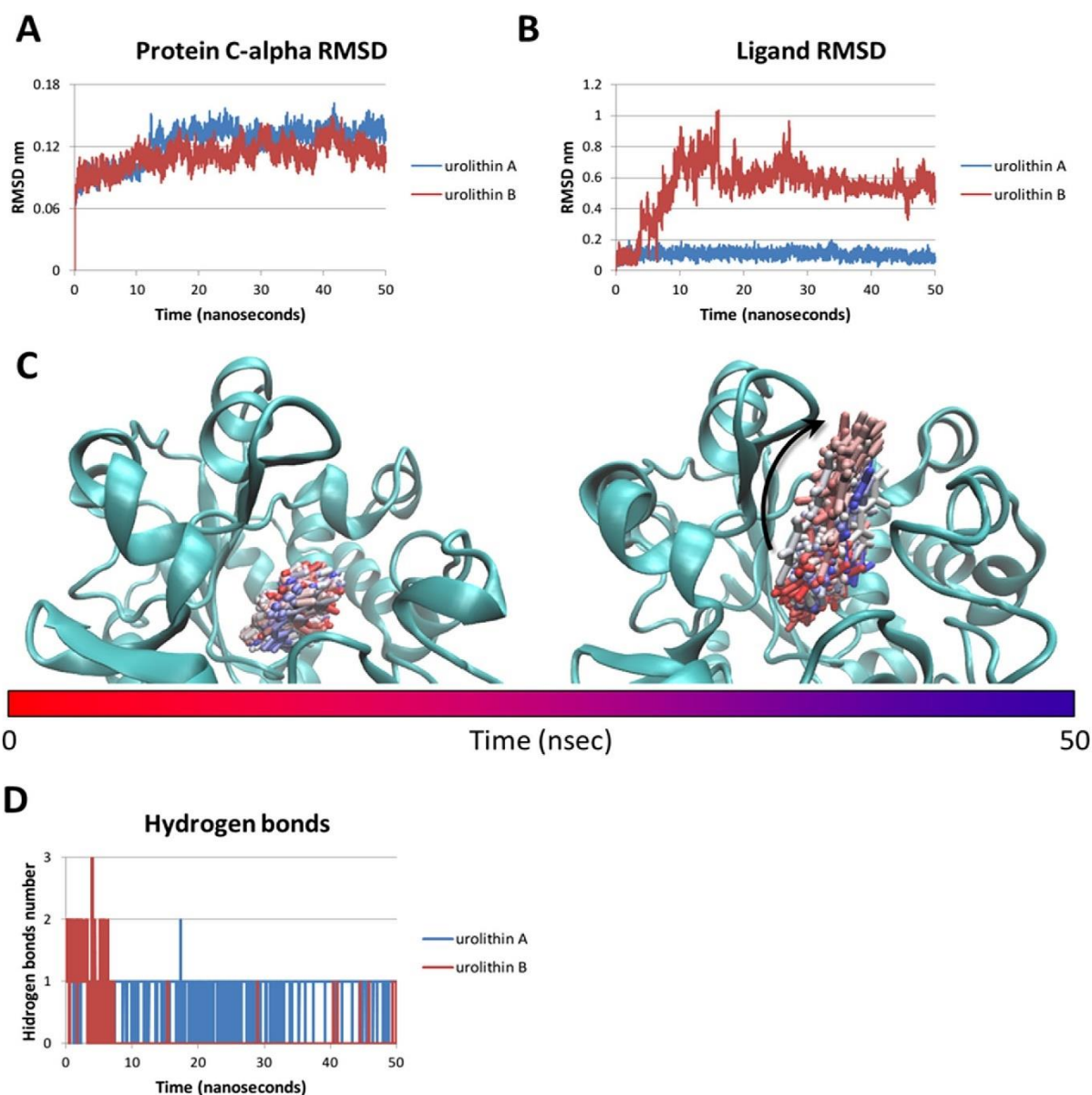


Figure 3. MD of EST. A) RMSD plots of protein C-alpha in complex with UroA or UroB. B) RMSD plot of UroA and UroB. C) Time-step representation of trajectories of UroA (on the right) and UroB (on the left). The from-red-to-blue color switch indicates stepwise changes of ligand coordinates over the time. The black arrow indicates the outward trajectory. D) Hydrogen bonds between EST and UroA or UroB over the time.

more favored interaction for UroA than UroB: the latter showed an early loss of hydrogen bonds, while the former was found most frequently engaging the protein with at least one hydrogen bond (Figure 3D). The hydrogen bonds loss of UroB could reasonably explain its trajectory outward the binding site. Overall, these results described EST as a possible target of both urolithin, though UroA seemed interacting more favorably than UroB.

17 β -hydroxysteroid dehydrogenase (17 β -HSD). The enzyme modulates the potency of steroids interconverting inactive 17-

keto-steroids and their more active 17 β -hydroxy forms.^[32] The fishing study found an orthologous of human 17 β -HSDs from the fungus *Cochliobolus lunatus*. This enzyme is however considered representative of the class of enzymes it belongs to, providing a valid benchmark model to study human orthologous.^[33] Therefore, the fungal 17 β -HSD was considered for docking simulations and pharmacophoric analysis to check the capability of UroA to fit its ligand binding site. As described for EST, the ability of UroA to interact with 17 β -HSD was assessed comparing

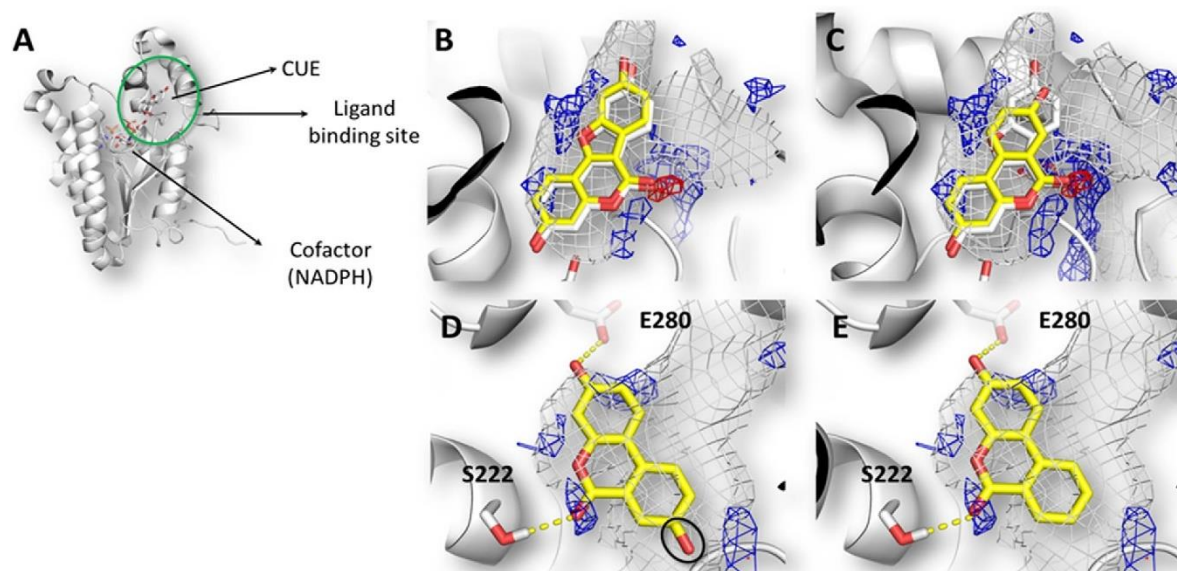


Figure 4. Docking simulations and pharmacophoric analysis of 17β -HSD. The protein is represented in cartoon. Ligands and residues involved in polar interaction are represented in sticks. Yellow dotted lines indicate polar contacts. Black rings indicate hydroxyl group proximal to hydrophilic space. White, blue and red meshes indicate spaces suitable to receive hydrophobic, H-bond donor and H-bond acceptor groups, respectively. A) Graphical representation of fungal 17β -HSD (PDB code 3HB5). B) Superimposition of crystallographic and computed pose of CUE (white and yellow, respectively) as in the structure having PDB code 3QWI. C) Superimposition of calculated pose of UroA and crystallographic pose of CUE (white and yellow, respectively) as in the structure having PDB code 3QWI. D) Calculated pose of UroA. E) Calculated pose of UroB.

its docking pose with the crystallographic architecture of the similar ligand identified by ligand-based virtual screening (CUE; Table 1). The calculated pose of CUE (76.6 score units) was in agreement with its crystallographic architecture (Figure 4B), supporting the procedure efficacy to provide reliable binding architectures. The calculated pose of UroA (76.2 score units) overlapped the crystallographic pose or CUE satisfying the pharmacophorical requirements of pocket (Figure 4C). The potential of urolithins to interact with 17β -HSD pocket was inferred accordingly. Therefore, the interaction of UroA and UroB with the human orthologous 17β -HSD1, which converts E1 to the more potent E2,^[27] was calculated. Concerning docking simulations and pharmacophoric analysis, UroA and UroB (58.6 and 59.2 score units, respectively) were found matching pharmacophorical requirements of 17β -HSD1 pocket. However, UroA placed the hydroxyl group in position #8 close to a hydrophilic pocket patch possibly resulting in a more favored interaction than UroB (Figure 4D,E).

Regarding MD, the RMSD analysis unveiled that complex geometry with both urolithins was found overall stable, with a steady-state fluctuation along the all simulation (Figure 5A,B). Moreover, the analysis of urolithins trajectories revealed their capability to stably persist within the catalytic site (Figure 5C). These results were in line with the stable network of hydrogen bonds found for both urolithins (Figure 5D).

On this basis, UroA and UroB were found stably interacting with the human 17β -HSD1 and a degree of inhibitory activity was inferred for them accordingly.

3.2. Experimental Assessment

The computational results collected for UroA and UroB pointed to a possible degree of inhibitory activity against 17β -HSD1, and its actual inhibition was checked experimentally. Nonetheless, a degree of interaction with EST may also be expected (see Section 3.1.2). Specifically, in silico analysis aimed at: i) defining the theoretical capability of urolithins to interact with 17β -HSD1; and ii) providing a qualitative estimate of their likeliness as inhibitors. Therefore, computational outcomes were not quantitatively compared to the results collected in vitro.

3.2.1. Cell-Free Inhibitory Assay

As a preliminary screening, UroA and UroB were tested at $20\ \mu\text{M}$ in a 17β -HSD1 cell-free inhibition assay. Genistein ($20\ \mu\text{M}$), a strong 17β -HSD1 inhibitor previously described,^[34] was used as positive control. The inhibition percentage observed for UroA, UroB and genistein with respect to the control (DMSO) was 82%, 64%, and 95%, respectively (mean value of 3 independent measurements, standard deviation < 10 %). These results proved the actual capability of both urolithins to inhibit 17β -HSD1, in agreement with computational findings.

3.2.2. Cell-Based Model

The capability of UroA or UroB to inhibit 17β -HSD1 was then assessed in a cell-based model checking the conversion of E1 to

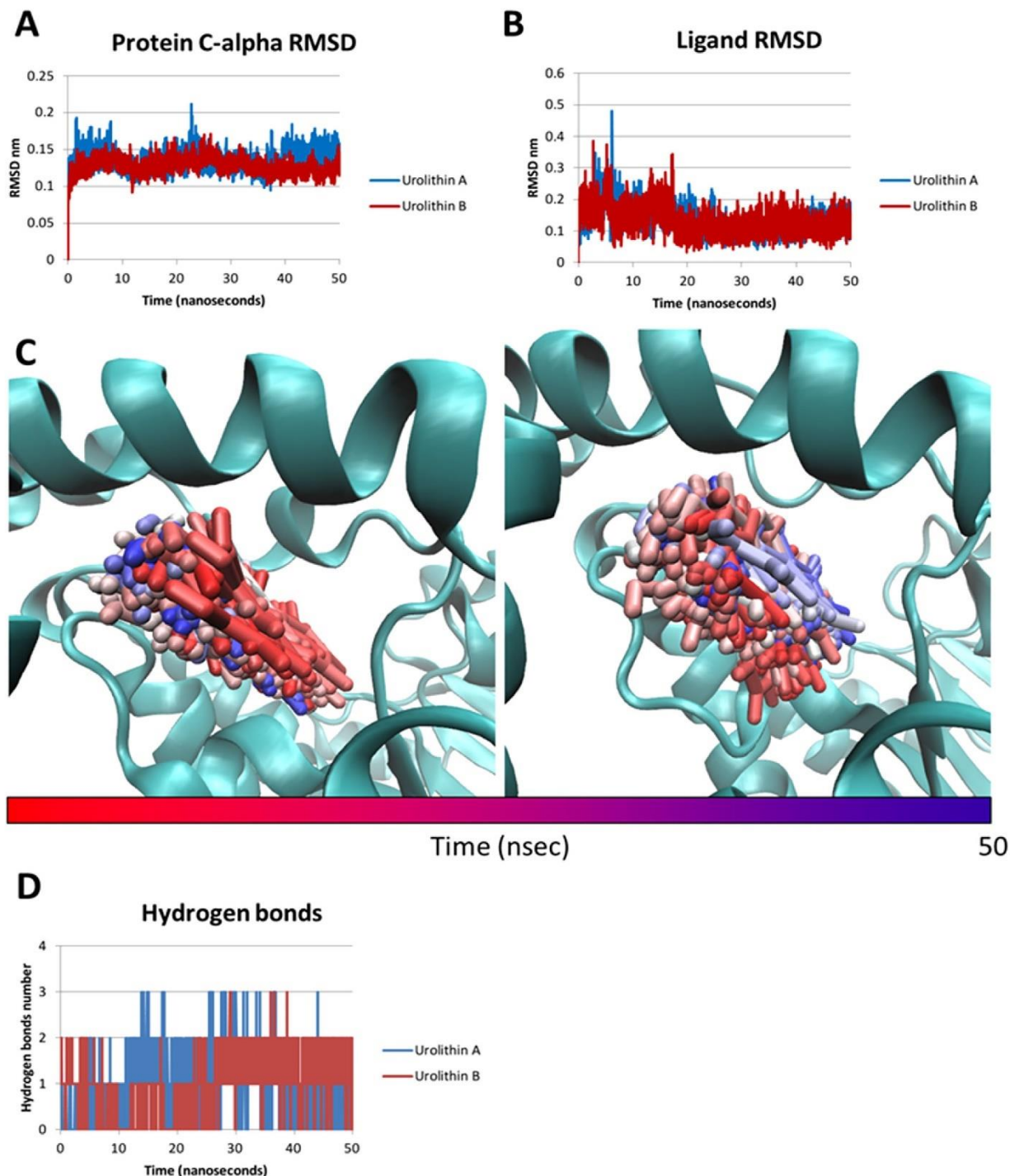


Figure 5. MD of 17β -HSD1. A) RMSD plots of protein C-alpha in complex with UroA or UroB. B) RMSD plot of UroA and UroB. C) Time-step representation of trajectories of UroA (on the right) and UroB (on the left). The from-red-to-blue color switch indicates the stepwise changes of ligand coordinates over the time. D) Hydrogen bonds number between 17β -HSD and UroA or UroB over the time.

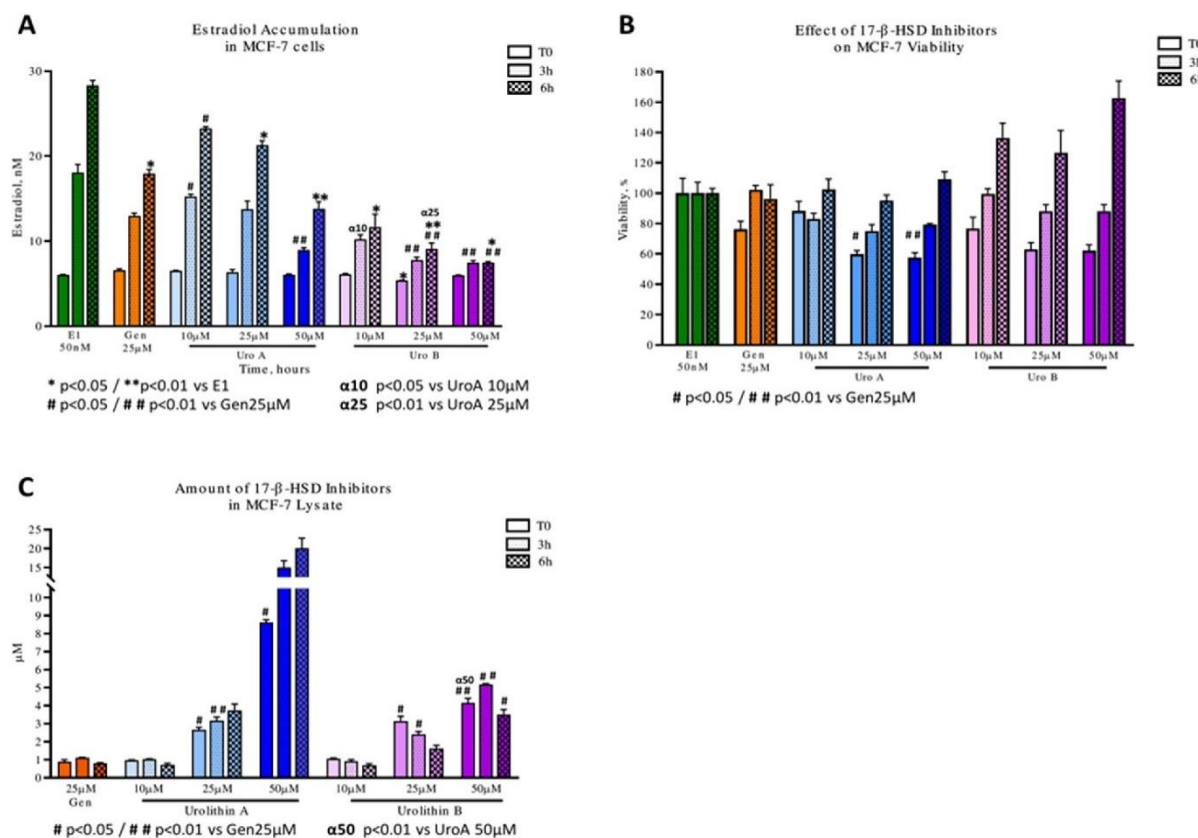


Figure 6. Results of cell-based 17β-HSD1 inhibitory assay. A) E2 accumulation in untreated cells (E1) or treated with, genistein, UroA or UroB. B) Cell viability of untreated cells (E1) or upon treatment with, genistein, UroA, or UroB. C) Cell internalization of genistein, UroA or UroB.

E2 in MCF-7 cells as formerly shown.^[35] MCF-7 cells represent a gold standard to check the estrogenicity of compounds, including urolithins.^[14] Moreover, previous studies proved the expression of 17β-HSD1 gene in MCF-7 electing this cell line as suitable for studying a ligand-dependent inhibition of 17β-HSD1.^[36,37] Nonetheless, this cell-based assay could not isolate precisely the role of 17β-HSD1 from that of other enzymes possibly involved in the modulation of E2 level. However, the integrated use of cell-free measurements (see above) consistently confirmed the actual role of 17β-HSD1 inhibition to reduce the level of E2, though the involvement of other ancillary mechanisms could not be excluded.

Inhibitory activity of UroA or UroB was tested at 10, 25, or 50 μM upon three or six treatment hours (3 and 6 h, respectively; **Figure 6**). Genistein (25 μM) was used as a positive control. The treatment with E1 alone served as reference control to measure the full transformation of E1 to E2. Genistein significantly reduced the production of E2 at 6 h compared to the cells treated with E1 alone ($p < 0.05$; **Figure 6A**). UroA 25 and 50 μM significantly reduced E2 production at 6 h compared to E1 alone ($p < 0.05$). Also, UroA 50 μM at 6 h was found more effective than the equimolar treatment with genistein. Concerning UroB, all examined concentrations were found able to significantly re-

duce E2 production at 6h in comparison to the treatment with E1 alone ($p < 0.05$). Additionally, UroB 25 and 50 μM at 3 or 6 h were found more efficient than genistein ($p < 0.05$). Moreover, comparing UroA with UroB, the latter appeared significantly more effective than the former at 10 μM upon 3 h of treatment and at 25 μM upon 6 h of treatment ($p < 0.01$). Keeping in mind that the inhibition of 17β-HSD1 leads to a depletion of E2, eventually resulting in anti-estrogenic effects, the lower inhibitory activity of UroA compared to UroB was in line with the higher estrogenicity of the former, as previously described.^[14]

Cell viability was also assessed via MTT assay for all tested conditions and no significant differences were found for UroB when compared to the corresponding time point controls with E1 alone or genistein (**Figure 6B**). Conversely, UroA 25 and 50 μM at the time zero were found able to slightly reduce cell viability more than the respective controls ($p < 0.05$), though at 3 and 6 h cell viability was comparable either to that of the treatments with genistein or E1 alone. All investigated compounds showed at the time zero a mean value lower than the one observed when cells were exposed to E1 alone. The reduction of viability observed in these treatments was in line with the anti-proliferative action against breast cancer cells previously described for urolithins and other polyphenols.^[38,39] However, transient adaptive mechanisms to

xenobiotics treatments at a very short exposure time tested are likely to be involved as well.

The accumulation of genistein, UroA, and UroB by cells was also checked measuring the compounds in cell lysates (Figure 6C). The treatment time did not affect significantly their accumulation. However, a higher mean accumulation for both urolithins with respect to genistein was found at 25 and 50 μM for all investigated time points, with a higher average concentration-dependent accumulation of UroA compared to UroB. However, keeping in mind that cells may express phase II enzymes,^[10] the diverse detection of UroA with respect to UroB in cell lysate might be due to a differential metabolic transformation of these compounds.

These results are important in the light of data collected in cell-free trials as, despite the lower inhibitory activity of both urolithins in comparison to genistein, the treatment with UroB at 25 and 50 μM resulted in a time-dependent higher inhibition compared to genistein 25 μM . The more pronounced accumulation of urolithins in comparison to genistein is reasonably crucial to determine the strong E2 reduction observed. However, the formation of more potent inhibitory metabolites due to cell metabolism cannot be excluded. Specifically, UroB could provide inhibitory metabolites more potent than UroA. This may rationally explain the inverted rank observed in the two assays (the cell-based assay UroB produced a stronger inhibition than UroA while the latter was a stronger inhibitor in the cell-free system). Furthermore, effects on other enzymes either involved in E2 formation or depletion may also differentiate the activity of urolithins. For instance, the inhibition of aromatase, an enzyme involved in the E2 biosynthesis, has been proved for UroA.^[40] Moreover, considering the capability of cells to express phase-II enzymes,^[10] a differential formation of phase-II metabolites from the two compounds possibly resulting in the diverse observed outcomes cannot be excluded. Generally, this and other similar phenomena related to a different enzyme inhibition by urolithins are likely to diversify their estrogenic/anti-estrogenic action, potentially resulting in diverse effects on estrogens levels either in cell systems or in living organisms.

Notably, the concentration of aglycones assessed in this study may exceed what commonly found in plasma upon consumption of food rich in urolithin precursors. However, the overall reported plasma levels of urolithin metabolites may span over a wide range, including those assessed in this study (e.g., ref. [41]). Moreover, plasma levels of urolithin conjugates three times higher than the highest concentration assessed here have been reported in a 3-day pilot walnut intervention study in human volunteers.^[42] This is particularly relevant in the light of the β -glucuronidase activity of tumor cells (including MCF-7), that can release aglycones from polyphenol conjugates, as previously shown (e.g., ref. [43]). Specifically, a significant role of β -glucuronidases, which are highly expressed in solid tumors, has been observed in the wide release of urolithin A and B aglycones from their respective glucuronides.^[44] Actually, the real internal level of aglycones at the site of action (i.e., the concentration at the district of protein-ligand interaction) is hard to estimate a priori, but it may poorly reflect the circulating level in plasma under some circumstances (e.g., in the case of cells with a high expression of β -glucuronidases). Indeed, conjugates-reverting activity of certain cell lines (e.g., MCF-7) and the high

plasma concentration of urolithin conjugates might result in a potentially high transient concentration of aglycones at the site of interaction. This made the assessment of aglycones at the tested concentrations reasonable to consistently describe urolithins in a representative mechanistic model system, accounting for the reversible conjugation–deconjugation phenomenon.

4. Concluding Remarks

The identification of previously unknown biological targets underlying urolithins effect on the estrogenic system is advisable towards a comprehensive understanding of their biological roles. In this context, computer-aided target fishing approaches may support a straightforward identification of novel and unexpected protein targets. This study described, for the first time, 17 β -HSD1 among the biological targets of UroA and UroB. In particular, even though the real relevance to the in vivo condition could not be easily extrapolated, the collected results clearly pointed out: i) the capability of certain dibenzo- α -pyrones to interact and inhibit this enzyme in vitro (UroA and UroB were used as case study); ii) cells prone of conjugates-reverting activity may be exposed to 17 β -HSD1 inhibition by UroA and UroB. Although the outcomes of cell-based assays could not exclude the existence of other 17 β -HSD-independent mechanisms, the evidence produced through cell-free conditions proved the actual inhibition of 17 β -HSD1. These results highlighted a new mechanism, with possible implications in living organisms, the relevance of which is worth additional research to better understand urolithin bioactivity. Of note, the inhibitory activity described in this study might cause anti-estrogenic effects. However, the overall effect of UroA and UroB in vivo shall need to be interpreted from a more general point of view considering the complex network of mechanisms involved, also in the light of the likely combined action of chemical mixtures of food origin. The provided results also underlined the need to carefully investigate the differential cellular fate of UroA and UroB as they might generate a pattern of metabolites with a different inhibitory action against 17 β -HSD1. Particularly, the phase-II conjugates deserve a high priority. Moreover, the results collected clearly described the multi-target activity of this class of compounds, which may have a manifold action on urolithins estrogenicity. Specifically, UroA and UroB might have differential estrogenic/anti-estrogenic effects at both ligand-dependent and ligand-independent levels, acting on enzymes directly involved in the estrogens level (e.g., EST and 17 β -HSD1) or on proteins involved in the regulation/expression of ERs (e.g., CK2).

As a general remark, this work represents a proof of principle towards a better comprehension of the mechanisms of action of urolithins bioactivity. In this context, the study provided a knowledge-based foothold to better understand the possible effects of urolithins on the estrogenic system from a molecular standpoint. Further studies need to be carried out to address more comprehensively the inhibitory potential of other urolithin metabolites and the design of future in vitro to in vivo extrapolation studies is desirable to better link our evidence to the in vivo conditions. However, this work provided a compelling line-of-evidence to consider the inhibition of 17 β -HSD1 in future investigations to better describe the modulatory effects of ellagitannins derivatives in vivo.

Acknowledgements

This research benefits from the HPC (high performance computing) facility of the University of Parma, Italy. The authors would like to acknowledge Prof. Gabriele Cruciani for the courtesy of FLAP software (www.moldiscovery.com).

Conflict of Interest

The authors declare no conflict of interest.

Authors Contributions

L.D. and M.M. contributed equally to this work. L.D., C.D., G.G., and D.D. conceptualization, writing-original draft preparation, data discussion; M.M., A.F., M.L., B.R., and P.P. supervision of cell-based experiments and data discussion; M.F. and A.M. supervision of cell-free experiments.

Keywords

17 β -hydroxysteroid dehydrogenase type 1, estrogenic activity, food bioactives, target fishing, urolithins

Received: March 27, 2020
Revised: June 23, 2020
Published online: July 20, 2020

- [1] S. Alfei, F. Turrini, S. Catena, P. Zunin, M. Grilli, A. M. Pittaluga, R. Boggia, *Eur. J. Med. Chem.* **2019**, *183*, 111724.
- [2] J. M. Landete, *Food Res. Int.* **2011**, *44*, 1150.
- [3] F. A. Tomas-Barberan, A. Gonzalez-Sarrias, R. Garcia-Villalba, M. A. Nunez-Sanchez, M. V. Selma, M. T. Garcia-Conesa, J. C. Espin, *Mol. Nutr. Food Res.* **2017**, *61*, 1500901.
- [4] A. Cortes-Martin, R. Garcia-Villalba, A. Gonzalez-Sarrias, M. Romo-Vaquero, V. Loria-Kohen, A. Ramirez-de-Molina, F. A. Tomás-Barberán, M. V. Selma, J. C. Espin, *Food Funct.* **2018**, *9*, 4100.
- [5] M. Romo-Vaquero, R. Garcia-Villalba, A. Gonzalez-Sarrias, D. Beltrán, F. A. Tomás-Barberán, J. C. Espin, M. V. Selma, *J. Funct. Foods* **2015**, *17*, 785.
- [6] P. Saha, B. San Yeoh, R. Singh, B. Chandrasekar, P. K. Vemula, B. Haribabu, M. Vijay-Kumar, V. R. Jala, *PLoS One* **2016**, *11*, e0156811.
- [7] P. Mena, M. Dall'Asta, L. Calani, F. Brighenti, D. Del Rio, *Eur. J. Nutr.* **2017**, *56*, 99.
- [8] M. A. Avila-Galvez, J. A. Gimenez-Bastida, A. Gonzalez-Sarrias, J. C. Espin, *Food Funct.* **2019**, *10*, 3135.
- [9] M. A. Nunez-Sanchez, R. Garcia-Villalba, T. Monedero-Saiz, N. V. Garcia-Talavera, M. B. Gómez-Sánchez, C. Sánchez-Álvarez, A. M. García-Albert, F. J. Rodríguez-Gil, M. Ruiz-Marín, F. A. Pastor-Quirante, F. Martínez-Díaz, M. J. Yáñez-Gascón, A. González-Sarrias, F. A. Tomás-Barberán, J. C. Espin, *Mol. Nutr. Food Res.* **2014**, *58*, 1199.
- [10] G. Aragonés, F. Danesi, D. Del Rio, P. Mena, *Trends Food Sci. Technol.* **2017**, *69*, 230.
- [11] M. V. Selma, D. Beltran, M. C. Luna, M. Romo-Vaquero, R. García-Villalba, A. Mira, J. C. Espin, F. A. Tomás-Barberán, *Front. Microbiol.* **2017**, *8*, 1521.
- [12] L. Mele, P. Mena, A. Piemontese, V. Marino, N. López-Gutiérrez, F. Bernini, F. Brighenti, I. Zanotti, D. Del Rio, *Arch. Biochem. Biophys.* **2016**, *599*, 42.
- [13] L. Dellafiara, P. Mena, P. Cozzini, F. Brighenti, D. Del Rio, *Food Funct.* **2013**, *4*, 1442.
- [14] M. Larrosa, A. Gonzalez-Sarrias, M. T. Garcia-Conesa, F. A. Tomas-Barberan, J. C. Espin, *J. Agric. Food Chem.* **2006**, *54*, 1611.
- [15] D. G. Skledar, T. Tomasic, M. S. Dolenc, L. P. Masic, A. Zega, *Chemosphere* **2019**, *220*, 706.
- [16] W. Zhang, J. H. Chen, I. Aguilera-Barrantes, C. W. Shiao, X. Sheng, L. S. Wang, G. D. Stoner, Y. W. Huang, *Mol. Nutr. Food Res.* **2016**, *60*, 2387.
- [17] H. S. Aiyer, A. M. Warri, D. R. Woode, L. Hilakivi-Clarke, R. Clarke, *J. Agric. Food Chem.* **2012**, *60*, 5693.
- [18] M. Larrosa, M. T. Garcia-Conesa, J. C. Espin, F. A. Tomas-Barberan, *Mol. Aspects Med.* **2010**, *31*, 513.
- [19] L. Dellafiara, G. Aichinger, E. Geib, L. Sánchez-Barrionuevo, M. Brock, D. Cánovas, C. Dall'Asta, D. Marko, *Food Chem.* **2019**, *270*, 61.
- [20] M. Baroni, G. Cruciani, S. Sciabola, F. Perruccio, J. S. Mason, *J. Chem. Inf. Model.* **2007**, *47*, 279.
- [21] L. Dellafiara, P. Mena, D. Del Rio, P. Cozzini, *J. Agric. Food Chem.* **2014**, *62*, 5881.
- [22] L. Dellafiara, M. Marchetti, F. Spyrikis, V. Orlandi, B. Campanini, G. Cruciani, P. Cozzini, A. Mozzarelli, *Bioorg. Med. Chem. Lett.* **2015**, *25*, 4297.
- [23] M. J. Abraham, T. Murtola, R. Schulz, S. Páll, J. C. Smith, B. Hess, E. Lindahl, *SoftwareX* **2015**, *1–2*, 19.
- [24] R. B. Best, X. Zhu, J. Shim, P. E. Lopes, J. Mittal, M. Feig, A. D. MacKerell Jr., *J. Chem. Theory Comput.* **2012**, *8*, 3257.
- [25] V. Zoete, M. A. Cuendet, A. Grosdidier, O. Michielin, *J. Comput. Chem.* **2011**, *32*, 2359.
- [26] L. Dellafiara, G. Galaverna, G. Cruciani, C. Dall'Asta, *Food Chem. Toxicol.* **2019**, *130*, 199.
- [27] P. Kruchten, R. Werth, S. Marchais-Oberwinkler, M. Frotscher, R. W. Hartmann, *Mol. Cell. Endocrinol.* **2009**, *301*, 154.
- [28] N. Wale, G. Karypis, *J. Chem. Inf. Model.* **2009**, *49*, 2190.
- [29] M. D. Williams, T. Nguyen, P. P. Carriere, S. L. Tilghman, C. Williams, *Int. J. Environ. Res. Public Health* **2016**, *13*, 36.
- [30] W. G. Garbacz, M. Jiang, W. Xie, *Adv. Exp. Med. Biol.* **2017**, *1043*, 455.
- [31] E. Sonneveld, J. A. Riteco, H. J. Jansen, B. Pieterse, A. Brouwer, W. G. Schoonen, B. van der Burg, *Toxicol. Sci.* **2006**, *89*, 173.
- [32] D. Poirier, *Curr. Med. Chem.* **2003**, *10*, 453.
- [33] A. Cassetta, J. Stojan, I. Krastanova, K. Kristan, M. Brunskole Šveglj, D. Lamba, T. Lanišnik Rižner, *J. Steroid Biochem. Mol. Biol.* **2017**, *171*, 80.
- [34] D. Schuster, L. G. Nashev, J. Kirchmair, C. Laggner, G. Wolber, T. Langer, A. Odermatt, *J. Med. Chem.* **2008**, *51*, 4188.
- [35] J. D. Brooks, L. U. Thompson, *J. Steroid Biochem. Mol. Biol.* **2005**, *94*, 461.
- [36] G. S. Chetrite, J. R. Pasqualini, *J. Steroid Biochem. Mol. Biol.* **2001**, *76*, 95.
- [37] E. Hilborn, O. Stal, A. Alexeyenko, A. Jansson, *Oncotarget* **2017**, *8*, 62183.
- [38] N. Panth, B. Manandhar, K. R. Paudel, *Phytother. Res.* **2017**, *31*, 568.
- [39] A. Uifalean, S. Schneider, C. Ionescu, M. Lalk, C. A. Iuga, *Molecules* **2016**, *21*, E13.
- [40] L. S. Adams, Y. J. Zhang, N. P. Seeram, D. Heber, S. A. Chen, *Cancer Prev. Res.* **2010**, *3*, 108.
- [41] J. C. Espin, M. Larrosa, M. T. Garcia-Conesa, F. Tomas-Barberan, *Evid. Based Complement. Alternat. Med.* **2013**, *2013*, 270418.
- [42] B. Pfundstein, R. Haubner, G. Würtele, N. Gehres, C. M. Ulrich, R. W. Owen, *J. Agric. Food Chem.* **2014**, *62*, 10264.
- [43] B. Yuan, L. L. Wang, Y. Jin, H. J. Zhen, P. Xu, Y. Xu, C. Li, H. Xu, *AAPS J.* **2012**, *14*, 329.
- [44] J. P. Piwowarski, I. Stanisławska, S. Granica, J. Stefańska, A. K. Kiss, *Drug Metab. Dispos.* **2017**, *45*, 657.

4. Discussion and conclusions

The main goal of the thesis was to create inhibitors that can be used to treat estrogen dependent diseases (EDDs), such as non-small cell lung cancer (NSCLC) and endometriosis, by inhibiting peripheral E2 development via targeting the enzymes responsible for E2 synthesis in the diseased tissues, such as STS and 17 β -HSD1. In comparison to the current endocrine treatments for EDDs, this novel approach is now seen as a safer therapeutic strategy with the possibility of fewer adverse effects since systemic estrogen action should be less affected. The work was divided into two approaches to achieve the goal of this study: the first is the development of a new class of non-steroidal and selective inhibitors of 17 β -HSD1 capable of improving the treatment of NSCLC, chapter 3.1, and the second is the synthesis of sulfamate compounds that are drugs for STS inhibition and prodrugs for 17 β -HSD1 inhibition as a new therapeutic option for the treatment of endometriosis (drug-prodrug approach), chapter 3.2. For description of the compounds listed in this section, a capital letter for the respective manuscript accompanying an Arabic number for compound numbers in the respective manuscript are used.

4.1 Synthesis of inhibitors of 17 β -HSD1 for treatment non-small cell lung cancer (NSCLC)

As stated in the introduction, lung cancer is the world's most frequent cause of death associated with cancer, and more than 85 percent of cases represented by NSCLC. Consequently, it is imperative to discover more effective medicines with innovative modes of action. According to rising evidence over the last two decades, estrogens play a key role in lung tumorigenesis in both men and women and 17 β -HSD1, which catalyzes the weakly active E1 to the potent estrogen E2, is widely expressed in NSCLC cells, and help to stimulate tumor progression. Thus, 17 β -HSD1 inhibition appears to be a promising therapeutic alternative for NSCLC. A small library of 2,5- disubstituted furane amide derivatives was synthesized and tested towards 17 β -HSD1 in cell-free assays and they displayed exceptionally high 17 β -HSD1 inhibitory activity, (results were shown in chapter 3.1). Additionally, the selectivity of the compounds over 17 β -HSD2 was studied, and it was discovered that **A1** and **A2** (Figure 17) were extremely selective over 17 β -HSD2 (selectivity factors = 563 and 145, respectively), suggesting that methyl groups improved selectivity over 17 β -HSD2. Compound **A1** was the most promising compound in the series and thus had been tested for its affinity to the estrogen receptors α and β (ERs) and it showed low affinity with a relative binding affinity (RBA) below 0.1%.

Furthermore, the effectiveness of compound **A1** was explored in cellular studies using NSCLC Calu-1 cell lines, and it completely inhibited E1-dependent Calu-1 cell proliferation at low nanomolar concentrations, providing the first compelling proof that 17 β -HSD1 is an appropriate target for the treatment of NSCLC, opening up new perspectives to deal with this deadly disease, which is urgently required. In contrast to the previously discovered 2,5-disubstituted thiophene amide derivatives which had short half-lives (< 5 minutes), compound **A1** had a 50-minute half-life in human liver S9 fraction (phase I and II metabolism). It can be concluded that the furan ring plays a major role in the stability of such compounds. In addition, cytotoxicity for **A1** was tested in the MTT assay using HEK293 cells, and no toxic impact was observed up to 6.25 M, which was more than 1000 times the IC₅₀ value. This section of the study provided the first proof that a highly selective 17 β -HSD1 inhibitor may be used to suppress NSCLC cell proliferation.

4.2 Dual inhibition of STS and 17 β -HSD1: a novel drug-prodrug approach for the treatment of endometriosis

In recent years, the steroidogenic enzymes STS and 17 β -HSD1 have gained attention as promising therapeutic targets for endometriosis, as their inhibition has the ability to effectively reduce estrogen levels in the peripheral and local tissues without the common hypo-estrogenic side effects that characterize the existing treatment options. It was found that, both STS and 17 β -HSD1 have been shown to be over-expressed in endometriosis compared to normal endometrial tissue. This section of the project looked at the design and synthesis of a variety of non-steroidal molecules that function as dual inhibitors of STS and 17 β -HSD1 (DSHIs) as a new strategy for the treatment of endometriosis. Agents that inhibit multiple enzymes in the steroidogenic pathway can help to block estrogen biosynthesis in endometriotic tissues more effectively, which might be capable of providing the effects of a combination therapy as a single drug. To see whether this idea could also be generalized to the dual inhibition of STS and 17 β -HSD1, a number of novel compounds were synthesized by introducing the pharmacophore required for inhibition of STS (aryl-O-sulfamate moiety) into *in-house* 17 β -HSD1 inhibitors. We hoped to engineer inhibitory action against STS into these compounds, and the parent phenols will be released *in vivo* to inhibit 17 β -HSD1 through chemical hydrolysis and/or sulfatase-mediated cleavage of their corresponding sulfamates after STS inactivation. As a result, sulfamate final compounds are drugs for STS inhibition and prodrugs for 17 β -HSD1 inhibition. Several sulfamates were synthesized and tested in cellular assays for STS inhibition, using T47D breast cancer cell lines and their precursor phenols were also synthesized and tested

towards 17 β -HSD1 in both cell-free and cellular assays. Structure activity relationship (SAR) studies have been performed on this class and is presented in chapter 3.2. It was discovered that the optimal position of the sulfamate moiety to the attachment point of the ring was in *meta* or *para* positions (position 3: **B13** and 4: **B14** on ring C in Figure 17), while the compound with an *ortho* sulfamate group showed no STS inhibitory activity. Further, STS inhibitory activity was improved relative to **B13** with the inclusion of electron-withdrawing groups into ring C (F: **B18, B20**; Cl: **B16, B19**), while methyl as an electron-donating group decreased it. When the phenyl moiety of ring A (Figure 17) was substituted with pyridine (**B28-B30**), the STS inhibitory activity was reduced 10 to 40-fold compared to **B13**. The replacement of the furan ring (B) with oxazole **B36** and thiazole **B37** resulted in a 2-fold reduction for the inhibition of STS, whereas oxadiazole had a drastic decrease in inhibitory function, compared to **B13**. 2,4-thiazole **B37** had a 2-fold increase in potency when compared to its isomer 2,5-thiazole. As a conclusion, furan derivatives (**B13, B16, B18-B20, and B22-B24**), oxazole **B36**, and 2,4-thiazole **B37** displayed nanomolar IC₅₀ values when tested against STS in T47D cells, suggesting good cell penetration and also, they were able to significantly inhibit STS in an irreversible mode of action. The hydroxyl group has been shown in the literature to play an important role in the inhibition of 17 β -HSD1 and this was proved by testing the most active sulfamate compounds towards 17 β -HSD1 in cell-free assays, and the results showed that the tested sulfamates were inactive against 17 β -HSD1. So, the corresponding phenolic derivatives were synthesized and screened against 17 β -HSD1 in both cell-free and cellular assays. It was discovered that for good 17 β -HSD1 activity, the hydroxyl group of ring C should be in the *para* **B1** or *meta* position **B2**, as the *ortho* position abolished the activity (Figure 17). In addition, the introduction of electronegative atoms (F: **B6, B8**; Cl: **B4, B7**) and electron donation group (CH₃: **B5**) enhanced the inhibitory activity against 17 β -HSD1. In comparison to **B1**, the pyridine derivatives **B26** and **B27** displayed a 2-3-fold decrease in cellular 17 β -HSD1 inhibitory activity, while **B25** completely abolished the activity (Figure 17). For ring B, 2,4-thiazole **B33** improved 17 β -HSD1 inhibitory activity relative to furan **B1**, while the other heterocyclic rings; oxadiazole, oxazole, and 2,5-thiazole decreased it. Moreover, the selectivity of all 17 β -HSD1 inhibitors over 17 β -HSD2 was tested. In comparison to **B1** (SF = 51), insertion of Cl (**B4**, SF = 74), CH₃ (**B5**, SF = 150), and F (**B6**, SF = 85) in position 3 (*ortho* to OH) of ring C (Figure 17) improved selectivity and compounds with substituents in position 3 (*ortho* to OH) were more selective than those with substituents in position 2 (*meta* to OH). Pyridine derivatives **B26** and **B27** were highly selective for 17 β -HSD2. In terms of the effect of different middle rings on selectivity over 17 β -HSD2, 2,4-thiazole **B33** displayed a significant improvement in selectivity

(SF= 115) and oxazole **B32** gave the same selectivity factor as **B1**, while furan substitution with oxadiazole and 2,5-thiazole resulted in compounds with reduced selectivity over 17 β -HSD2. It's also important that the compounds should have no or just a minor affinity for ERs, as binding to these receptors may interfere with therapeutic efficacy. Thus, the ER α binding affinities of sulfamate derivatives **B13**, **B16**, **B19**, **B23**, and **B37**, as well as their corresponding phenols **B1**, **B4**, **B7**, **B11**, and **B33**, were examined, and the compounds displayed low binding affinities. Metabolic stability plays an important role in maximizing the bioavailability of new drugs, which improves their probability of effectiveness after their *in vivo* application. Therefore, the most active sulfamates **B13**, **B16**, **B18-B20**, **B22-B24**, **B36**, and **B37** were tested for their metabolic stability, using human and mouse hepatic S9 fractions. Oxazole **B36** had the highest metabolic stability profile, with $t_{1/2}$ of 181 and 47 minutes, in both human and mouse hepatic S9 fractions, respectively. 2,4-thiazole **B37** was less metabolically stable than oxazole **B36** in both human, $t_{1/2}$ = 50 min and mouse, $t_{1/2}$ = 15 min hepatic S9 fractions. Furthermore, furan containing compounds **B13**, **B16**, **B18-B20**, and **B22-B24** showed moderate metabolic stability, $t_{1/2}$ = 47, 48, 43, 39, 51, 34, 44 and 24 min, respectively, supporting a reasonable metabolic profile. In addition, MTT assays were performed using HEK-293 cells to assess the potential cytotoxicity of **B13**, **B16**, **B19**, and **B37**, as well as their conjugate phenols **B1**, **B4**, **B7**, and **B33**. At a concentration of 20 μ M, cell growth was inhibited by 11.7% to 30.0%, indicating low cytotoxicity. The prodrug-drug principle was confirmed after a quantitative assay was developed to track and monitor the time-dependent formation of the phenolic compound (17 β -HSD1 inhibitor), following incubation of its parent sulfamate (STS inhibitor) under cellular (T47D/DMEM) and cell-free (phosphate buffer) conditions, and simultaneously evaluate the percentage inhibition of 17 β -HSD1 as a function of time. For the isolation, identification, and quantification of both sulfamate and phenolic compounds, a reliable and sensitive LC-MS/MS analytical system was developed and optimized. Four sulfamated compounds (**B13**, **B16**, **B19** and **B37**) were used for incubation and the expected phenolic derivatives (**B1**, **B4**, **B7** and **B33**) were monitored. The percentage inhibition of 17 β -HSD1 was found to be associated with the time-dependent release of the phenolic compound, indicating a close relationship between phenol formation and inactivation of the enzyme. Also, the compounds had various half-life times ranging from hours to days, based on the substitution pattern of the compounds. These findings reflect the efficient and successful implementation of the drug-prodrug concept and also showed that a new structural group of DSHIs was established, from which new compounds with therapeutic potential for endometriosis treatment can be further developed.

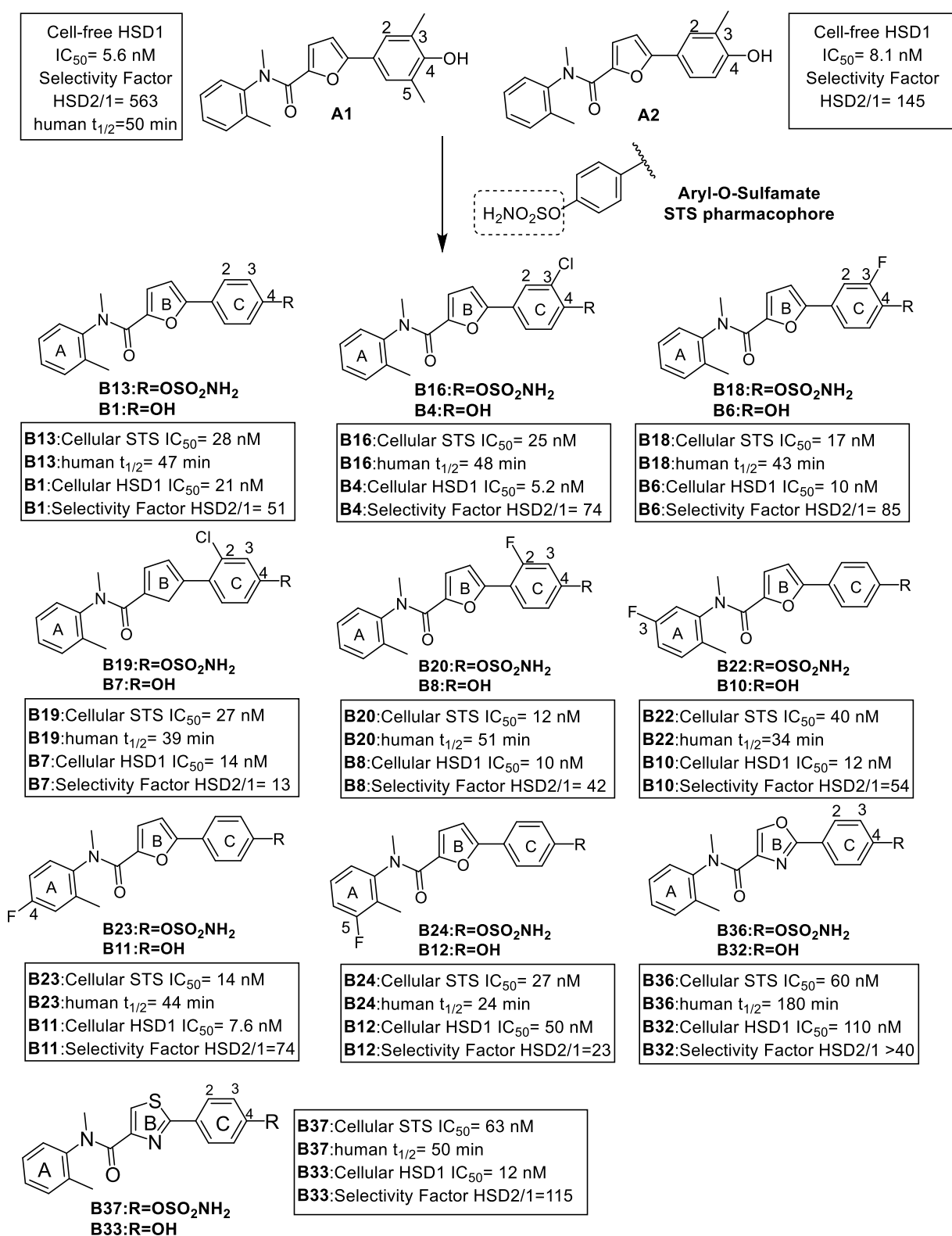


Figure 17: Biological data of the most potent compounds in the thesis

5. Supporting information

This section contains the supporting information of the studies presented in chapter 3.1 and 3.2. It contains further experimental details, as well as additional figures and results.

5.1 Supporting Information for Publication A

5.1.1 Chemical Methods

Chemical names follow IUPAC nomenclature. Starting materials were purchased from Aldrich, Acros, Combi-Blocks or Fluorochem and were used without purification. Normal pressure column chromatography was performed on silica gel (70-200 μm) and reaction progress was monitored by TLC on Alugram SIL G/UV254 (Macherey-Nagel). Visualization was accomplished with UV light. ^1H and ^{13}C NMR spectra were measured on a Bruker-500 (at 500 MHz and 126 MHz, respectively) or Bruker-300 (at 300 MHz and 75 MHz, respectively).

Chemical shifts are reported in δ (parts per million: ppm), using residual peaks of the deuterated solvents as internal standard: $(\text{CD}_3)_2\text{SO}$ (DMSO-*d*6): 2.50 ppm (^1H NMR), 39.52 ppm (^{13}C NMR); $(\text{CD}_3)_2\text{CO}$ (Acetone-*d*6): 2.05 ppm (^1H NMR), 29.84 ppm and 206.26 ppm (^{13}C NMR); CDCl_3 (Chloroform-*d*): 2.05 ppm (^1H NMR), 29.84 ppm and 206.26 ppm (^{13}C NMR). Signals are described as br (broad), s (singlet), d (doublet), t (triplet), dd (doublet of doublets), ddd (doublet of doublet of doublets), dt (doublet of triplets) and m (multiplet). All coupling constants (J) are given in Hertz (Hz). Melting points (mp) were measured in open capillaries on a Stuart Scientific SMP3 apparatus and are uncorrected.

Mass spectrometry was performed on a TSQ Quantum (ThermoFisher, Dreieich, Germany). The triple quadrupole mass spectrometer was equipped with an electrospray interface (ESI). The purity of the compounds was assessed by LC/MS. The Surveyor-LC-system consisted of a pump, an auto sampler, and a PDA detector. The system was operated by the standard software Xcalibur. A RP C18 NUCLEODUR 100-5 (3 mm) column (Macherey-Nagel GmbH, Dühren, Germany) was used as stationary phase. All solvents were HPLC grade. In a gradient run the percentage of acetonitrile (containing 0.1 % trifluoroacetic acid) was increased from an initial concentration of 20% at 0 min to 100 % at 12 min and kept at 100 % for 3 min. The injection volume was 20 μL and flow rate was set to 700 $\mu\text{L}/\text{min}$. MS analysis was carried out at a needle voltage of 3000 V and a capillary temperature of 350 $^\circ\text{C}$. Mass spectra were acquired in positive mode, using an electron spray ionization method, from 100 to 1000 m/z and UV spectra were recorded at the wave length of 254 nm and in some cases at 360 nm. IR spectra were recorded for selected compounds on a Bruker Vector 33 spectrometer (neat sample).

All microwave irradiation experiments were carried out in a 507 CEM-Discover microwave apparatus.

All tested compounds exhibited $\geq 95\%$ chemical purity as measured by LC/MS.

Method A, general procedure for amide formation:

A mixture of 5-bromofuran-2-carboxylic acid (1 eq), thionyl chloride (2.5 eq) and DMF (5 drops) in toluene (10 mL) was refluxed at 110°C for 4 hours. The reaction mixture was cooled to room temperature; the solvent and the excess of thionyl chloride were removed under reduced pressure. The corresponding *N*-methylamine (1 eq) and Et₃N (1 eq) in CH₂Cl₂ (10 mL) was added at 0°C under N₂ atmosphere to the acyl chloride. After 30 minutes at 0°C, the ice bath was removed and the solution was warmed up and stirred at room temperature overnight. The reaction mixture was extracted twice with CH₂Cl₂ (2 × 15 mL); the organic layer was dried over MgSO₄, filtered and the solution was concentrated under reduced pressure. The residue was purified by silica gel column chromatography using hexanes and EtOAc as eluent or by trituration in a mixture of diethyl ether / petroleum ether to afford the desired compound.

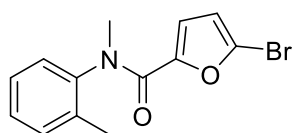
Method B, general procedure for Suzuki-Miyaura coupling:

In a sealed tube the previously prepared 5-bromo-*N*-heteroaryl-furan-2-carboxamide derivative (1 eq.) was introduced followed by the corresponding boronic acid (1.5 eq.), cesium carbonate (3 eq.), tetrakis (triphenylphosphine)palladium (0.02 eq.) and a mixture of DME/EtOH/H₂O (1:1:1, v:v:v, 3 mL) as solvent. The reactor was flushed with N₂ and submitted to microwave irradiation (150°C, 150 W) for 20 minutes. After cooling to room temperature, a mixture of EtOAc/H₂O (1:1, v:v, 2 mL) was added to stop the reaction. The aqueous layer was extracted with EtOAc (3 × 10 mL). The organic layer was washed once with brine and once with water, dried over MgSO₄, filtered and the solution was concentrated under reduced pressure. The residue was purified by column chromatography using hexanes and EtOAc as eluent to afford the desired compound.

Method C, general procedure for ether cleavage:

To a solution of methoxyaryl compounds (1 eq.) in dry dichloromethane (5 mL/mmol of reactant), boron trifluoride-dimethyl sulfide complex (6 eq./methoxy function) was added dropwise at 0 °C and stirred for 6-14 h at room temperature. After the reaction was finished, the reaction mixture was diluted with dichloromethane and 5% aqueous NaHCO₃ was added until neutral pH was obtained. The aqueous layer was extracted with dichloromethane. The combined organic layers were washed with brine, dried over sodium sulfate, evaporated to dryness under reduced pressure. The product was purified by column chromatography using EtOAc as eluent to afford the desired compound.

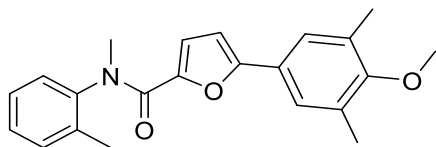
5-bromo-*N*-methyl-*N*-(*o*-tolyl)furan-2-carboxamide **1b**



The title compound was prepared by reaction of 5-bromofuran-2-carboxylic acid (500 mg, 2.6 mmol), thionyl chloride (0.5 mL, 6.8 mmol) and *N*,2-dimethylaniline (315 mg, 2.6 mmol) according to method A. The residue was purified by silica gel column chromatography (*n*-hexane/ethyl acetate 70:30) to afford the desired product as grey solid (349 mg, 45 %). C₁₃H₁₂BrNO₂; MW 294; mp: 93 – 95°C; MS (ESI) 294, 296 [M+H]⁺; ¹H NMR (500 MHz, DMSO-*d*₆) δ 7.39 – 7.32 (m, 2H), 7.34 – 7.24 (m, 2H), 6.47 (d, *J* = 3.6 Hz, 1H), 5.51 (d, *J* = 3.6

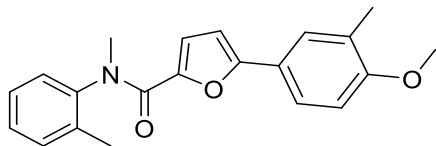
Hz, 1H), 3.21 (s, 3H), 2.12 (s, 3H); ^{13}C NMR (126 MHz, Acetone- d_6) δ 158.3, 150.6, 142.5, 138.7, 131.1, 129.5, 129.2, 128.2, 125.1, 118.9, 113.9, 38.4, 21.2.

5-(4-methoxy-3,5-dimethylphenyl)-*N*-methyl-*N*-(*o*-tolyl)furan-2-carboxamide **1a**



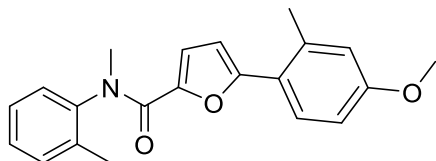
The title compound was prepared by reaction of **1b** (500 mg, 1.70 mmol), (4-methoxy-3,5-dimethylphenyl) boronic acid (367 mg, 2.04 mmol), cesium carbonate (1662 mg, 5.10 mmol) and tetrakis(triphenylphosphine) palladium (39 mg, 0.02 eq.) according to method B. The residue was purified by silica gel column chromatography (*n*-hexane/ethyl acetate 70:30) to afford the desired product as yellow solid (75 mg, 65%). $\text{C}_{22}\text{H}_{23}\text{NO}_3$; MW 349; mp : 128-132 °C MS (ESI) 350 $[\text{M}+\text{H}]^+$; ^1H NMR (500 MHz, Acetone- d_6) δ 7.33-7.43 (m, 3H), 7.29 (dd, $J = 2, 8$ Hz, 1H), 6.94 (brs, 2H), 6.64 (d, $J = 3$ Hz, 1H), 6.62 (d, $J = 3$ Hz, 1H), 3.68 (s, 3H), 3.30 (s, 3H), 2.22 (s, 9H); ^{13}C NMR (126 MHz, Acetone- d_6) δ 159.1, 158.4, 156.0, 148.1, 144.6, 136.8, 132.2, 132.1, 129.2, 129.1, 128.3, 126.3, 125.6, 119.3, 106.4, 60.6, 37.5, 17.6, 16.1; IR (cm^{-1}) 3049, 2981, 2924, 2856, 1626.

5-(4-methoxy-3-methylphenyl)-*N*-methyl-*N*-(*o*-tolyl)furan-2-carboxamide **2a**



The title compound was prepared by reaction of **1b** (500 mg, 1.70 mmol), (4-methoxy-3-methylphenyl) boronic acid (339 mg, 2.04 mmol), cesium carbonate (1662 mg, 5.10 mmol) and tetrakis(triphenylphosphine) palladium (39 mg, 0.02 eq.) according to method B. The residue was purified by silica gel column chromatography (*n*-hexane/ethyl acetate 90:10) to afford the desired product as colorless oil (213 mg, 37%). $\text{C}_{21}\text{H}_{21}\text{NO}_3$; MW 335; MS (ESI) 336 $[\text{M}+\text{H}]^+$; ^1H NMR (500 MHz, Acetone- d_6) δ 7.44 – 7.26 (m, 4H), 7.19 (dd, $J = 8.6, 2.3$ Hz, 1H), 7.04 – 7.00 (m, 1H), 6.87 (d, $J = 8.5$ Hz, 1H), 6.58 (d, $J = 3.6$ Hz, 1H), 6.51 (d, $J = 3.6$ Hz, 1H), 3.83 (s, 3H), 3.29 (s, 3H), 2.22 (s, 3H), 2.15 (s, 3H); ^{13}C NMR (126 MHz, Acetone- d_6) δ 159.2, 159.1, 156.4, 147.6, 144.5, 136.8, 132.2, 129.2, 129.1, 128.3, 127.5, 127.3, 124.3, 123.1, 119.2, 111.1, 105.5, 55.9, 37.4, 17.6, 16.2; IR and (cm^{-1}) 3052, 2933, 2838, 1627.

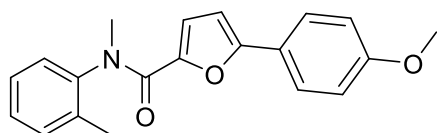
5-(4-methoxy-2-methylphenyl)-*N*-methyl-*N*-(*o*-tolyl)furan-2-carboxamide **3a**



The title compound was prepared by reaction of **1b** (500 mg, 1.70 mmol), (4-methoxy-2-methylphenyl) boronic acid (339 mg, 2.04 mmol), cesium carbonate (1662 mg, 5.10 mmol) and

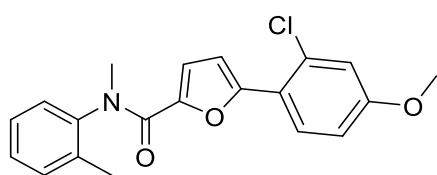
tetrakis(triphenylphosphine) palladium (39 mg, 0.02 eq.) according to method B. The residue was purified by silica gel column chromatography (*n*-hexane/ethyl acetate 90:10) to afford the desired product as white solid (247 mg, 41%). C₂₁H₂₁NO₃; MW 335; mp : 90-93 °C MS (ESI) 336 [M+H]⁺; ¹H NMR (500 MHz, Acetone-*d*₆) δ 7.27-7.40 (m, 4H), 6.99 (d, *J* = 7 Hz, 1H), 6.78 (s, 1H), 6.72 (dd, *J* = 2 Hz, 8 Hz, 1H), 6.42 (d, *J* = 3 Hz, 1H), 6.33 (d, *J* = 3 Hz, 1H), 3.79 (s, 3H), 3.29 (s, 3H), 2.35 (s, 3H), 2.22 (s, 3H); ¹³C NMR (126 MHz, Acetone-*d*₆) δ 160.6, 159.3, 155.6, 147.2, 144.4, 137.6, 136.7, 132.3, 129.6, 129.2, 129.1, 128.4, 122.8, 118.6, 117.2, 112.4, 109.4, 55.6, 37.4, 22.1, 17.6 ; IR (cm⁻¹) 3052, 2960, 2936, 2859, 2835, 1639.

5-(4-methoxyphenyl)-*N*-methyl-*N*-(*o*-tolyl)furan-2-carboxamide **4a**



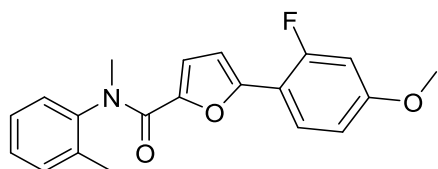
The title compound was prepared by reaction of **1b** (80 mg, 0.27 mmol), (4-methoxyphenyl)boronic acid (54 mg, 0.35 mmol), cesium carbonate (266 mg, 0.82 mmol) and tetrakis(triphenylphosphine) palladium (6 mg, 0.02 eq.) according to method B. The residue was purified by silica gel column chromatography (*n*-hexane/ethyl acetate 70:30) to afford the desired product as yellow solid (52 mg, 29%). C₂₀H₁₉NO₃; MW 321; mp: 92-95 °C; MS (ESI) 322 [M+H]⁺; ¹H NMR (500 MHz, DMSO-*d*₆) δ 7.42 – 7.26 (m, 4H), 7.23 (d, *J* = 8.7 Hz, 2H), 6.90 (d, *J* = 8.8 Hz, 2H), 6.71 (d, *J* = 3.6 Hz, 1H), 6.36 (d, *J* = 3.6 Hz, 1H), 3.77 (s, 3H), 3.24 (s, 3H), 2.16 (s, 3H); ¹³C NMR (126 MHz, Acetone-*d*₆) δ 160.9, 159.1, 156.0, 147.6, 144.4, 136.7, 132.1, 129.2, 129.0, 128.2, 126.6, 123.5, 119.0, 114.9, 105.6, 55.7, 37.3, 17.5.

5-(2-chloro-4-methoxyphenyl)-*N*-methyl-*N*-(*o*-tolyl)furan-2-carboxamide **5a**



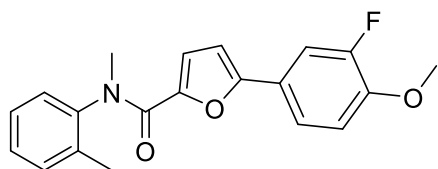
The title compound was prepared by reaction of **1b** (500 mg, 1.70 mmol), (2-chloro-4-methoxyphenyl) boronic acid (380 mg, 2.04 mmol), cesium carbonate (1662 mg, 5.10 mmol) and tetrakis(triphenylphosphine) palladium (39 mg, 0.02 eq.) according to method B. The residue was purified by silica gel column chromatography (*n*-hexane/ethyl acetate 90:10) to afford the desired product as white solid (150 mg, 25%). C₂₁H₁₈ClNO₃; MW 356; mp : 92-94 °C; MS (ESI) 356, 358 [M+H]⁺; ¹H NMR (500 MHz, Acetone-*d*₆) δ 7.41 – 7.28 (m, 4H), 7.00 (d, *J* = 2.6 Hz, 1H), 6.95 (d, *J* = 8.9 Hz, 1H), 6.89 (d, *J* = 3.7 Hz, 1H), 6.86 (dd, *J* = 8.9, 2.6 Hz, 1H), 6.50 (d, *J* = 3.7 Hz, 1H), 3.84 (s, 3H), 3.30 (s, 3H), 2.21 (s, 3H); ¹³C NMR (126 MHz, Acetone-*d*₆) δ 161.0, 159.0, 152.1, 147.7, 144.4, 136.8, 132.3, 131.8, 130.2, 129.22, 129.16, 128.4, 121.7, 118.7, 116.4, 114.4, 111.2, 56.2, 37.5, 17.6; IR (cm⁻¹) 2996, 2944, 2915, 2844, 1619.

5-(2-fluoro-4-methoxyphenyl)-*N*-methyl-*N*-(*o*-tolyl)furan-2-carboxamide **6a**



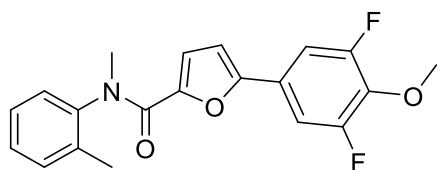
The title compound was prepared by reaction of **1b** (80 mg, 0.27 mmol), (2-fluoro-4-methoxyphenyl)boronic acid (60 mg, 0.35 mmol), cesium carbonate (266 mg, 0.82 mmol) and tetrakis(triphenylphosphine) palladium (6 mg, 0.02 eq.) according to method B. The residue was purified by silica gel column chromatography (*n*-hexane/ethyl acetate 80:20) to afford the desired product as yellow oil (60 mg, 67%). C₂₀H₁₈FNO₃; MW 339; MS (ESI) 340 [M+H]⁺; ¹H NMR (500 MHz, Acetone-*d*₆) δ 7.41 – 7.28 (m, 4H), 6.97 (t, *J* = 8.8 Hz, 1H), 6.81 – 6.72 (m, 2H), 6.55 (t, *J* = 3.7 Hz, 1H), 6.49 (d, *J* = 3.6 Hz, 1H), 3.84 (s, 3H), 3.30 (s, 3H), 2.22 (s, 3H); ¹³C NMR (126 MHz, Acetone-*d*₆) δ 162.2, 162.1, 161.7, 159.7, 159.0, 150.2, 147.6, 145.3, 144.4, 136.8, 132.2, 129.2, 129.1, 128.4, 128.1, 128.0, 119.1, 111.54, 111.52, 111.48, 111.40, 110.0, 109.9, 102.8, 102.6, 56.3, 37.4, 17.6.

5-(3-fluoro-4-methoxyphenyl)-*N*-methyl-*N*-(*o*-tolyl)furan-2-carboxamide **7a**



The title compound was prepared by reaction of **1b** (100 mg, 0.34 mmol), (3-fluoro-4-methoxyphenyl) boronic acid (75 mg, 0.44 mmol), cesium carbonate (332 mg, 1.02 mmol) and tetrakis(triphenylphosphine) palladium (8 mg, 0.02 eq.) according to method B. The residue was purified by silica gel column chromatography (*n*-hexane/ethyl acetate 70:30), to afford the desired product as a yellow oil (75 mg, 65%). C₂₀H₁₈FNO₃; MW 339; MS (ESI) 340 [M+H]⁺; ¹H NMR (500 MHz, Chloroform-*d*) δ 7.28 – 7.20 (m, 2H), 7.18 (dt, *J* = 7.5, 4.4 Hz, 1H), 7.12 – 7.07 (m, 1H), 6.93 (ddd, *J* = 8.5, 2.1, 1.3 Hz, 1H), 6.82 – 6.71 (m, 2H), 6.35 (d, *J* = 3.6 Hz, 1H), 6.26 (d, *J* = 3.6 Hz, 1H), 3.77 (s, 3H), 3.26 (s, 3H), 2.13 (s, 3H); ¹³C NMR (126 MHz, Acetone-*d*₆) δ 158.9, 154.7, 154.1, 152.1, 148.8, 148.7, 148.1, 144.3, 136.7, 132.1, 129.12, 128.3, 123.9, 123.8, 121.49, 121.46, 119.1, 114.71, 114.70, 112.7, 112.5, 106.7, 56.6, 37.4, 17.5.

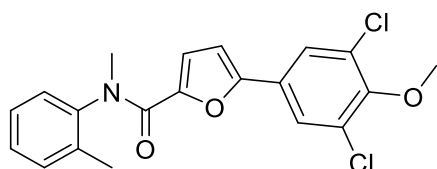
5-(3,5-difluoro-4-methoxyphenyl)-*N*-methyl-*N*-(*o*-tolyl)furan-2-carboxamide **9a**



The title compound was prepared by reaction of **1b** (500 mg, 1.70 mmol), (3,5-difluoro-4-methoxyphenyl) boronic acid (383 mg, 2.04 mmol), cesium carbonate (1662 mg, 5.10 mmol) and tetrakis(triphenylphosphine) palladium (39 mg, 0.02 eq.) according to method B. The residue was purified by silica gel column chromatography (*n*-hexane/ethyl acetate 70:30) to

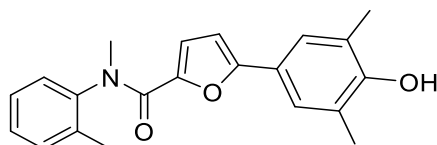
afford the desired product as yellow oil (236 mg, 39%). $C_{20}H_{17}F_2NO_3$; MW 357; mp : 70-72 °C; MS (ESI) 358 $[M+H]^+$; 1H NMR (500 MHz, Acetone- d_6) δ 7.30-7.43 (m, 4H), 6.89 (d, $J = 9$ Hz, 2H), 6.84 (d, $J = 4$ Hz, 1H), 6.64 (d, $J = 4$ Hz, 1H), 3.97 (s, 3H), 3.31 (s, 3H), 2.23 (s, 3H); ^{13}C NMR (126 MHz, Acetone- d_6) δ 158.8, 157.81, 157.7, 155.85, 155.80, 153.2, 148.9, 144.3, 137.2, 136.8, 132.2, 129.3, 129.2, 128.4, 126.1, 126.0, 125.9, 119.3, 109.1, 108.9, 108.8, 108.6, 62.4, 37.5, 17.6; IR (cm^{-1}) 2921, 2847, 1625.

5-(3,5-dichloro-4-methoxyphenyl)-*N*-methyl-*N*-(*o*-tolyl)furan-2-carboxamide **10a**



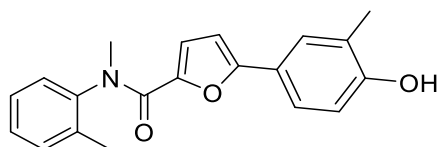
The title compound was prepared by reaction of **1b** (500 mg, 1.70 mmol), (3,5-dichloro-4-methoxyphenyl) boronic acid (450 mg, 2.04 mmol), cesium carbonate (1662 mg, 5.10 mmol) and tetrakis(triphenylphosphine) palladium (39 mg, 0.02 eq.) according to method B. The residue was purified by silica gel column chromatography (*n*-hexane/ethyl acetate 80:20) to afford the desired product as yellow solid (438 mg, 39%). $C_{20}H_{17}Cl_2NO_3$; MW 390; mp : 114-117 °C MS (ESI) 390, 392 $[M+H]^+$; 1H NMR (300 MHz, Acetone- d_6) δ 7.31-7.46 (m, 4H), 7.24 (s, 2H), 6.94 (d, $J = 4$ Hz, 1H), 6.78 (d, $J = 4$ Hz, 1H), 3.89 (s, 3H), 3.33 (s, 3H), 2.25 (s, 3H); ^{13}C NMR (75 MHz, Acetone- d_6) δ 158.7, 152.8, 152.5, 149.3, 144.3, 136.7, 132.2, 130.5, 129.5, 129.1, 128.4, 128.3, 125.2, 119.4, 109.0, 61.3, 37.5, 17.6.

5-(4-hydroxy-3,5-dimethylphenyl)-*N*-methyl-*N*-(*o*-tolyl)furan-2-carboxamide **1**



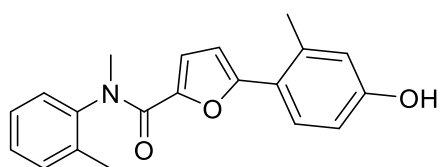
The title compound was prepared by reaction of **1a** (260 mg, 0.74 mmol) and $BF_3 \cdot SMe_2$ (470 μ L, 4.44 mmol) according to method C. The residue was purified by silica gel column chromatography (*n*-hexane/ethyl acetate 60:40) to afford the desired product as yellow solid (74 mg, 30%). $C_{21}H_{21}NO_3$; MW 335; mp: 175-178 °C; MS (ESI) 336 $[M+H]^+$; 1H NMR (300 MHz, Chloroform- d) δ 7.21 (dt, $J = 16.6, 4.3$ Hz, 3H), 7.10 (d, $J = 7.3$ Hz, 1H), 6.78 (s, 2H), 6.37 (d, $J = 3.6$ Hz, 1H), 6.21 (d, $J = 3.5$ Hz, 1H), 6.03 (s, 1H), 3.27 (s, 3H), 2.15 – 2.08 (m, 9H); ^{13}C NMR (75 MHz, Chloroform- d) δ 159.6, 156.5, 153.4, 145.4, 143.1, 135.8, 131.4, 128.4, 128.1, 127.4, 124.8, 123.9, 121.6, 119.5, 104.4, 37.6, 17.4, 16.0; IR (cm^{-1}) 3274, 2952, 2912, 1614, 1592.

5-(4-hydroxy-3-methylphenyl)-*N*-methyl-*N*-(*o*-tolyl)furan-2-carboxamide **2**



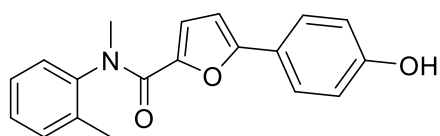
The title compound was prepared by reaction of **2a** (224 mg, 0.67 mmol) and $\text{BF}_3 \cdot \text{SMe}_2$ (420 μL , 4.02 mmol) according to method C. The residue was purified by crystallization in water and ethanol to afford the desired product as green solid (140 mg, 65%). $\text{C}_{20}\text{H}_{19}\text{NO}_3$; MW 321; mp: 183-186 °C; MS (ESI) 322 $[\text{M}+\text{H}]^+$; ^1H NMR (500 MHz, $\text{DMSO}-d_6$) δ 9.66 (s, 1H), 7.42 – 7.25 (m, 4H), 7.02 (d, 1H), 6.87 (s, 1H), 6.71 (d, $J = 8.3$ Hz, 1H), 6.60 (d, $J = 3.7$ Hz, 1H), 6.42 (d, $J = 3.7$ Hz, 1H), 3.23 (s, 3H), 2.14 (s, 3H), 2.08 (s, 3H); ^{13}C NMR (126 MHz, $\text{DMSO}-d_6$) δ 157.9, 156.0, 155.3, 145.4, 142.9, 135.2, 131.1, 128.18, 128.11, 127.3, 126.3, 124.3, 123.0, 120.2, 118.5, 114.7, 104.4, 36.9, 17.0, 15.7; IR (cm^{-1}) 3132, 2907, 1573.

5-(4-hydroxy-2-methylphenyl)-*N*-methyl-*N*-(*o*-tolyl)furan-2-carboxamide **3**



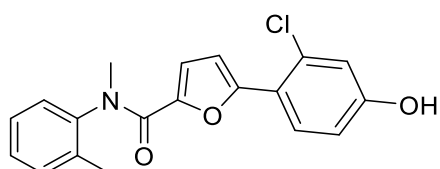
The title compound was prepared by reaction of **3a** (200 mg, 0.60 mmol) and $\text{BF}_3 \cdot \text{SMe}_2$ (468 μL , 3.60 mmol) according to method C. The residue was purified by silica gel column chromatography (*n*-hexane/ethyl acetate 60:40) to afford the desired product as white solid (178 mg, 92%). $\text{C}_{20}\text{H}_{19}\text{NO}_3$; MW 321; mp: 219-221 °C; MS (ESI) 322 $[\text{M}+\text{H}]^+$; ^1H NMR (500 MHz, $\text{DMSO}-d_6$) δ 9.64 (s, 1H), 7.26-7.38 (m, 4H), 6.83 (d, $J = 8$ Hz, 1H), 6.62 (s, 1H), 6.55 (d, $J = 7$ Hz, 1H), 6.42 (d, $J = 3$ Hz, 1H), 6.20 (d, $J = 3$ Hz, 1H), 3.23 (s, 3H), 2.23 (s, 3H), 2.15 (s, 3H); ^{13}C NMR (126 MHz, $\text{DMSO}-d_6$) δ 158.0, 157.5, 154.6, 145.1, 142.8, 136.3, 135.2, 131.2, 128.4, 128.2, 128.1, 127.4, 119.8, 117.8, 117.6, 113.0, 108.1, 36.9, 21.3, 17.0; IR (cm^{-1}) 3243, 3056, 2966, 2920, 2853, 1616.

5-(4-hydroxyphenyl)-*N*-methyl-*N*-(*o*-tolyl)furan-2-carboxamide **4**



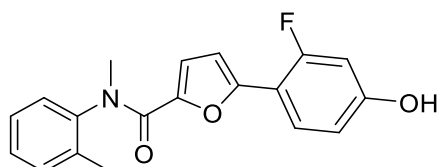
The title compound was prepared by reaction of **4a** (50 mg, 0.16 mmol) and $\text{BF}_3 \cdot \text{SMe}_2$ (100 μL , 0.96 mmol) according to method C. The residue was purified silica gel column chromatography (*n*-hexane/ethyl acetate 60:40) to afford the desired product as yellow solid (45 mg, 92%). $\text{C}_{19}\text{H}_{17}\text{NO}_3$; MW 307; mp: 172-175 °C; MS (ESI) 308 $[\text{M}+\text{H}]^+$; ^1H NMR (500 MHz, $\text{DMSO}-d_6$) δ 9.76 (s, 1H), 7.41 – 7.25 (m, 4H), 7.13 (d, $J = 8.4$ Hz, 2H), 6.72 (d, $J = 8.7$ Hz, 2H), 6.61 (d, $J = 3.6$ Hz, 1H), 6.30 (d, $J = 3.6$ Hz, 1H), 3.23 (s, 3H), 2.15 (s, 3H); ^{13}C NMR (126 MHz, $\text{DMSO}-d_6$) δ 157.95, 157.94, 155.1, 145.4, 142.8, 135.2, 131.1, 128.16, 128.13, 127.3, 125.6, 120.4, 118.3, 115.5, 104.5, 36.8, 16.9.

5-(2-chloro-4-hydroxyphenyl)-*N*-methyl-*N*-(*o*-tolyl)furan-2-carboxamide **5**



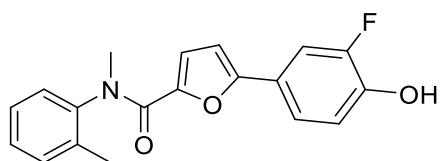
The title compound was prepared by reaction of **5a** (120 mg, 0.34 mmol) and $\text{BF}_3 \cdot \text{SMe}_2$ (265 μL , 2.04 mmol) according to method C. The residue was purified by silica gel column chromatography (*n*-hexane/ethyl acetate 60:40) to afford the desired product as white solid (89 mg, 77%). $\text{C}_{19}\text{H}_{16}\text{ClNO}_3$; MW 342; mp: 198-201 °C; MS (ESI) 342, 344 $[\text{M}+\text{H}]^+$; ^1H NMR (500 MHz, $\text{DMSO}-d_6$) δ 10.27 (s, 1H), 7.42 – 7.26 (m, 4H), 6.85 (d, $J = 2.4$ Hz, 1H), 6.83 – 6.78 (m, 2H), 6.69 (dd, $J = 8.7, 2.5$ Hz, 1H), 6.36 (d, $J = 3.7$ Hz, 1H), 3.24 (s, 3H), 2.15 (s, 3H); ^{13}C NMR (126 MHz, $\text{DMSO}-d_6$) δ 158.2, 157.7, 151.0, 145.6, 142.7, 135.2, 131.2, 130.2, 129.2, 128.2, 128.1, 127.4, 118.5, 117.9, 116.8, 114.7, 109.7, 36.9, 16.9; IR (cm^{-1}) 3064, 2993, 2877, 2775, 2691, 1562.

5-(2-fluoro-4-hydroxyphenyl)-*N*-methyl-*N*-(*o*-tolyl)furan-2-carboxamide **6**



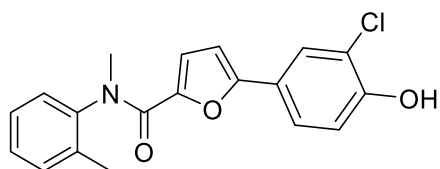
The title compound was prepared by reaction of **6a** (57 mg, 0.17 mmol) and $\text{BF}_3 \cdot \text{SMe}_2$ (110 μL , 1.01 mmol) according to method C. The residue was purified by silica gel column chromatography (*n*-hexane/ethyl acetate 60:40) to afford the desired product as yellow oil (10 mg, 18%). $\text{C}_{19}\text{H}_{16}\text{FNO}_3$; MW 325; MS (ESI) 326 $[\text{M}+\text{H}]^+$; ^1H NMR (500 MHz, $\text{DMSO}-d_6$) δ 10.29 (s, 1H), 7.42 – 7.26 (m, 4H), 6.82 (t, $J = 8.8$ Hz, 1H), 6.62 (dd, $J = 13.1, 2.3$ Hz, 1H), 6.58 (dd, $J = 8.6, 2.4$ Hz, 1H), 6.50 (t, $J = 3.6$ Hz, 1H), 6.35 (d, $J = 3.6$ Hz, 1H), 3.24 (s, 3H), 2.15 (s, 3H); ^{13}C NMR (126 MHz, $\text{DMSO}-d_6$) δ 160.2, 159.3, 159.2, 158.2, 157.7, 149.23, 145.5, 142.7, 135.2, 131.1, 128.2, 128.1, 127.4, 126.9, 126.8, 118.2, 112.02, 108.5, 108.45, 108.40, 108.3, 103.2, 103.0, 36.9, 16.9.

5-(3-fluoro-4-hydroxyphenyl)-*N*-methyl-*N*-(*o*-tolyl)furan-2-carboxamide **7**



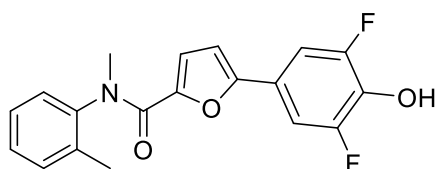
The title compound was prepared by reaction of **7a** (60 mg, 0.18 mmol) and $\text{BF}_3 \cdot \text{SMe}_2$ (110 μL , 1.06 mmol) according to method C. The residue was purified by silica gel column chromatography (*n*-hexane/ethyl acetate 60:40) to afford the desired product as yellow solid (55 mg, 95%). $\text{C}_{19}\text{H}_{16}\text{FNO}_3$; MW 325; mp: 190-192 °C; MS (ESI) 326 $[\text{M}+\text{H}]^+$; ^1H NMR (500 MHz, $\text{DMSO}-d_6$) δ 10.22 (s, 1H), 7.42 – 7.26 (m, 4H), 7.00 – 6.92 (m, 2H), 6.89 (t, $J = 8.8$ Hz, 1H), 6.73 (d, $J = 3.6$ Hz, 1H), 6.44 (d, $J = 3.6$ Hz, 1H), 3.24 (s, 3H), 2.15 (s, 3H); ^{13}C NMR (126 MHz, $\text{DMSO}-d_6$) δ 157.7, 153.7, 151.9, 150.0, 146.0, 145.4, 145.3, 142.8, 135.2, 131.1, 128.2, 128.1, 127.3, 121.0, 120.9, 120.68, 120.65, 118.4, 118.02, 118.00, 111.9, 111.8, 105.8, 36.9, 16.9.

5-(3-chloro-4-hydroxyphenyl)-*N*-methyl-*N*-(*o*-tolyl)furan-2-carboxamide **8**



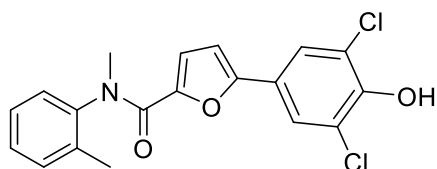
The title compound was prepared by reaction of **1b** (80 mg, 0.27 mmol), (3-chloro-4-hydroxyphenyl) boronic acid (61 mg, 0.35 mmol), cesium carbonate (266 mg, 0.82 mmol) and tetrakis(triphenylphosphine) palladium (6 mg, 0.02 eq.) according to method B. The residue was purified by crystallization in ethanol and water, to afford the desired product as white solid (36 mg, 39%). $C_{19}H_{16}ClNO_3$; MW 342; mp: 77 – 80 °C; MS (ESI) 342, 344 $[M+H]^+$; 1H NMR (500 MHz, DMSO- d_6) δ 10.53 (s, 1H), 7.43 – 7.26 (m, 4H), 7.14 (dd, $J = 8.5, 2.2$ Hz, 1H), 7.08 (d, $J = 2.2$ Hz, 1H), 6.90 (d, $J = 8.5$ Hz, 1H), 6.75 (d, $J = 3.6$ Hz, 1H), 6.50 (d, $J = 3.6$ Hz, 1H), 3.24 (s, 3H), 2.15 (s, 3H); ^{13}C NMR (126 MHz, DMSO- d_6) δ 157.7, 153.43, 153.42, 146.0, 142.7, 135.2, 131.0, 128.3, 128.0, 127.3, 125.2, 124.0, 121.5, 120.2, 118.5, 116.8, 105.7, 36.9, 16.9.

5-(3,5-difluoro-4-hydroxyphenyl)-*N*-methyl-*N*-(*o*-tolyl)furan-2-carboxamide **9**



The title compound was prepared by reaction of **9a** (180 mg, 0.50 mmol) and $BF_3 \cdot SMe_2$ (320 μ L, 3.00 mmol) according to method C. The residue was purified by silica gel column chromatography (*n*-hexane/ethyl acetate 60:40) to afford the desired product as yellow solid (140 mg, 81%). $C_{19}H_{15}F_2NO_3$; MW 343; mp: 176-178 °C; MS (ESI) 344 $[M+H]^+$; 1H NMR (500 MHz, Acetone- d_6) δ 9.25 (s, 1H), 7.30-7.42 (m, 4H), 6.88 (d, $J = 7$ Hz, 2H), 6.75 (d, $J = 3$ Hz, 1H), 6.59 (d, $J = 3$ Hz, 1H), 3.31 (s, 3H), 2.22 (s, 3H); ^{13}C NMR (126 MHz, Acetone- d_6) δ 158.9, 154.55, 154.50, 153.9, 152.6, 152.5, 148.4, 144.3, 136.8, 135.2, 135.0, 134.9, 132.2, 129.3, 129.2, 128.4, 122.1, 122.0, 121.9, 119.3, 108.7, 108.6, 108.5, 108.4, 107.5, 37.5, 17.6; IR (cm^{-1}) 3056, 2930, 1623.

5-(3,5-dichloro-4-hydroxyphenyl)-*N*-methyl-*N*-(*o*-tolyl)furan-2-carboxamide **10**



The title compound was prepared by reaction of **10a** (240 mg, 0.61 mmol) and $BF_3 \cdot SMe_2$ (476 μ L, 3.66 mmol) according to method C. The residue was purified by silica gel column chromatography (*n*-hexane/ethyl acetate 60:40) to afford the desired product as orange solid (117 mg, 51%). $C_{19}H_{15}Cl_2NO_3$; MW 376; mp: 134-137 °C; MS (ESI) 376, 378 $[M+H]^+$; 1H NMR (500 MHz, Acetone- d_6) δ 9.08 (s, 1H), 7.34-7.43 (m, 3H), 7.30 (d, $J = 8$ Hz, 1H), 7.19 (s, 2H), 6.80 (d, $J = 3$ Hz, 1H), 6.71 (d, $J = 3$ Hz, 1H), 3.31 (s, 3H), 2.23 (s, 3H); ^{13}C NMR (126

MHz, Acetone-*d*₆) δ 158.9, 153.2, 150.0, 148.6, 144.3, 136.7, 132.2, 129.5, 129.1, 128.3, 125.0, 124.1, 123.4, 119.4, 107.5, 37.5, 17.6; IR (cm⁻¹) 3129, 2957, 2923, 2853, 1620.

5.1.2 Biological Methods

[2,4,6,7-³H]-E2 and [2,4,6,7-³H]-E1 were purchased from Perkin-Elmer, Boston. Quickszint Flow 302 scintillator fluid was bought from Zinsser Analytic, Frankfurt. Other chemicals were purchased from Sigma, Roth or Merck.

***h*17 β -HSD1 and *h*17 β -HSD2 enzyme preparation.** Cytosolic (*h*17 β -HSD1) and microsomal (*h*17 β -HSD2) fractions were obtained from human placenta according to previously described procedures.¹⁻⁵ Fresh tissue was homogenized and the enzymes were separated from the mitochondria, cell membrane, nucleus and other rests by fractional centrifugation at 1000 g, 10.000 g and 150.000 g. The pellet fraction containing the microsomal *h*17 β -HSD2 was used for the determination of *h*17 β -HSD2 inhibition, while *h*17 β -HSD1 was obtained after precipitation with ammonium sulfate from the cytosolic fraction for use of testing of *h*17 β -HSD1 inhibition. Aliquots containing *h*17 β -HSD1 or *h*17 β -HSD2 were stored frozen.

Inhibition of *h*17 β -HSD2 in cell-free assay. Inhibitory activities were evaluated following an established method with minor modifications.^{6,7} Briefly, the enzyme preparation was incubated with NAD⁺ [1500 μ M] in the presence of potential inhibitors at 37 °C in a phosphate buffer (50 mM) supplemented with 20% of glycerol and EDTA 1mM. Inhibitor stock solutions were prepared in DMSO. Final concentration of DMSO was adjusted to 1% in all samples. The enzymatic reaction was started by addition of a mixture of unlabelled- and [³H]-E2 (final concentration: 500 nM, 0.11 μ Ci) at 37 °C. After 20 min, the incubation was stopped with HgCl₂ and the mixture was extracted with ether. After evaporation, the steroids were dissolved in acetonitrile/water (45:55). E1 and E2 were separated using acetonitrile/water (45:55) as mobile phase in a C18 RP chromatography column (Nucleodur C18, 3 μ m, Macherey-Nagel, Düren) connected to a HPLC-system (Agilent 1100 Series, Agilent Technologies, Waldbronn). Detection and quantification of the steroids were performed using a radioflow detector (Berthold Technologies, Bad Wildbad). The conversion rate was calculated according to the following equation: %conversion = (%E1/(%E1+%E2)) \times 100. Each value was calculated from at least two independent experiments.

Inhibition of *h*17 β -HSD1 in a in cell-free assay. The 17 β -HSD1 inhibition assay was performed similarly to the *h*17 β -HSD2 test. The human cytosolic enzyme was incubated with NADH [500 μ M] while the rat recombinant enzyme was reacted with NADPH [500 μ M]. Test compound and a mixture of unlabelled- and [³H]-E1 (final concentration: 500 nM, 0.15 μ Ci) were added and mixed for 10 min at 37°C. Further treatment of the samples and HPLC separation was carried out as mentioned above for *h*17 β -HSD2.

Estrogen receptor affinity in a cell-free assay. The binding affinity of compound **1** to ER α and ER β was determined according to the recommendations of the US Environmental Protection Agency (EPA) by their Endocrine Disruptor Screening Program (EDSP)⁸ using recombinant human proteins. Briefly, 1 nM of ER α and 4 nM of ER β , respectively, were

incubated with [³H]-E2 (3 nM for ER α and 10 nM for ER β) and test compound (3 μ M for ER α and 10 μ M for ER β) for 16-20 h at 4°C.

The potential inhibitors were dissolved in DMSO (2% final concentration). Evaluation of non-specific-binding was performed with unlabeled E2 at concentrations 100-fold of [³H]-E2 (300 nM for ER α and 1000 nM for ER β). After incubation, ligand-receptor complexes were selectively bound to hydroxyapatite (83.5 g/LinTE-buffer). The bound complex was washed three times and resuspended in ethanol. For radiodetection, scintillator cocktail (Quickszint 212, Zinsser Analytic, Frankfurt) was added and samples were measured in a liquid scintillation counter (1450 LSC & Luminescence Counter, Perkin Elmer).

From these results the percentage of [³H]-E2 displacement by the compounds was calculated. The plot of % displacement versus compound concentration resulted in sigmoidal binding curves. The compound concentrations necessary to displace 50% of the receptor bound [³H]-E2 were determined. Unlabeled E2 IC₅₀ values were determined in each experiment and used as reference. The E2 IC₅₀ determined were 3 \pm 20% nM for ER α and 10 \pm 20% nM for ER β . Relative Binding Affinity was determined by applying the following equation: RBA [%] = (IC₅₀(E2)/IC₅₀(compound)) · 100.¹⁰ This results in a RBA value of 100% for E2. After the assay was established and validated, a modification was made to increase throughput. Compounds were tested at concentrations of 1000 times the IC₅₀(E2). Compounds with less than 50% displacement of [³H]-E2 at a concentration of 1000 times IC₅₀(E2) were classified as RBA <0.1%.

Metabolic stability in a cell-free assay. Compound **1** was tested according to established method.⁹⁻¹¹ For evaluation of phase I and II metabolic stability 1 μ M compound was incubated with 1 mg/ml pooled mammalian liver S9 fraction (BD Gentest), 2 mM NADPH regenerating system, 1 mM UDPGA and 0.1 mM PAPS at 37°C for 0, 5, 15 and 60 minutes at a final volume of 100 μ L. The incubation was stopped by precipitation of S9 enzymes with 2 volumes of cold acetonitrile containing internal standard. Concentration of the remaining test compound at the different time points was analyzed by LC-MS/MS and used to determine half-life (t_{1/2}).

MTT-Cytotoxicity assay. The number of living cells was evaluated measuring the reduction of 3-(4,5-dimethylthiazol-2-yl)-2,5-diphenyltetrazoliumbromide (MTT). Experiments were performed in 96-well cell culture plates in DMEM supplemented with 10% FCS. Cells were incubated for 66 h with 6.25, 12.50, 25, 50, and 100 μ M of test compound at 37 °C in a humidified atmosphere at 5% CO₂. For cleavage reaction MTT-solution (5mg/mL in PBS) was added and incubation was continued for another 66 h. Reaction stop and cell lysis were carried out by addition of sodium dodecyl sulphate (SDS) in 0.01N HCl (10%). The produced blue formazan was quantified spectrophotometrically at 590nm as described by Denizot and Lang¹² with minor modifications.

Cell culture. The human NSCLC cell line Calu-1 (squamous cell carcinoma) was purchased from the American Type Culture Collection (Rockville, MD). Cells were routinely maintained in RPMI 1640 medium, supplemented with 10% heat-inactivated fetal bovine serum (FBS), 2mM glutamine and penicillin-streptomycin-amphotericin B solution (10,000 units penicillin, 10 mg streptomycin and 25 μ g amphotericin B/mL). Sigma-Aldrich Co. (St. Louis, MO) at

37°C in a humidified incubator with 5% CO₂. Prior to all experiments, cells were grown overnight in a phenol red-free RPMI 1640 medium, supplemented with 10% charcoal-dextran-stripped FBS, Sigma-Aldrich Co. (St. Louis, MO). The stock solutions of **1** (5.43 mM) and estrone (E1) (7 mg/ml) were prepared in DMSO, aliquoted and stored at -20° C until use. The investigated compounds were diluted in the culture medium to the desired concentration (50 nM or 500 nM for **1** and 5 µM for E1) and added to cell cultures during all experiments. The same volume of DMSO was used as a vehicle control and its final concentration in culture medium never exceeded 0.1%.

Impact of E1 and 1 treatment on Calu-1 cells growth in real time conditions. The xCELLigence RTCA DP System, ACEA Biosciences (San Diego, CA), with 16-well E-Plates was employed for label-free, real-time monitoring of cell proliferation. It is an electrical impedance-based cell proliferation assay, where the impedance values from microelectrodes located at the bottom of each well in E-plate are measured and converted by the software into the Cell Index. Therefore, when cells adhere to the well surface and start to proliferate, the change in electrode impedance is recorded. At the beginning of the experiment 150 µL of phenol red-free RPMI 1640, supplemented with 10% charcoal-dextran-stripped FBS was added to each well and the background impedance was measured after 30 minutes of incubation. Next, Calu-1 cells were harvested by a standard trypsinization method, counted automatically with EVETM cell counter; NanoEnTek Inc. (Seoul, Korea), suspended in a phenol red-free RPMI 1640 medium, supplemented with 10% charcoal-dextran-stripped FBS and seeded into 16-well E-Plates at a concentration of 3,5 x 10³ cells/well to a final volume of 200 µl per well. In order to avoid evaporation of medium, water was added to the spaces between all wells. E-plate was allowed to incubate at room temperature for 30 minutes and then was inserted into the xCELLigence RTCA DP device for continuous recording of impedance overnight. The next day culture media were changed and for another 50 hrs Calu-1 cells were cultured in the following experimental groups: (1) control – medium alone (phenol red-free RPMI 1640 medium, supplemented with 10% charcoal-dextran-stripped FBS), (2) medium with **1** at the concentration of 50 nM, (3) medium with **1** at the concentration of 500 nM, (4) vehicle control – medium with DMSO. Afterwards, media were replaced once again and cells were exposed to the compounds for 75 hrs of incubation in the following groups: (1) 5 µM E1, (2) 5 µM E1 and 50 nM **1**, (3) 5 µM E1 and 500 nM **1**, (4) vehicle control – medium with DMSO. Cell growth in real time was monitored from the beginning of an experiment till 150 h and the electrical impedance was measured at 15-minutes intervals throughout the cultivation period. Cell index was normalized (normalized cell index) at the time point of E1 and **1** administration using software provided by the manufacturer (RTCA Software, v. 1.2, November 2009). Four replicates of each compound concentration for Calu-1 cell line were used.

5.1.3 Computational Details

Docking simulations. As a first step, the Restrained ElectroStatic Potential (RESP) charges¹³ were computed for **1** to enhance the accuracy of the following docking simulations. In particular, **1** was optimized at the Density Functional Theory level using the hybrid B3LYP functional¹⁴ and the Pople6-311++G(d,p) basis set. Molecular electrostatic potential (MEP) was thus computed on such structure, at Hartree-Fock (HF) level of theory, using a smaller basis set

(6-31G(d)). Finally, the charge values were fitted in order to reproduce the computed MEPs. All these calculations were performed with the Gaussian 09¹⁵ package apart from the charges fitting performed using Antechamber, a freely accessible AmberTools program. Next, docking simulations were performed on the crystal structure of a ternary complex (*h17 β* -HSD1-inhibitor-NADP⁺ available from PDB with code 3HB5¹⁶). The 3HB5 X-ray solved structure was first pre-treated using the protein preparation module of Schrodinger suite 2015-3¹⁷, which enables to add missing hydrogen atoms and to determine the optimal protonation states for histidine residues. The obtained structure was used for docking simulations performed by GLIDE v6.8,¹⁸ which is part of the Schrodinger Suite. During the docking process, the receptor protein was held fixed, while full conformational flexibility was allowed for the ligand. The described protocol was performed employing the default Force Field OPLS_2005, except for the atomic charges, which were derived following the RESP protocol, as described above. A cubic grid set on the center of mass of the cognate ligand having an edge of 13 Å for the inner box and of 30 Å for the outerbox was used. All simulations were performed flagging the extra precision (XP) mode. In order to ensure an adequate sampling of the conformational space, 20000 poses per ligand were generated in the initial phase and, among them, 10000 were selected for post-docking minimization. Note that docking simulations were performed including NADPH as cofactor, given its occurrence at much higher concentration with respect to NADP⁺ in living cells.¹⁹ The herein described protocol was set on the basis of docking calibration studies aimed at reproducing the X-ray pose of the 3HB5 cognate ligand.

All the docking parameters employed in our studies were initially calibrated trying to reproduce as good as possible the X-ray binding conformation of the cognate ligand (i.e., 3([(9beta,14beta,16alpha,17alpha)-3,17-dihydroxyestra-1,3,5(10)-trien-16-yl]methyl)benzamide, hereafter referred to as E2B) embedded into 3HB5 available from PDB. In this respect, Figure S1 shows unequivocally the goodness of the superimposition between docking and X-ray poses showing a value of root-mean-square deviation (RMSD) equal to 0.64 Å.

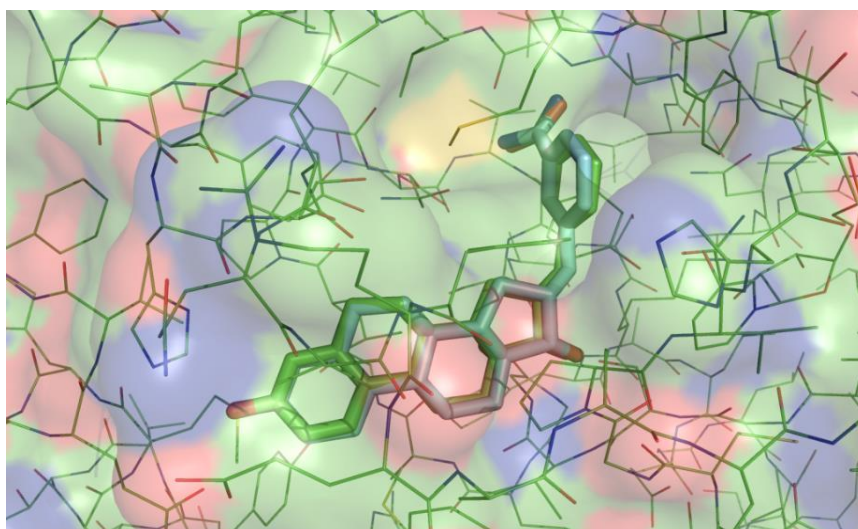


Figure S1. Crystal structure pose (in green) and top-scored docking pose (in cyan) of E2B in the ternary complex of *h17 β* -HSD1 (PDB code: 3HB5).

Density functional theory. All DFT calculations were carried out using the Gaussian 09 package.¹⁵ Geometry optimizations were performed at the B3LYP²/6-311++G(d,p) level of theory. In order to take into account, the solvation effect, all calculations were carried out using the polarizable continuum model (PCM) for water, as implemented in Gaussian 09.

Model validation. The robustness of the found correlation was challenged by performing a randomization analysis. In order to assess the risk of chance correlation 1 million of y-scrambled models were generated and for each of them the value of r^2 was computed. Notably, the found correlation can be considered statistically significant if for all the randomized models a value of r^2 lower than that observed for the non-randomized model is detected (Figure S2).

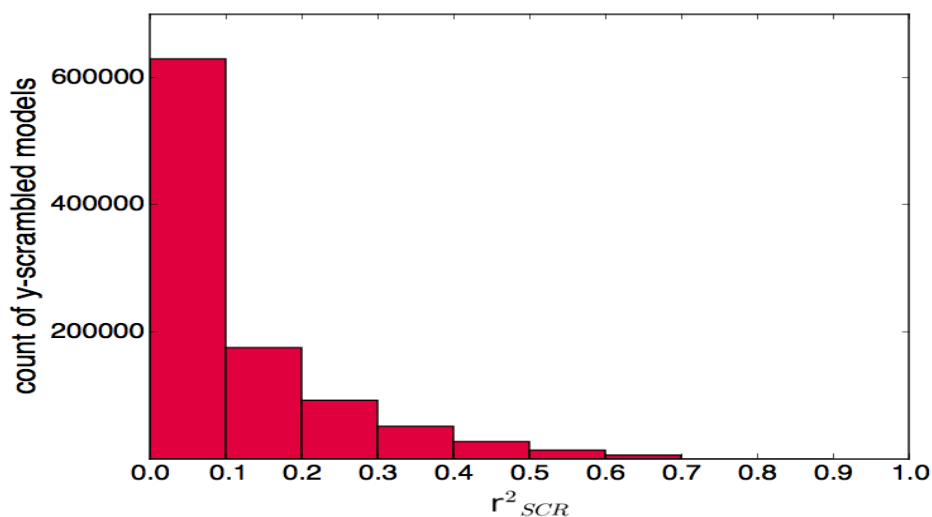
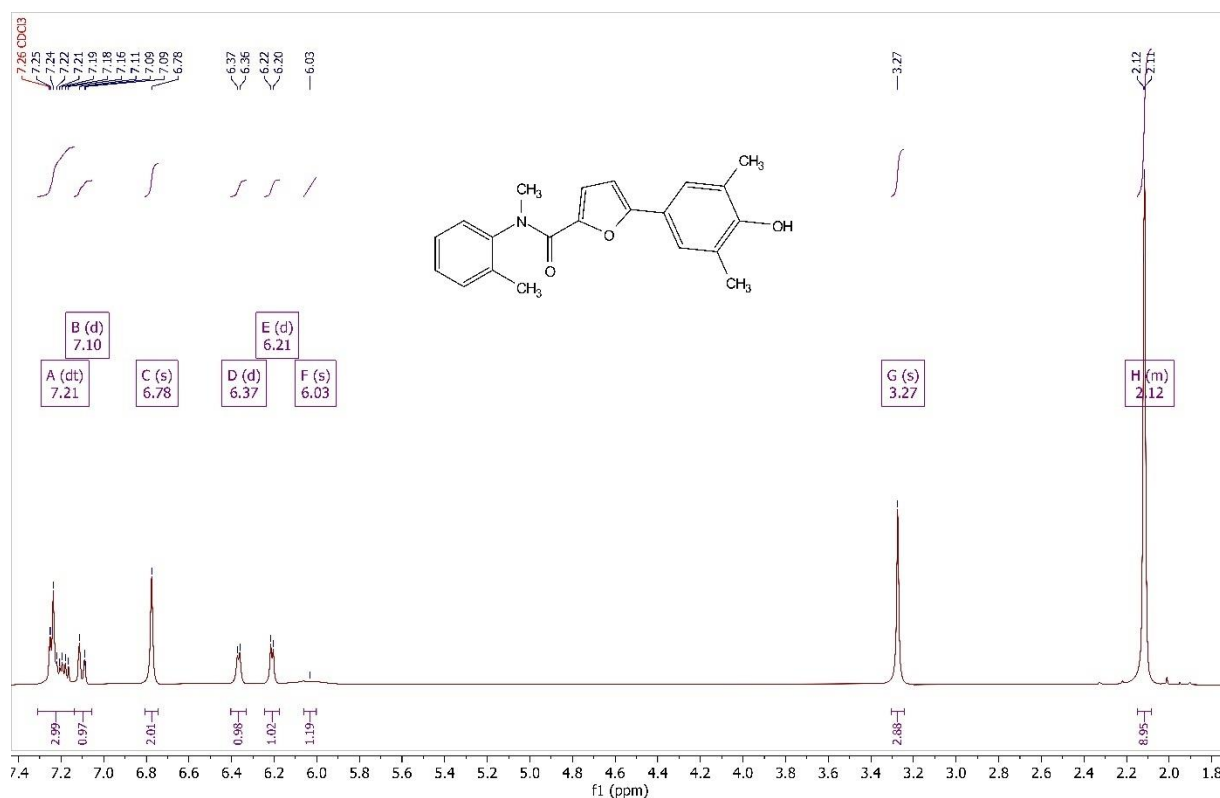


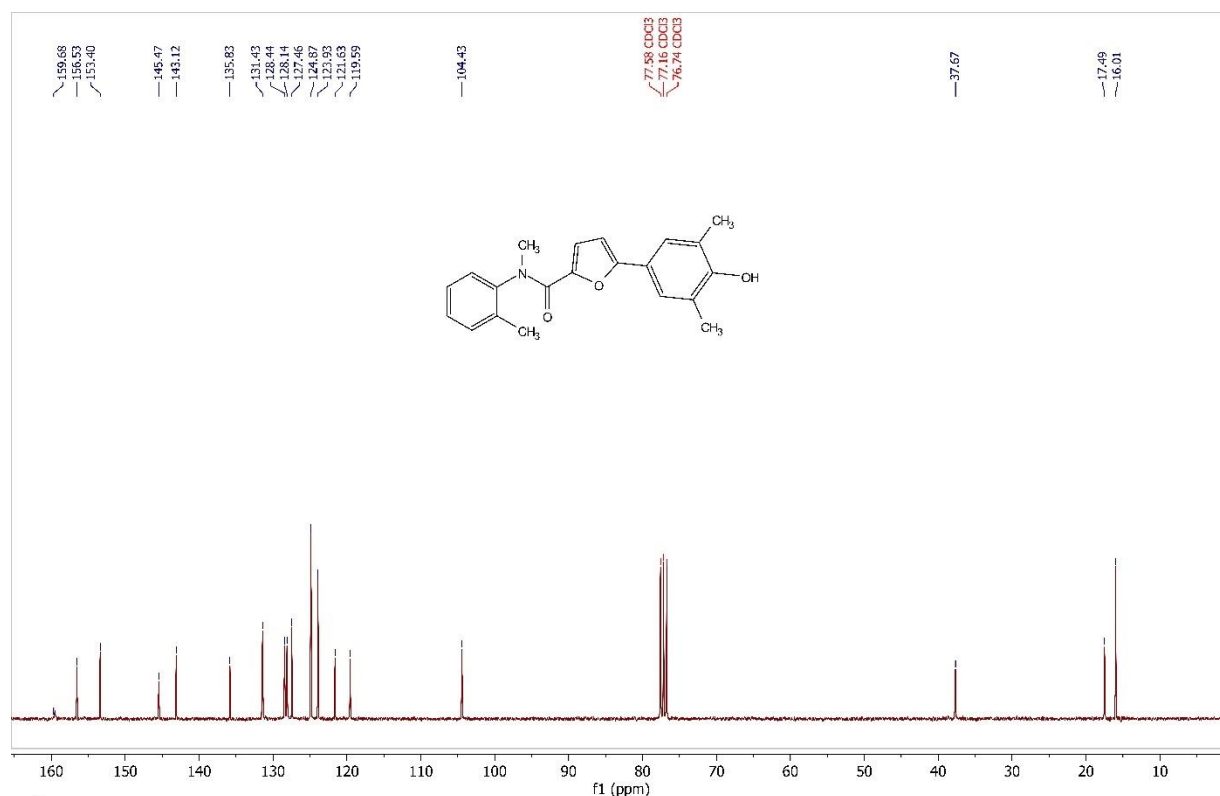
Figure S2. Histogram of r^2_{SCR} vs. number of randomized models over 1 million y-scrambling runs.

5.1.4 Representative ^1H -NMR and ^{13}C -NMR spectra

Compound 1:

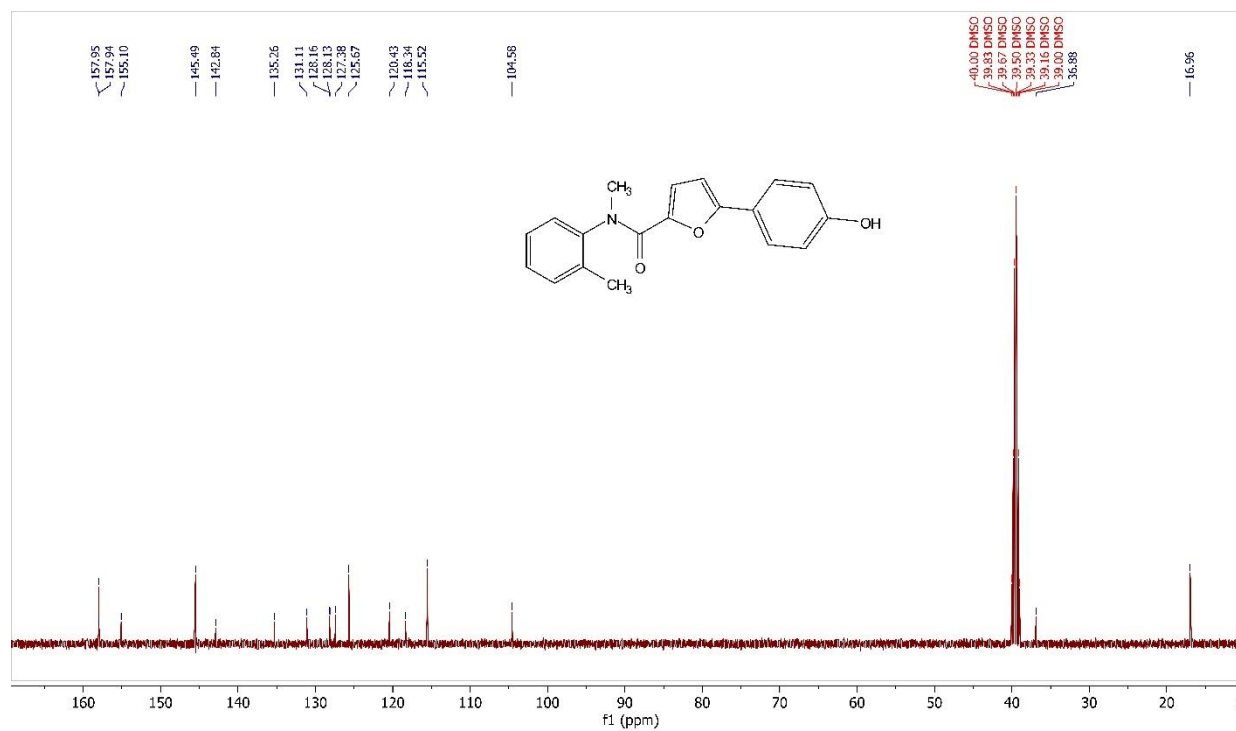
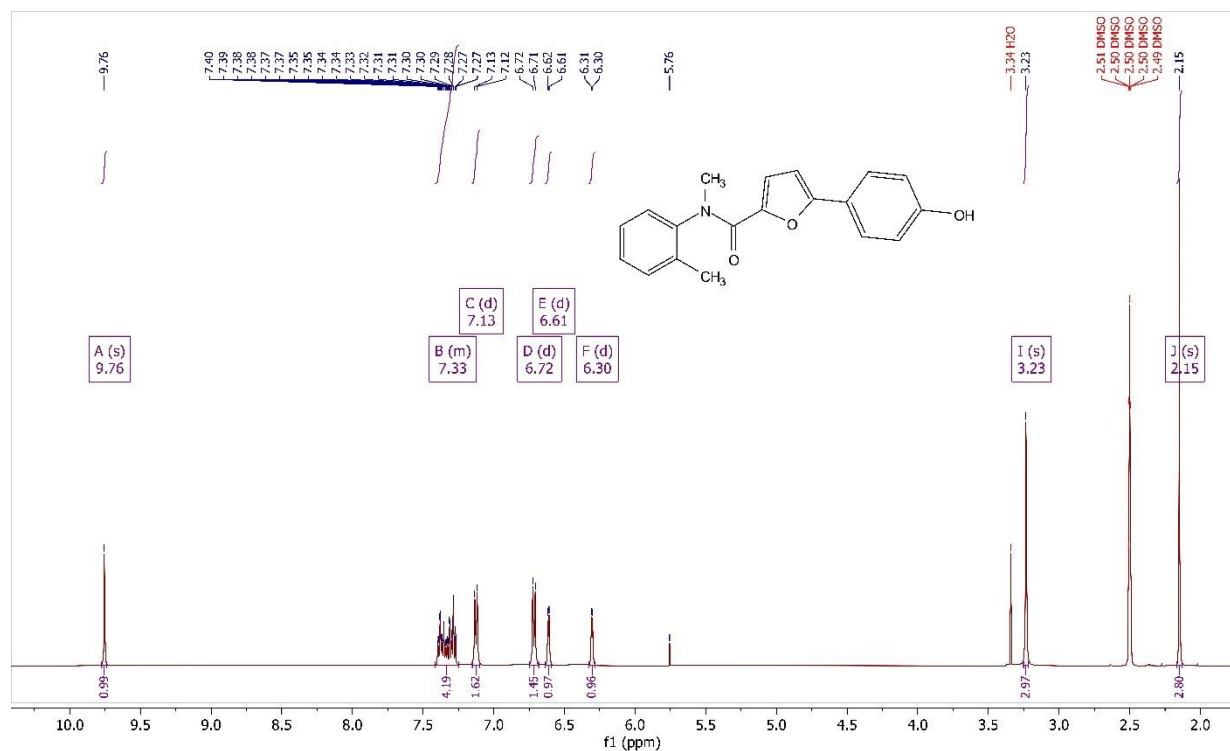


^{13}C NMR (75 MHz, Chloroform-*d*) δ 159.6, 156.5, 153.4, 145.4, 143.1, 135.8, 131.4, 128.4, 128.1, 127.4, 124.8, 123.9, 121.6, 119.5, 104.4, 37.6, 17.4, 16.0.

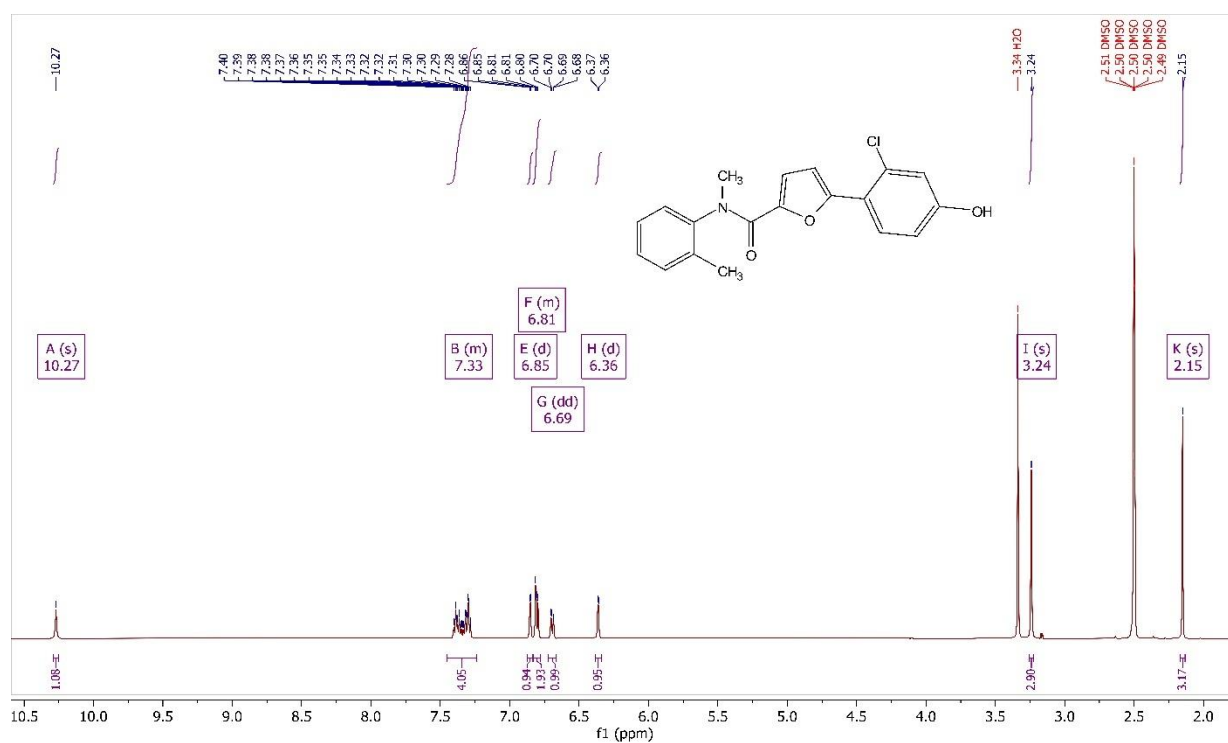


^{13}C NMR (75 MHz, Chloroform-*d*) δ 159.6, 156.5, 153.4, 145.4, 143.1, 135.8, 131.4, 128.4, 128.1, 127.4, 124.8, 123.9, 121.6, 119.5, 104.4, 37.6, 17.4, 16.0.

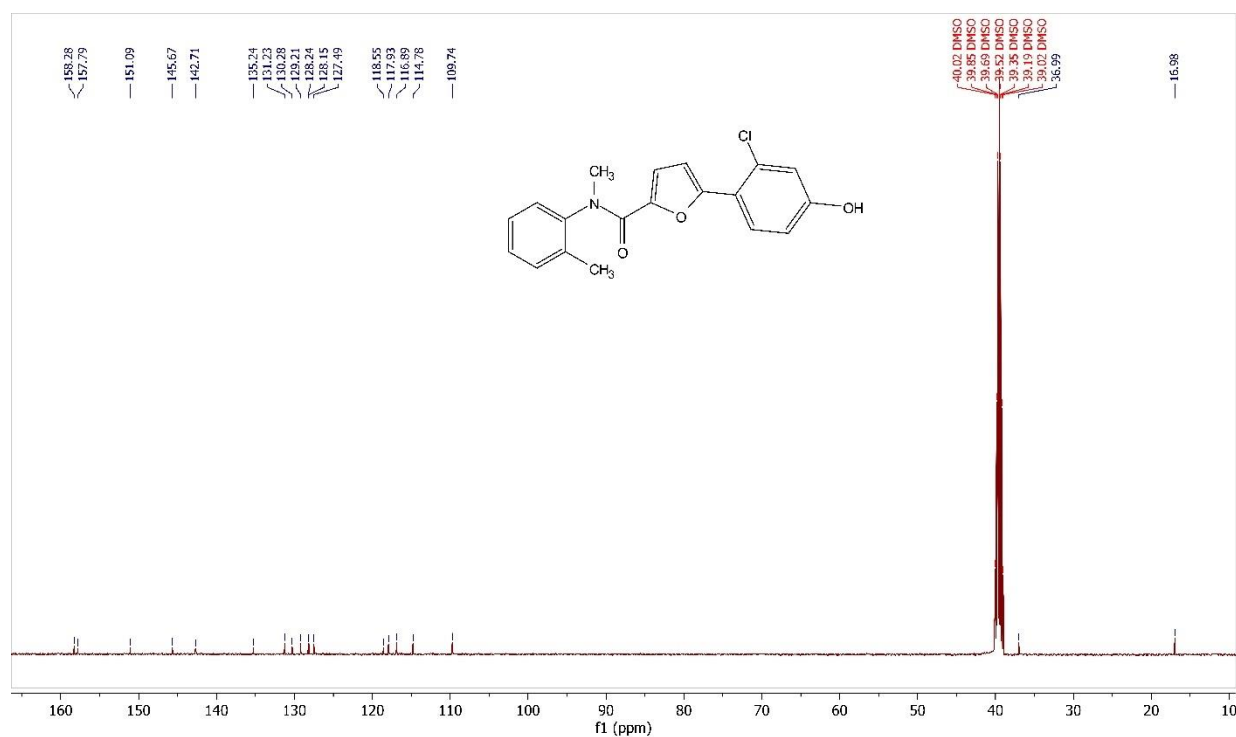
Compound 4:



Compound 5:

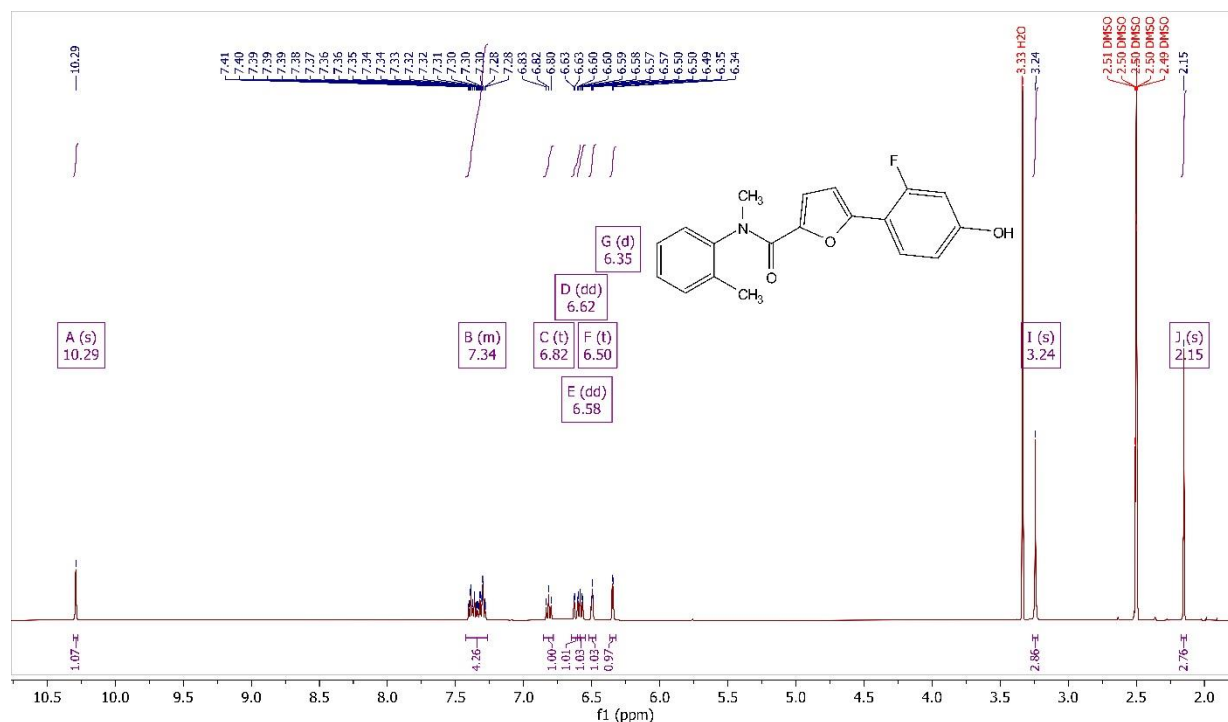


¹H NMR (500 MHz, DMSO-*d*₆) δ 10.27 (s, 1H), 7.42 – 7.26 (m, 4H), 6.85 (d, *J* = 2.4 Hz, 1H), 6.83 – 6.78 (m, 2H), 6.69 (dd, *J* = 8.7, 2.5 Hz, 1H), 6.36 (d, *J* = 3.7 Hz, 1H), 3.24 (s, 3H), 2.15 (s, 3H).

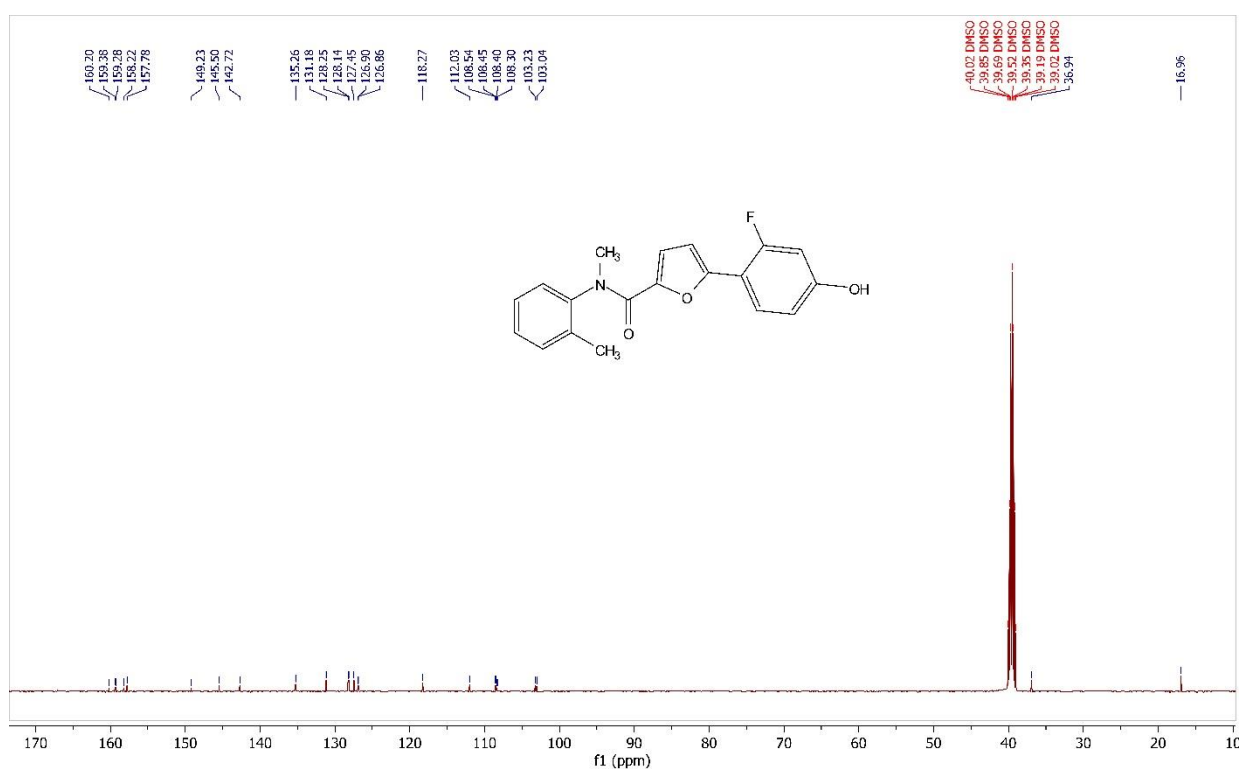


¹³C NMR (126 MHz, DMSO-*d*₆) δ 158.2, 157.7, 151.0, 145.6, 142.7, 135.2, 131.2, 130.2, 129.2, 128.2, 128.1, 127.4, 118.5, 117.9, 116.8, 114.7, 109.7, 36.9, 16.9.

Compound 6:

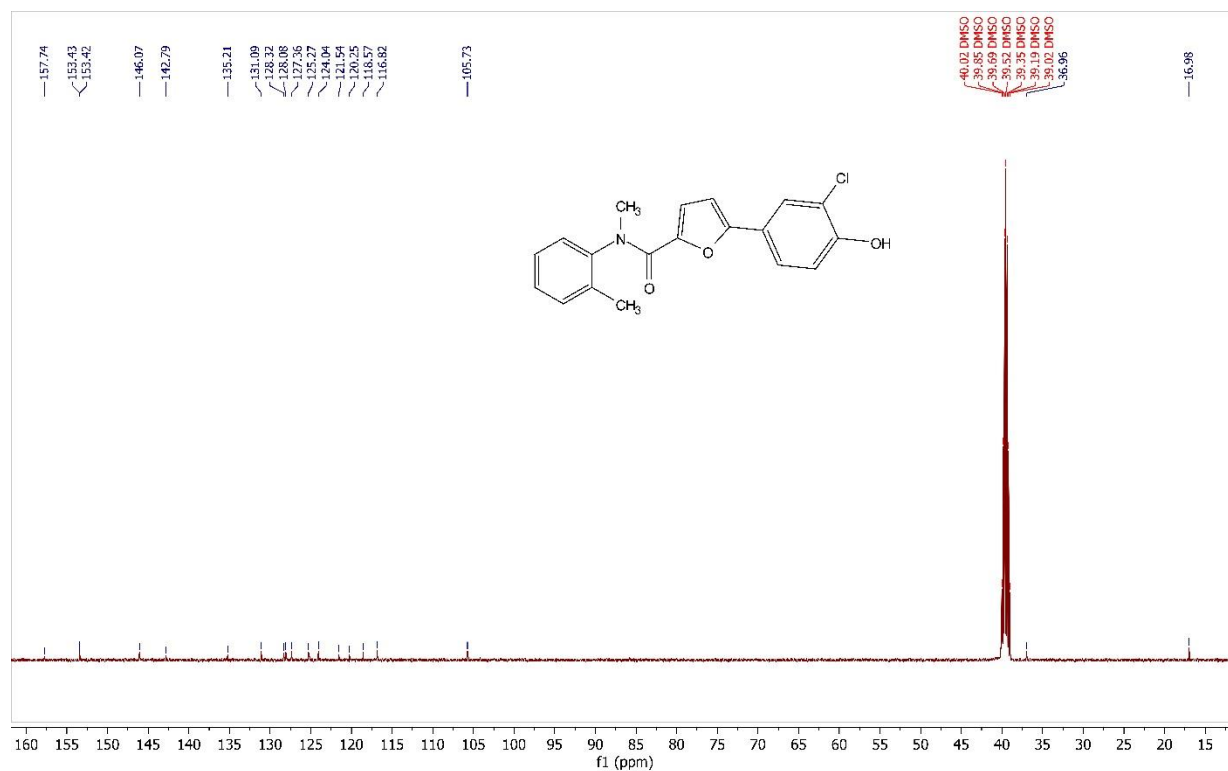
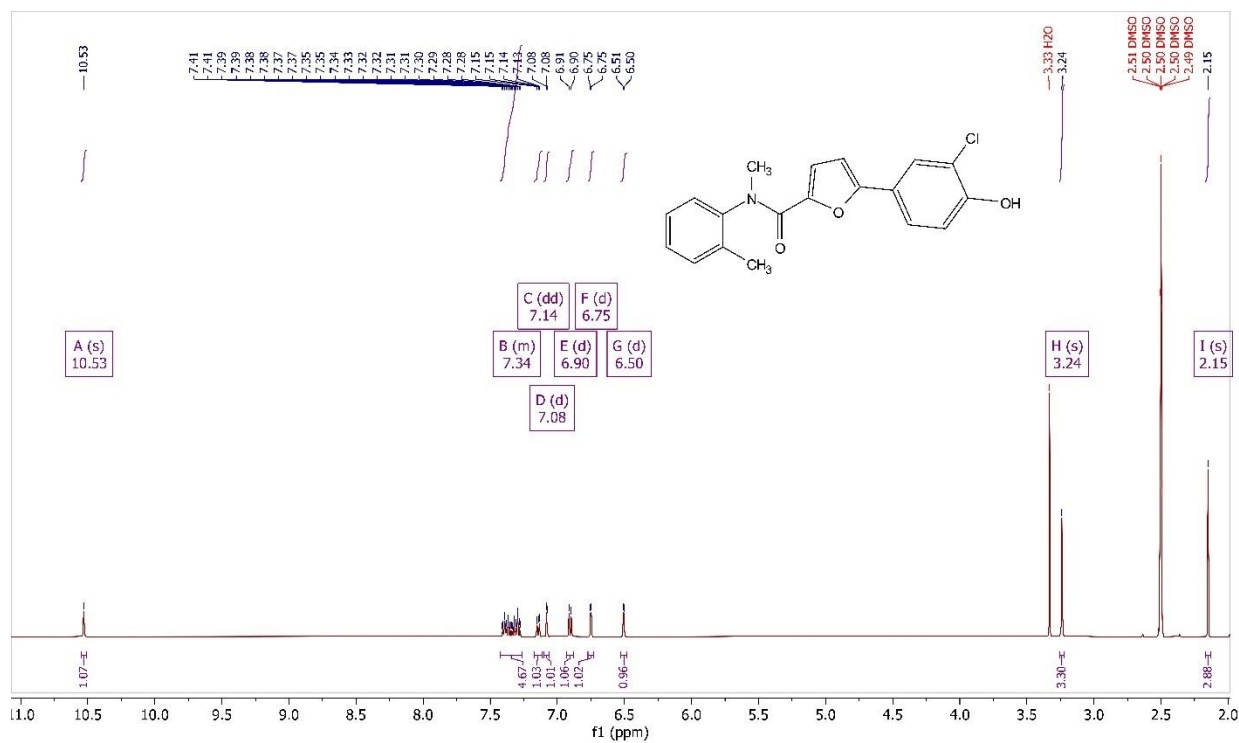


¹H NMR (500 MHz, DMSO-*d*₆) δ 10.29 (s, 1H), 7.42 – 7.26 (m, 4H), 6.82 (t, *J* = 8.8 Hz, 1H), 6.62 (dd, *J* = 13.1, 2.3 Hz, 1H), 6.58 (dd, *J* = 8.6, 2.4 Hz, 1H), 6.50 (t, *J* = 3.6 Hz, 1H), 6.35 (d, *J* = 3.6 Hz, 1H), 3.24 (s, 3H), 2.15 (s, 3H).



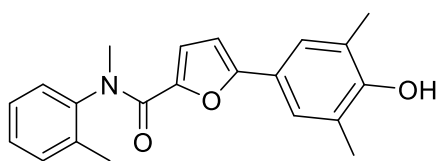
¹³C NMR (126 MHz, DMSO-*d*₆) δ 160.2, 159.3, 159.2, 158.2, 157.7, 149.2, 145.5, 142.7, 135.2, 131.1, 128.2, 128.1, 127.4, 126.9, 126.8, 118.2, 112.0, 108.5, 108.45, 108.40, 108.3, 103.2, 103.0, 36.9, 16.9.

Compound 8:

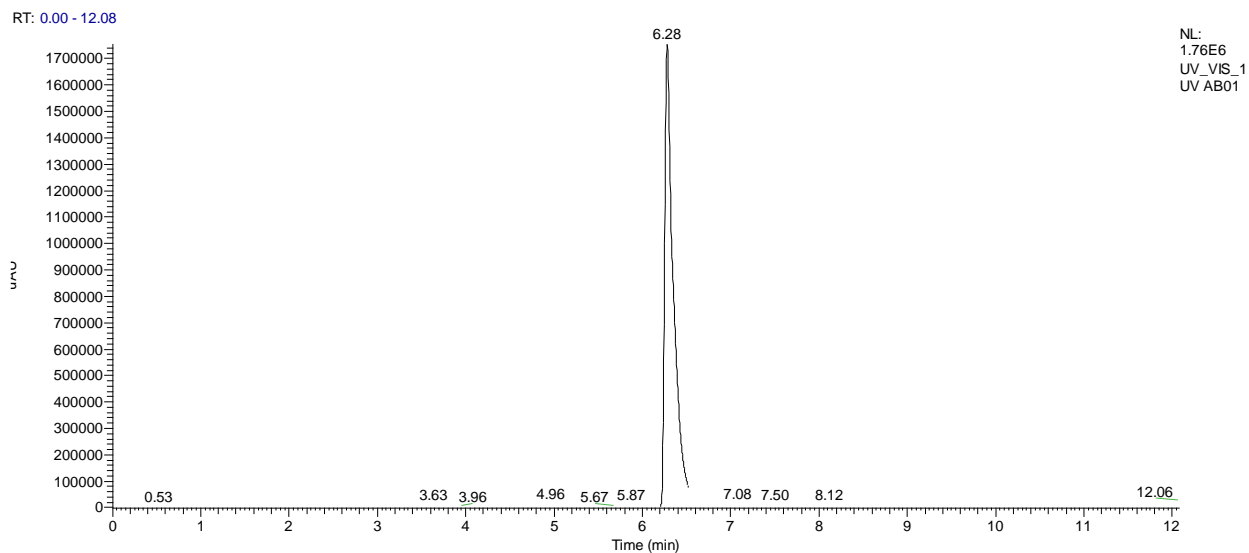


5.1.5 Representative MS spectra

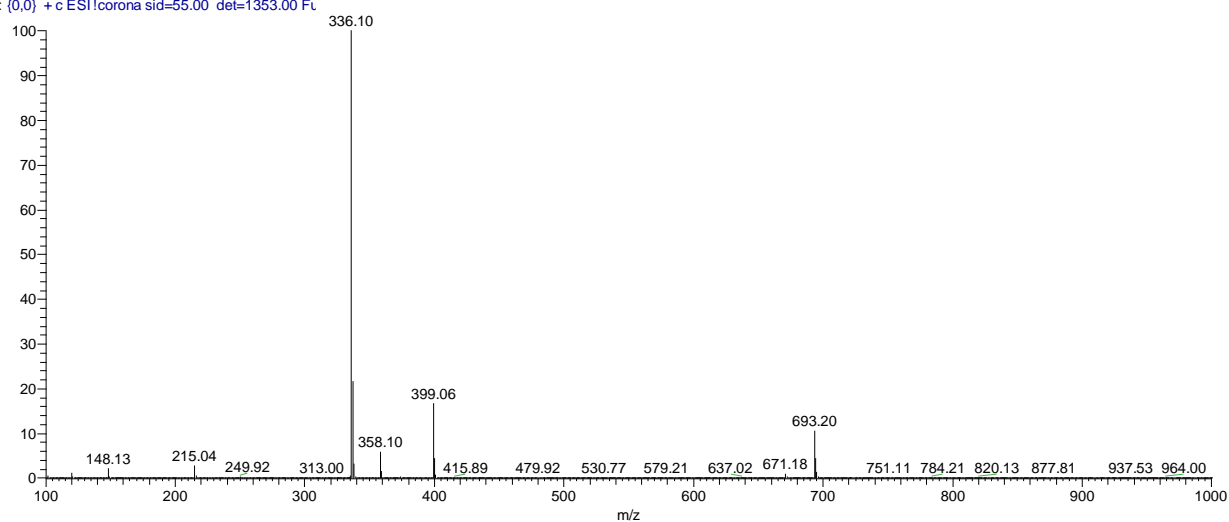
Compound 1:

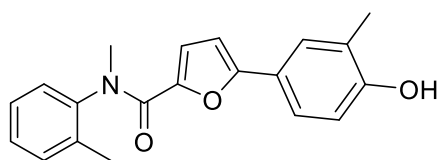


Molecular Weight: 335.40

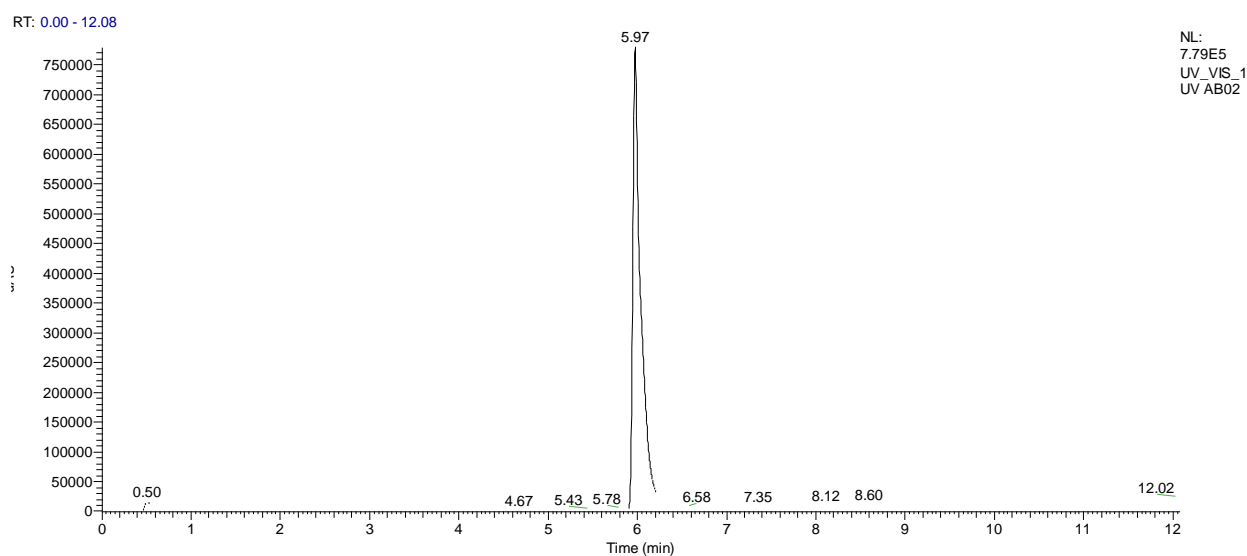


AB01 #284-318 RT: 6.02-6.74 AV: 35 NL: 4.21E6
T: (0,0) + c ESI | corona sid=55.00 det=1353.00 Fu

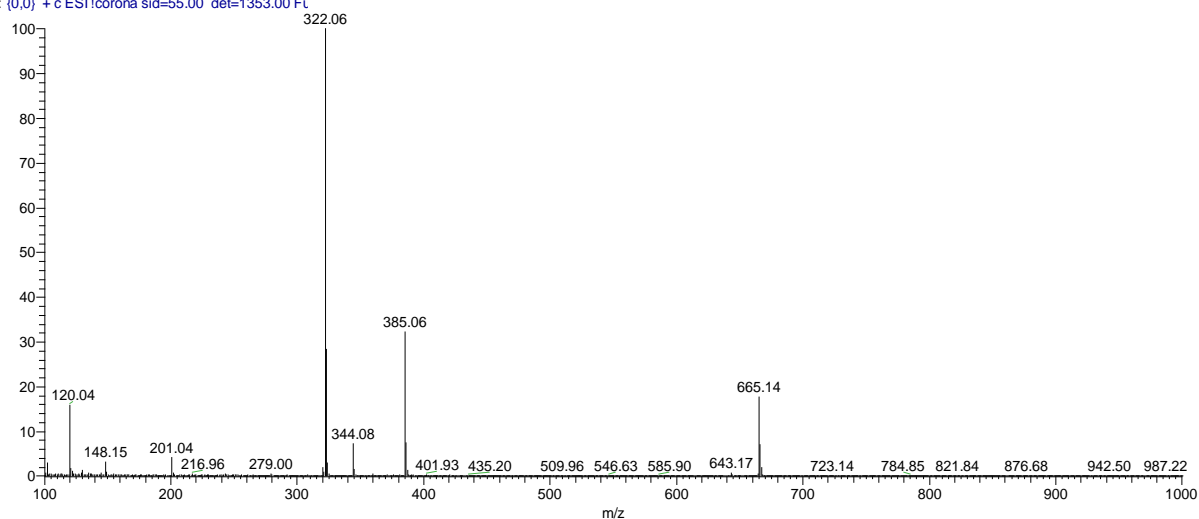


Compound 2:

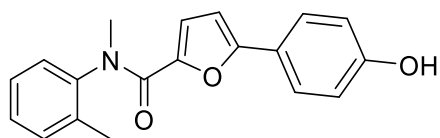
Molecular Weight: 321.38



AB02 #273-296 RT: 5.78-6.27 AV: 24 NL: 6.52E5
T: (0.0) + c ESI Icorona sid=55.00 det=1353.00 Ft

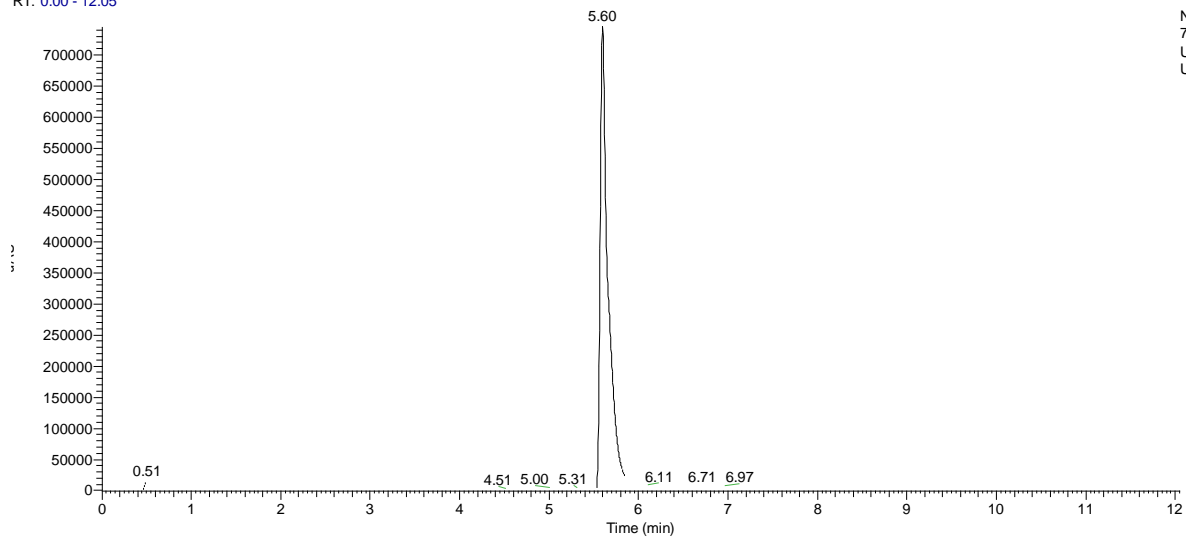
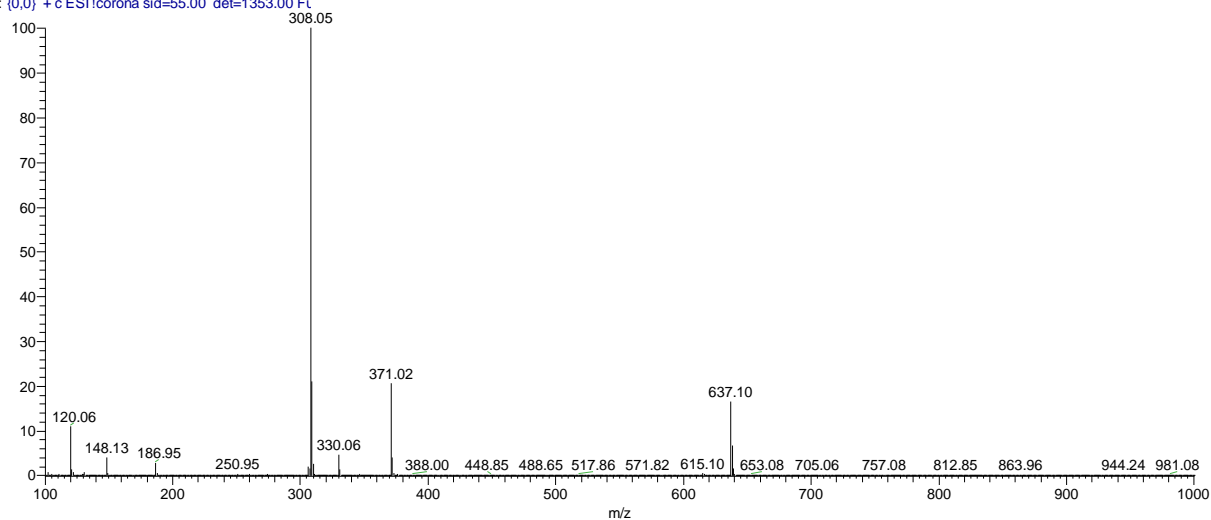


Compound 4:

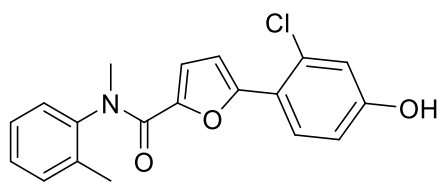


Molecular Weight: 307.35

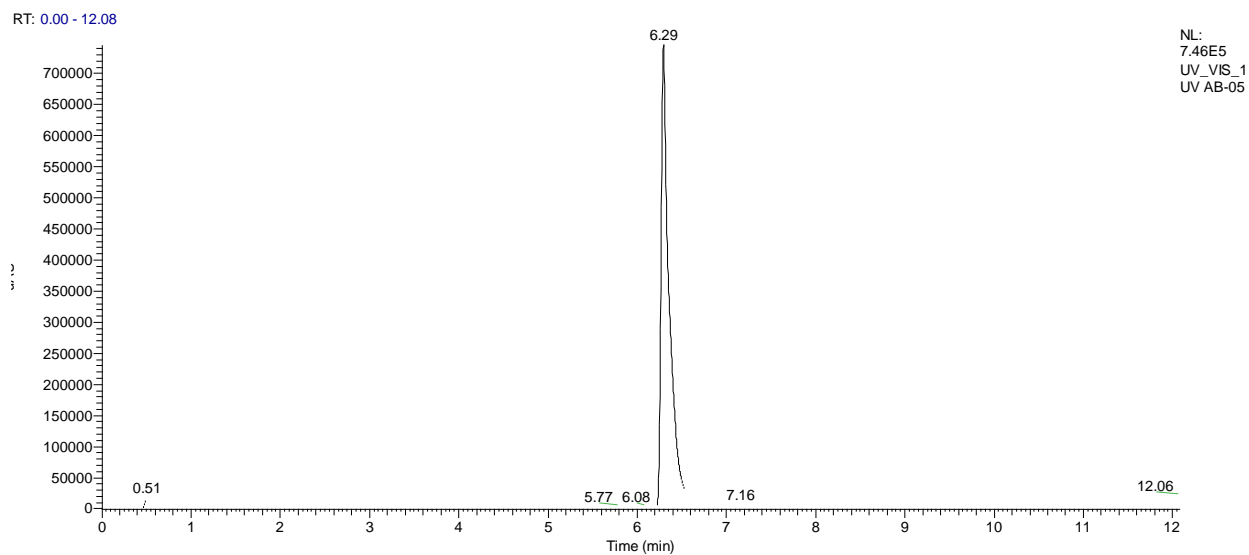
RT: 0.00 - 12.05

NL:
7.45E5
UV_VIS_1
UV AB-04AB-04 #241-288 RT: 5.10-6.10 AV: 48 NL: 1.69E6
T: (0,0) + c ESI!corona sid=55.00 det=1353.00 Ft

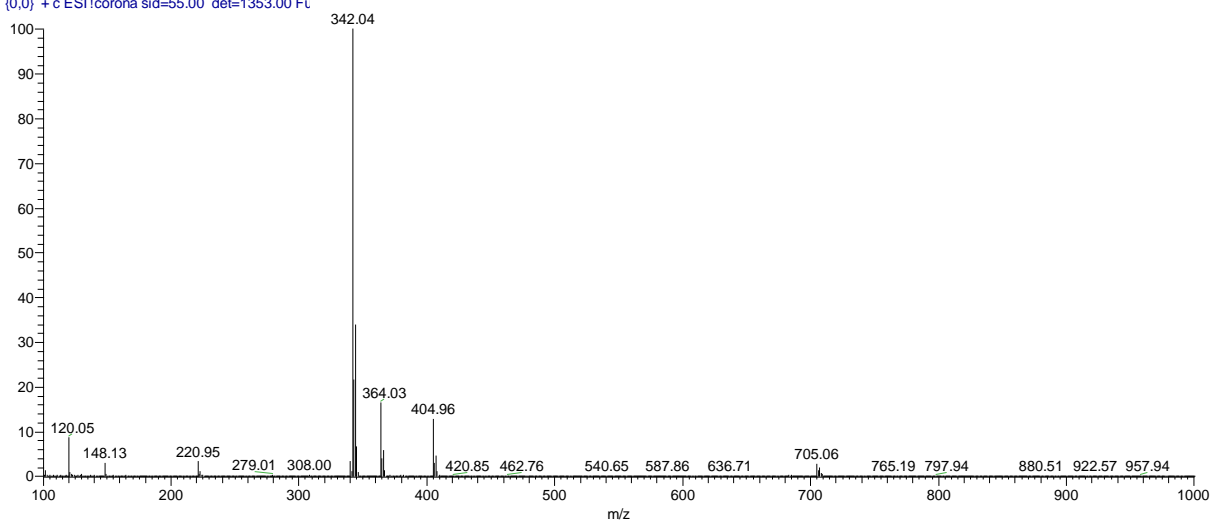
Compound 5:



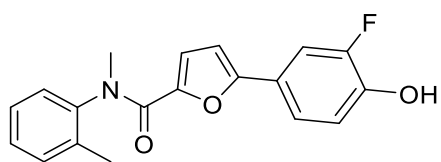
Molecular Weight: 341.79



AB-05 #278-318 RT: 5.89-6.74 AV: 41 NL: 1.30E6
T: {0,0} + c ESI Icorona sid=55.00 det=1353.00 Fu

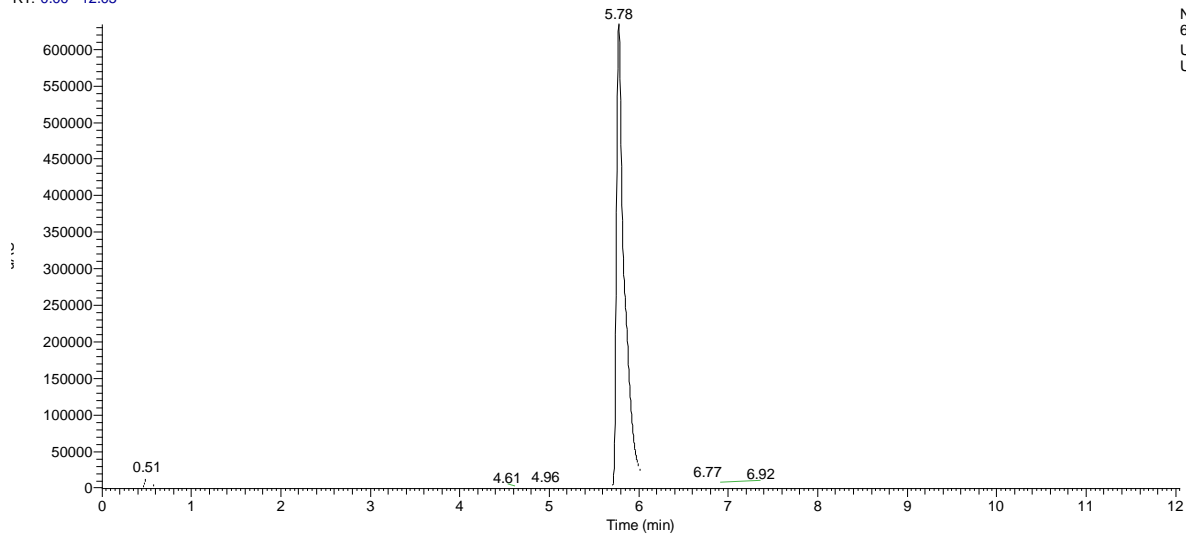
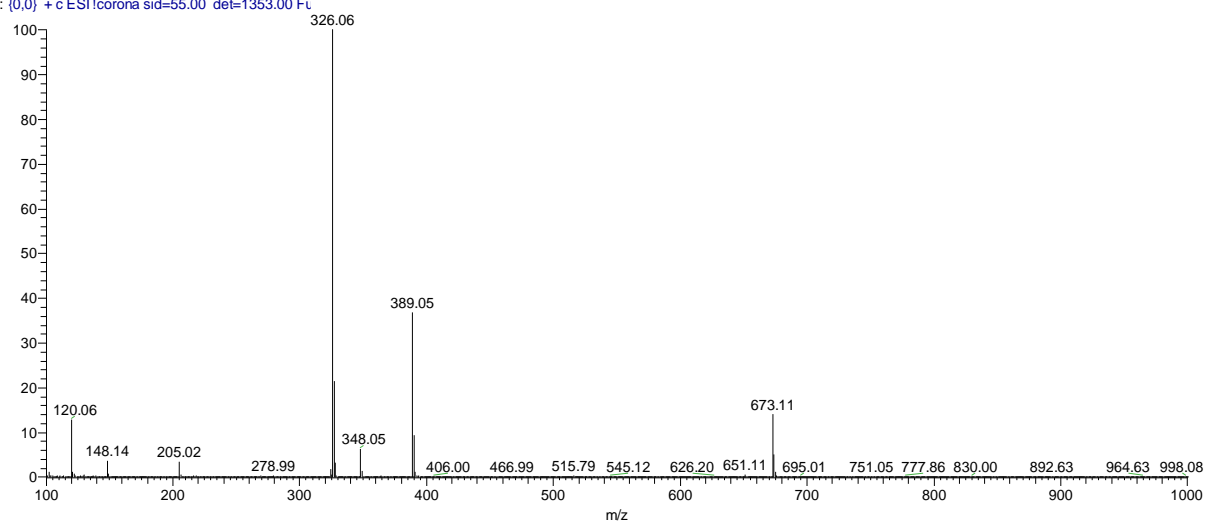


Compound 7:

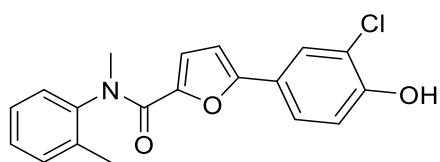


Molecular Weight: 325.34

RT: 0.00 - 12.05

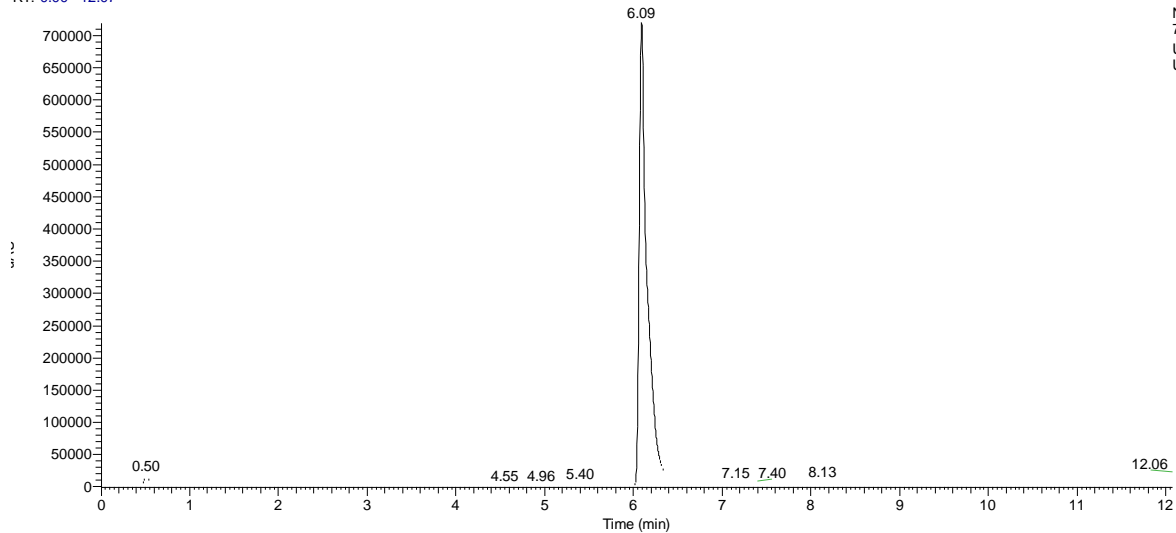
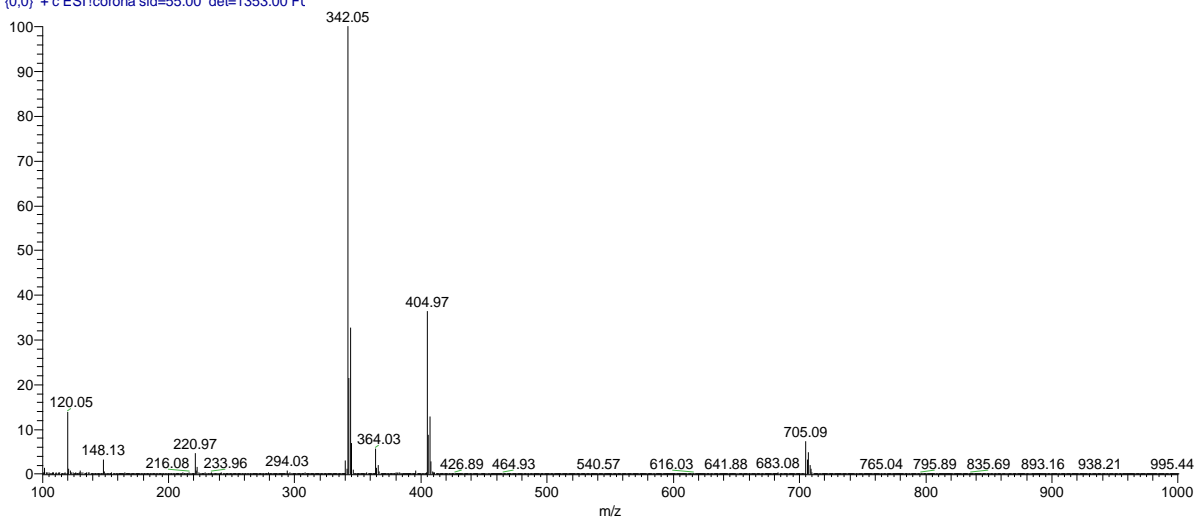
NL:
6.34E5
UV_VIS_1
UV AB-07AB-07 #265-290 RT: 5.61-6.15 AV: 26 NL: 1.26E6
T: (0,0) + c ESI!corona sid=55.00 det=1353.00 F1

Compound 8:



Molecular Weight: 341.79

RT: 0.00 - 12.07

NL:
7.19E5
UV_VIS_1
UV AB-08-AB-08-#253-324 RT: 5.36-6.87 AV: 72 NL: 1.10E6
T: (0,0) + c ESI Icorona sid=55.00 det=1353.00 Ft

5.1.6 Overview on molecular formulas and MS data

Table S1: Overview on molecular formulas, required masses and found masses for compounds **1a – 10a**, **1b** and **1 – 10**

Compound	Molecular Formula	Mass required (Exact Mass)	Mass found [M+H] ⁺
1b	C ₁₃ H ₁₂ BrNO ₂	293.01	293.98 , 295.97*
1a	C ₂₂ H ₂₃ NO ₃	349.17	350.18
2a	C ₂₁ H ₂₁ NO ₃	335.15	336.15
3a	C ₂₁ H ₂₁ NO ₃	335.15	336.27
4a	C ₂₀ H ₁₉ NO ₃	321.14	322.12
5a	C ₂₀ H ₁₈ ClNO ₃	355.10	356.06, 358.07*
6a	C ₂₀ H ₁₈ FNO ₃	339.13	340.13
7a	C ₂₀ H ₁₈ FNO ₃	339.13	340.22
9a	C ₂₀ H ₁₇ F ₂ NO ₃	357.12	357.90
10a	C ₂₀ H ₁₇ Cl ₂ NO ₃	389.06	390.15, 392.09*
1	C ₂₁ H ₂₁ NO ₃	335.15	336.10
2	C ₂₀ H ₁₉ NO ₃	321.14	322.06
3	C ₂₀ H ₁₉ NO ₃	321.14	322.20
4	C ₁₉ H ₁₇ NO ₃	307.12	308.05
5	C ₁₉ H ₁₆ ClNO ₃	341.08	342.04, 344.09*
6	C ₁₉ H ₁₆ FNO ₃	325.11	326.01
7	C ₁₉ H ₁₆ FNO ₃	325.11	326.06
8	C ₁₉ H ₁₆ ClNO ₃	341.08	342.05, 344.01*
9	C ₁₉ H ₁₅ F ₂ NO ₃	343.10	344.22
10	C ₁₉ H ₁₅ Cl ₂ NO ₃	375.04	376.14, 378.10*

*Higher value corresponds to molecular species containing the heavier halogen isotope (Cl, Br).

5.1.7 References

- (1) Marchais-Oberwinkler, S.; Wetzel, M.; Ziegler, E.; Kruchten, P.; Werth, R.; Henn, C.; Hartmann, R. W.; Frotscher, M., New Drug-Like Hydroxyphenylnaphthol Steroidomimetics As Potent and Selective 17 β -Hydroxysteroid Dehydrogenase Type 1 Inhibitors for the Treatment of Estrogen-Dependent Diseases. *J. Med. Chem.* **2011**, *54* (2), 534-547.
- (2) Perspicace, E.; Giorgio, A.; Carotti, A.; Marchais-Oberwinkler, S.; Hartmann, R. W., Novel N-methylsulfonamide and retro-N-methylsulfonamide derivatives as 17 β -hydroxysteroid dehydrogenase type 2 (17 β -HSD2) inhibitors with good ADME-related physicochemical parameters. *Eur. J. Med. Chem.* **2013**, *69*, 201-215.
- (3) Zhu, D.-W.; Lee, X.; Breton, R.; Ghosh, D.; Pang born, W.; Duax, W.; Lin, S.-X., Crystallization and preliminary X-ray diffraction analysis of the complex of human placental 17 β -hydroxysteroid dehydrogenase with NADP+. *J. Mol. Biol.* **1993**, *234* (1), 242-244.
- (4) Puranen, T. J.; Poutanen, M. H.; Peltoketo, H. E.; Vihko, P. T.; Vihko, R. K., Site-directed mutagenesis of the putative active site of human 17 β -hydroxysteroid dehydrogenase type 1. *Biochem. J.* **1994**, *304* (1), 289-293.
- (5) Jazbutyte, V.; Hu, K.; Kruchten, P.; Bey, E.; Maier, S. K.; Fritzeimer, K. H.; Prella, K.; Hegele-Hartung, C.; Hartmann, R. W.; Neyses, L.; Ertl, G.; Pelzer, T. Aging reduces the efficacy of estrogen substitution to attenuate cardiac hypertrophy in female spontaneously hypertensive rats. *Hypertension* **2006**, *48* (4), 579-586.
- (6) Xu, K.; Wetzel, M.; Hartmann, R. W.; Marchais-Oberwinkler, S. Synthesis and biological evaluation of spiro- δ -lactones as inhibitors of 17 β -hydroxysteroid dehydrogenase type 2 (17 β -HSD2). *Lett. Drug Des. Discov.* **2011**, *8* (5), 406-421.
- (7) Lin, S. X.; Yang, F.; Jin, J. Z.; Breton, R.; Zhu, D. W.; Luu-The, V.; Labrie, F. Subunit identity of the dimeric 17 beta-hydroxysteroid dehydrogenase from human placenta. *J. Biol. Chem.* **1992**, *274* (23), 28762-28770.
- (8) EDSP, Protocol for the In Vitro Estrogen Receptor Saturation Binding and Competitive Binding Assays Using Rat Uterine Cytosol. Available via EPA. http://www.epa.gov/endo/pubs/assayvalidation/appendix1_er_ruc.pdf. **2009**.
- (9) Di, L.; Kerns, E. H.; Hong, Y.; Kleintop, T. A.; McConnell, O. J.; Huryn, D. M. Optimization of a higher throughput microsomal stability screening assay for profiling drug discovery candidates. *J. Biomol. Screen.* **2003**, *8* (4), 453-462.
- (10) Moreno-Farre, J.; Workman, P.; Raynud, F. Analysis of potential drug-drug interactions for anticancer agents in human liver microsomes by high throughput liquid chromatography/mass spectrometry assay. *Aust.-Asian J. Cancer* **2007**, *6*, 55-69.
- (11) Hui, J. P. M.; Grossert, J. S.; Cutler, M. J.; Melanson, J. E. Strategic identification of *in vitro* metabolites of 13-desmethyl spiroside C using liquid chromatography/high-resolution mass spectrometry. *Rapid. Commun. Mass. Sp.* **2011**, *26* (3), 345-354.
- (12) Denizot, F.; Lang, R. Rapid colorimetric assay for cell growth and survival. Modifications to the tetrazolium dye procedure giving improved sensitivity and reliability. *J. Immunol.Methods* **1986**, *89* (2), 271-277.
- (13) Cornell, W. D.; Cieplak, P.; Bayly, C. I.; Kollmann, P. A. Application of RESP charges to calculate conformational energies, hydrogen bond energies, and free energies of solvation. *J. Am. Chem. Soc.* **1993**, *115* (21), 9620-9631.
- (14) Becke, A. D. Density-functional thermochemistry. III. The role of exact exchange. *J. Chem. Phys.* **1993**, *98*, 5648-5652.

-
- (15) Frisch, M. J.; Trucks, G. W.; Schlegel, H. B.; Scuseria, G. E.; Robb, M. A.; Cheeseman, J. R.; Scalmani, G.; Barone, V.; Mennucci, B.; Petersson, G. A.; Nakatsuji, H.; Caricato, M.; Li, X.; Hratchian, H. P.; Izmaylov, A. F.; Bloino, J.; Zheng, G.; Sonnenberg, J. L.; Hada, M.; Ehara, M.; Toyota, K.; Fukuda, R.; Hasegawa, J.; Ishida, M.; Nakajima, T.; Honda, Y.; Kitao, O.; Nakai, H.; Vreven, T.; Montgomery, J. A., Jr.; Peralta, J. E.; Ogliaro, F.; Bearpark, M.; Heyd, J. J.; Brothers, E.; Kudin, K. N.; Staroverov, V. N.; Kobayashi, R.; Normand, J.; Raghavachari, K.; Rendell, A.; Burant, J. C.; Iyengar, S. S.; Tomasi, J.; Cossi, M.; Rega, N.; Millam, J. M.; Klene, M.; Knox, J. E.; Cross, J. B.; Bakken, V.; Adamo, C.; Jaramillo, J.; Gomperts, R.; Stratmann, R. E.; Yazyev, O.; Austin, A. J.; Cammi, R.; Pomelli, C.; Ochterski, J. W.; Martin, R. L.; Morokuma, K.; Zakrzewski, V. G.; Voth, G. A.; Salvador, P.; Dannenberg, J. J.; Dapprich, S.; Daniels, A. D.; Farkas, Ö.; Foresman, J. B.; Ortiz, J. V.; Cioslowski, J.; Fox, D. J. *Gaussian 09*, revision A.2, Gaussian, Inc.: Wallingford, CT, **2009**.
- (16) Mazumdar, M.; Fournier, D.; Zhu, D. W.; Cadot, C.; Poirier, D.; Lin, S. X. Binary and ternary crystal structure analyses of a novel inhibitor with 17beta-HSD type 1: a lead compound for breast cancer therapy. *Biochem. J.* **2009**, *424* (3), 357-366.
- (17) Schrödinger Suite 2015-3: Schrödinger, LLC, New York, NY, **2015**.
- (18) Small-Molecule Drug Discovery Suite 2015-3: Glide, version 6.8, Schrödinger, LLC, New York, **2015**.
- (19) Sherbet, D. P.; Papari-Zareei, M.; Khan, N.; Sharma, K. K.; Brandmaier, A.; Rambally, S.; Chattopadhyay, A.; Andersson, S.; Agarwal, A. K.; Auchus, R. J. Cofactors, redox state, and directional preferences of hydroxysteroid dehydrogenases. *Mol. Cell. Endocrinol.* **2007**, *265-266*, 83-88.

5.2 Supporting Information for Publication B

5.2.1 Synthesis of compounds **1a**, **5a-12a**, **25a-27a**, **32a-34a**, **1b**, **9b**, **10b-12b**, **25b**, **26b**, **31b-34b**, **10c**, **31c**, **32c**, **1-12**, **25-27** and **31-34**

5-bromo-N-methyl-N-(o-tolyl)furan-2-carboxamide (1b). The title compound was prepared according to method A and B using 5-bromofuran-2-carboxylic acid (1.90 g, 10 mmol), thionyl chloride (1.45 ml, 20 mmol) and DMF (30 drops) in toluene (50 ml). The corresponding N,2-dimethylaniline (1.25 ml, 10 mmol) and Et₃N (2.79 ml, 20 mmol) in DCM (50 ml) was added to the acyl chloride. The residue was purified by silica gel column chromatography (petroleum ether /ethyl acetate 5:1) to give 2.1 g (7.13 mmol/ 71 %) of the analytically pure compound (purity: 96.99 %). C₁₃H₁₂BrNO₂; MW 294.15; ¹H NMR (500 MHz, DMSO-*d*₆) δ 7.39 – 7.32 (m, 2H), 7.34 – 7.24 (m, 2H), 6.47 (d, *J* = 3.6 Hz, 1H), 5.51 (d, *J* = 3.6 Hz, 1H), 3.21 (s, 3H), 2.12 (s, 3H); MS (ESI): 293.75, 295.95 (M+H)⁺.

5-(4-methoxyphenyl)-N-methyl-N-(o-tolyl)furan-2-carboxamide (1a). The title compound was prepared according to method D by the reaction of **1b** (0.535 g, 1.82 mmol, 1 equiv) and (4-methoxyphenyl)boronic acid (0.414 g, 2.73 mmol, 1.5 equiv) in the presence of cesium carbonate (2.37 g, 7.28 mmol, 4 equiv) and tetrakis(triphenylphosphine) palladium (105 mg, 0.091 mmol, 0.05 equiv) in DME/water 1:1 (50 ml). The product was purified by column chromatography (petroleum ether /ethyl acetate 4:1) to give 0.5 g (1.55 mmol/ 85 %) of the analytically pure compound (purity: 98.48 %). C₂₀H₁₉NO₃; MW 321.38; ¹H NMR (500 MHz, DMSO-*d*₆) δ 7.42 – 7.26 (m, 4H), 7.23 (d, *J* = 8.7 Hz, 2H), 6.90 (d, *J* = 8.8 Hz, 2H), 6.71 (d, *J* = 3.6 Hz, 1H), 6.36 (d, *J* = 3.6 Hz, 1H), 3.77 (s, 3H), 3.24 (s, 3H), 2.16 (s, 3H); MS (ESI): 322.12 (M+H)⁺.

5-(4-hydroxyphenyl)-N-methyl-N-(o-tolyl)furan-2-carboxamide (1). The title compound was prepared according to method E by the reaction of **1a** (0.4 g, 1.24 mmol, 1 equiv) and BF₃.SMe₂ (1.30 ml, 12.4 mmol, 10 equiv) in dichloromethane (50 ml). The product was purified by column chromatography (dichloromethane/methanol 98.5:1.5) to give 0.29 g (0.944 mmol/ 76 %) of the analytically pure compound (purity: 99.36 %). C₁₉H₁₇NO₃; MW 307.35; mp: 172-175 °C; ¹H NMR (500 MHz, DMSO-*d*₆) δ 9.76 (s, 1H), 7.41 – 7.25 (m, 4H), 7.13 (d, *J* = 8.4 Hz, 2H), 6.72 (d, *J* = 8.7 Hz, 2H), 6.61 (d, *J* = 3.6 Hz, 1H), 6.30 (d, *J* = 3.6 Hz, 1H), 3.23 (s, 3H), 2.15 (s, 3H); ¹³C NMR (126 MHz, DMSO-*d*₆) δ 157.95, 157.94, 155.10, 145.49, 142.84, 135.26, 131.11, 128.16, 128.13, 127.38, 125.66, 120.43, 118.34, 115.52, 104.58, 36.88, 16.96; MS (ESI): 308.12 (M+H)⁺.

5-(3-hydroxyphenyl)-N-methyl-N-(o-tolyl)furan-2-carboxamide (2). The title compound was prepared according to method D by the reaction of **1b** (0.294 g, 1 mmol, 1 equiv) and (3-hydroxyphenyl)boronic acid (0.206 g, 1.5 mmol, 1.5 equiv) in the presence of cesium carbonate (1.3 g, 4 mmol, 4 equiv) and tetrakis(triphenylphosphine) palladium (57 mg, 0.05 mmol, 0.05 equiv) in DME/water 1:1 (50 ml). The product was purified by column chromatography (petroleum ether /ethyl acetate 3:1) to give 0.234 g (0.76 mmol/ 76 %) of the analytically pure compound (purity: 98.92 %). C₁₉H₁₇NO₃; MW 307.35; mp: 134-136 °C; ¹H NMR (500 MHz, Acetone-*d*₆) δ 8.43 (s, 1H), 7.43 – 7.26 (m, 4H), 7.15 (t, *J* = 7.9 Hz, 1H), 6.94 – 6.90 (m, 1H), 6.84 (d, *J* = 7.7 Hz, 1H), 6.77 (dd, *J* = 8.0, 2.5 Hz, 1H), 6.67 (d, *J* = 3.6 Hz, 1H), 6.29 (d, *J* =

3.7 Hz, 1H), 3.30 (s, 3H), 2.23 (s, 3H); ^{13}C NMR (126 MHz, Acetone- d_6) δ 159.15, 158.57, 155.87, 147.97, 144.15, 136.70, 132.18, 131.92, 130.67, 129.22, 129.15, 128.30, 118.66, 116.47, 116.38, 111.81, 107.25, 37.29, 17.52; MS (ESI): 308.00 (M+H) $^+$.

5-(2-hydroxyphenyl)-N-methyl-N-(o-tolyl)furan-2-carboxamide (3). The title compound was prepared according to method D by the reaction of **1b** (0.294 g, 1 mmol, 1 equiv) and (2-hydroxyphenyl)boronic acid (0.206 g, 1.5 mmol, 1.5 equiv) in the presence of cesium carbonate (1.3 g, 4 mmol, 4 equiv) and tetrakis(triphenylphosphine) palladium (57 mg, 0.05 mmol, 0.05 equiv) in DME/water 1:1 (50 ml). The product was purified by column chromatography (petroleum ether /ethyl acetate 3:1) to give 0.222 g (0.72 mmol/ 72 %) of the analytically pure compound (purity: 98.24 %). $\text{C}_{19}\text{H}_{17}\text{NO}_3$; MW 307.35; mp: 197-199 $^\circ\text{C}$; ^1H NMR (500 MHz, DMSO- d_6) δ 10.21 (s, 1H), 7.42 – 7.26 (m, 4H), 7.10 (ddd, $J = 8.7, 7.2, 1.7$ Hz, 1H), 6.90 – 6.84 (m, 1H), 6.81 (dd, $J = 8.8, 2.5$ Hz, 2H), 6.75 – 6.69 (m, 1H), 6.46 (d, $J = 3.6$ Hz, 1H), 3.25 (s, 3H), 2.16 (s, 3H); ^{13}C NMR (126 MHz, DMSO- d_6) δ 157.97, 154.06, 151.77, 145.14, 142.86, 135.16, 131.12, 129.21, 128.10, 128.04, 127.38, 125.41, 118.91, 118.32, 116.07, 115.92, 110.39, 36.99, 16.97; MS (ESI): 308.01 (M+H) $^+$.

5-(3-chloro-4-hydroxyphenyl)-N-methyl-N-(o-tolyl)furan-2-carboxamide (4). The title compound was prepared according to method D by the reaction of **1b** (0.294 g, 1 mmol, 1 equiv) and (3-chloro-4-hydroxyphenyl)boronic acid (0.259 g, 1.5 mmol, 1.5 equiv) in the presence of cesium carbonate (1.3 g, 4 mmol, 4 equiv) and tetrakis(triphenylphosphine) palladium (57 mg, 0.05 mmol, 0.05 equiv) in DME/water 1:1 (50 ml). The product was purified by column chromatography (petroleum ether /ethyl acetate 3:1) to give 0.233 g (0.68 mmol/ 68 %) of the analytically pure compound (purity: 98.59 %). $\text{C}_{19}\text{H}_{16}\text{ClNO}_3$; MW 341.79; mp: 77-80 $^\circ\text{C}$; ^1H NMR (500 MHz, DMSO- d_6) δ 10.53 (s, 1H), 7.43 – 7.26 (m, 4H), 7.14 (dd, $J = 8.5, 2.2$ Hz, 1H), 7.08 (d, $J = 2.2$ Hz, 1H), 6.90 (d, $J = 8.5$ Hz, 1H), 6.75 (d, $J = 3.6$ Hz, 1H), 6.50 (d, $J = 3.6$ Hz, 1H), 3.24 (s, 3H), 2.15 (s, 3H); ^{13}C NMR (126 MHz, DMSO- d_6) δ 157.74, 153.43, 153.42, 146.07, 142.79, 135.21, 131.09, 128.32, 128.08, 127.36, 125.27, 124.04, 121.54, 120.25, 118.57, 116.82, 105.73, 36.96, 16.98; MS (ESI): 342.07, 344.11 (M+H) $^+$.

5-(4-methoxy-3-methylphenyl)-N-methyl-N-(o-tolyl)furan-2-carboxamide (5a). The title compound was prepared according to method D by the reaction of **1b** (0.441 g, 1.49 mmol, 1 equiv) and (4-methoxy-3-methylphenyl)boronic acid (0.373 g, 2.24 mmol, 1.5 equiv) in the presence of cesium carbonate (1.94 g, 5.96 mmol, 4 equiv) and tetrakis(triphenylphosphine) palladium (86 mg, 0.074 mmol, 0.05 equiv) in DME/water 1:1 (60 ml). The product was purified by column chromatography (petroleum ether /ethyl acetate 3:1) to give 0.44 g (1.31 mmol/ 88 %) of the analytically pure compound (purity: 99.99 %). $\text{C}_{21}\text{H}_{21}\text{NO}_3$; MW 335.40; ^1H NMR (500 MHz, Acetone- d_6) δ 7.44 – 7.26 (m, 4H), 7.19 (dd, $J = 8.6, 2.3$ Hz, 1H), 7.04 – 7.00 (m, 1H), 6.87 (d, $J = 8.5$ Hz, 1H), 6.58 (d, $J = 3.6$ Hz, 1H), 6.51 (d, $J = 3.6$ Hz, 1H), 3.83 (s, 3H), 3.29 (s, 3H), 2.22 (s, 3H), 2.15 (s, 3H); MS (ESI): 336.18 (M+H) $^+$.

5-(4-hydroxy-3-methylphenyl)-N-methyl-N-(o-tolyl)furan-2-carboxamide (5). The title compound was prepared according to method E by the reaction of **5a** (0.420 g, 1.25 mmol, 1 equiv) and $\text{BF}_3 \cdot \text{SMe}_2$ (1.31 ml, 12.52 mmol, 10 equiv) in dichloromethane (30 ml). The product was purified by column chromatography (petroleum ether /ethyl acetate 2:1) to give 0.29 g (0.9 mmol/ 72 %) of the analytically pure compound (purity: 99.99 %). $\text{C}_{20}\text{H}_{19}\text{NO}_3$; MW 321.38;

mp: 183-186 °C; ^1H NMR (500 MHz, DMSO- d_6) δ 9.66 (s, 1H), 7.42 – 7.25 (m, 4H), 7.02 (d, 1H), 6.87 (s, 1H), 6.71 (d, $J = 8.3$ Hz, 1H), 6.60 (d, $J = 3.7$ Hz, 1H), 6.42 (d, $J = 3.7$ Hz, 1H), 3.23 (s, 3H), 2.14 (s, 3H), 2.08 (s, 3H); ^{13}C NMR (126 MHz, DMSO- d_6) δ 157.91, 156.09, 155.32, 145.49, 142.94, 135.25, 131.12, 128.18, 128.11, 127.39, 126.38, 124.32, 123.08, 120.27, 118.57, 114.75, 104.43, 36.98, 17.02, 15.74; MS (ESI): 322.15 (M+H) $^+$.

5-(3-fluoro-4-methoxyphenyl)-N-methyl-N-(o-tolyl)furan-2-carboxamide (**6a**). The title compound was prepared according to method D by the reaction of **1b** (0.294 g, 1 mmol, 1 equiv) and (3-fluoro-4-methoxyphenyl)boronic acid (0.254 g, 1.5 mmol, 1.5 equiv) in the presence of cesium carbonate (1.3 g, 4 mmol, 4 equiv) and tetrakis(triphenylphosphine) palladium (57 mg, 0.05 mmol, 0.05 equiv) in DME/water 1:1 (50 ml). The product was purified by column chromatography (petroleum ether /ethyl acetate 4:1) to give 0.292 g (0.86 mmol/ 86 %) of the analytically pure compound (purity: 98.26 %). $\text{C}_{20}\text{H}_{18}\text{FNO}_3$; MW 339.37; ^1H NMR (500 MHz, Chloroform- d) δ 7.28 – 7.20 (m, 2H), 7.18 (dt, $J = 7.5, 4.4$ Hz, 1H), 7.12 – 7.07 (m, 1H), 6.93 (ddd, $J = 8.5, 2.1, 1.3$ Hz, 1H), 6.82 – 6.71 (m, 2H), 6.35 (d, $J = 3.6$ Hz, 1H), 6.26 (d, $J = 3.6$ Hz, 1H), 3.77 (s, 3H), 3.26 (s, 3H), 2.13 (s, 3H); MS (ESI): 340.07 (M+H) $^+$.

5-(3-fluoro-4-hydroxyphenyl)-N-methyl-N-(o-tolyl)furan-2-carboxamide (**6**). The title compound was prepared according to method E by the reaction of **6a** (0.250 g, 0.736 mmol, 1 equiv) and $\text{BF}_3\cdot\text{SMe}_2$ (0.775 ml, 7.36 mmol, 10 equiv) in dichloromethane (30 ml). The product was purified by column chromatography (dichloromethane/methanol 98:2) to give 0.185 g (0.56 mmol/ 77 %) of the analytically pure compound (purity: 98.48 %). $\text{C}_{19}\text{H}_{16}\text{FNO}_3$; MW 325.34; mp: 190-192 °C; ^1H NMR (500 MHz, DMSO- d_6) δ 10.22 (s, 1H), 7.42 – 7.26 (m, 4H), 7.00 – 6.92 (m, 2H), 6.89 (t, $J = 8.8$ Hz, 1H), 6.73 (d, $J = 3.6$ Hz, 1H), 6.44 (d, $J = 3.6$ Hz, 1H), 3.24 (s, 3H), 2.15 (s, 3H); ^{13}C NMR (126 MHz, DMSO- d_6) δ 157.78, 152.83 (d, $J = 224.5$ Hz), 150.02, 146.00, 145.42 (d, $J = 12.3$ Hz), 142.82, 135.25, 131.11, 128.18 (d, $J = 12.8$ Hz), 127.39, 121.00 (d, $J = 7.2$ Hz), 120.66 (d, $J = 3.1$ Hz), 118.49, 118.02, 118.00, 111.90 (d, $J = 20.4$ Hz), 105.80, 36.96, 16.98; MS (ESI): 326.01 (M+H) $^+$.

5-(2-chloro-4-methoxyphenyl)-N-methyl-N-(o-tolyl)furan-2-carboxamide (**7a**). The title compound was prepared according to method D by the reaction of **1b** (0.600 g, 2.03 mmol, 1 equiv) and (2-chloro-4-methoxyphenyl)boronic acid (0.57 g, 3.05 mmol, 1.5 equiv) in the presence of cesium carbonate (2.64 g, 8.12 mmol, 4 equiv) and tetrakis(triphenylphosphine) palladium (117 mg, 0.101 mmol, 0.05 equiv) in DME/water 1:1 (60 ml). The product was purified by column chromatography (petroleum ether /ethyl acetate 3:1) to give 0.585 g (1.64 mmol/ 81 %) of the analytically pure compound (purity: 98.33 %). $\text{C}_{20}\text{H}_{18}\text{ClNO}_3$; MW 355.82; ^1H NMR (500 MHz, Acetone- d_6) δ 7.41 – 7.28 (m, 4H), 7.00 (d, $J = 2.6$ Hz, 1H), 6.95 (d, $J = 8.9$ Hz, 1H), 6.89 (d, $J = 3.7$ Hz, 1H), 6.86 (dd, $J = 8.9, 2.6$ Hz, 1H), 6.50 (d, $J = 3.7$ Hz, 1H), 3.84 (s, 3H), 3.30 (s, 3H), 2.21 (s, 3H); MS (ESI): 356.06, 358.07 (M+H) $^+$.

5-(2-chloro-4-hydroxyphenyl)-N-methyl-N-(o-tolyl)furan-2-carboxamide (**7**). The title compound was prepared according to method E by the reaction of **7a** (0.585 g, 1.64 mmol, 1 equiv) and $\text{BF}_3\cdot\text{SMe}_2$ (1.72 ml, 16.44 mmol, 10 equiv) in dichloromethane (50 ml). The product was purified by column chromatography (dichloromethane/methanol 98:2) to give 0.4 g (1.17 mmol/ 71 %) of the analytically pure compound (purity: 98.40 %). $\text{C}_{19}\text{H}_{16}\text{ClNO}_3$; MW 341.79; mp: 198-201 °C; ^1H NMR (500 MHz, DMSO- d_6) δ 10.27 (s, 1H), 7.42 – 7.26 (m, 4H), 6.85 (d,

$J = 2.4$ Hz, 1H), 6.83 – 6.78 (m, 2H), 6.69 (dd, $J = 8.7, 2.5$ Hz, 1H), 6.36 (d, $J = 3.7$ Hz, 1H), 3.24 (s, 3H), 2.15 (s, 3H); ^{13}C NMR (126 MHz, DMSO- d_6) δ 158.28, 157.79, 151.09, 145.67, 142.71, 135.24, 131.23, 130.28, 129.21, 128.24, 128.15, 127.49, 118.54, 117.93, 116.89, 114.79, 109.74, 36.99, 16.98; MS (ESI): 342.02, 344.09 (M+H) $^+$.

5-(2-fluoro-4-methoxyphenyl)-N-methyl-N-(o-tolyl)furan-2-carboxamide (8a). The title compound was prepared according to method D by the reaction of **1b** (0.700 g, 2.37 mmol, 1 equiv) and (2-fluoro-4-methoxyphenyl)boronic acid (0.606 g, 3.56 mmol, 1.5 equiv) in the presence of cesium carbonate (3.08 g, 9.48 mmol, 4 equiv) and tetrakis(triphenylphosphine) palladium (137 mg, 0.118 mmol, 0.05 equiv) in DME/water 1:1 (80 ml). The product was purified by column chromatography (petroleum ether /ethyl acetate 4:1) to give 0.674 g (1.98 mmol/ 83 %) of the analytically pure compound (purity: 99.99 %). $\text{C}_{20}\text{H}_{18}\text{FNO}_3$; MW 339.37; ^1H NMR (500 MHz, Acetone- d_6) δ 7.41 – 7.28 (m, 4H), 6.97 (t, $J = 8.8$ Hz, 1H), 6.81 – 6.72 (m, 2H), 6.55 (t, $J = 3.7$ Hz, 1H), 6.49 (d, $J = 3.6$ Hz, 1H), 3.84 (s, 3H), 3.30 (s, 3H), 2.22 (s, 3H); MS (ESI): 340.13 (M+H) $^+$.

5-(2-fluoro-4-hydroxyphenyl)-N-methyl-N-(o-tolyl)furan-2-carboxamide (8). The title compound was prepared according to method E by the reaction of **8a** (0.674 g, 1.98 mmol, 1 equiv) and $\text{BF}_3 \cdot \text{SMe}_2$ (2.08 ml, 19.86 mmol, 10 equiv) in dichloromethane (50 ml). The product was purified by column chromatography (dichloromethane/methanol 99.5:0.5) to give 0.55 g (1.69 mmol/ 85 %) of the analytically pure compound (purity: 99.04 %). $\text{C}_{19}\text{H}_{16}\text{FNO}_3$; MW 325.34; mp: 185-187 °C; ^1H NMR (500 MHz, DMSO- d_6) δ 10.29 (s, 1H), 7.42 – 7.26 (m, 4H), 6.82 (t, $J = 8.8$ Hz, 1H), 6.62 (dd, $J = 13.1, 2.3$ Hz, 1H), 6.58 (dd, $J = 8.6, 2.4$ Hz, 1H), 6.50 (t, $J = 3.6$ Hz, 1H), 6.35 (d, $J = 3.6$ Hz, 1H), 3.24 (s, 3H), 2.15 (s, 3H); ^{13}C NMR (126 MHz, DMSO- d_6) δ 160.19, 159.32 (d, $J = 12.0$ Hz), 158.21, 157.77, 149.20 (d, $J = 2.6$ Hz), 144.10 (d, $J = 255.13$ Hz), 135.25, 131.16, 128.18 (d, $J = 12.9$ Hz), 127.44, 126.87 (d, $J = 5.0$ Hz), 118.26, 112.01, 112.00, 108.48 (d, $J = 10.6$ Hz), 108.34 (d, $J = 12.4$ Hz), 103.12 (d, $J = 23.4$ Hz), 36.93, 16.95; MS (ESI): 326.06 (M+H) $^+$.

5-bromo-N-(2-fluoro-6-methylphenyl)furan-2-carboxamide (9b). The title compound was prepared according to method A and B using 5-bromofuran-2-carboxylic acid (1.90 g, 10 mmol), thionyl chloride (1.45 ml, 20 mmol) and DMF (30 drops) in toluene (50 ml). The corresponding 2-fluoro-6-methylaniline (1.11 ml, 10 mmol) and Et_3N (2.79 ml, 20 mmol) in DCM (50 ml) was added to the acyl chloride. The residue was purified by silica gel column chromatography (petroleum ether /ethyl acetate 4:1) to give 1.5 g (5.03 mmol/ 50 %) of the analytically pure compound (purity: 96.76 %). $\text{C}_{12}\text{H}_9\text{BrFNO}_2$; MW 298.11; ^1H NMR (300 MHz, DMSO- d_6) δ 9.93 (s, 1H), 7.34 (d, $J = 3.6$ Hz, 1H), 7.31 – 7.19 (m, 1H), 7.18 – 7.06 (m, 2H), 6.84 (d, $J = 3.6$ Hz, 1H), 2.21 (s, 3H); MS (ESI): 297.82, 299.85 (M+H) $^+$.

5-bromo-N-(2-fluoro-6-methylphenyl)-N-methylfuran-2-carboxamide (9a). The title compound was prepared according to method C using 5-bromo-N-(2-fluoro-6-methylphenyl)furan-2-carboxamide (0.5 g, 1.67 mmol, 1 equiv), NaH (0.08 g, 3.35 mmol, 2 equiv) and iodomethane (0.103 ml, 1.67 mmol, 1 equiv) in DMF (30 ml). The product was purified by column chromatography (dichloromethane/methanol 99.5:0.5) to give 0.27 g (0.86 mmol/ 51 %) of the analytically pure compound (purity: 98.10 %). $\text{C}_{13}\text{H}_{11}\text{BrFNO}_2$; MW 312.14; ^1H NMR (500 MHz, Methanol- d_4) δ 7.38 (td, $J = 8.0, 5.6$ Hz, 1H), 7.21 – 7.13 (m, 1H), 7.13 – 7.06 (m, 1H),

6.35 (d, $J = 3.6$ Hz, 1H), 6.04 (d, $J = 3.6$ Hz, 1H), 3.29 (s, 3H), 2.24 (s, 3H); MS (ESI): 312.02, 313.91 (M+H)⁺.

N-(2-fluoro-6-methylphenyl)-5-(4-hydroxyphenyl)-*N*-methylfuran-2-carboxamide (**9**). The title compound was prepared according to method D by the reaction of **9a** (0.168 g, 0.538 mmol, 1 equiv) and (4-hydroxyphenyl) boronic acid (0.111 g, 0.807 mmol, 1.5 equiv) in the presence of cesium carbonate (0.701 g, 2.15 mmol, 4 equiv) and tetrakis(triphenylphosphine) palladium (31 mg, 0.026 mmol, 0.05 equiv) in DME/water 1:1 (50 ml). The product was purified by column chromatography (petroleum ether /ethyl acetate 2:1) to give 0.098 g (0.3 mmol/ 56 %) of the analytically pure compound (purity: 99.99 %). C₁₉H₁₆FNO₃; MW 325.34; mp: 171-173 °C; ¹H NMR (500 MHz, Chloroform-*d*) δ 7.41 – 7.26 (m, 3H), 7.25 (s, 1H), 7.11 (ddt, $J = 7.8, 1.6, 0.8$ Hz, 1H), 7.06 (dddd, $J = 9.0, 8.2, 1.4, 0.6$ Hz, 1H), 6.93 – 6.86 (m, 2H), 6.37 – 6.30 (m, 2H), 3.37 (s, 3H), 2.25 (s, 3H); ¹³C NMR (126 MHz, Chloroform-*d*) δ 159.98, 158.93 (d, $J = 233.7$ Hz), 156.78 (d, $J = 52.2$ Hz), 145.28, 138.80, 130.85 (d, $J = 13.3$ Hz), 129.40 (d, $J = 8.6$ Hz), 126.55 (d, $J = 3.3$ Hz), 126.44, 122.34, 119.06, 116.22, 115.90, 114.40 (d, $J = 20.4$ Hz), 104.90, 36.63, 17.38; MS (ESI): 325.94 (M+H)⁺.

5-bromo-*N*-(5-fluoro-2-methylphenyl)furan-2-carboxamide (**10c**). The title compound was prepared according to method A and B using 5-bromofuran-2-carboxylic acid (1.90 g, 10 mmol), thionyl chloride (1.45 ml, 20 mmol) and DMF (30 drops) in toluene (50 ml). The corresponding 5-fluoro-2-methylaniline (1.11 ml, 10 mmol) and Et₃N (2.79 ml, 20 mmol) in DCM (50 ml) was added to the acyl chloride. The residue was purified by silica gel column chromatography (petroleum ether /ethyl acetate 4:1) to give 2.1 g (7.04 mmol/ 70 %) of the analytically pure compound (purity: 98.19 %). C₁₂H₉BrFNO₂; MW 298.11; ¹H NMR (500 MHz, DMSO-*d*₆) δ 9.88 (s, 1H), 7.35 (d, $J = 3.5$ Hz, 1H), 7.29 (ddd, $J = 8.5, 6.5, 0.9$ Hz, 1H), 7.23 (dd, $J = 10.3, 2.8$ Hz, 1H), 7.02 (td, $J = 8.5, 2.8$ Hz, 1H), 6.84 (d, $J = 3.6$ Hz, 1H), 2.19 (s, 3H); MS (ESI): 298.02, 300.00 (M+H)⁺.

5-bromo-*N*-(5-fluoro-2-methylphenyl)-*N*-methylfuran-2-carboxamide (**10b**). The title compound was prepared according to method C using 5-bromo-*N*-(5-fluoro-2-methylphenyl)furan-2-carboxamide (1.766 g, 5.92 mmol, 1 equiv), NaH (0.284 g, 11.85 mmol, 2 equiv) and iodomethane (0.368 ml, 5.92 mmol, 1 equiv) in DMF (60 ml). The product was purified by column chromatography (petroleum ether /ethyl acetate 4:1) to give 1.45 g (4.64 mmol/ 78 %) of the analytically pure compound (purity: 99.97 %). C₁₃H₁₁BrFNO₂; MW 312.14; ¹H NMR (500 MHz, DMSO-*d*₆) δ 7.39 (dd, $J = 8.6, 6.4$ Hz, 1H), 7.29 (dd, $J = 9.5, 2.7$ Hz, 1H), 7.22 (td, $J = 8.5, 2.7$ Hz, 1H), 6.52 (d, $J = 3.6$ Hz, 1H), 5.83 (d, $J = 3.7$ Hz, 1H), 3.21 (s, 3H), 2.08 (s, 3H); MS (ESI): 311.98, 313.96 (M+H)⁺.

N-(5-fluoro-2-methylphenyl)-5-(4-methoxyphenyl)-*N*-methylfuran-2-carboxamide (**10a**). The title compound was prepared according to method D by the reaction of **10b** (1.13 g, 3.64 mmol, 1 equiv) and (4-methoxyphenyl)boronic acid (0.830 g, 5.46 mmol, 1.5 equiv) in the presence of cesium carbonate (4.74 g, 14.56 mmol, 4 equiv) and tetrakis(triphenylphosphine) palladium (210 mg, 0.182 mmol, 0.05 equiv) in DME/water 1:1 (80 ml). The product was purified by column chromatography (petroleum ether /ethyl acetate 4:1) to give 1.05 g (3.09 mmol/ 85 %) of the analytically pure compound (purity: 96.64 %). C₂₀H₁₈FNO₃; MW 339.37; ¹H NMR (500 MHz, DMSO-*d*₆) δ 7.45 – 7.39 (m, 1H), 7.30 (dd, $J = 9.7, 2.8$ Hz, 1H), 7.27 – 7.20 (m, 3H),

6.92 (d, $J = 8.5$ Hz, 2H), 6.76 (dd, $J = 3.7, 1.7$ Hz, 1H), 6.58 – 6.53 (m, 1H), 3.77 (s, 3H), 3.24 (s, 3H), 2.12 (s, 3H); MS (ESI): 340.12 (M+H)⁺.

N-(5-fluoro-2-methylphenyl)-5-(4-hydroxyphenyl)-*N*-methylfuran-2-carboxamide (**10**). The title compound was prepared according to method E by the reaction of **10a** (1.00 g, 2.94 mmol, 1 equiv) and BF₃.SMe₂ (3.1 ml, 29.46 mmol, 10 equiv) in dichloromethane (80 ml). The product was purified by column chromatography (petroleum ether /ethyl acetate 2:1) to give 0.711 g (2.18 mmol/ 74 %) of the analytically pure compound (purity: 97.27 %). C₁₉H₁₆FNO₃; MW 325.34; mp: 184-186 °C; ¹H NMR (500 MHz, DMSO-*d*₆) δ 9.79 (s, 1H), 7.44 – 7.38 (m, 1H), 7.28 (dd, $J = 9.5, 2.7$ Hz, 1H), 7.26 – 7.19 (m, 1H), 7.15 – 7.10 (m, 2H), 6.73 (d, $J = 8.3$ Hz, 2H), 6.66 (d, $J = 3.5$ Hz, 1H), 6.51 (s, 1H), 3.23 (s, 3H), 2.10 (s, 3H); ¹³C NMR (126 MHz, DMSO-*d*₆) δ 160.78 (d, $J = 243.4$ Hz), 158.00, 157.78, 155.21, 145.34, 143.92 (d, $J = 10.1$ Hz), 132.22 (d, $J = 8.8$ Hz), 131.53 (d, $J = 3.6$ Hz), 125.59, 120.36, 118.70, 115.55, 115.19 (d, $J = 21.7$ Hz), 114.93 (d, $J = 20.5$ Hz), 104.71, 36.72, 16.26; MS (ESI): 326.14 (M+H)⁺.

5-bromo-*N*-(4-fluoro-2-methylphenyl)furan-2-carboxamide (**11b**). The title compound was prepared according to method A and B using 5-bromofuran-2-carboxylic acid (1.90 g, 10 mmol), thionyl chloride (1.45 ml, 20 mmol) and DMF (30 drops) in toluene (50 ml). The corresponding 4-fluoro-2-methylaniline (1.11 ml, 10 mmol) and Et₃N (2.79 ml, 20 mmol) in DCM (50 ml) was added to the acyl chloride. The residue was purified by silica gel column chromatography (petroleum ether /ethyl acetate 4:1) to give 2.53 g (8.48 mmol/ 84 %) of the analytically pure compound (purity: 98.11 %). C₁₂H₉BrFNO₂; MW 298.11; ¹H NMR (500 MHz, DMSO-*d*₆) δ 9.88 (s, 1H), 7.34 – 7.26 (m, 2H), 7.14 (ddd, $J = 9.6, 3.0, 0.8$ Hz, 1H), 7.04 (td, $J = 8.6, 3.0$ Hz, 1H), 6.83 (d, $J = 3.6$ Hz, 1H), 2.20 (s, 3H); MS (ESI): 297.99, 300.03 (M+H)⁺.

5-bromo-*N*-(4-fluoro-2-methylphenyl)-*N*-methylfuran-2-carboxamide (**11a**). The title compound was prepared according to method C using 5-bromo-*N*-(4-fluoro-2-methylphenyl)furan-2-carboxamide (1.119 g, 3.75 mmol, 1 equiv), NaH (0.18 g, 7.5 mmol, 2 equiv) and iodomethane (0.233 ml, 3.75 mmol, 1 equiv) in DMF (40 ml). The product was purified by column chromatography (petroleum ether /ethyl acetate 4:1) to give 0.80 g (2.56 mmol/ 86 %) of the analytically pure compound (purity: 97.32 %). C₁₃H₁₁BrFNO₂; MW 312.14; ¹H NMR (500 MHz, DMSO-*d*₆) δ 7.34 (dd, $J = 8.7, 5.5$ Hz, 1H), 7.25 (dd, $J = 9.5, 3.0$ Hz, 1H), 7.13 (td, $J = 8.5, 3.1$ Hz, 1H), 6.51 (d, $J = 3.6$ Hz, 1H), 5.73 (d, $J = 3.6$ Hz, 1H), 3.20 (s, 3H), 2.12 (s, 3H); MS (ESI): 311.98, 313.97 (M+H)⁺.

N-(4-fluoro-2-methylphenyl)-5-(4-hydroxyphenyl)-*N*-methylfuran-2-carboxamide (**11**). The title compound was prepared according to method D by the reaction of **11a** (0.750 g, 2.4 mmol, 1 equiv) and (4-hydroxyphenyl) boronic acid (0.496 g, 3.6 mmol, 1.5 equiv) in the presence of cesium carbonate (3.12 g, 9.6 mmol, 4 equiv) and tetrakis(triphenylphosphine) palladium (138 mg, 0.12 mmol, 0.05 equiv) in DME/water 1:1 (80 ml). The product was purified by column chromatography (petroleum ether /ethyl acetate 2:1) to give 0.55 g (1.69 mmol/ 70 %) of the analytically pure compound (purity: 95.22 %). C₁₉H₁₆FNO₃; MW 325.34; mp: 196-198 °C; ¹H NMR (500 MHz, DMSO-*d*₆) δ 9.78 (s, 1H), 7.35 (dd, $J = 8.7, 5.5$ Hz, 1H), 7.27 (dd, $J = 9.8, 3.0$ Hz, 1H), 7.15 (dd, $J = 8.6, 3.3$ Hz, 3H), 6.73 (d, $J = 8.5$ Hz, 2H), 6.65 (d, $J = 3.6$ Hz, 1H), 6.43 (d, $J = 3.6$ Hz, 1H), 3.22 (s, 3H), 2.15 (s, 3H); ¹³C NMR (126 MHz, DMSO-*d*₆) δ 161.26 (d, $J = 244.8$ Hz), 157.98, 155.14, 145.42, 139.18 (d, $J = 2.6$ Hz), 138.19 (d, $J = 8.7$ Hz), 130.06

(d, $J = 9.1$ Hz), 125.59, 125.58, 120.40, 118.62, 117.41 (d, $J = 22.3$ Hz), 115.53, 113.91 (d, $J = 22.2$ Hz), 104.66, 36.92, 17.04; MS (ESI): 326.11 (M+H)⁺.

5-bromo-N-(3-fluoro-2-methylphenyl)furan-2-carboxamide (12b). The title compound was prepared according to method A and B using 5-bromofuran-2-carboxylic acid (1.90 g, 10 mmol), thionyl chloride (1.45 ml, 20 mmol) and DMF (30 drops) in toluene (50 ml). The corresponding 5-fluoro-2-methylaniline (1.11 ml, 10 mmol) and Et₃N (2.79 ml, 20 mmol) in DCM (50 ml) was added to the acyl chloride. The residue was purified by silica gel column chromatography (dichloromethane/methanol 99.5:0.5) to give 2.31 g (7.77 mmol/ 77 %) of the analytically pure compound (purity: 96.67 %). C₁₂H₉BrFNO₂; MW 298.11; ¹H NMR (500 MHz, DMSO-*d*₆) δ 10.05 (s, 1H), 7.34 (d, $J = 3.6$ Hz, 1H), 7.25 (tdd, $J = 8.2, 6.4, 0.7$ Hz, 1H), 7.20 – 7.13 (m, 1H), 7.09 (ddd, $J = 9.6, 8.3, 1.3$ Hz, 1H), 6.84 (d, $J = 3.5$ Hz, 1H), 2.09 (s, 3H); MS (ESI): 297.88, 299.97 (M+H)⁺.

5-bromo-N-(3-fluoro-2-methylphenyl)-N-methylfuran-2-carboxamide (12a). The title compound was prepared according to method C using 5-bromo-N-(3-fluoro-2-methylphenyl)furan-2-carboxamide (1.319 g, 7.77 mmol, 1 equiv), NaH (0.373 g, 15.55 mmol, 2 equiv) and iodomethane (0.483 ml, 7.77 mmol, 1 equiv) in DMF (70 ml). The product was purified by column chromatography (petroleum ether /ethyl acetate 3:1) to give 1.97 g (6.31 mmol/ 81 %) of the analytically pure compound (purity: 98.04 %). C₁₃H₁₁BrFNO₂; MW 312.14; ¹H NMR (500 MHz, DMSO-*d*₆) δ 7.37 – 7.24 (m, 2H), 7.18 – 7.13 (m, 1H), 6.51 (d, $J = 3.6$ Hz, 1H), 5.86 (d, $J = 3.6$ Hz, 1H), 3.22 (s, 3H), 2.04 (s, 3H); MS (ESI): 311.94, 313.95 (M+H)⁺.

N-(3-fluoro-2-methylphenyl)-5-(4-hydroxyphenyl)-N-methylfuran-2-carboxamide (12). The title compound was prepared according to method D by the reaction of **12a** (1.55 g, 4.97 mmol, 1 equiv) and (4-hydroxyphenyl) boronic acid (1.029 g, 7.45 mmol, 1.5 equiv) in the presence of cesium carbonate (6.47 g, 19.88 mmol, 4 equiv) and tetrakis(triphenylphosphine) palladium (287 mg, 0.248 mmol, 0.05 equiv) in DME/water 1:1 (100 ml). The product was purified by column chromatography (petroleum ether /ethyl acetate 2:1) to give 1.33 g (4.08 mmol/ 82 %) of the analytically pure compound (purity: 99.99 %). C₁₉H₁₆FNO₃; MW 325.34; mp: 195-197 °C; ¹H NMR (500 MHz, DMSO-*d*₆) δ 9.78 (s, 1H), 7.38 – 7.31 (m, 1H), 7.28 (t, $J = 8.9$ Hz, 1H), 7.17 (dd, $J = 7.8, 1.3$ Hz, 1H), 7.11 (d, $J = 8.2$ Hz, 2H), 6.75 – 6.70 (m, 2H), 6.66 (d, $J = 3.1$ Hz, 1H), 6.53 (t, $J = 2.5$ Hz, 1H), 3.24 (s, 3H), 2.07 (s, 3H); ¹³C NMR (126 MHz, DMSO-*d*₆) δ 161.09 (d, $J = 243.4$ Hz), 157.97 (d, $J = 10.4$ Hz), 155.20, 145.30, 144.55 (d, $J = 2.7$ Hz), 127.89 (d, $J = 9.4$ Hz), 125.54, 124.24, 122.85 (d, $J = 17.0$ Hz), 120.34, 118.79, 115.53, 115.44, 114.71 (d, $J = 22.4$ Hz), 104.72, 37.01, 9.29; MS (ESI): 326.07 (M+H)⁺.

5-bromo-N-(3-methylpyridin-2-yl)furan-2-carboxamide (25b). To a suspension of 5-bromofuran-2-carboxylic acid (1.00 g, 5.23 mmol, 1 equiv), DCC (1.08 g, 5.23 mmol, 1 equiv), DMAP (31 mg, 0.261 mmol, 0.05 equiv) in 40 ml DCM at 0 °C 4-methylpyridin-3-amine (0.565 g, 5.23 mmol, 1 equiv) was added. The mixture was stirred at room temperature overnight. The mixture was quenched with water (50 mL) and extracted three times with ethyl acetate (3 x 30 mL). The organic layer was washed with water, dried over MgSO₄, filtered and evaporated to dryness under reduced pressure. The residue was purified by silica gel column chromatography (dichloromethane/methanol 94:6) to give 0.956 g (3.4 mmol/ 65 %) of the analytically pure compound (purity: 99.99 %). C₁₁H₉BrN₂O₂; MW 281.11; ¹H NMR (500 MHz, DMSO-*d*₆) δ

10.52 (s, 1H), 8.31 (ddd, $J = 4.7, 1.9, 0.7$ Hz, 1H), 7.73 (ddd, $J = 7.6, 1.9, 0.8$ Hz, 1H), 7.41 (d, $J = 3.6$ Hz, 1H), 7.27 (dd, $J = 7.5, 4.8$ Hz, 1H), 6.84 (d, $J = 3.6$ Hz, 1H), 2.18 (s, 3H); MS (ESI): 280.95, 282.94 (M+H)⁺.

5-bromo-N-methyl-N-(3-methylpyridin-2-yl)furan-2-carboxamide (25a). The title compound was prepared according to method C using 5-bromo-N-(3-methylpyridin-2-yl)furan-2-carboxamide (0.866 g, 3.08 mmol, 1 equiv), NaH (0.147 g, 6.16 mmol, 2 equiv) and iodomethane (0.191 ml, 3.08 mmol, 1 equiv) in DMF (30 ml). The product was purified by column chromatography (dichloromethane/methanol 97:3) to give 0.754 g (2.55 mmol/ 82 %) of the analytically pure compound (purity: 99.99 %). C₁₂H₁₁BrN₂O₂; MW 295.14; ¹H NMR (300 MHz, DMSO-*d*₆) δ 8.35 (dd, $J = 4.8, 1.8$ Hz, 1H), 7.83 (ddd, $J = 7.6, 1.8, 0.9$ Hz, 1H), 7.40 (dd, $J = 7.6, 4.7$ Hz, 1H), 6.55 (d, $J = 3.5$ Hz, 1H), 6.13 (s, 1H), 3.25 (s, 3H), 2.17 (s, 3H); MS (ESI): 294.99, 297.00 (M+H)⁺.

5-(4-hydroxyphenyl)-N-methyl-N-(3-methylpyridin-2-yl)furan-2-carboxamide (25). The title compound was prepared according to method D by the reaction of **25a** (0.7 g, 2.37 mmol, 1 equiv) and (4-hydroxyphenyl) boronic acid (0.49 g, 3.55 mmol, 1.5 equiv) in the presence of cesium carbonate (3.08 g, 9.48 mmol, 4 equiv) and tetrakis(triphenylphosphine) palladium (136 mg, 0.118 mmol, 0.05 equiv) in DME/water 1:1 (40 ml). The product was purified by column chromatography (petroleum ether /ethyl acetate 1:1) to give 0.55 g (1.78 mmol/ 75 %) of the analytically pure compound (purity: 99.99 %). C₁₈H₁₆N₂O₃; MW 308.34; mp: 202-204 °C; ¹H NMR (500 MHz, DMSO-*d*₆) δ 9.79 (s, 1H), 8.35 (ddd, $J = 4.7, 2.0, 0.7$ Hz, 1H), 7.85 (ddd, $J = 7.6, 1.9, 0.8$ Hz, 1H), 7.39 (dd, $J = 7.6, 4.8$ Hz, 1H), 7.04 (s, 2H), 6.74 – 6.69 (m, 2H), 6.68 (s, 2H), 3.25 (s, 3H), 2.20 (s, 3H); ¹³C NMR (126 MHz, DMSO-*d*₆) δ 158.32, 157.99, 155.18, 155.08, 146.86, 145.69, 140.18, 130.24, 125.55, 123.67, 120.26, 118.52, 115.55, 104.75, 35.07, 16.70.; MS (ESI): 309.09 (M+H)⁺.

5-bromo-N-(4-methylpyridin-3-yl)furan-2-carboxamide (26b). To a suspension of 5-bromofuran-2-carboxylic acid (1.00 g, 5.23 mmol, 1 equiv), DCC (1.08 g, 5.23 mmol, 1 equiv), DMAP (31 mg, 0.261 mmol, 0.05 equiv) in 40 ml DCM at 0 °C 4-methylpyridin-3-amine (0.565 g, 5.23 mmol, 1 equiv) was added. The mixture was stirred at room temperature overnight. The mixture was quenched with water (50 mL) and extracted three times with ethyl acetate (3 x 30 mL). The organic layer was washed with water, dried over MgSO₄, filtered and evaporated to dryness under reduced pressure. The residue was purified by silica gel column chromatography (dichloromethane/methanol 94:6) to give 1.1 g (3.91 mmol/ 74 %) of the analytically pure compound (purity: 92.05 %). C₁₁H₉BrN₂O₂; MW 281.11; ¹H NMR (500 MHz, DMSO-*d*₆) δ 10.11 (s, 1H), 8.43 (s, 1H), 8.33 (d, $J = 5.0$ Hz, 1H), 7.38 – 7.29 (m, 2H), 6.85 (d, $J = 3.5$ Hz, 1H), 2.22 (s, 3H); MS (ESI): 280.93, 282.94 (M+H)⁺.

5-bromo-N-methyl-N-(4-methylpyridin-3-yl)furan-2-carboxamide (26a). The title compound was prepared according to method C using 5-bromo-N-(4-methylpyridin-3-yl)furan-2-carboxamide (0.94 g, 3.34 mmol, 1 equiv), NaH (0.16 g, 6.68 mmol, 2 equiv) and iodomethane (0.207 ml, 3.34 mmol, 1 equiv) in DMF (30 ml). The product was purified by column chromatography (petroleum ether /ethyl acetate 1:1) to give 0.65 g (2.2 mmol/ 65 %) of the analytically pure compound (purity: 97.69 %). C₁₂H₁₁BrN₂O₂; MW 295.14; ¹H NMR (500 MHz, DMSO-*d*₆) δ 8.48 (d, $J = 5.0$ Hz, 1H), 8.42 (s, 1H), 7.41 (d, $J = 5.0$ Hz, 1H), 6.52 (d, $J =$

3.6 Hz, 1H), 6.01 (d, $J = 3.7$ Hz, 1H), 3.24 (s, 3H), 2.19 (s, 3H); MS (ESI): 294.97, 296.97 (M+H)⁺.

5-(4-hydroxyphenyl)-N-methyl-N-(4-methylpyridin-3-yl)furan-2-carboxamide (26). The title compound was prepared according to method D by the reaction of **26a** (0.453 g, 1.53 mmol, 1 equiv) and (4-hydroxyphenyl) boronic acid (0.317 g, 2.3 mmol, 1.5 equiv) in the presence of cesium carbonate (1.99 g, 6.12 mmol, 4 equiv) and tetrakis(triphenylphosphine) palladium (88 mg, 0.076 mmol, 0.05 equiv) in DME/water 1:1 (40 ml). The product was purified by column chromatography (petroleum ether /ethyl acetate 4:1) to give 0.33 g (1.07 mmol/ 70 %) of the analytically pure compound (purity: 96.89 %). C₁₈H₁₆N₂O₃; MW 308.34; mp: 174-176 °C; ¹H NMR (500 MHz, DMSO-*d*₆) δ 9.78 (s, 1H), 8.51 – 8.45 (m, 2H), 7.45 (d, $J = 5.0$ Hz, 1H), 7.03 (d, $J = 8.2$ Hz, 2H), 6.72 (d, $J = 8.3$ Hz, 2H), 6.69 – 6.65 (m, 2H), 3.27 (s, 3H), 2.20 (s, 3H); ¹³C NMR (126 MHz, DMSO-*d*₆) δ 158.04, 157.97, 155.33, 148.91, 148.61, 145.36, 144.53, 139.93, 125.87, 125.56, 120.25, 119.18, 115.56, 104.77, 37.07, 16.42; MS (ESI): 309.14 (M+H)⁺.

5-bromo-N-(2-methylpyridin-3-yl)furan-2-carboxamide (27b). To a suspension of 5-bromofuran-2-carboxylic acid (1.00 g, 5.23 mmol, 1 equiv), DCC (1.08 g, 5.23 mmol, 1 equiv), DMAP (31 mg, 0.261 mmol, 0.05 equiv) in 40 ml DCM at 0 °C 4-methylpyridin-3-amine (0.565 g, 5.23 mmol, 1 equiv) was added. The mixture was stirred at room temperature overnight. The mixture was quenched with water (50 mL) and extracted three times with ethyl acetate (3 x 30 mL). The organic layer was washed with water, dried over MgSO₄, filtered and evaporated to dryness under reduced pressure. The residue was purified by silica gel column chromatography (dichloromethane/methanol 94:6) to give 1.3 g (4.62 mmol/ 88 %) of the analytically pure compound (purity: 99.99 %). C₁₁H₉BrN₂O₂; MW 281.11; ¹H NMR (500 MHz, DMSO-*d*₆) δ 10.33 (s, 1H), 8.52 (dd, $J = 5.2, 1.5$ Hz, 1H), 8.12 – 8.06 (m, 1H), 7.58 (dd, $J = 8.1, 5.2$ Hz, 1H), 7.41 (dd, $J = 3.6, 1.6$ Hz, 1H), 6.88 (d, $J = 3.5$ Hz, 1H), 2.52 (s, 3H); MS (ESI): 280.94, 282.94 (M+H)⁺.

5-bromo-N-methyl-N-(2-methylpyridin-3-yl)furan-2-carboxamide (27a). The title compound was prepared according to method C using 5-bromo-N-(2-methylpyridin-3-yl)furan-2-carboxamide (0.9 g, 3.2 mmol, 1 equiv), NaH (0.153 g, 6.4 mmol, 2 equiv) and iodomethane (0.199 ml, 3.20 mmol, 1 equiv) in DMF (30 ml). The product was purified by column chromatography (dichloromethane/methanol 97:3) to give 0.82 g (2.77 mmol/ 86 %) of the analytically pure compound (purity: 95.81 %). C₁₂H₁₁BrN₂O₂; MW 295.14; ¹H NMR (500 MHz, DMSO-*d*₆) δ 8.53 – 8.48 (m, 1H), 7.74 (dd, $J = 7.9, 1.7$ Hz, 1H), 7.35 (dd, $J = 7.9, 4.8$ Hz, 1H), 6.53 (d, $J = 3.5$ Hz, 1H), 6.00 (d, $J = 3.1$ Hz, 1H), 3.24 (s, 3H), 2.31 (s, 3H); MS (ESI): 294.97, 296.98 (M+H)⁺.

5-(4-hydroxyphenyl)-N-methyl-N-(2-methylpyridin-3-yl)furan-2-carboxamide (27). The title compound was prepared according to method D by the reaction of **27a** (0.6 g, 2.03 mmol, 1 equiv) and (4-hydroxyphenyl) boronic acid (0.42 g, 3.04 mmol, 1.5 equiv) in the presence of cesium carbonate (2.64 g, 8.12 mmol, 4 equiv) and tetrakis(triphenylphosphine) palladium (117 mg, 0.101 mmol, 0.05 equiv) in DME/water 1:1 (40 ml). The product was purified by column chromatography (petroleum ether /ethyl acetate 1:1) to give 0.466 g (1.15 mmol/ 74 %) of the analytically pure compound (purity: 99.99 %). C₁₈H₁₆N₂O₃; MW 308.34; mp: 199-201 °C; ¹H

NMR (500 MHz, DMSO- d_6) δ 9.78 (s, 1H), 8.54 – 8.49 (m, 1H), 7.75 (dd, $J = 7.9, 1.6$ Hz, 1H), 7.37 (dd, $J = 7.9, 4.7$ Hz, 1H), 7.03 (d, $J = 8.0$ Hz, 2H), 6.71 (d, $J = 8.2$ Hz, 2H), 6.67 (s, 2H), 3.26 (s, 3H), 2.35 (s, 3H); ^{13}C NMR (126 MHz, DMSO- d_6) δ 158.04, 157.77, 155.82, 155.37, 148.20, 145.40, 138.94, 135.91, 125.58, 122.60, 120.25, 119.23, 115.55, 104.76, 36.82, 20.24; MS (ESI): 309.11 (M+H) $^+$.

4-methoxybenzohydrazide (31d). The title compound was prepared by refluxing methyl 4-methoxybenzoate (1.00 g, 6.01 mmol, 1 equiv) with the mixture of hydrazine hydrate (2.91 ml, 60.17 mmol, 10 equiv) and methanol (15 mL) for 6 h. The excess hydrazine and methanol were evaporated to give the crude product which was recrystallized from methanol to give 0.85 g (5.11 mmol/ 85 %) of the analytically pure compound (purity: 96.49 %). $\text{C}_8\text{H}_{10}\text{N}_2\text{O}_2$; MW 166.18; ^1H NMR (500 MHz, DMSO- d_6) δ 9.60 (s, 1H), 7.80 (d, 2H), 6.97 (d, 2H), 4.41 (s, 2H), 3.79 (s, 3H); MS (ESI): 166.80 (M+H) $^+$.

Ethyl 5-(4-methoxyphenyl)-1,3,4-oxadiazole-2-carboxylate (31c). A mixture of 4-methoxybenzohydrazide (0.8 g, 4.81 mmol, 1 equiv), DIPEA (0.905 ml, 5.29 mmol, 1.1 equiv) and DMAP (58 mg, 0.481 mmol, 0.1 equiv) was dissolved in DCM (20 ml) and treated with ethyl 2-chloro-2-oxoacetate (0.592 ml, 5.29 mmol, 1.1 equiv) dropwise at 0 °C. The reaction mixture was slowly warmed to room temperature and stirred overnight. Later, it was treated with Et_3N (0.671 ml, 4.81 mmol, 1 equiv) /TsCl (0.916 g, 4.81 mmol, 1 equiv) and stirred it overnight. The reaction mixture was diluted with EtOAc/DCM and washed with water, saturated aqueous NaHCO_3 and saturated aqueous NaCl. The organic layer was collected, concentrated, and purified by column chromatography (petroleum ether /ethyl acetate 5:1) to give 0.98 g (3.94 mmol/ 82 %) of the analytically pure compound (purity: 94.79 %). $\text{C}_{12}\text{H}_{12}\text{N}_2\text{O}_4$; MW 248.08; ^1H NMR (500 MHz, DMSO- d_6) δ 8.01 (d, 2H), 7.18 (d, 2H), 4.45 (q, $J = 7.1$ Hz, 2H), 3.87 (s, 3H), 1.37 (t, $J = 7.1$ Hz, 3H); MS (ESI): 248.98 (M+H) $^+$.

Potassium 5-(4-methoxyphenyl)-1,3,4-oxadiazole-2-carboxylate (31b). Ethyl 5-(4-methoxyphenyl)-1,3,4-oxadiazole-2-carboxylate (0.9 g, 3.62 mmol, 1 equiv) was dissolved in THF/EtOH (10 mL/5 mL) and treated with KOH (0.203 g, 3.62 mmol, 1 equiv) in H_2O (1 mL) at 0°C, the resulting mixture stirred for 2 h at 0°C. The product, Potassium 5-(4-methoxyphenyl)-1,3,4-oxadiazole-2-carboxylate, precipitated out from the solution and was separated by filtration and used for the next step without further purification to give 0.88 g (3.4 mmol/ 94 %) of the desired potassium salt. $\text{C}_{10}\text{H}_7\text{KN}_2\text{O}_4$; MW 258.27; ^1H NMR (500 MHz, Deuterium Oxide) δ 7.75 (d, 2H), 6.97 (d, 2H), 3.85 (s, 3H).

5-(4-methoxyphenyl)-N-methyl-N-(o-tolyl)-1,3,4-oxadiazole-2-carboxamide (31a). To a stirred suspension of potassium 5-(4-methoxyphenyl)-1,3,4-oxadiazole-2-carboxylate (0.8 g, 3.09 mmol, 1 equiv) in acetonitrile (25 mL) at 0 °C, oxalyl chloride (0.471 g, 3.71 mmol, 1.2 equiv) was added dropwise over 10 min. DMF (5 drops) was added to the reaction mixture, and vigorous gas evolution was observed. The resulting reaction mixture was stirred for further 2 h to form acyl chloride. The solvent was removed under reduced pressure. N,2-dimethylaniline (0.386 ml, 3.09 mmol, 1 equiv) and DIPEA (1.37 ml, 7.72 mmol, 2.5 equiv) were dissolved in DCM (25 mL) and added at 0 °C to the acyl chloride. The reaction mixture was stirred for 30 min at 0 °C, after which it was allowed to warm up to room temperature and stirred overnight. The mixture was quenched with water (20 mL) and extracted twice with DCM (2 x 15 ml); the

organic layer was dried over MgSO₄, filtered and the solution was concentrated under reduced pressure. The residue was purified by silica gel column chromatography (petroleum ether /ethyl acetate 4:1) to give 0.7 g (2.16 mmol/ 70 %) of the analytically pure compound (purity: 99.99 %). C₁₈H₁₇N₃O₃; MW 323.35; ¹H NMR (300 MHz, DMSO-*d*₆) δ 7.77 – 7.65 (m, 2H), 7.37 – 7.24 (m, 3H), 7.20 (td, *J* = 7.2, 6.7, 1.8 Hz, 1H), 7.16 – 7.04 (m, 2H), 3.85 (s, 3H), 3.33 (s, 3H), 2.27 (s, 3H); MS (ESI): 323.99 (M+H)⁺.

5-(4-hydroxyphenyl)-N-methyl-N-(o-tolyl)-1,3,4-oxadiazole-2-carboxamide (31). The title compound was prepared according to method E by the reaction of **31a** (0.68 g, 2.10 mmol, 1 equiv) and BF₃.SMe₂ (2.21 ml, 21.02 mmol, 10 equiv) in dichloromethane (50 ml). The product was purified by column chromatography (dichloromethane/methanol 95:5) to give 0.5 g (1.61 mmol/ 77 %) of the analytically pure compound (purity: 99.00 %). C₁₇H₁₅N₃O₃; MW 309.33; mp: 210-212 °C; ¹H NMR (500 MHz, DMSO-*d*₆) δ 10.41 (s, 1H), 7.64 – 7.58 (m, 2H), 7.34 – 7.31 (m, 1H), 7.28 (ddd, *J* = 6.6, 3.7, 2.2 Hz, 2H), 7.23 – 7.17 (m, 1H), 6.93 – 6.85 (m, 2H), 3.33 (s, 3H), 2.26 (s, 3H); ¹³C NMR (126 MHz, DMSO-*d*₆) δ 164.01, 161.35, 157.24, 154.66, 140.91, 135.44, 131.02, 128.83, 128.79, 128.06, 127.10, 116.26, 112.90, 36.77, 17.03; MS (ESI): 309.93 (M+H)⁺.

Ethyl 2-(4-methoxyphenyl)oxazole-4-carboxylate (32c). A mixture of 4-methoxy benzamide (0.6 g, 3.96 mmol, 1 equiv) and ethyl bromopyruvate (0.597 ml, 4.76 mmol, 1.2 equiv) was refluxed in ethanol (40 ml) for 5 h. The solvent was removed under reduced pressure. The residue was quenched with water, then extracted twice with ethyl acetate (2 x 15 ml). The organic layers were combined, dried over magnesium sulfate and concentrated to dryness under reduced pressure. The product was purified by column chromatography (petroleum ether /ethyl acetate 3:1) to give 0.75 g (3.03 mmol/ 76 %) of the analytically pure compound (purity: 94.68 %). C₁₃H₁₃NO₄; MW 247.25; ¹H NMR (500 MHz, DMSO-*d*₆) δ 8.85 (s, 1H), 7.94 (d, 2H), 7.10 (d, 2H), 4.31 (q, *J* = 7.1 Hz, 2H), 3.83 (s, 3H), 1.30 (t, *J* = 7.1 Hz, 3H); MS (ESI): 247.98 (M+H)⁺.

2-(4-methoxyphenyl)oxazole-4-carboxylic acid (32b). Ethyl 2-(4-methoxyphenyl)oxazole-4-carboxylate (0.7 g, 2.83 mmol, 1 equiv) was dissolved in THF/EtOH (15 mL/7.5 mL) and treated with KOH (0.158 g, 2.83 mmol, 1 equiv) in H₂O (1 mL) at 0°C, the resulting mixture stirred for 2 h at 0°C. The solvent was removed under reduced pressure. The residue was quenched with water, acidified with 2 M HCl to pH 2 and extracted twice with ethyl acetate (2 x 10 ml). The organic layers were combined, dried over magnesium sulfate and concentrated to dryness under reduced pressure. The product was purified by column chromatography (petroleum ether /ethyl acetate 2:1) to give 0.45 g (2.05 mmol/ 72 %) of the analytically pure compound (purity: 95.74 %). C₁₁H₉NO₄; MW 219.20; ¹H NMR (500 MHz, DMSO-*d*₆) δ 13.09 (s, 1H), 8.77 (s, 1H), 7.94 (d, *J* = 9.0 Hz, 2H), 7.11 (d, *J* = 8.9 Hz, 1H), 3.84 (s, 3H); MS (ESI): 219.94 (M+H)⁺.

2-(4-methoxyphenyl)-N-methyl-N-(o-tolyl)oxazole-4-carboxamide (32a). The title compound was prepared according to method A and B using 2-(4-methoxyphenyl)oxazole-4-carboxylic acid (0.4 g, 1.82 mmol), thionyl chloride (0.264 ml, 3.64 mmol) and DMF (5 drops) in toluene (10 ml). The corresponding N,2-dimethylaniline (0.227 ml, 1.82 mmol) and Et₃N (0.508 ml, 3.64 mmol) in DCM (10 ml) was added to the acyl chloride. The residue was purified by silica

gel column chromatography (petroleum ether /ethyl acetate 2:1) to give 0.499 g (1.54 mmol/ 85 %) of the analytically pure compound (purity: 99.44 %). $C_{19}H_{18}N_2O_3$; MW 322.36; 1H NMR (500 MHz, DMSO- d_6) δ 7.70 – 7.64 (m, 2H), 7.46 (s, 1H), 7.35 – 7.25 (m, 2H), 7.28 – 7.21 (m, 2H), 7.05 – 6.99 (m, 2H), 3.79 (s, 3H), 3.24 (s, 3H), 2.17 (s, 3H); MS (ESI): 322.96 (M+H) $^+$.

2-(4-hydroxyphenyl)-N-methyl-N-(o-tolyl)oxazole-4-carboxamide (32). The title compound was prepared according to method E by the reaction of **32a** (0.45 g, 1.39 mmol, 1 equiv) and $BF_3 \cdot SMe_2$ (1.46 ml, 13.95 mmol, 10 equiv) in dichloromethane (30 ml). The product was purified by column chromatography (dichloromethane/methanol 97:3) to give 0.31 g (1.00 mmol/ 72 %) of the analytically pure compound (purity: 99.91 %). $C_{18}H_{16}N_2O_3$; MW 308.34; mp: 220-222 °C; 1H NMR (500 MHz, DMSO- d_6) δ 10.10 (s, 1H), 7.60 – 7.54 (m, 2H), 7.38 (s, 1H), 7.35 – 7.25 (m, 2H), 7.28 – 7.21 (m, 2H), 6.82 (dd, $J = 9.0, 2.5$ Hz, 2H), 3.24 (s, 3H), 2.17 (s, 3H); ^{13}C NMR (126 MHz, DMSO- d_6) δ 160.93, 159.98, 159.96, 142.42, 140.37, 136.02, 135.51, 130.94, 128.35, 128.32, 127.86, 127.12, 117.15, 115.82, 36.49, 17.10; MS (ESI): 308.98 (M+H) $^+$.

2-(4-methoxyphenyl)thiazole-4-carboxylic acid (33b). The title compound was prepared according to method D by the reaction of ethyl 2-bromothiazole-4-carboxylate (1.00 g, 4.23 mmol, 1 equiv) and (4-methoxyphenyl)boronic acid (0.965 g, 6.35 mmol, 1.5 equiv) in the presence of sodium carbonate (2.24 g, 21.15 mmol, 5 equiv) and tetrakis(triphenylphosphine) palladium (244 mg, 0.211 mmol, 0.05 equiv) in toluene/ethanol 1:1 (50 ml). The product was purified by column chromatography (dichloromethane/methanol 90:10) to give 0.87 g (3.69 mmol/ 87 %) of the analytically pure compound (purity: 99.99 %). $C_{11}H_9NO_3S$; MW 235.26; 1H NMR (500 MHz, DMSO- d_6) δ 13.05 (s, 1H), 8.41 (s, 1H), 7.91 (d, 2H), 7.08 (d, 2H), 3.83 (s, 3H); MS (ESI): 236.00 (M+H) $^+$.

2-(4-methoxyphenyl)-N-methyl-N-(o-tolyl)thiazole-4-carboxamide (33a). The title compound was prepared according to method A and B using 2-(4-methoxyphenyl)thiazole-4-carboxylic acid (0.85 g, 3.61 mmol), thionyl chloride (0.524 ml, 7.22 mmol) and DMF (10 drops) in toluene (20 ml). The corresponding N,2-dimethylaniline (0.45 ml, 3.6 mmol) and Et_3N (1.00 ml, 7.22 mmol) in DCM (20 ml) was added to the acyl chloride. The residue was purified by silica gel column chromatography (petroleum ether /ethyl acetate 3:1) to give 0.98 g (2.98 mmol/ 80 %) of the analytically pure compound (purity: 98.76 %). $C_{19}H_{18}N_2O_2S$; MW 338.43; 1H NMR (500 MHz, Acetone- d_6) δ 7.83 (s, 1H), 7.54 – 7.47 (m, 2H), 7.28 (ddt, $J = 7.5, 1.4, 0.7$ Hz, 1H), 7.22 – 7.05 (m, 3H), 6.95 – 6.88 (m, 2H), 3.82 (s, 3H), 3.32 (s, 3H), 2.29 (s, 3H); MS (ESI): 339.05 (M+H) $^+$.

2-(4-hydroxyphenyl)-N-methyl-N-(o-tolyl)thiazole-4-carboxamide (33). The title compound was prepared according to method E by the reaction of **33a** (0.650 g, 1.92 mmol, 1 equiv) and $BF_3 \cdot SMe_2$ (2.00 ml, 19.2 mmol, 10 equiv) in dichloromethane (40 ml). The product was purified by column chromatography (petroleum ether /ethyl acetate 2:1) to give 0.359 g (1.1 mmol/ 57 %) of the analytically pure compound (purity: 99.99 %). $C_{18}H_{16}N_2O_2S$; MW 324.40; mp: 237-239 °C; 1H NMR (500 MHz, DMSO- d_6) δ 9.97 (s, 1H), 7.81 (s, 1H), 7.40 – 7.34 (m, 2H), 7.30 – 7.23 (m, 1H), 7.21 – 7.10 (m, 3H), 6.75 (dd, $J = 9.0, 2.5$ Hz, 2H), 3.26 (s, 3H), 2.22 (s, 3H); ^{13}C NMR (126 MHz, DMSO- d_6) δ 165.68, 162.79, 159.52, 150.23, 143.44, 135.24, 130.51,

128.00, 127.76, 127.54, 126.66, 123.85, 122.97, 115.66, 36.83, 17.40; MS (ESI): 324.94 (M+H)⁺.

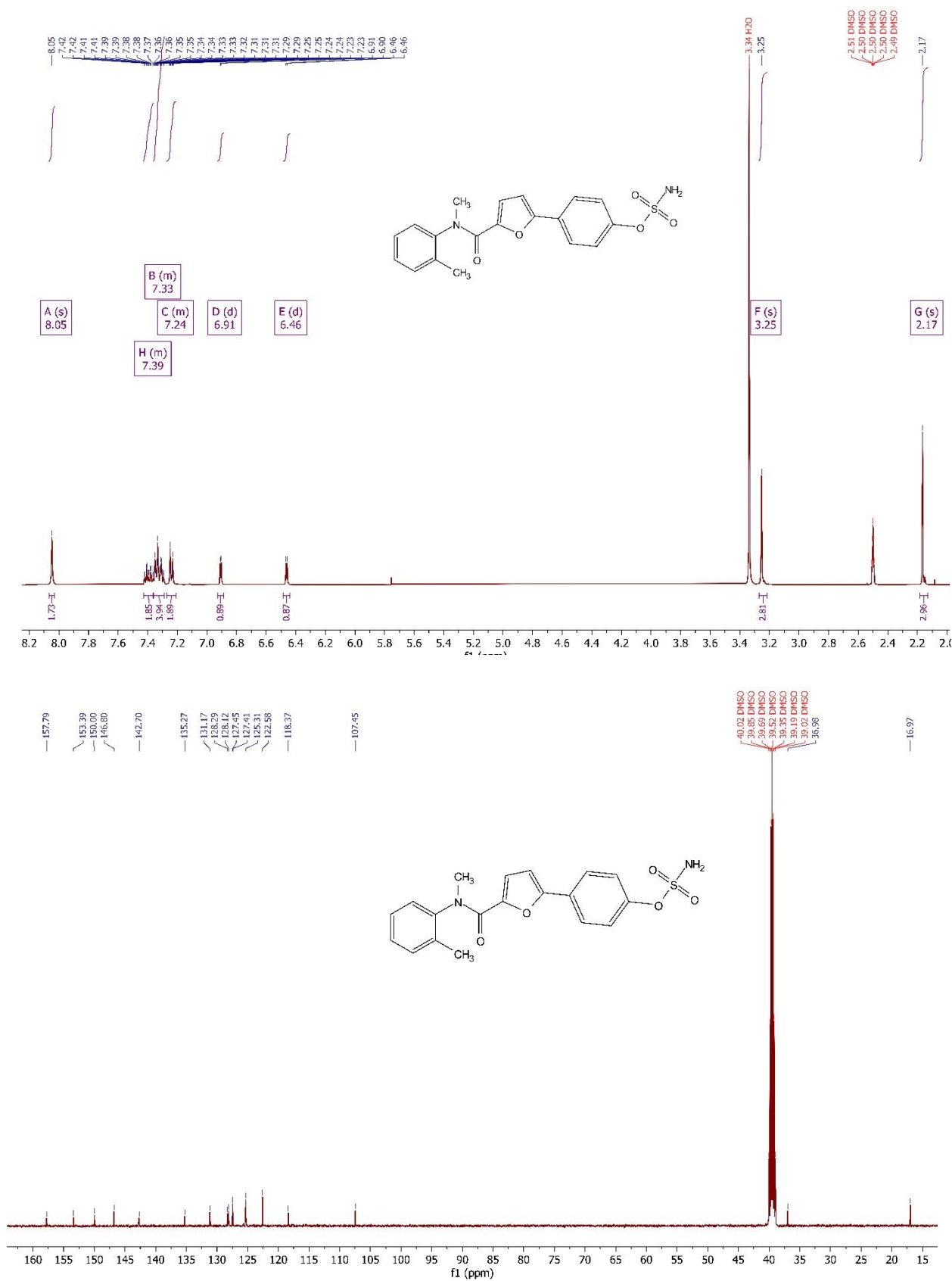
2-(4-methoxyphenyl)thiazole-5-carboxylic acid (34b). The title compound was prepared according to method D by the reaction of methyl 2-bromothiazole-5-carboxylate (1.00 g, 4.5 mmol, 1 equiv) and (4-methoxyphenyl)boronic acid (1.02 g, 6.75 mmol, 1.5 equiv) in the presence of sodium carbonate (2.38 g, 22.5 mmol, 5 equiv) and tetrakis(triphenylphosphine) palladium (260 mg, 0.225 mmol, 0.05 equiv) in toluene/ethanol 1:1 (50 ml). The product was purified by column chromatography (dichloromethane/methanol 90:10) to give 0.89 g (3.78 mmol/ 84 %) of the analytically pure compound (purity: 94.68 %). C₁₁H₉NO₃S; MW 235.26; ¹H NMR (500 MHz, DMSO-*d*₆) δ 13.50 (s, 1H), 8.35 (s, 1H), 8.00 – 7.93 (m, 2H), 7.12 – 7.05 (m, 2H), 3.84 (s, 3H); MS (ESI): 236.01 (M+H)⁺.

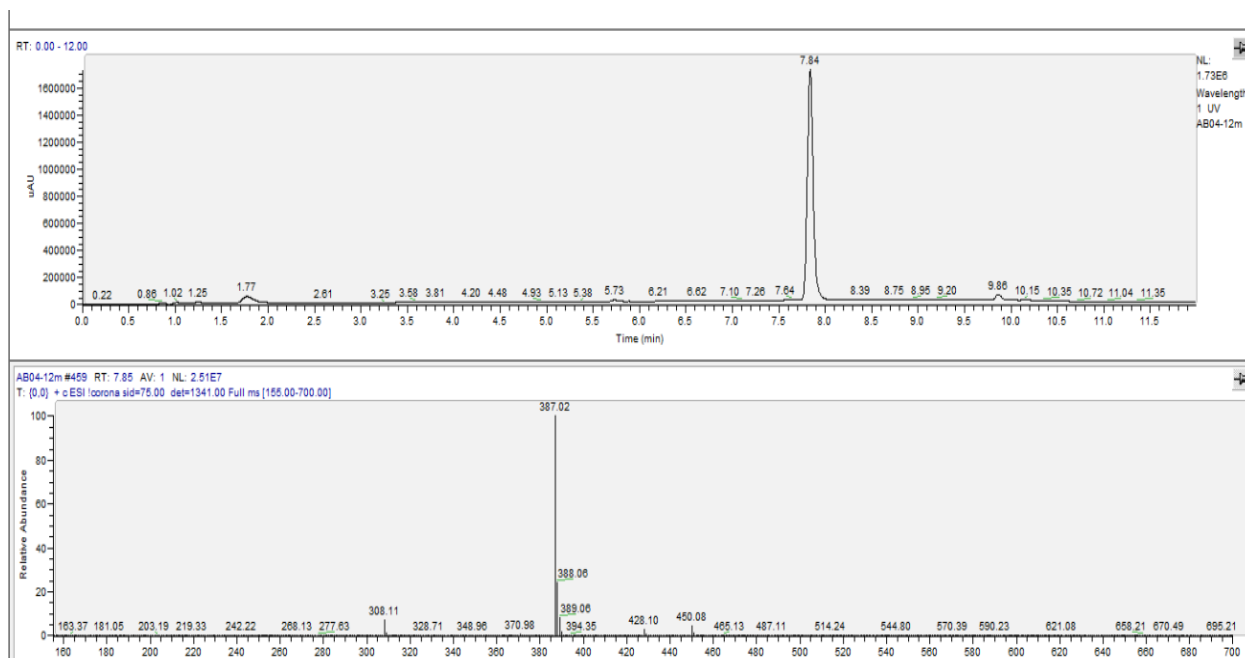
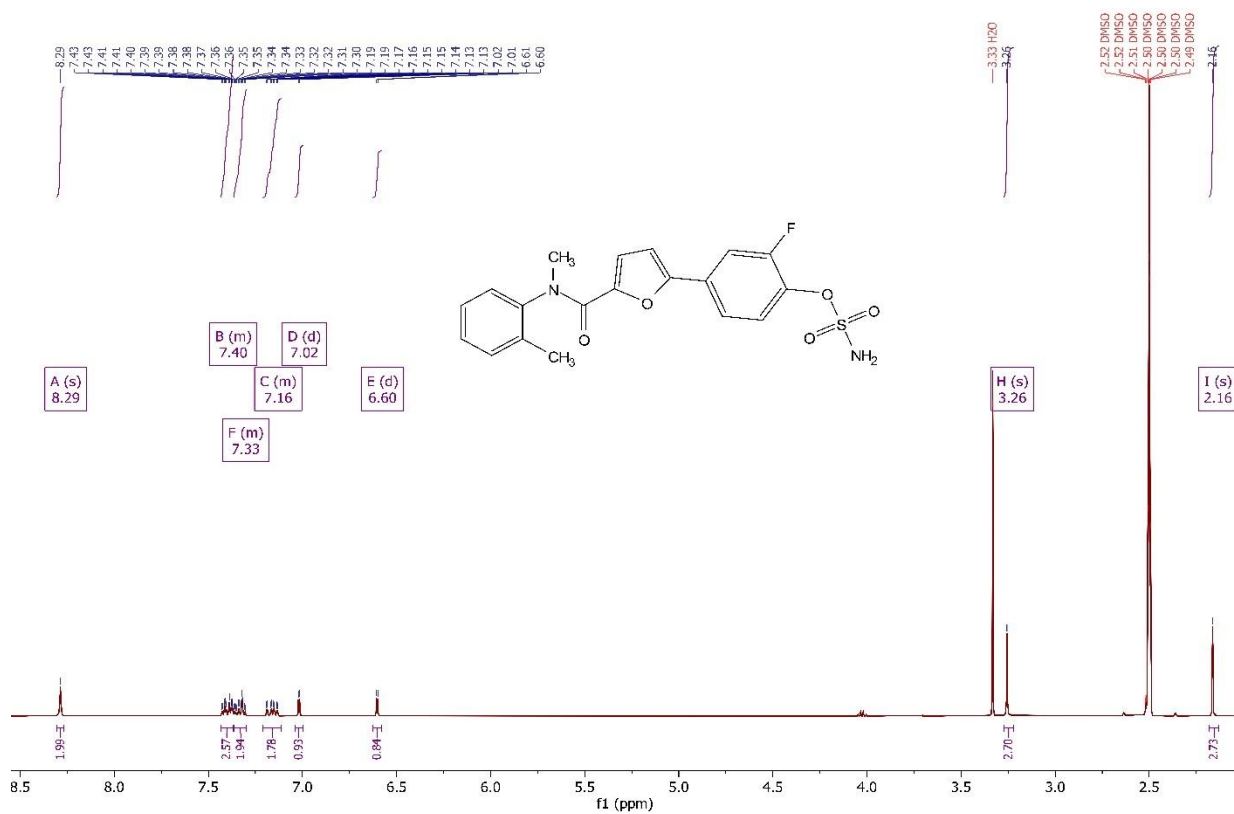
2-(4-methoxyphenyl)-N-methyl-N-(o-tolyl)thiazole-5-carboxamide (34a). The title compound was prepared according to method A and B using 2-(4-methoxyphenyl)thiazole-5-carboxylic acid (0.80 g, 3.4 mmol), thionyl chloride (0.493 ml, 6.8 mmol) and DMF (10 drops) in toluene (20 ml). The corresponding N,2-dimethylaniline (0.424 ml, 3.4 mmol) and Et₃N (0.95 ml, 6.8 mmol) in DCM (20 ml) was added to the acyl chloride. The residue was purified by silica gel column chromatography (petroleum ether /ethyl acetate 4:1) to give 0.85 g (2.51 mmol/ 73 %) of the analytically pure compound (purity: 95.60 %). C₁₉H₁₈N₂O₂S; MW 338.43; ¹H NMR (500 MHz, Acetone-*d*₆) δ 7.82 – 7.75 (m, 2H), 7.48 – 7.40 (m, 2H), 7.43 – 7.35 (m, 2H), 7.15 (s, 1H), 7.03 – 6.96 (m, 2H), 3.85 (s, 3H), 3.33 (s, 3H), 2.23 (s, 3H); MS (ESI): 339.05 (M+H)⁺.

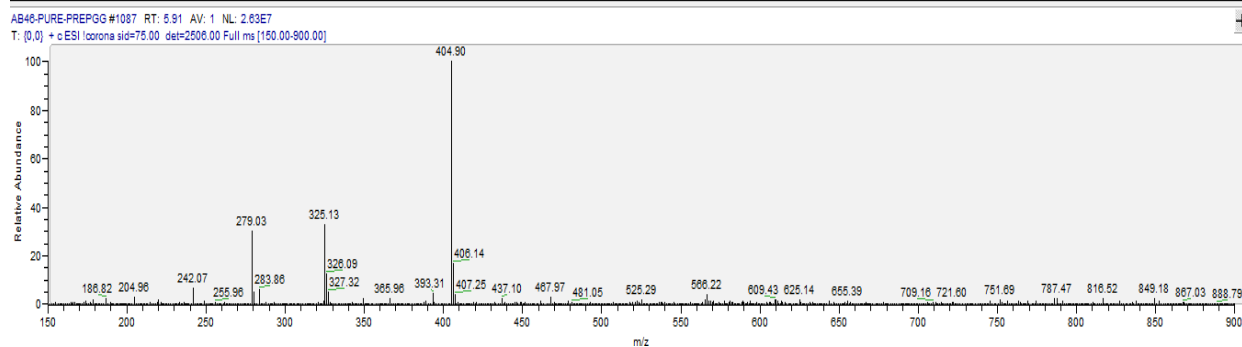
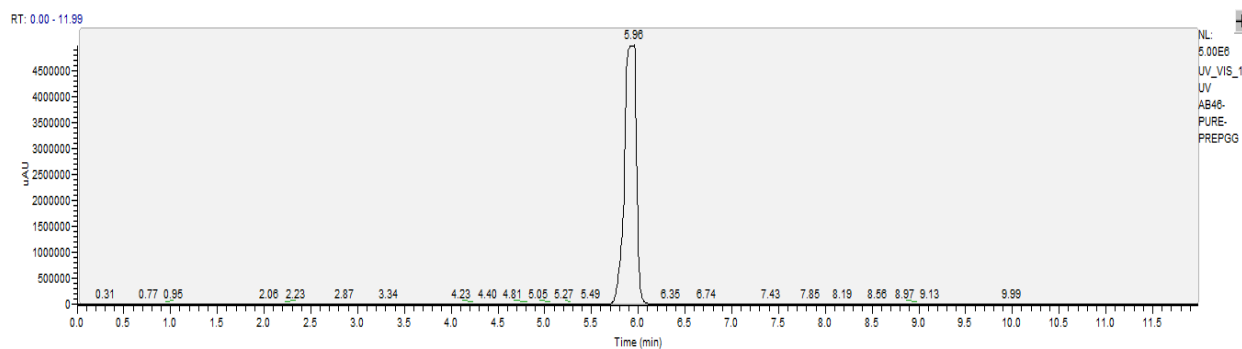
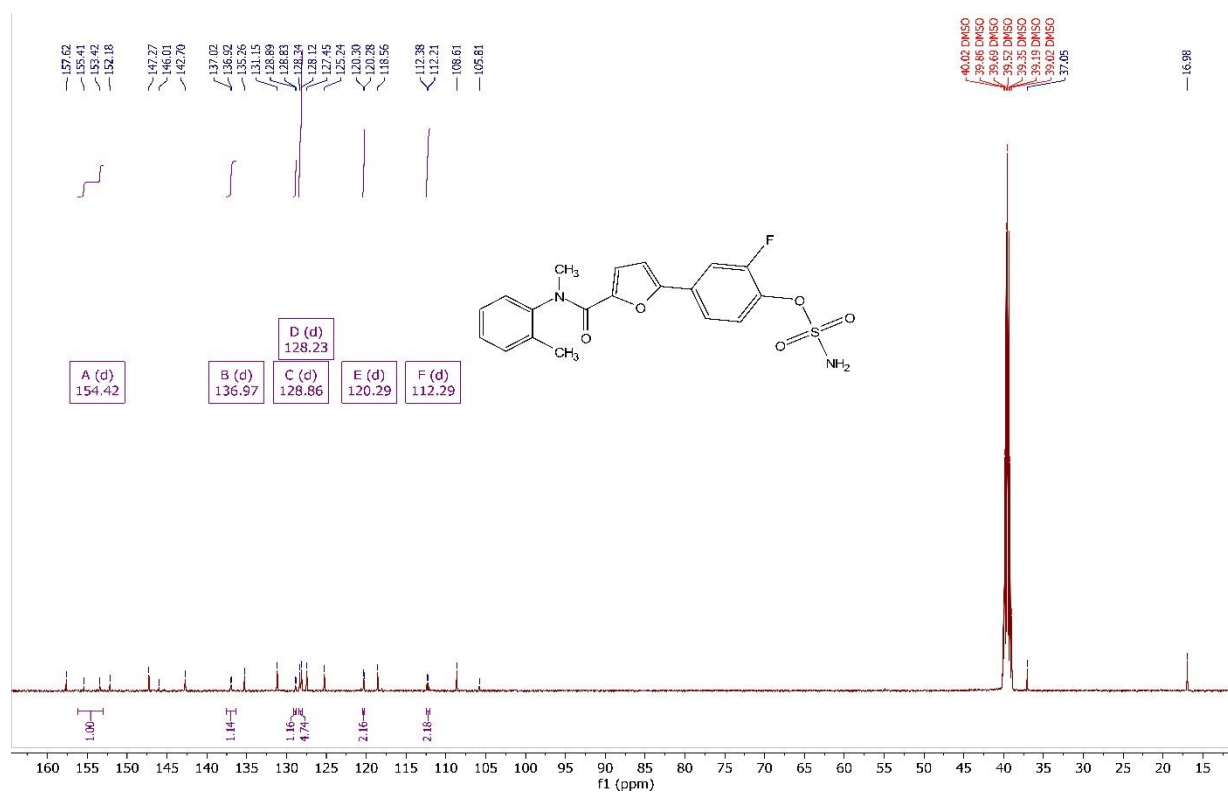
2-(4-hydroxyphenyl)-N-methyl-N-(o-tolyl)thiazole-5-carboxamide (34). The title compound was prepared according to method E by the reaction of **34a** (0.8 g, 2.36 mmol, 1 equiv) and BF₃.SMe₂ (2.48 ml, 23.6 mmol, 10 equiv) in dichloromethane (50 ml). The product was purified by column chromatography (petroleum ether /ethyl acetate 3:1) to give 0.5 g (1.54 mmol/ 65 %) of the analytically pure compound (purity: 99.00 %). C₁₈H₁₆N₂O₂S; MW 324.40; mp: 219-221 °C; ¹H NMR (500 MHz, DMSO-*d*₆) δ 10.12 (s, 1H), 7.64 – 7.59 (m, 2H), 7.43 (dt, *J* = 8.8, 5.8 Hz, 2H), 7.37 (dd, *J* = 5.1, 2.3 Hz, 2H), 7.10 (s, 1H), 6.82 (dd, *J* = 9.1, 2.5 Hz, 2H), 3.27 (s, 3H), 2.16 (s, 3H); ¹³C NMR (126 MHz, DMSO-*d*₆) δ 170.94, 160.22, 160.09, 146.43, 141.59, 135.98, 131.66, 131.36, 129.40, 128.99, 128.04, 127.89, 123.50, 116.00, 36.96, 16.88; MS (ESI): 324.98 (M+H)⁺.

5.2.2 Representative $^1\text{H-NMR}$, $^{13}\text{C-NMR}$ and MS spectra of compounds 13, 17, 19, 33 and 37

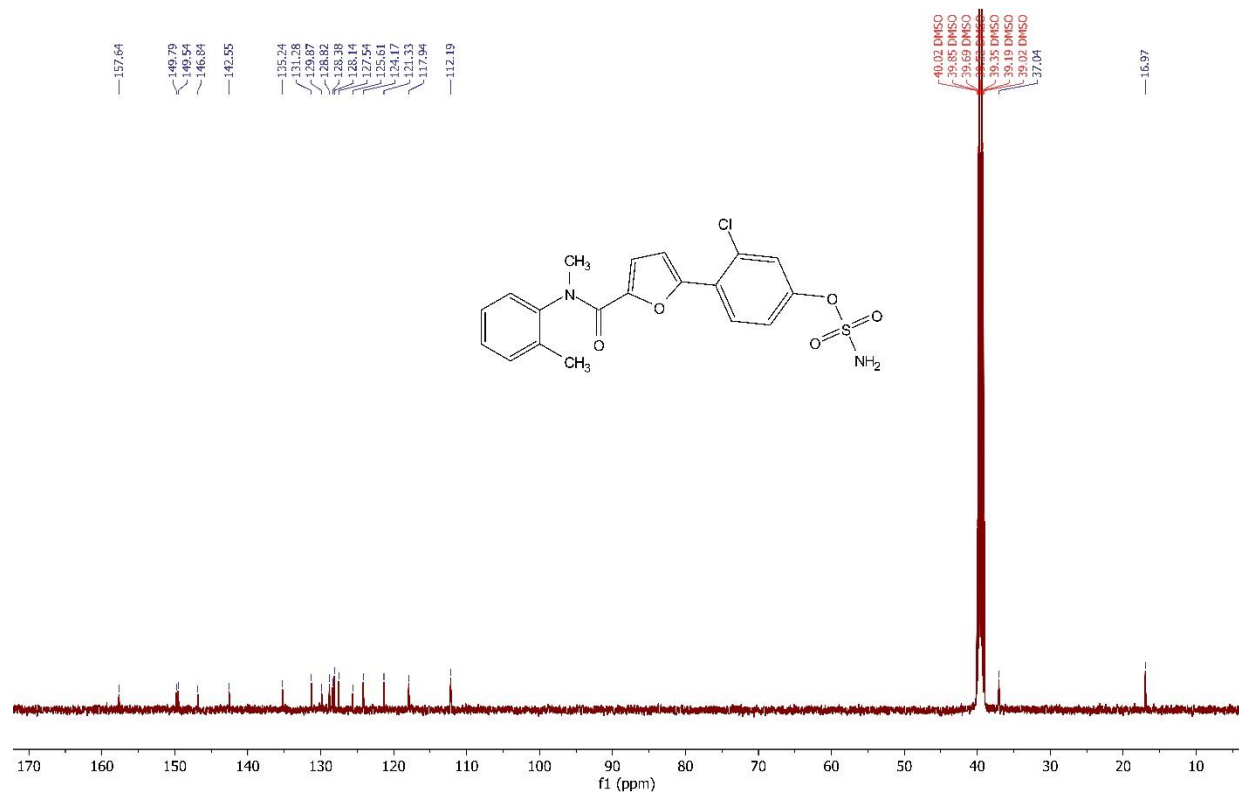
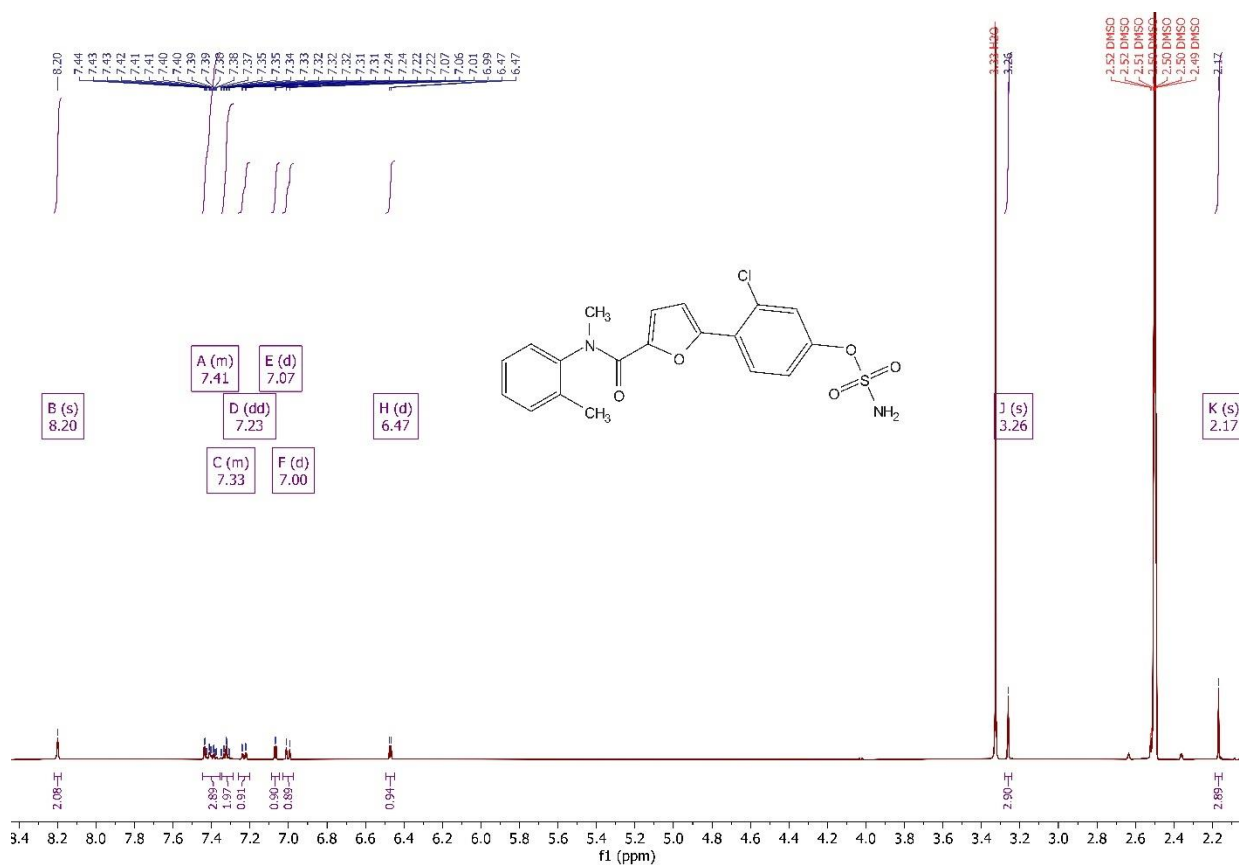
Compound 13:

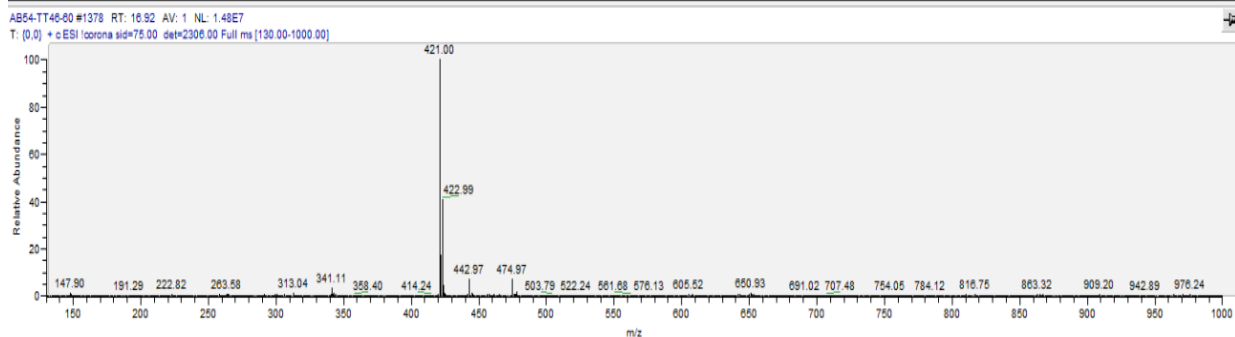
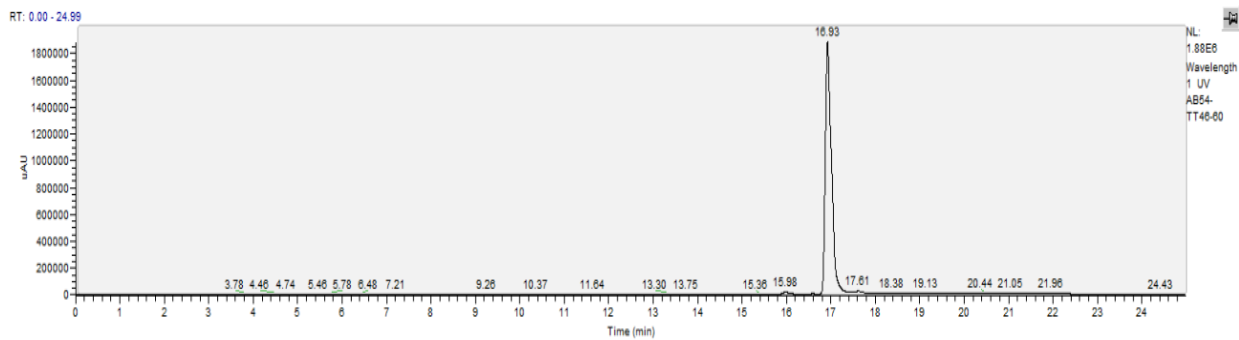
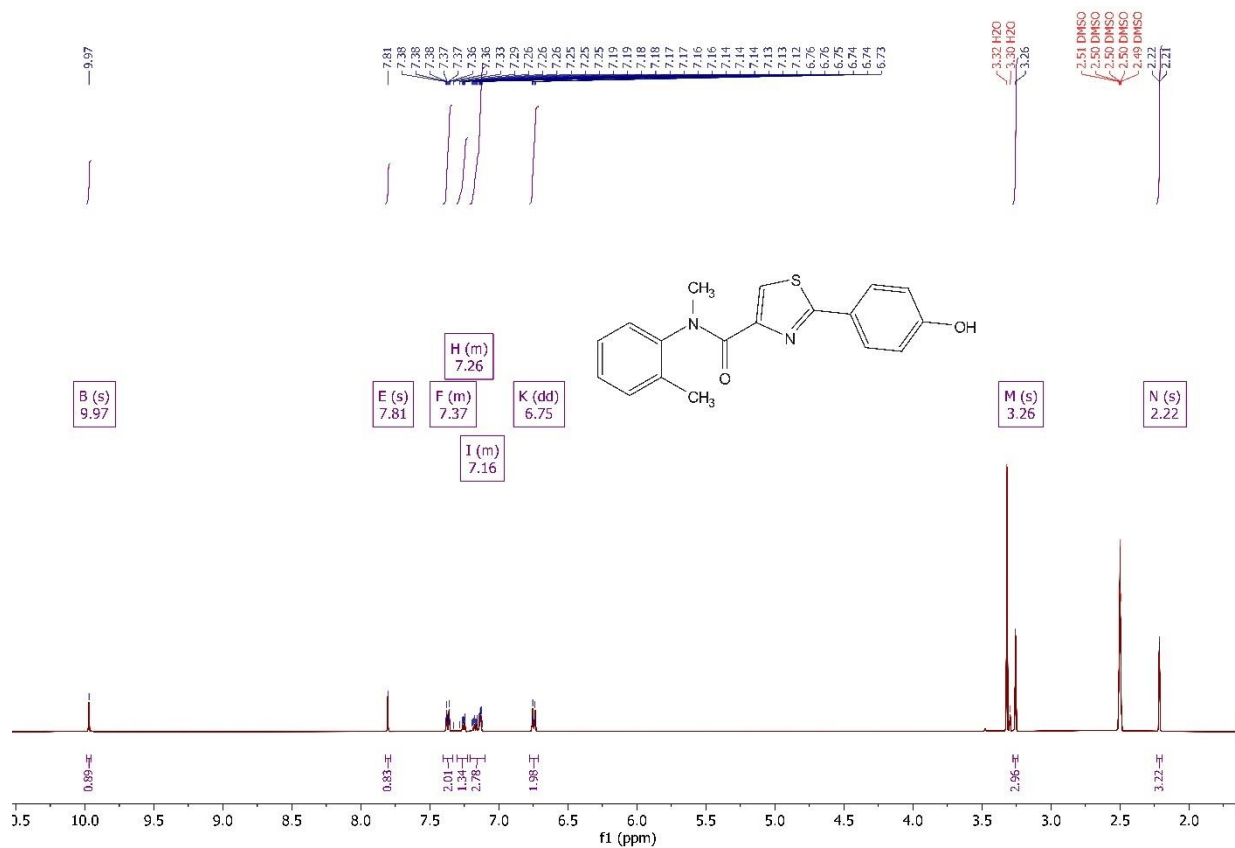


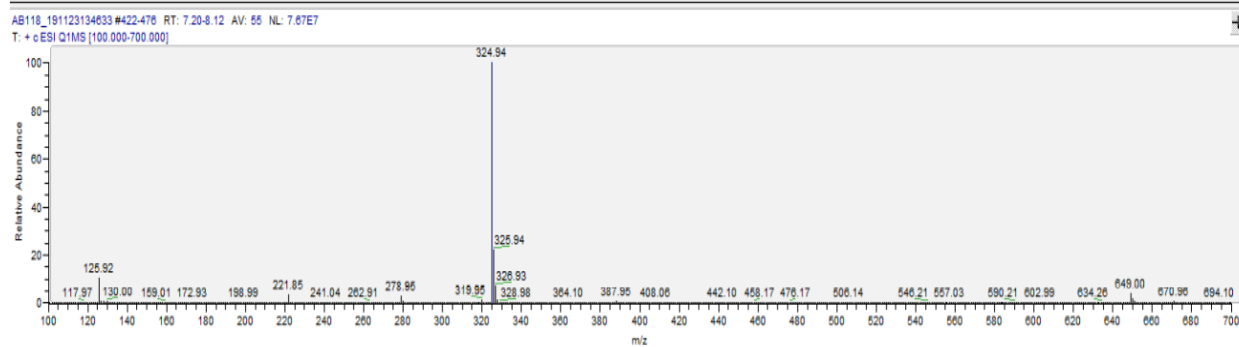
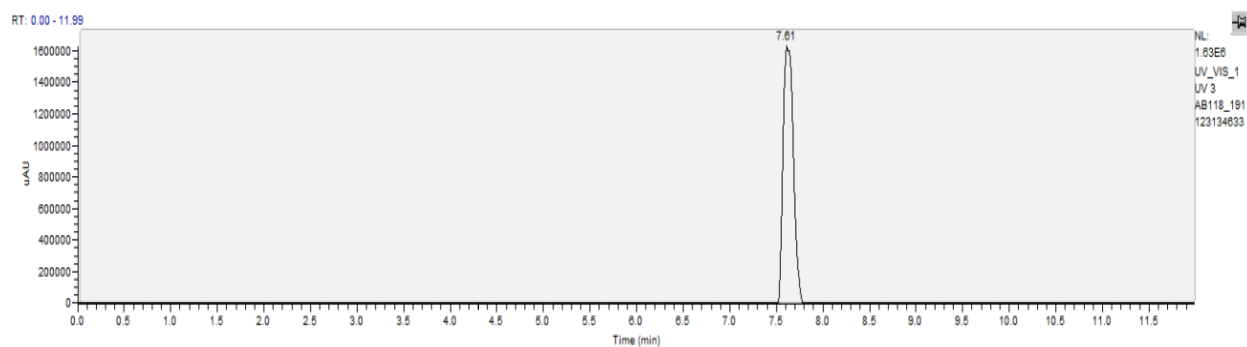
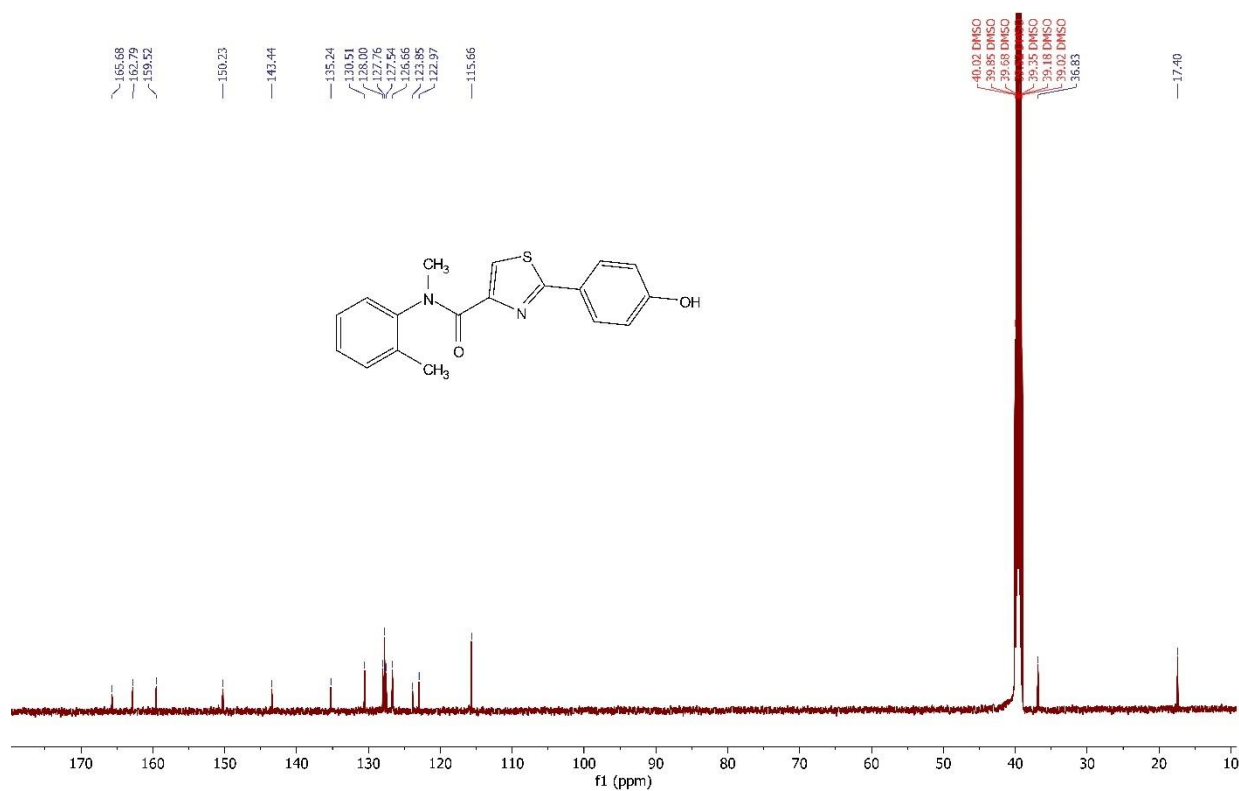
**Compound 17:**



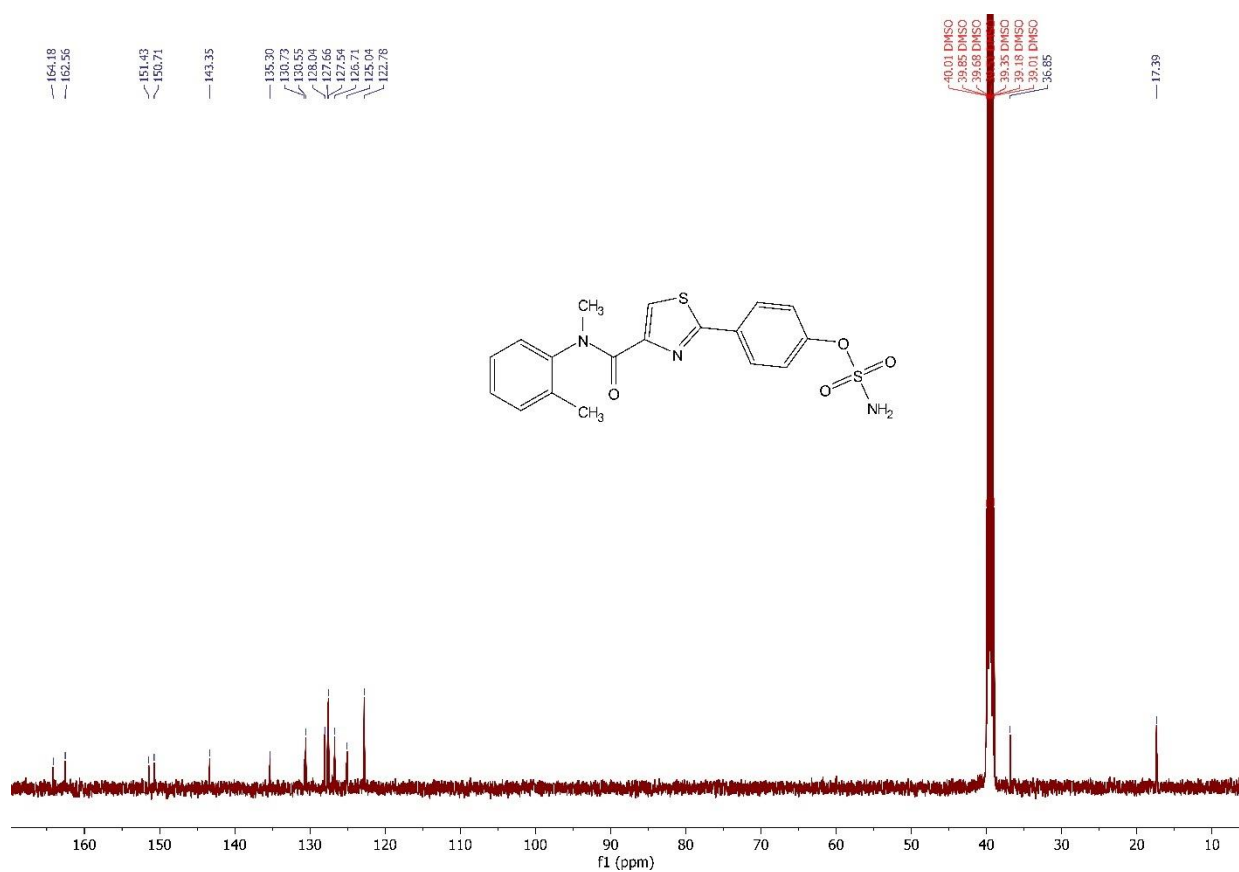
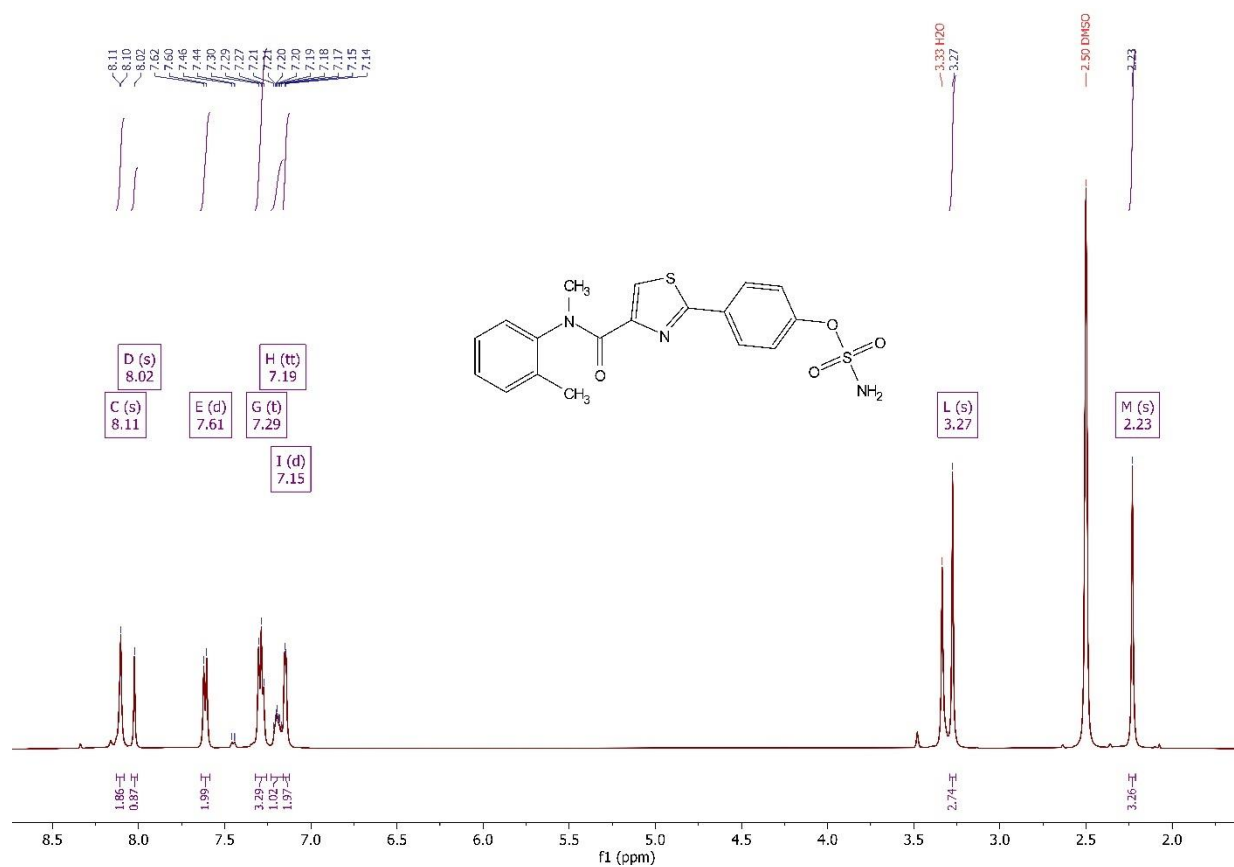
Compound 19:

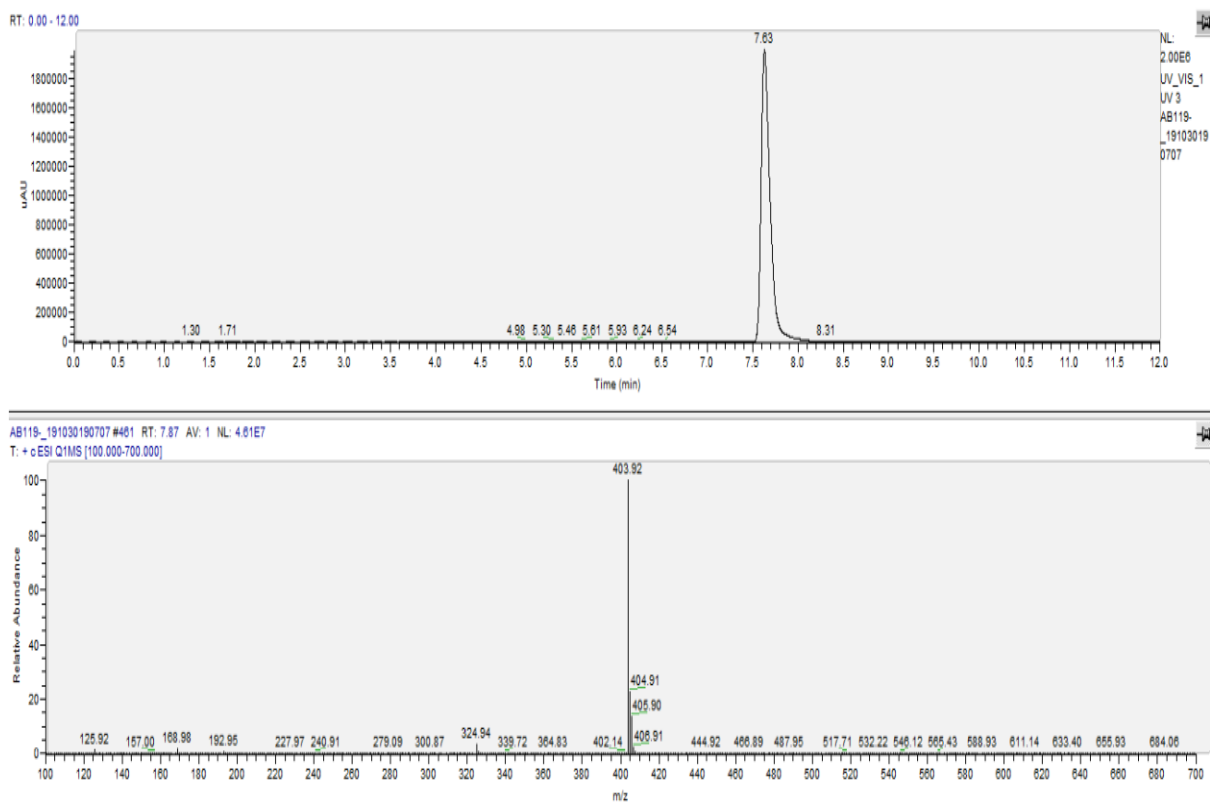


**Compound 33:**



Compound 37:





5.2.3 Validation of drug-prodrug concept (compounds **16**, **19**, and **37**)

To study the effect of the presence of an electronegative atom such as chlorine on the stability of the sulfamate moiety, two compounds were studied **16** and **19**, compound **16** contains chlorine *ortho* to the sulfamate while **19** had its chlorine *meta* to it. It is expected that compound **13** (unsubstituted sulfamate) will be more stable than compound **19** (*m*-chloro sulfamate) which in turn is assumed to be more stable than compound **16** (*o*-chloro sulfamate). Regarding **16**, the results revealed that it was completely hydrolyzed after 6 h incubation of 10 nM of it in phosphate buffer. 50 % inhibition of 17 β -HSD1 was reached quickly (below 1 h) and after 22 % of it converted to **4** (2.2 nM), see Figure 1. This is approximately equal to the cell-free IC₅₀ of 17 β -HSD1 for **4**, which is 2.7 nM.

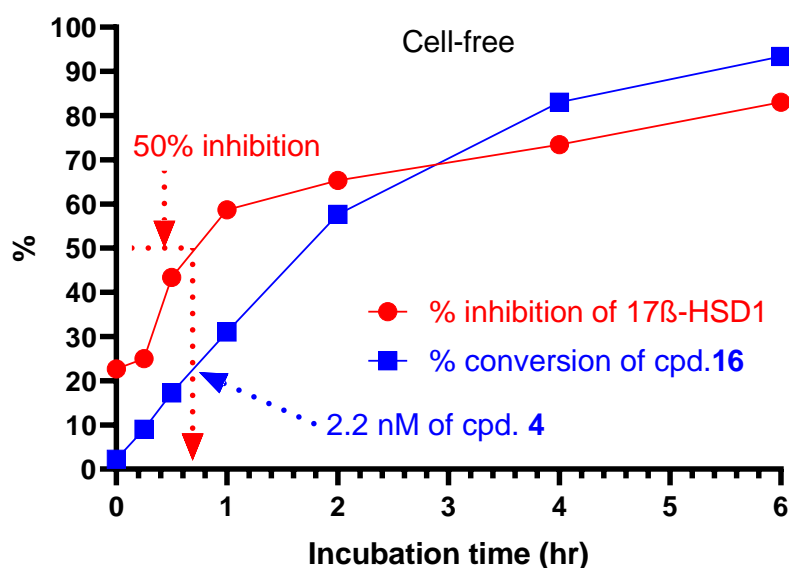


Figure 1. Plots of percentage conversion of **16** to **4** and the percentage inhibition of 17β-HSD1 at starting concentration of 10 nM of **16** in a cell-free system. Each point in the figure represents mean value of two independent experiments each conducted in duplicates, standard deviation less than 20 %.

However, in a cellular assay using T47D/DMEM, **16** hydrolyzes too quickly (Figure 2) to see a steady rise in % inhibition because **4** is very potent in cellular systems with 5.2 nM IC_{50} for 17β-HSD1. Also, T47D cells contain esterases that can accelerate hydrolysis of **16** to its phenolic compound **4** (this may explain why it was more stable in phosphate buffer than in T47D/DMEM).

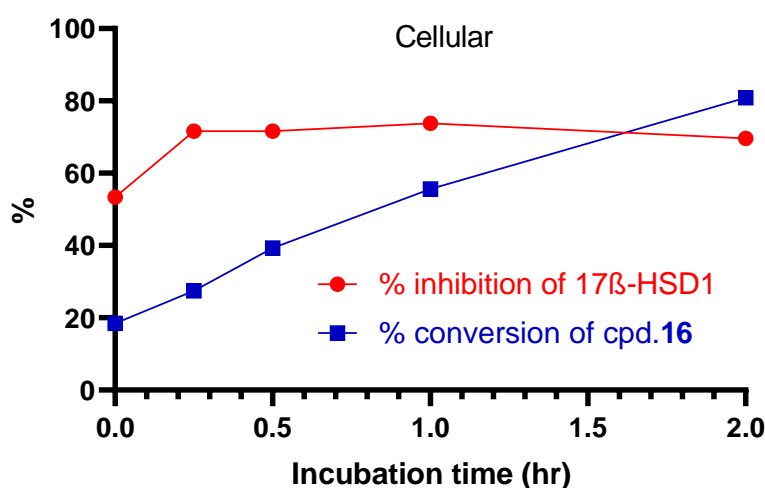


Figure 2. Plots of percentage conversion of **16** to **4** and the percentage inhibition of 17β-HSD1 at starting concentration of 10 nM of **16** in a cellular system. Each point in the figure represents

mean value of two independent experiments each conducted in duplicates, standard deviation less than 20 %.

During validation of the proposed drug-prodrug concept for dual inhibition of STS and 17 β -HSD1, the chosen prodrugs should ideally have suitable stability, but this was not the case with **16**. Its instability compared to **13** could be explained by the *ortho*-chloro substituent to the sulfamate group, which makes it more liable for hydrolysis. Compound **19** -with *meta* chlorine to sulfamate moiety- was completely hydrolyzed to its phenolic derivative **7** in phosphate buffer, after 12 h and in T47D/DMEM, after 9h. So, **19** showed an intermediate stability between **13** (unsubstituted sulfamate) and **16** (*ortho* substituted sulfamate). 32.5 nM (50 % of **19**) of **7** was reached after 6 h giving 50 % inhibition of 17 β -HSD1 (cell-free IC₅₀ for 17 β -HSD1 of **7** equals 32 nM), see Figure 3. In a cellular assay, 50 % inhibition of 17 β -HSD1 was reached after 45 % of 30 nM **19** was hydrolyzed to **7** to give 13.5 nM (cellular IC₅₀ for 17 β -HSD1 of **7** equals 14 nM), see Figure 4. In conclusion, the prodrug principle was validated, in which the inhibition of 17 β -HSD1 was performed exclusively by the released drug upon incubation of the prodrug in biological systems.

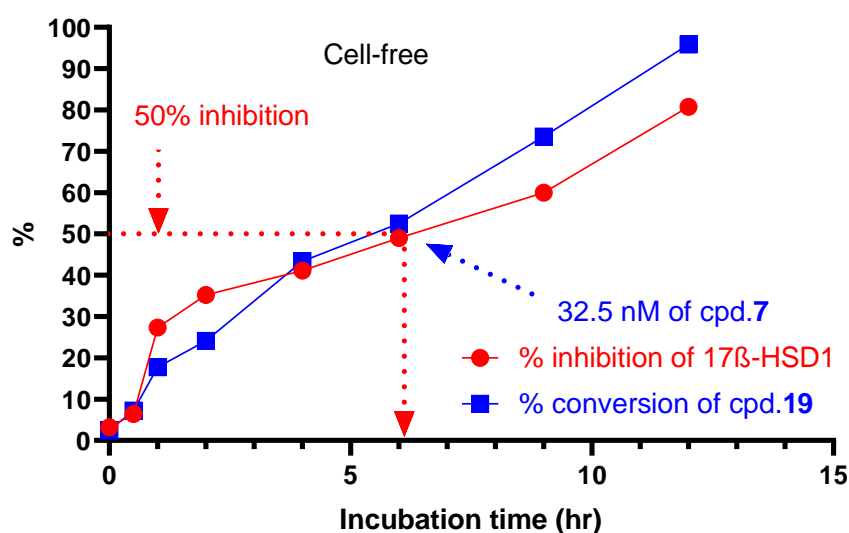


Figure 3. Plots of percentage conversion of **19** to **7** and the percentage inhibition of 17 β -HSD1 at starting concentration of 75 nM of **19** in a cell-free system. Each point in the figure represents mean value of two independent experiments each conducted in duplicates, standard deviation less than 20 %.

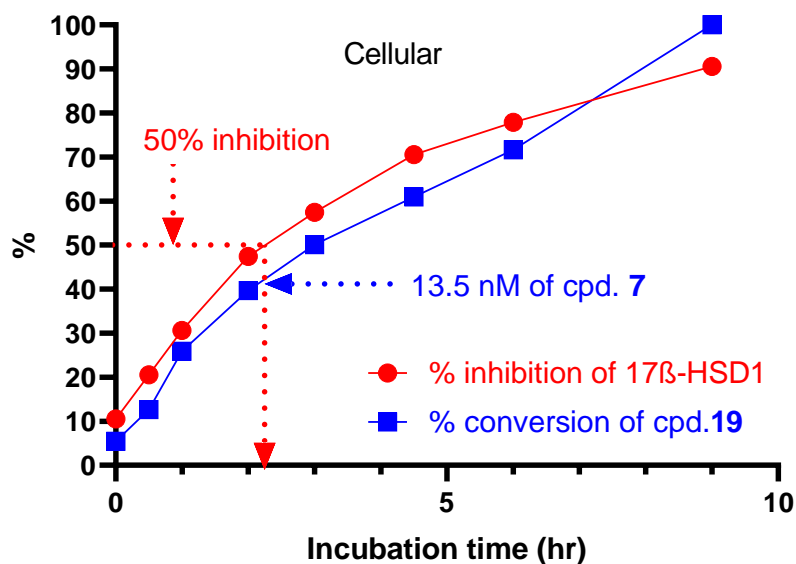


Figure 4. Plots of percentage conversion of **19** to **7** and the percentage inhibition of 17β-HSD1 at starting concentration of 30 nM of **19** in a cellular system. Each point in the figure represents mean value of two independent experiments each conducted in duplicates, standard deviation less than 20 %.

Another example, thiazole **37** was less stable than the corresponding furan **13** in both cell-free (% conversion of **37** to **33** = 65 % after 24 h) and cellular (% conversion of **37** to **33** = 99 % after 12 h) assays. Upon incubation of 75 nM of **37** in phosphate buffer, it had been noticed that 50 % inhibition of 17β-HSD1 had been attained when 50 % of **37** converted to **33** (37.5 nM) as shown in Figure 5, and that is approximately equivalent to the cell-free IC₅₀ of 17β-HSD1 inhibitor **33**, which is 34 nM. Concerning cellular validation, starting concentration of 30 nM of **37** gave 50 % inhibition of 17β-HSD1 after 42 % of it hydrolyzed to **33** (12.6 nM) as illustrated in Figure 6, (cellular IC₅₀ of **33** = 12 nM).

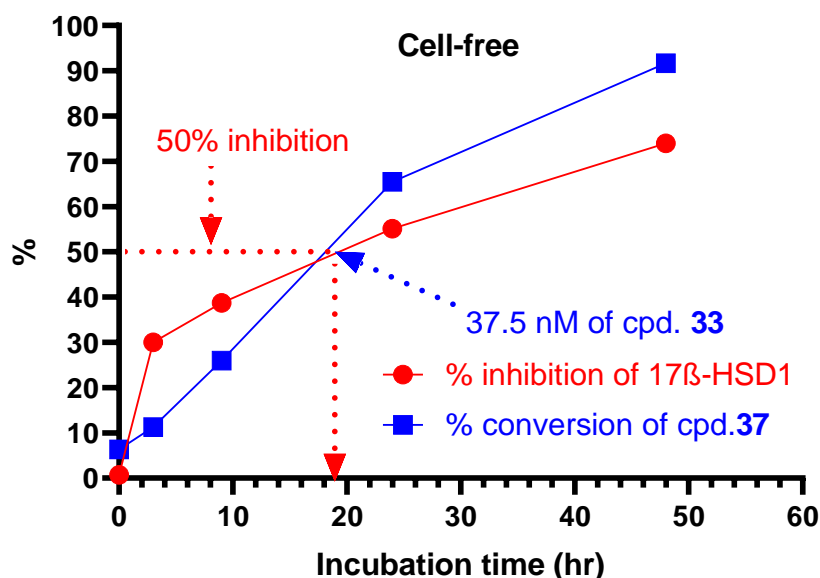


Figure 5. Plots of percentage conversion of **37** to **33** and the percentage inhibition of 17β-HSD1 at starting concentration of 75 nM of **37** in a cell-free system. Each point in the figure represents mean value of two independent experiments each conducted in duplicates, standard deviation less than 20 %.

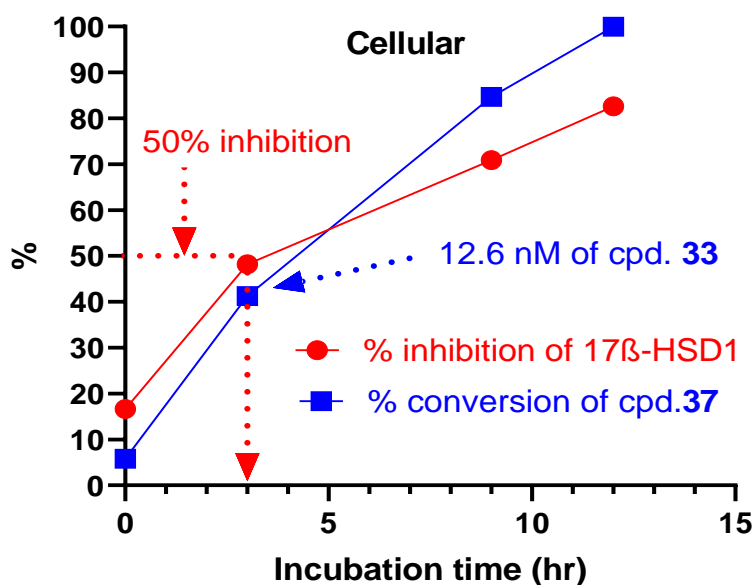


Figure 6. Plots of percentage conversion of **37** to **33** and the percentage inhibition of 17β-HSD1 at starting concentration of 30 nM of **37** in a cellular system. Each point in the figure represents mean value of two independent experiments each conducted in duplicates, standard deviation less than 20 %.

5.2.4 Validation of drug-prodrug concept for compound **13** at different starting concentrations

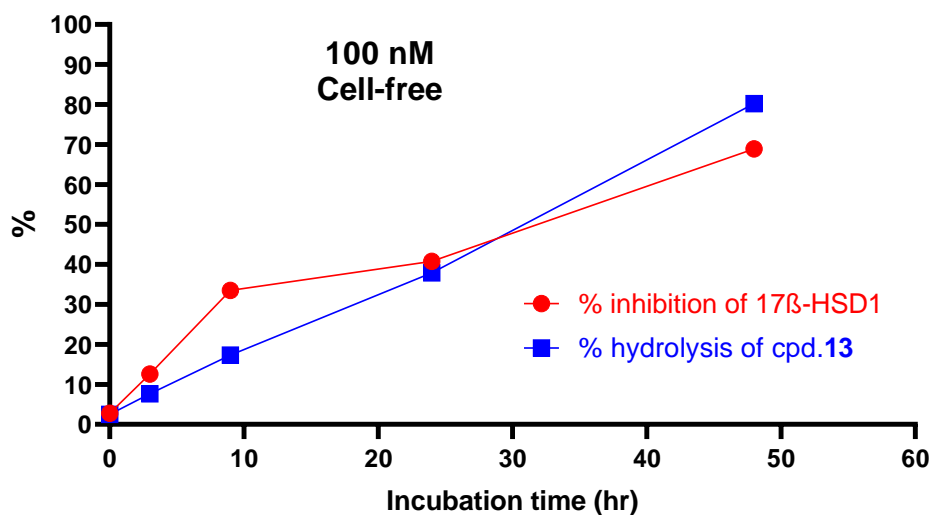


Figure 7. Plots of percentage conversion of **13** to **1** and the percentage inhibition of 17β-HSD1 at starting concentration of 100 nM of **13** in a cell-free system. Each point in the figure represents the mean value of two independent experiments each conducted in duplicates, standard deviation less than 20 %.

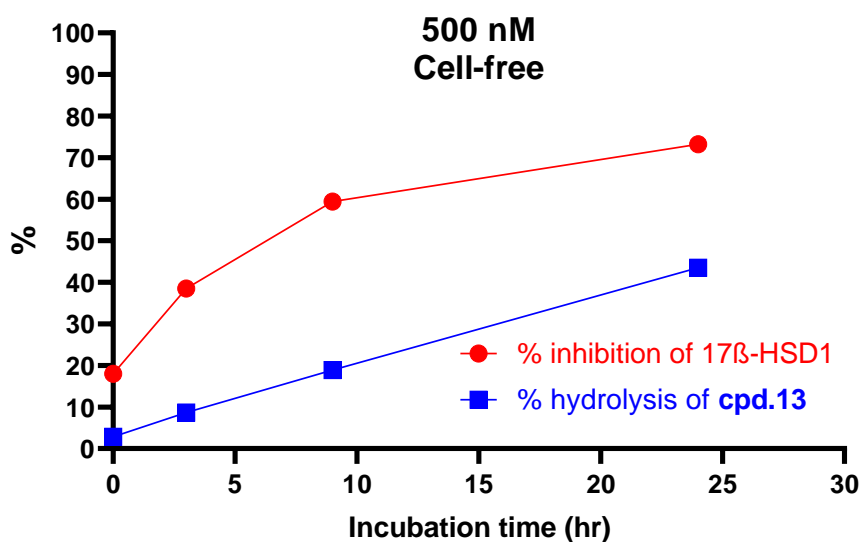


Figure 8. Plots of percentage conversion of **13** to **1** and the percentage inhibition of 17β-HSD1 at starting concentration of 500 nM of **13** in a cell-free system. Each point in the figure represents the mean value of two independent experiments each conducted in duplicates, standard deviation less than 20 %.

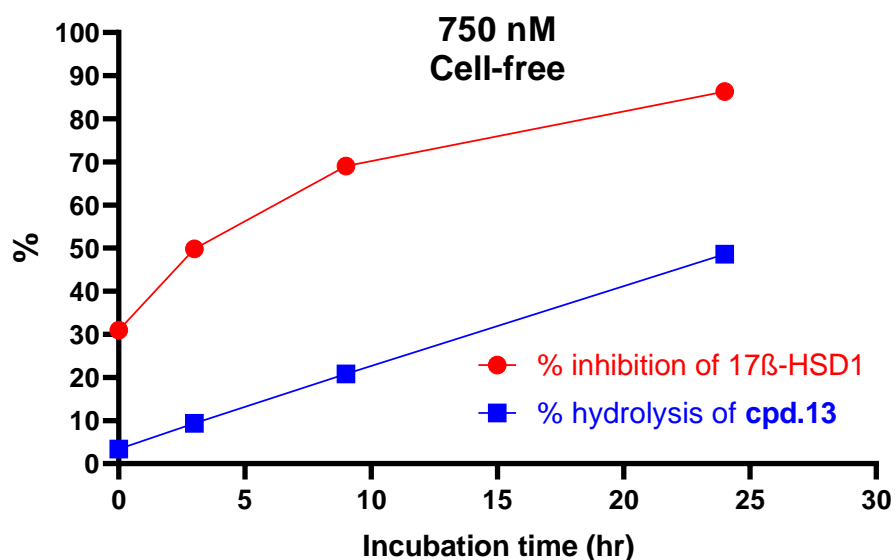


Figure 9. Plots of percentage conversion of **13** to **1** and the percentage inhibition of 17β-HSD1 at starting concentration of 750 nM of **13** in a cell-free system. Each point in the figure represents the mean value of two independent experiments each conducted in duplicates, standard deviation less than 20 %.

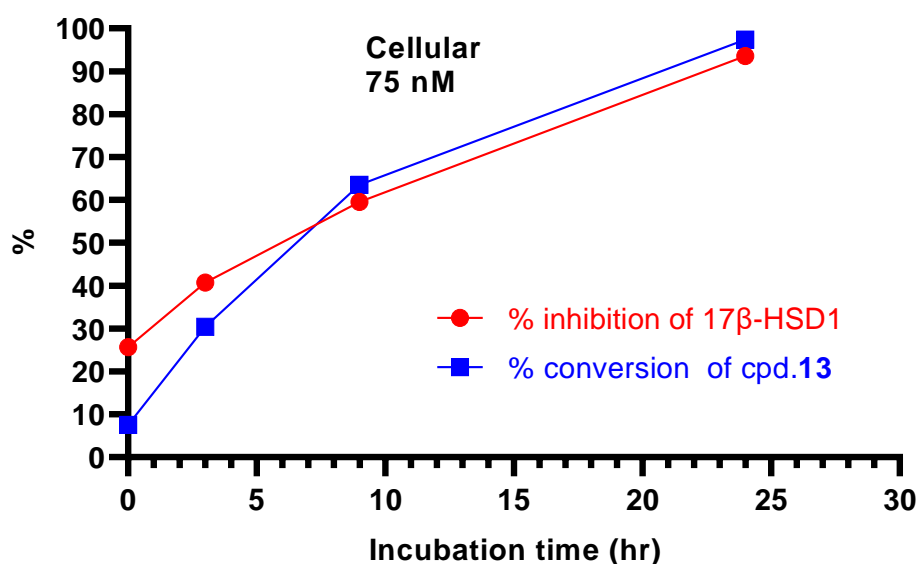


Figure 10. Plots of percentage conversion of **13** to **1** and the percentage inhibition of 17β-HSD1 at starting concentration of 75 nM of **13** in a cellular system. Each point in the figure represents the mean value of two independent experiments each conducted in duplicates, standard deviation less than 20 %.

5.2.5 HEK-293 cell growth inhibition assay and cytotoxicity data

Cells were grown in Dulbecco's Modified Eagle's Medium (DMEM, Sigma) containing 10 % fetal calf serum (FCS, Sigma). All cell media contained in addition penicillin G (final concentration 100 U/mL) and streptomycin sulfate (final concentration 100 mg/mL) and were maintained at 37 °C and 5 % CO₂ in a humidified incubator. Cells were seeded in 96-well standard assay microplates at a density of 45000 cells per well, then allowed to adhere overnight before compound addition. After 24 h, cells were treated with different concentrations of the compounds (maximum concentration: 20 μM). Cells were incubated for additional 48 h at 37 °C, after which 20 μL of MTT reagent (prepared as 5 mg/mL phosphate buffer saline, PBS) were added and then incubated for additional 1 h. After that, 100 μL of sodium dodecylsulfate (SDS, prepared as 10% in 0.01-N HCl) were added and incubated for at least 2 h at 37 °C to allow for cell lysis. Absorbance was then measured at a wavelength of 570 nm in a plate reader (PolarStar, BMG Labtech, Freiburg, Germany). Tunicamycin was used as a positive control (50 % growth inhibition at 0.1 μM). Proliferation in the presence of the vehicle was arbitrarily set to 0 % growth inhibition.

Table S1. Cytotoxicity data for sulfamates 13, 16, 19 and 37 and the conjugate phenols 1, 4, 7 and 33.

Cpd	Structure	Cell Growth Inhibition at 20 μM ^[a]
13		12.8 %
1		11.7 %
16		53.6%
4		54.6%
19		30.0 %
7		25.1%
37		15.1%
33		25.9 %

^[a] Mean value of at least two independent experiments, standard deviations less than 15 %

6. References

1. Tatiana Ruiz-Cortés, Z., Gonadal sex steroids: Production, action and interactions in mammals. *Steroids-from physiology to clinical medicine*. Intechopen: **2012**, 3-44.
2. Miller, W. L.; Auchus, R. J., The molecular biology, biochemistry, and physiology of human steroidogenesis and its disorders. *Endocr. Rev.* **2011**, 32 (1), 81-151.
3. Labrie, F.; Luu-The, V.; Lin, S.-X.; Simard, J.; Labrie, C., Role of 17 β -hydroxysteroid dehydrogenases in sex steroid formation in peripheral intracrine tissues. *Trends Endocrinol. Metab.* **2000**, 11 (10), 421-427.
4. Labrie, F., Intracrinology. *Mol. Cell. Endocrinol.* **1991**, 78 (3), C113-C118.
5. Labrie, F.; Luu-The, V.; Labrie, C.; Bélanger, A.; Simard, J.; Lin, S.-X.; Pelletier, G., Endocrine and intracrine sources of androgens in women: Inhibition of breast cancer and other roles of androgens and their precursor dehydroepiandrosterone. *Endocr. Rev.* **2003**, 24 (2), 152-182.
6. Suzuki, T.; Miki, Y.; Nakamura, Y.; Moriya, T.; Ito, K.; Ohuchi, N.; Sasano, H., Sex steroid-producing enzymes in human breast cancer. *Endocr. Relat. Cancer* **2005**, 12 (4), 701-720.
7. Veler, C. D.; Thayer, S.; Doisy, E. A., The preparation of the crystalline follicular ovarian hormone: theelin. *J. Biol. Chem.* **1930**, 87 (2), 357-371.
8. Cui, J.; Shen, Y.; Li, R., Estrogen synthesis and signaling pathways during aging: From periphery to brain. *Trends Mol. Med.* **2013**, 19 (3), 197-209.
9. Prossnitz, E. R.; Barton, M., The G-protein-coupled estrogen receptor GPER in health and disease. *Nat. Rev. Endocrinol.* **2011**, 7 (12), 715-726.
10. Miller, W. L., Molecular biology of steroid hormone synthesis. *Endocr. Rev.* **1988**, 9 (3), 295-318.
11. Payne, A. H.; Hales, D. B., Overview of steroidogenic enzymes in the pathway from cholesterol to active steroid hormones. *Endocr. Rev.* **2004**, 25 (6), 947-970.
12. Ryan, K. J.; Smith, O. W., Biogenesis of steroid hormones in the human ovary. *Recent Prog. Horm. Res.* **1965**, 21, 367-409.
13. Hall, P. F., Cytochrome P-450 C21sc: One enzyme with two actions: Hydroxylase and lyase. *J. Steroid Biochem. Mol. Biol.* **1991**, 40 (4), 527-532.
14. Attar, E.; Bulun, S., Aromatase and other steroidogenic genes in endometriosis: translational aspects. *Hum. Reprod. Update* **2006**, 12 (1), 49-56.
15. Penning, T. M., Molecular endocrinology of hydroxysteroid dehydrogenases. *Endocr. Rev.* **1997**, 18 (3), 281-305.
16. Peltoketo, H.; Simard, J.; Adamski, J., 17 β -hydroxysteroid dehydrogenase (HSD)/17-ketosteroid reductase (KSR) family; nomenclature and main characteristics of the 17HSD/KSR enzymes. *J. Mol. Endocrinol.*, **1999**, 23 (1), 1-11.
17. Arlt, W.; Haas, J.; Callies, F.; Reincke, M.; Hübler, D.; Oettel, M.; Ernst, M.; Schulte, H. M.; Allolio, B., Biotransformation of oral dehydroepiandrosterone in elderly men: significant increase in circulating estrogens. *J. Clin. Endocrinol. Metab.* **1999**, 84 (6), 2170-2176.
18. Arlt, W.; Justl, H.-G.; Callies, F.; Reincke, M.; Hübler, D.; Oettel, M.; Ernst, M.; Schulte, H. M.; Allolio, B., Oral dehydroepiandrosterone for adrenal androgen replacement: pharmacokinetics and peripheral conversion to androgens and estrogens in young healthy females after dexamethasone suppression. *J. Clin. Endocrinol. Metab.* **1998**, 83 (6), 1928-1934.
19. Labrie, F.; Bélanger, A.; Bélanger, P.; Bérubé, R.; Martel, C.; Cusan, L.; Gomez, J.; Candas, B.; Chaussade, V.; Castiel, I., Metabolism of DHEA in postmenopausal women

- following percutaneous administration. *J. Steroid Biochem. Mol. Biol.* **2007**, *103* (2), 178-188.
20. Morales, A.; Haubrich, R.; Hwang, J.; Asakura, H.; Yen, S. C., The effect of six months treatment with a 100 mg daily dose of dehydroepiandrosterone (DHEA) on circulating sex steroids, body composition and muscle strength in age-advanced men and women. *Clin. Endocrinol. (Oxf.)* **1998**, *49* (4), 421-432.
 21. Liu, L.; Kang, J.; Ding, X.; Chen, D.; Zhou, Y.; Ma, H., Dehydroepiandrosterone-regulated testosterone biosynthesis via activation of the ERK1/2 signaling pathway in primary rat leydig cells. *Cell. Physiol. Biochem.* **2015**, *36* (5), 1778-1792.
 22. Simpson, E. R., Sources of estrogen and their importance. *J. Steroid Biochem. Mol. Biol.* **2003**, *86* (3-5), 225-230.
 23. McNatty, K. P.; Makris, A.; Degrazia, C.; Rapin, O.; Ryan, K. J., The production of progesterone, androgens, and estrogens by granulosa cells, thecal tissue, and stromal tissue from human ovaries in vitro. *J. Clin. Endocrinol. Metab.* **1979**, *49* (5), 687-699.
 24. Norman, A. W. Steroid hormones: Chemistry, biosynthesis, and metabolism. *Hormones* **1997**, 49-86.
 25. Buffet, N. C.; Djakoure, C.; Maitre, S. C.; Bouchard, P., Regulation of the human menstrual cycle. *Front. Neuroendocrinol.* **1998**, *19* (3), 151-186.
 26. Nilsson, S.; Gustafsson, J.-Å., Estrogen receptor transcription and transactivation basic aspects of estrogen action. *Breast Cancer Res.* **2000**, *2* (5), 1-7.
 27. Shi, H.; Kumar, S. P. D. S.; Liu, X., G protein-coupled estrogen receptor in energy homeostasis and obesity pathogenesis. *Prog. Mol. Biol. Transl. Sci.* **2013**, *114*, 193-250.
 28. Nilsson, S.; Makela, S.; Treuter, E.; Tujague, M.; Thomsen, J.; Andersson, G.; Enmark, E.; Pettersson, K.; Warner, M.; Gustafsson, J.-Å., Mechanisms of estrogen action. *Physiol. Rev.* **2001**, *81* (4), 1535-1565.
 29. Morselli, E.; Santos, R. S.; Criollo, A.; Nelson, M. D.; Palmer, B. F.; Clegg, D. J., The effects of oestrogens and their receptors on cardiometabolic health. *Nat. Rev. Endocrinol.* **2017**, *13* (6), 352-364.
 30. Jia, M.; Dahlman-Wright, K.; Gustafsson, J.-Å., Estrogen receptor alpha and beta in health and disease. *Best Pract. Res. Clin. Endocrinol. Metab.* **2015**, *29* (4), 557-568.
 31. Hall, J. M.; Couse, J. F.; Korach, K. S., The multifaceted mechanisms of estradiol and estrogen receptor signaling. *J. Biol. Chem.* **2001**, *276* (40), 36869-36872.
 32. Ballard, P. L.; Baxter, J. D.; Higgins, S. J.; Rousseau, G. G.; Tomkins, G. M., General presence of glucocorticoid receptors in mammalian tissues. *Endocrinology* **1974**, *94* (4), 998-1002.
 33. Kumar, V.; Chambon, P., The estrogen receptor binds tightly to its responsive element as a ligand-induced homodimer. *Cell* **1988**, *55* (1), 145-156.
 34. Turner, R. T.; Riggs, B. L.; Spelsberg, T. C., Skeletal effects of estrogen. *Endocr. Rev.* **1994**, *15* (3), 275-300.
 35. Robker, R. L.; Richards, J. S., Hormone-induced proliferation and differentiation of granulosa cells: A coordinated balance of the cell cycle regulators cyclin D2 and p27^{Kip1}. *Mol. Endocrinol.* **1998**, *12* (7), 924-940.
 36. Adashi, E., Immune modulators in the context of the ovulatory process: A Role for Interleukin-1. *Am. J. Reprod. Immunol.* **1996**, *35* (3), 190-194.
 37. Drummond, A. E.; Findlay, J. K., The role of estrogen in folliculogenesis. *Mol. Cell. Endocrinol.* **1999**, *151* (1-2), 57-64.
 38. Groothuis, P.; Dassen, H.; Romano, A.; Punyadeera, C., Estrogen and the endometrium: lessons learned from gene expression profiling in rodents and human. *Hum. Reprod. Update* **2007**, *13* (4), 405-417.
 39. Dickson, R. B.; Stancel, G. M., Chapter 8: Estrogen receptor-mediated processes in normal and cancer cells. *JNCI Monographs* **2000**, *2000* (27), 135-145.

40. Gustafsson, J.-Å.; Warner, M., Estrogen receptor β in the breast: Role in estrogen responsiveness and development of breast cancer. *J. Steroid Biochem. Mol. Biol.* **2000**, *74* (5), 245-248.
41. Pepe, G. J.; Albrecht, E. D., Actions of placental and fetal adrenal steroid hormones in primate pregnancy. *Endocr. Rev.* **1995**, *16* (5), 608-648.
42. Albrecht, E. D.; Aberdeen, G. W.; Pepe, G. J., The role of estrogen in the maintenance of primate pregnancy. *Am. J. Obstet. Gynecol.* **2000**, *182* (2), 432-438.
43. Cauley, J. A.; Robbins, J.; Chen, Z.; Cummings, S. R.; Jackson, R. D.; LaCroix, A. Z.; LeBoff, M.; Lewis, C. E.; McGowan, J.; Neuner, J., Effects of estrogen plus progestin on risk of fracture and bone mineral density: The women's health initiative randomized trial. *JAMA* **2003**, *290* (13), 1729-1738.
44. Mendelsohn, M. E.; Karas, R. H., The protective effects of estrogen on the cardiovascular system. *N. Engl. J. Med.* **1999**, *340* (23), 1801-1811.
45. Van Amelsvoort, T.; Compton, J.; Murphy, D., In vivo assessment of the effects of estrogen on human brain. *Trends Endocrinol. Metab.* **2001**, *12* (6), 273-276.
46. Fink, G.; Sumner, B. E.; Rosie, R.; Grace, O.; Quinn, J. P., Estrogen control of central neurotransmission: effect on mood, mental state, and memory. *Cell. Mol. Neurobiol.* **1996**, *16* (3), 325-344.
47. Stahl, S. M., Effects of estrogen on the central nervous system. *J. Clin. Psychiatry* **2001**, *62* (5), 317-318.
48. Roof, R. L.; Hall, E. D., Gender differences in acute CNS trauma and stroke: neuroprotective effects of estrogen and progesterone. *J. Neurotrauma* **2000**, *17* (5), 367-388.
49. Sherwin, B. B., Estrogen and memory in women: How can we reconcile the findings? *Horm. Behav.* **2005**, *47* (3), 371-375.
50. Olsen, N. J.; Kovacs, W. J., Gonadal steroids and immunity. *Endocr. Rev.* **1996**, *17* (4), 369-384.
51. Deroo, B. J.; Korach, K. S., Estrogen receptors and human disease. *J. Clin. Invest.* **2006**, *116* (3), 561-570.
52. Brown, S. B.; Hankinson, S. E., Endogenous estrogens and the risk of breast, endometrial, and ovarian cancers. *Steroids* **2015**, *99*, 8-10.
53. Travis, R. C.; Key, T. J., Oestrogen exposure and breast cancer risk. *Breast Cancer Res.* **2003**, *5* (5), 239-247.
54. Yager, J. D.; Davidson, N. E., Estrogen carcinogenesis in breast cancer. *N. Engl. J. Med.* **2006**, *354* (3), 270-282.
55. Grady, D.; Gebretsadik, T.; Kerlikowske, K.; Ernster, V.; Petitti, D., Hormone replacement therapy and endometrial cancer risk: A meta-analysis. *Obstet. Gynecol.* **1995**, *85* (2), 304-313.
56. Chlebowski, R.; Anderson, G.; Sarto, G.; Haque, R.; Runowicz, C.; Aragaki, A.; Thomson, C.; Howard, B.; Wactawski-Wende, J.; Chen, C., Continuous combined estrogen plus progestin and endometrial cancer: The women's health initiative randomized trial. *J. Natl. Cancer Inst.* **2016**, *108* (3), 1-10.
57. Cuna, S.; Hoffmann, P.; Pujol, P., Estrogens and epithelial ovarian cancer. *Gynecol. Oncol.* **2004**, *94* (1), 25-32.
58. Rodriguez, C.; Patel, A. V.; Calle, E. E.; Jacob, E. J.; Thun, M. J., Estrogen replacement therapy and ovarian cancer mortality in a large prospective study of US women. *JAMA* **2001**, *285* (11), 1460-1465.
59. Burney, R. O.; Giudice, L. C., Pathogenesis and pathophysiology of endometriosis. *Fertil. Steril.* **2012**, *98* (3), 511-519.

60. Kitawaki, J.; Kado, N.; Ishihara, H.; Koshiba, H.; Kitaoka, Y.; Honjo, H., Endometriosis: the pathophysiology as an estrogen-dependent disease. *J. Steroid Biochem. Mol. Biol.* **2002**, *83* (1-5), 149-155.
61. Márquez-Garbán, D. C.; Chen, H.W.; Fishbein, M. C.; Goodglick, L.; Pietras, R. J., Estrogen receptor signaling pathways in human non-small cell lung cancer. *Steroids* **2007**, *72* (2), 135-143.
62. Zhang, G.; Liu, X.; Farkas, A. M.; Parwani, A. V.; Lathrop, K. L.; Lenzner, D.; Land, S. R.; Srinivas, H., Estrogen receptor β functions through nongenomic mechanisms in lung cancer cells. *Mol. Endocrinol.* **2009**, *23* (2), 146-156.
63. Hershberger, P. A.; Stabile, L. P.; Kanterewicz, B.; Rothstein, M. E.; Gubish, C. T.; Land, S.; Shuai, Y.; Siegfried, J. M.; Nichols, M., Estrogen receptor beta (ER β) subtype-specific ligands increase transcription, p44/p42 mitogen activated protein kinase (MAPK) activation and growth in human non-small cell lung cancer cells. *J. Steroid Biochem. Mol. Biol.* **2009**, *116* (1-2), 102-109.
64. Fan, S.; Liao, Y.; Liu, C.; Huang, Q.; Liang, H.; Ai, B.; Fu, S.; Zhou, S., Estrogen promotes tumor metastasis via estrogen receptor beta-mediated regulation of matrix-metalloproteinase-2 in non-small cell lung cancer. *Oncotarget.* **2017**, *8* (34), 56443-56459.
65. Liu, C.; Liao, Y.; Fan, S.; Fu, X.; Xiong, J.; Zhou, S.; Zou, M.; Wang, J., G-protein-coupled estrogen receptor antagonist G15 decreases estrogen-induced development of non-small cell lung cancer. *Oncol. Res.* **2019**, *27* (3), 283-292.
66. Pacifici, R., Estrogen, cytokines, and pathogenesis of postmenopausal osteoporosis. *J. Bone Miner. Res.* **1996**, *11* (8), 1043-1051.
67. Riggs, B. L.; Khosla, S.; Melton III, L. J., A unitary model for involutional osteoporosis: estrogen deficiency causes both type I and type II osteoporosis in postmenopausal women and contributes to bone loss in aging men. *J. Bone Miner. Res.* **1998**, *13* (5), 763-773.
68. Black, D. M.; Rosen, C. J., Postmenopausal osteoporosis. *N. Engl. J. Med.* **2016**, *374* (3), 254-262.
69. Bray, F.; Ferlay, J.; Soerjomataram, I.; Siegel, R. L.; Torre, L. A.; Jemal, A., Global cancer statistics 2018: GLOBOCAN estimates of incidence and mortality worldwide for 36 cancers in 185 countries. *CA Cancer J. Clin.* **2018**, *68* (6), 394-424.
70. Gasperino, J., Gender is a risk factor for lung cancer. *Med. Hypotheses* **2011**, *76* (3), 328-331.
71. Schwartz, A. G.; Prysak, G. M.; Murphy, V.; Lonardo, F.; Pass, H.; Schwartz, J.; Brooks, S., Nuclear estrogen receptor β in lung cancer: Expression and survival differences by sex. *Clin. Cancer Res.* **2005**, *11* (20), 7280-7287.
72. Papadopoulos, A.; Guida, F.; Leffondré, K.; Cénéé, S.; Cyr, D.; Schmaus, A.; Radoï, L.; Paget-Bailly, S.; Carton, M.; Menvielle, G., Heavy smoking and lung cancer: Are women at higher risk? Result of the ICARE study. *Br. J. Cancer* **2014**, *110* (5), 1385-1391.
73. Ryu, J.-S.; Jeon, S.-H.; Kim, J.-S.; Lee, J. H.; Kim, S. H.; Hong, J. T.; Jeong, J. H.; Jeong, J. J.; Lee, M. D.; Min, S. J., Gender differences in susceptibility to smoking among patients with lung cancer. *Korean J. Intern. Med.* **2011**, *26* (4), 427-431.
74. Guo, H.; Huang, K.; Zhang, X.; Zhang, W.; Guan, L.; Kuang, D.; Deng, Q.; Deng, H.; Zhang, X.; He, M., Women are more susceptible than men to oxidative stress and chromosome damage caused by polycyclic aromatic hydrocarbons exposure. *Environ. Mol. Mutagen.* **2014**, *55* (6), 472-481.
75. Spivack, S. D.; Hurteau, G. J.; Reilly, A. A.; Aldous, K. M.; Ding, X.; Kaminsky, L. S., CYP1B1 expression in human lung. *Drug Metab. Disposition* **2001**, *29* (6), 916-922.
76. Cavalieri, E.; Chakravarti, D.; Guttenplan, J.; Hart, E.; Ingle, J.; Jankowiak, R.; Muti, P.; Rogan, E.; Russo, J.; Santen, R., Catechol estrogen quinones as initiators of breast

- and other human cancers: implications for biomarkers of susceptibility and cancer prevention. *Biochim. Biophys. Acta - Rev. Cancer* **2006**, *1766* (1), 63-78.
77. Belous, A. R.; Hachey, D. L.; Dawling, S.; Roodi, N.; Parl, F. F., Cytochrome P450 1B1-mediated estrogen metabolism results in estrogen-deoxyribonucleoside adduct formation. *Cancer Res.* **2007**, *67* (2), 812-817.
 78. Weinberg, O. K.; Marquez-Garban, D. C.; Fishbein, M. C.; Goodglick, L.; Garban, H. J.; Dubinett, S. M.; Pietras, R. J., Aromatase inhibitors in human lung cancer therapy. *Cancer Res.* **2005**, *65* (24), 11287-11291.
 79. Stabile, L. P.; Davis, A. L. G.; Gubish, C. T.; Hopkins, T. M.; Luketich, J. D.; Christie, N.; Finkelstein, S.; Siegfried, J. M., Human non-small cell lung tumors and cells derived from normal lung express both estrogen receptor α and β and show biological responses to estrogen. *Cancer Res.* **2002**, *62* (7), 2141-2150.
 80. Pietras, R. J.; Márquez, D. C.; Chen, H. W.; Tsai, E.; Weinberg, O.; Fishbein, M., Estrogen and growth factor receptor interactions in human breast and non-small cell lung cancer cells. *Steroids* **2005**, *70* (5-7), 372-381.
 81. Fasco, M. J.; Hurteau, G. J.; Spivack, S. D., Gender-dependent expression of alpha and beta estrogen receptors in human nontumor and tumor lung tissue. *Mol. Cell. Endocrinol.* **2002**, *188* (1-2), 125-140.
 82. Jala, V. R.; Radde, B. N.; Haribabu, B.; Klinge, C. M., Enhanced expression of G-protein coupled estrogen receptor (GPER/GPR30) in lung cancer. *BMC Cancer* **2012**, *12* (1), 1-12.
 83. Liu, C.; Liao, Y.; Fan, S.; Tang, H.; Jiang, Z.; Zhou, B.; Xiong, J.; Zhou, S.; Zou, M.; Wang, J., G protein-coupled estrogen receptor (GPER) mediates NSCLC progression induced by 17 β -estradiol (E 2) and selective agonist G1. *Med. Oncol.* **2015**, *32* (4), 104.
 84. Słowikowski, B. K.; Lianeri, M.; Jagodziński, P. P., Exploring estrogenic activity in lung cancer. *Mol. Biol. Rep.* **2017**, *44* (1), 35-50.
 85. Hsu, L.-H.; Chu, N.-M.; Kao, S.-H., Estrogen, estrogen receptor and lung cancer. *Int. J. Mol. Sci.* **2017**, *18* (8), 1713.
 86. Niikawa, H.; Suzuki, T.; Miki, Y.; Suzuki, S.; Nagasaki, S.; Akahira, J.; Honma, S.; Evans, D. B.; Hayashi, S.-i.; Kondo, T., Intratumoral estrogens and estrogen receptors in human non-small cell lung carcinoma. *Clin. Cancer Res.* **2008**, *14* (14), 4417-4426.
 87. Verma, M. K.; Miki, Y.; Sasano, H., Aromatase in human lung carcinoma. *Steroids* **2011**, *76* (8), 759-764.
 88. Marquez-Garban, D. C.; Chen, H.-W.; Goodglick, L.; Fishbein, M. C.; Pietras, R. J., Targeting aromatase and estrogen signaling in human non-small cell lung cancer. *Ann. N.Y. Acad. Sci.* **2009**, *1155*, 194-205.
 89. Verma, M. K.; Miki, Y.; Abe, K.; Suzuki, T.; Niikawa, H.; Suzuki, S.; Kondo, T.; Sasano, H., Intratumoral localization and activity of 17 β -hydroxysteroid dehydrogenase type 1 in non-small cell lung cancer: A potent prognostic factor. *J. Transl. Med.* **2013**, *11* (1), 1-11.
 90. Drzewiecka, H.; Jagodzinski, P. P., Conversion of estrone to 17-beta-estradiol in human non-small-cell lung cancer cells in vitro. *Biomed. Pharmacother.* **2012**, *66* (7), 530-534.
 91. Drzewiecka, H.; Gałęcki, B.; Jarmołowska-Jurczyszyn, D.; Kluk, A.; Dyszkiewicz, W.; Jagodziński, P. P., Increased expression of 17-beta-hydroxysteroid dehydrogenase type 1 in non-small cell lung cancer. *Lung Cancer* **2015**, *87* (2), 107-116.
 92. Giudice, L. C., Endometriosis. Clinical practice. *N. Engl. J. Med.* **2010**, *362* (25), 2389-2398.
 93. Nap, A. W.; Groothuis, P. G.; Demir, A. Y.; Evers, J. L.; Dunselman, G. A., Pathogenesis of endometriosis. *Best Pract. Res. Clin. Obstet. Gynaecol.* **2004**, *18* (2), 233-244.
 94. Konings, G.; Brentjens, L.; Delvoux, B.; Linnanen, T.; Cornel, K.; Koskimies, P.; Bongers, M.; Kruitwagen, R.; Xanthoulea, S.; Romano, A., Intracrine regulation of

- estrogen and other sex steroid levels in endometrium and non-gynecological tissues; pathology, physiology, and drug discovery. *Front. Pharmacol.* **2018**, *9* (940), 1-51.
95. Ferreira, A. L. L.; Bessa, M. M. M.; Drezett, J.; de Abreu, L. C., Quality of life of the woman carrier of endometriosis: systematized review. *Reprodução & Climatério* **2016**, *31* (1), 48-54.
 96. Berkley, K. J.; Rapkin, A. J.; Papka, R. E., The pains of endometriosis. *Science* **2005**, *308* (5728), 1587-1589.
 97. Nnoaham, K. E.; Hummelshoj, L.; Webster, P.; d'Hooghe, T.; de Cicco Nardone, F.; de Cicco Nardone, C.; Jenkinson, C.; Kennedy, S. H.; Zondervan, K. T.; Study, W. E. R. F. G., Impact of endometriosis on quality of life and work productivity: a multicenter study across ten countries. *Fertil. Steril.* **2011**, *96* (2), 366-373.
 98. Van Gorp, T.; Amant, F.; Neven, P.; Vergote, I.; Moerman, P., Endometriosis and the development of malignant tumours of the pelvis. A review of literature. *Best Pract. Res. Clin. Obstet. Gynaecol.* **2004**, *18* (2), 349-371.
 99. Chene, G.; Ouellet, V.; Rahimi, K.; Barres, V.; Provencher, D.; Mes-Masson, A. M., The ARID1A pathway in ovarian clear cell and endometrioid carcinoma, contiguous endometriosis, and benign endometriosis. *Int. J. Gynecol. Obstet.* **2015**, *130* (1), 27-30.
 100. Bulun, S. E., Endometriosis. *N. Engl. J. Med.* **2009**, *360* (3), 268-279.
 101. Tsai, S. J.; Wu, M. H.; Lin, C.-C.; Sun, H. S.; Chen, H. M., Regulation of steroidogenic acute regulatory protein expression and progesterone production in endometriotic stromal cells. *J. Clin. Endocrinol. Metab.* **2001**, *86* (12), 5765-5773.
 102. Sampson, J. A., Peritoneal endometriosis due to the menstrual dissemination of endometrial tissue into the peritoneal cavity. *Am. J. Obstet. Gynecol.* **1927**, *14* (4), 422-469.
 103. Halme, J.; Hammond, M. G.; Hulka, J. F.; Raj, S. G.; Talbert, L. M., Retrograde menstruation in healthy women and in patients with endometriosis. *Obstet. Gynecol.* **1984**, *64* (2), 151-154.
 104. Sasson, I. E.; Taylor, H. S., Stem cells and the pathogenesis of endometriosis. *Ann. N.Y. Acad. Sci.* **2008**, *1127*, 106-115.
 105. Matsuura, K.; Ohtake, H.; Katabuchi, H.; Okamura, H., Coelomic metaplasia theory of endometriosis: Evidence from in vivo studies and an in vitro experimental model. *Gynecol. Obstet. Invest.* **1999**, *47* (Suppl. 1), 18-22.
 106. Rosenfeld, D. L.; Lecher, B. D., Endometriosis in a patient with Rokitansky-Kuster-Hauser syndrome. *Am. J. Obstet. Gynecol.* **1981**, *139* (1), 105.
 107. Bulun, S. E.; Lin, Z.; Imir, G.; Amin, S.; Demura, M.; Yilmaz, B.; Martin, R.; Utsunomiya, H.; Thung, S.; Gurates, B., Regulation of aromatase expression in estrogen-responsive breast and uterine disease: from bench to treatment. *Pharmacol. Rev.* **2005**, *57* (3), 359-383.
 108. Bulun, S. E.; Zeitoun, K. M.; Takayama, K.; Sasano, H., Estrogen biosynthesis in endometriosis: molecular basis and clinical relevance. *J. Mol. Endocrinol.* **2000**, *25* (1), 35-42.
 109. Attar, E.; Tokunaga, H.; Imir, G.; Yilmaz, M. B.; Redwine, D.; Putman, M.; Gurates, B.; Attar, R.; Yaegashi, N.; Hales, D. B., Prostaglandin E2 via steroidogenic factor-1 coordinately regulates transcription of steroidogenic genes necessary for estrogen synthesis in endometriosis. *J. Clin. Endocrinol. Metab.* **2009**, *94* (2), 623-631.
 110. Mounsey, A.; Wilgus, A.; Slawson, D. C., Diagnosis and management of endometriosis. *Am. Fam. Physician* **2006**, *74* (4), 594-600.
 111. Ferrero, S.; Evangelisti, G.; Barra, F., Current and emerging treatment options for endometriosis. *Expert Opin. Pharmacother.* **2018**, *19* (10), 1109-1125.

112. Ferrero, S.; Alessandri, F.; Racca, A.; Leone Roberti Maggiore, U., Treatment of pain associated with deep endometriosis: Alternatives and evidence. *Fertil. Steril.* **2015**, *104* (4), 771-792.
113. Barra, F.; Scala, C.; Mais, V.; Guerriero, S.; Ferrero, S., Investigational drugs for the treatment of endometriosis, an update on recent developments. *Expert Opin. Investig. Drugs* **2018**, *27* (5), 445-458.
114. Laschke, M. W.; Elitzsch, A.; Scheuer, C.; Vollmar, B.; Menger, M. D., Selective cyclooxygenase-2 inhibition induces regression of autologous endometrial grafts by down-regulation of vascular endothelial growth factor-mediated angiogenesis and stimulation of caspase-3-dependent apoptosis. *Fertil. Steril.* **2007**, *87* (1), 163-171.
115. Ebert, A. D.; Bartley, J.; David, M., Aromatase inhibitors and cyclooxygenase-2 (COX-2) inhibitors in endometriosis: new questions-old answers ? *Eur. J. Obstet. Gynecol. Reprod. Biol.* **2005**, *122* (2), 144-150.
116. Dunselman, G.; Vermeulen, N.; Becker, C.; Calhaz-Jorge, C.; D'Hooghe, T.; De Bie, B.; Heikinheimo, O.; Horne, A.; Kiesel, L.; Nap, A., ESHRE guideline: Management of women with endometriosis. *Hum. Reprod.* **2014**, *29* (3), 400-412.
117. Secky, L.; Svoboda, M.; Klameth, L.; Bajna, E.; Hamilton, G.; Zeillinger, R.; Jäger, W.; Thalhammer, T., The sulfatase pathway for estrogen formation: targets for the treatment and diagnosis of hormone-associated tumors. *J. Drug Deliv.* **2013**, *2013*, 1-13.
118. Miki, Y.; Suzuki, T.; Tazawa, C.; Yamaguchi, Y.; Kitada, K.; Honma, S.; Moriya, T.; Hirakawa, H.; Evans, D. B.; Hayashi, S. I., Aromatase localization in human breast cancer tissues: possible interactions between intratumoral stromal and parenchymal cells. *Cancer Res.* **2007**, *67* (8), 3945-3954.
119. Simpson, E. R.; Davis, S. R., Minireview: Aromatase and the regulation of estrogen biosynthesis—some new perspectives. *Endocrinology* **2001**, *142* (11), 4589-4594.
120. Simpson, E.; Rubin, G.; Clyne, C.; Robertson, K.; O'Donnell, L.; Davis, S.; Jones, M., Local estrogen biosynthesis in males and females. *Endocr. Relat. Cancer* **1999**, *6* (2), 131-137.
121. Stocco, C., Tissue physiology and pathology of aromatase. *Steroids* **2012**, *77* (1-2), 27-35.
122. Simard, J.; Vincent, A.; Duchesne, R.; Labrie, F., Full oestrogenic activity of C19- Δ^5 adrenal steroids in rat pituitary lactotrophs and somatotrophs. *Mol. Cell. Endocrinol.* **1988**, *55* (2), 233-242.
123. Trottier, A.; Maltais, R.; Ayan, D.; Barbeau, X.; Roy, J.; Perreault, M.; Poulin, R.; Lagüe, P.; Poirier, D., Insight into the mode of action and selectivity of PBRM, a covalent steroidal inhibitor of 17 β -hydroxysteroid dehydrogenase type 1. *Biochem. Pharmacol.* **2017**, *144*, 149-161.
124. Apa, R.; Lanzone, A.; Miceli, F.; Mastrandrea, M.; Caruso, A.; Mancuso, S.; Canipari, R., Growth hormone induces in vitro maturation of follicle- and cumulus-enclosed rat oocytes. *Mol. Cell. Endocrinol.* **1994**, *106* (1), 207-212.
125. Poulin, R.; Labrie, F., Stimulation of cell proliferation and estrogenic response by adrenal C₁₉- Δ^5 -steroids in the ZR-75-1 human breast cancer cell line. *Cancer Res.* **1986**, *46* (10), 4933-4937.
126. Dauvois, S.; Labrie, F., Androstenedione and androst-5-ene-3 β ,17 β -diol stimulate DMBA-induced rat mammary tumors-role of aromatase. *Breast Cancer Res. Treat.* **1989**, *13* (1), 61-69.
127. Morohashi, K.; Baba, T.; Tanaka, M., Steroid hormones and the development of reproductive organs. *Sex. Dev.* **2013**, *7* (1-3), 61-79.
128. Huhtinen, K.; Ståhle, M.; Perheentupa, A.; Poutanen, M., Estrogen biosynthesis and signaling in endometriosis. *Mol. Cell. Endocrinol.* **2012**, *358* (2), 146-154.

129. Konings, G.; Brentjens, L.; Delvoux, B.; Linnanen, T.; Cornel, K.; Koskimies, P.; Bongers, M.; Kruitwagen, R.; Xanthoulea, S.; Romano, A., Intracrine regulation of estrogen and other sex steroid levels in endometrium and non-gynecological tissues; Pathology, physiology, and drug discovery. *Front. Pharmacol.* **2018**, *9* (940), 1-51.
130. Heilier, J.-F.; Donnez, O.; Van Kerckhove, V.; Lison, D.; Donnez, J., Expression of aromatase (P450 aromatase/CYP19) in peritoneal and ovarian endometriotic tissues and deep endometriotic (adenomyotic) nodules of the rectovaginal septum. *Fertil. Steril.* **2006**, *85* (5), 1516-1518.
131. Fusi, L.; Purohit, A.; Brosens, J.; Woo, L. W. L.; Potter, B. V. L.; Reed, M. J., Inhibition of steroid sulfatase activity in endometriotic implants by STX64 (667Coumate): A potential new therapy. *Sci. World J.* **2008**, *8*, 1325-1327.
132. Noel, C.; Reed, M.; Jacobs, H.; James, V., The plasma concentration of oestrone sulphate in postmenopausal women: lack of diurnal variation, effect of ovariectomy, age and weight. *J. Steroid Biochem.* **1981**, *14* (11), 1101-1105.
133. Pasqualini, J.; Gelly, C.; Nguyen, B.-L.; Vella, C., Importance of estrogen sulfates in breast cancer. *J. Steroid Biochem.* **1989**, *34* (1-6), 155-163.
134. Laplante, Y.; Rancourt, C.; Poirier, D., Relative involvement of three 17 β -hydroxysteroid dehydrogenases (types 1, 7 and 12) in the formation of estradiol in various breast cancer cell lines using selective inhibitors. *Mol. Cell. Endocrinol.* **2009**, *301* (1-2), 146-153.
135. Šmuc, T.; Hevir, N.; Ribič-Pucelj, M.; Husen, B.; Thole, H.; Rižner, T. L., Disturbed estrogen and progesterone action in ovarian endometriosis. *Mol. Cell. Endocrinol.* **2009**, *301* (1), 59-64.
136. Santner, S.; Feil, P.; Santen, R., In situ estrogen production via the estrone sulfatase pathway in breast tumors: Relative importance versus the aromatase pathway. *J. Clin. Endocrinol. Metab.* **1984**, *59* (1), 29-33.
137. Khurana, A.; Belefrod, D.; He, X.; Chien, J.; Shridhar, V., Role of heparan sulfatases in ovarian and breast cancer. *Am. J. Cancer Res.* **2013**, *3* (1), 34-45.
138. Obaya, A. J., Molecular cloning and initial characterization of three novel human sulfatases. *Gene* **2006**, *372*, 110-117.
139. Sardiello, M.; Annunziata, I.; Roma, G.; Ballabio, A., Sulfatases and sulfatase modifying factors: an exclusive and promiscuous relationship. *Hum. Mol. Genet.* **2005**, *14* (21), 3203-3217.
140. Hanson, S. R.; Best, M. D.; Wong, C. H., Sulfatases: structure, mechanism, biological activity, inhibition, and synthetic utility. *Angew. Chem. Int. Ed.* **2004**, *43* (43), 5736-5763.
141. Chapman, E.; Best, M. D.; Hanson, S. R.; Wong, C. H., Sulfotransferases: Structure, mechanism, biological activity, inhibition, and synthetic utility. *Angew. Chem. Int. Ed.* **2004**, *43* (27), 3526-3548.
142. Stein, C.; Hille, A.; Seidel, J.; Rijnbout, S.; Waheed, A.; Schmidt, B.; Geuze, H.; von Figura, K., Cloning and expression of human steroid-sulfatase. Membrane topology, glycosylation, and subcellular distribution in BHK-21 cells. *J. Biol. Chem.* **1989**, *264* (23), 13865-13872.
143. Anson, D. S.; Taylor, J. A.; Bielicki, J.; Harper, G. S.; Peters, C.; Gibson, G. J.; Hopwood, J. J., Correction of human mucopolysaccharidosis type-VI fibroblasts with recombinant N-acetylgalactosamine-4-sulphatase. *Biochem. J* **1992**, *284* (3), 789-794.
144. Franco, B.; Meroni, G.; Parenti, G.; Levilliers, J.; Bernard, L.; Gebbia, M.; Cox, L.; Maroteaux, P.; Sheffield, L.; Rappold, G. A., A cluster of sulfatase genes on Xp22. 3: mutations in chondrodysplasia punctata (CDPX) and implications for warfarin embryopathy. *Cell* **1995**, *81* (1), 15-25.
145. Puca, A. A.; Zollo, M.; Repetto, M.; Andolfi, G.; Guffanti, A.; Simon, G.; Ballabio, A.; Franco, B., Identification by shotgun sequencing, genomic organization, and

- functional analysis of a fourth arylsulfatase gene (ARSF) from the Xp22. 3 region. *Genomics* **1997**, *42* (2), 192-199.
146. Ferrante, P.; Messali, S.; Meroni, G.; Ballabio, A., Molecular and biochemical characterisation of a novel sulphatase gene: Arylsulfatase G (ARSG). *Eur. J. Hum. Genet.* **2002**, *10* (12), 813-818.
147. Wiegmann, E. M.; Westendorf, E.; Kalus, I.; Pringle, T. H.; Lübke, T.; Dierks, T., Arylsulfatase K, a novel lysosomal sulfatase. *J. Biol. Chem.* **2013**, *288* (42), 30019-30028.
148. Tomatsu, S.; Fukuda, S.; Masue, M.; Sukegawa, K.; Fukao, T.; Yamagishi, A.; Hori, T.; Iwata, H.; Ogawa, T.; Nakashima, Y., Morquio disease: Isolation, characterization and expression of full-length cDNA for human N-acetylgalactosamine-6-sulfate sulfatase. *Biochem. Biophys. Res. Commun.* **1991**, *181* (2), 677-683.
149. Scott, H. S.; Blanch, L.; Guo, X.-H.; Freeman, C.; Orsborn, A.; Baker, E.; Sutherland, G. R.; Morris, C. P.; Hopwood, J. J., Cloning of the sulphamidase gene and identification of mutations in Sanfilippo A syndrome. *Nat. Genet.* **1995**, *11* (4), 465-467.
150. Freeman, C.; Hopwood, J. J., Glucuronate-2-sulphatase activity in cultured human skin fibroblast homogenates. *Biochem. J* **1991**, *279* (2), 399-405.
151. Bielicki, J.; Hopwood, J. J.; Melville, L. E.; anson, S. D., Recombinant human sulphamidase: Expression, amplification, purification and characterization. *Biochem. J* **1998**, *329* (1), 145-150.
152. Morimoto-Tomita, M.; Uchimura, K.; Werb, Z.; Hemmerich, S.; Rosen, S. D., Cloning and characterization of two extracellular heparin-degrading endosulfatases in mice and humans. *J. Biol. Chem.* **2002**, *277* (51), 49175-49185.
153. Miki, Y.; Nakata, T.; Suzuki, T.; Darnel, A. D.; Moriya, T.; Kaneko, C.; Hidaka, K.; Shiotsu, Y.; Kusaka, H.; Sasano, H., Systemic distribution of steroid sulfatase and estrogen sulfotransferase in human adult and fetal tissues. *J. Clin. Endocrinol. Metab.* **2002**, *87* (12), 5760-5768.
154. Foster, P. A.; Chander, S. K.; Newman, S. P.; Woo, L. L.; Sutcliffe, O. B.; Bubert, C.; Zhou, D.; Chen, S.; Potter, B. V.; Reed, M. J., A new therapeutic strategy against hormone-dependent breast cancer: The preclinical development of a dual aromatase and sulfatase inhibitor. *Clin. Cancer Res.* **2008**, *14* (20), 6469-6477.
155. Hernandez-Guzman, F. G.; Higashiyama, T.; Pangborn, W.; Osawa, Y.; Ghosh, D., Structure of human estrone sulfatase suggests functional roles of membrane association. *J. Biol. Chem.* **2003**, *278* (25), 22989-22997.
156. Mostafa, Y. A.; Taylor, S. D., Steroid derivatives as inhibitors of steroid sulfatase. *J. Steroid Biochem. Mol. Biol.* **2013**, *137*, 183-198.
157. Pasqualini, J. R.; Chetrite, G.; Blacker, C.; Feinstein, M. C.; Delalonde, L.; Talbi, M.; Maloche, C., Concentrations of estrone, estradiol, and estrone sulfate and evaluation of sulfatase and aromatase activities in pre- and postmenopausal breast cancer patients. *J. Clin. Endocrinol. Metab.* **1996**, *81* (4), 1460-1464.
158. Ruder, H. J.; Loriaux, L.; Lipsett, M., Estrone sulfate: Production rate and metabolism in man. *J. Clin. Investig.* **1972**, *51* (4), 1020-1033.
159. Suzuki, M.; Ishida, H.; Shiotsu, Y.; Nakata, T.; Akinaga, S.; Takashima, S.; Utsumi, T.; Saeki, T.; Harada, N., Expression level of enzymes related to in situ estrogen synthesis and clinicopathological parameters in breast cancer patients. *J. Steroid Biochem. Mol. Biol.* **2009**, *113* (3-5), 195-201.
160. Utsumi, T.; Yoshimura, N.; Takeuchi, S.; Maruta, M.; Maeda, K.; Harada, N., Elevated steroid sulfatase expression in breast cancers. *J. Steroid Biochem. Mol. Biol.* **2000**, *73* (3-4), 141-145.
161. Suzuki, T.; Nakata, T.; Miki, Y.; Kaneko, C.; Moriya, T.; Ishida, T.; Akinaga, S.; Hirakawa, H.; Kimura, M.; Sasano, H., Estrogen sulfotransferase and steroid sulfatase in human breast carcinoma. *Cancer Res.* **2003**, *63* (11), 2762-2770.

162. Šmuc, T.; Pucelj, M. R.; Šinkovec, J.; Husen, B.; Thole, H.; Rižner, T. L., Expression analysis of the genes involved in estradiol and progesterone action in human ovarian endometriosis. *Gynecol. Endocrinol.* **2007**, *23* (2), 105-111.
163. Adamson, G. D.; Pasta, D. J., Endometriosis fertility index: The new, validated endometriosis staging system. *Fertil. Steril.* **2010**, *94* (5), 1609-1615.
164. Purohit, A.; Fusi, L.; Brosens, J.; Woo, L.; Potter, B.; Reed, M., Inhibition of steroid sulphatase activity in endometriotic implants by 667 COUMATE: A potential new therapy. *Hum. Reprod.* **2008**, *23* (2), 290-297.
165. Dassen, H.; Punyadeera, C.; Kamps, R.; Delvoux, B.; Van Langendonck, A.; Donnez, J.; Husen, B.; Thole, H.; Dunselman, G.; Groothuis, P., Estrogen metabolizing enzymes in endometrium and endometriosis. *Hum. Reprod.* **2007**, *22* (12), 3148-3158.
166. Colette, S.; Defrère, S.; Van Kerk, O.; Van Langendonck, A.; Dolmans, M. M.; Donnez, J., Differential expression of steroidogenic enzymes according to endometriosis type. *Fertil. Steril.* **2013**, *100* (6), 1642-1649.
167. Šmuc, T.; Ruprecht, R.; Šinkovec, J.; Adamski, J.; Rižner, T. L., Expression analysis of estrogen-metabolizing enzymes in human endometrial cancer. *Mol. Cell. Endocrinol.* **2006**, *248* (1), 114-117.
168. Utsunomiya, H.; Ito, K.; Suzuki, T.; Kitamura, T.; Kaneko, C.; Nakata, T.; Niikura, H.; Okamura, K.; Yaegashi, N.; Sasano, H., Steroid sulfatase and estrogen sulfotransferase in human endometrial carcinoma. *Clin. Cancer Res.* **2004**, *10* (17), 5850-5856.
169. Salah, M.; Abdelsamie, A. S.; Frotscher, M., First dual inhibitors of steroid sulfatase (STS) and 17 β -hydroxysteroid dehydrogenase type 1 (17 β -HSD1): Designed multiple ligands as novel potential therapeutics for estrogen-dependent diseases. *J. Med. Chem.* **2017**, *60* (9), 4086-4092.
170. Hoffmann, F.; Maser, E., Carbonyl reductases and pluripotent hydroxysteroid dehydrogenases of the short-chain dehydrogenase/reductase superfamily. *Drug Metab. Rev.* **2007**, *39* (1), 87-144.
171. Maser, E., Xenobiotic carbonyl reduction and physiological steroid oxidoreduction: the pluripotency of several hydroxysteroid dehydrogenases. *Biochem. Pharmacol.* **1995**, *49* (4), 421-440.
172. Matsunaga, T.; Shintani, S.; Hara, A., Multiplicity of mammalian reductases for xenobiotic carbonyl compounds. *Drug Metab. Pharmacokinet.* **2006**, *21* (1), 1-18.
173. Moeller, G.; Adamski, J., Integrated view on 17beta-hydroxysteroid dehydrogenases. *Mol. Cell. Endocrinol.* **2009**, *301* (1-2), 7-19.
174. Meier, M.; Möller, G.; Adamski, J., Perspectives in understanding the role of human 17 β -hydroxysteroid dehydrogenases in health and disease. *Ann. N.Y. Acad. Sci.* **2009**, *1155* (1), 15-24.
175. Luu-The, V., Analysis and characteristics of multiple types of human 17 β -hydroxysteroid dehydrogenase. *J. Steroid Biochem. Mol. Biol.* **2001**, *76* (1-5), 143-151.
176. Prehn, C.; Möller, G.; Adamski, J., Recent advances in 17beta-hydroxysteroid dehydrogenases. *J. Steroid Biochem. Mol. Biol.* **2009**, *114* (1), 72-77.
177. Penning, T. M.; Byrns, M. C., Steroid hormone transforming aldo-keto reductases and cancer. *Ann. N.Y. Acad. Sci.* **2009**, *1155*, 33-42.
178. Lukacik, P.; Kavanagh, K. L.; Oppermann, U., Structure and function of human 17 β -hydroxysteroid dehydrogenases. *Mol. Cell. Endocrinol.* **2006**, *248* (1-2), 61-71.
179. Kowalik, D. P., SDR and AKR enzymes as a target of rational inhibitor development and research on functions of new SDR members. Doctoral Dissertation, Technische Universität München, **2016**, 211 p.
180. Marchais-Oberwinkler, S.; Henn, C.; Möller, G.; Klein, T.; Negri, M.; Oster, A.; Spadaro, A.; Werth, R.; Wetzels, M.; Xu, K.; Frotscher, M.; Hartmann, R. W.; Adamski,

- J., 17 β -Hydroxysteroid dehydrogenases (17 β -HSDs) as therapeutic targets: Protein structures, functions, and recent progress in inhibitor development. *J. Steroid Biochem. Mol. Biol.* **2011**, *125* (1), 66-82.
181. Mindnich, R.; Möller, G.; Adamski, J., The role of 17 beta-hydroxysteroid dehydrogenases. *Mol. Cell. Endocrinol.* **2004**, *218* (1-2), 7-20.
182. Vihko, P.; Herrala, A.; Härkönen, P.; Isomaa, V.; Kaija, H.; Kurkela, R.; Pulkka, A., Control of cell proliferation by steroids: The role of 17HSDs. *Mol. Cell. Endocrinol.* **2006**, *248* (1-2), 141-148.
183. Vihko, P.; Herrala, A.; Härkönen, P.; Isomaa, V.; Kaija, H.; Kurkela, R.; Li, Y.; Patrikainen, L.; Pulkka, A.; Soronen, P., Enzymes as modulators in malignant transformation. *J. Steroid Biochem. Mol. Biol.* **2005**, *93* (2-5), 277-283.
184. Poutanen, M.; Miettinen, M.; Vihko, R., Differential estrogen substrate specificities for transiently expressed human placental 17 beta-hydroxysteroid dehydrogenase and an endogenous enzyme expressed in cultured COS-m6 cells. *Endocrinology* **1993**, *133* (6), 2639-2644.
185. Geissler, W. M.; Davis, D. L.; Wu, L.; Bradshaw, K. D.; Patel, S.; Mendonca, B. B.; Elliston, K. O.; Wilson, J. D.; Russell, D. W.; Andersson, S., Male pseudohermaphroditism caused by mutations of testicular 17 β -hydroxysteroid dehydrogenase 3. *Nat. Genet.* **1994**, *7* (1), 34-39.
186. Rasiah, K. K.; Gardiner-Garden, M.; Padilla, E. J.; Möller, G.; Kench, J. G.; Alles, M. C.; Eggleton, S. A.; Stricker, P. D.; Adamski, J.; Sutherland, R. L., HSD17B4 overexpression, an independent biomarker of poor patient outcome in prostate cancer. *Mol. Cell. Endocrinol.* **2009**, *301* (1-2), 89-96.
187. Stanbrough, M.; Bubley, G. J.; Ross, K.; Golub, T. R.; Rubin, M. A.; Penning, T. M.; Febbo, P. G.; Balk, S. P., Increased expression of genes converting adrenal androgens to testosterone in androgen-independent prostate cancer. *Cancer Res.* **2006**, *66* (5), 2815-2825.
188. Jin, Y.; Penning, T. M., Aldo-keto reductases and bioactivation/detoxication. *Annu. Rev. Pharmacol. Toxicol.* **2007**, *47*, 263-292.
189. Penning, T. M.; Burczynski, M. E.; Jez, J. M.; Hung, C.-F.; Lin, H.-K.; Ma, H.; Moore, M.; Palackal, N.; Ratnam, K., Human 3 α -hydroxysteroid dehydrogenase isoforms (AKR1C1–AKR1C4) of the aldo-keto reductase superfamily: Functional plasticity and tissue distribution reveals roles in the inactivation and formation of male and female sex hormones. *Biochem. J.* **2000**, *351* (1), 67-77.
190. Biswas, M. G.; Russell, D. W., Expression cloning and characterization of oxidative 17 β - and 3 α -hydroxysteroid dehydrogenases from rat and human prostate. *J. Biol. Chem.* **1997**, *272* (25), 15959-15966.
191. Luu-The, V.; Tremblay, P.; Labrie, F., Characterization of type 12 17 β -hydroxysteroid dehydrogenase, an isoform of type 3 17 β -hydroxysteroid dehydrogenase responsible for estradiol formation in women. *Mol. Endocrinol.* **2006**, *20* (2), 437-443.
192. Haynes, B. P.; Straume, A. H.; Geisler, J.; A'Hern, R.; Helle, H.; Smith, I. E.; Lønning, P. E.; Dowsett, M., Intratumoral estrogen disposition in breast cancer. *Clin. Cancer Res.* **2010**, *16* (6), 1790-1801.
193. Marijanovic, Z.; Laubner, D.; Moller, G.; Gege, C.; Husen, B.; Adamski, J.; Breitling, R., Closing the gap: identification of human 3-ketosteroid reductase, the last unknown enzyme of mammalian cholesterol biosynthesis. *Mol. Endocrinol.* **2003**, *17* (9), 1715-1725.
194. Krazeisen, A.; Breitling, R.; Imai, K.; Fritz, S.; Möller, G.; Adamski, J., Determination of cDNA, gene structure and chromosomal localization of the novel human 17 β -hydroxysteroid dehydrogenase type 7. *FEBS Lett.* **1999**, *460* (2), 373-379.

195. Moeller, G.; Adamski, J., Multifunctionality of human 17 β -hydroxysteroid dehydrogenases. *Mol. Cell. Endocrinol.* **2006**, *248* (1-2), 47-55.
196. Fomitcheva, J.; Baker, M. E.; Anderson, E.; Lee, G. Y.; Aziz, N., Characterization of Ke 6, a new 17 β -hydroxysteroid dehydrogenase, and its expression in gonadal tissues. *J. Biol. Chem.* **1998**, *273* (35), 22664-22671.
197. Su, J.; Lin, M.; Napoli, J. L., Complementary deoxyribonucleic acid cloning and enzymatic characterization of a novel 17 β /3 α -hydroxysteroid/retinoid short chain dehydrogenase/reductase. *Endocrinology* **1999**, *140* (11), 5275-5284.
198. He, X.-Y.; Schulz, H.; Yang, S.-Y., A human brain L-3-hydroxyacyl-coenzyme A dehydrogenase is identical to an amyloid β -peptide-binding protein involved in Alzheimer's disease. *J. Biol. Chem.* **1998**, *273* (17), 10741-10746.
199. He, X. Y.; Merz, G.; Yang, Y. Z.; Mehta, P.; Schulz, H.; Yang, S. Y., Characterization and localization of human type10 17 β -hydroxysteroid dehydrogenase. *Eur. J. Biochem.* **2001**, *268* (18), 4899-4907.
200. Vinklarova, L.; Schmidt, M.; Benek, O.; Kuca, K.; Gunn-Moore, F.; Musilek, K., Friend or enemy? Review of 17 β -HSD10 and its role in human health or disease. *J. Neurochem.* **2020**, *155* (3), 231-249.
201. Brereton, P.; Suzuki, T.; Sasano, H.; Li, K.; Duarte, C.; Obeyesekere, V.; Haeseleer, F.; Palczewski, K.; Smith, I.; Komesaroff, P., Pan1b (17 β HSD11)-enzymatic activity and distribution in the lung. *Mol. Cell. Endocrinol.* **2001**, *171* (1-2), 111-117.
202. Chai, Z.; Brereton, P.; Suzuki, T.; Sasano, H.; Obeyesekere, V.; Escher, G.; Saffery, R.; Fuller, P.; Enriquez, C.; Krozowski, Z., 17 β -hydroxysteroid dehydrogenase type XI localizes to human steroidogenic cells. *Endocrinology* **2003**, *144* (5), 2084-2091.
203. Blanchard, P.G., Differential androgen and estrogen substrates specificity in the mouse and primates type 12 17 β -hydroxysteroid dehydrogenase. *J. Endocrinol.* **2007**, *194* (2), 449-455.
204. Moon, Y.-A.; Horton, J. D., Identification of two mammalian reductases involved in the two-carbon fatty acyl elongation cascade. *J. Biol. Chem.* **2003**, *278* (9), 7335-7343.
205. Horiguchi, Y.; Araki, M.; Motojima, K., 17 β -Hydroxysteroid dehydrogenase type 13 is a liver-specific lipid droplet-associated protein. *Biochem. Biophys. Res. Commun.* **2008**, *370* (2), 235-238.
206. Sivik, T.; Vikingsson, S.; Gréen, H.; Jansson, A., Expression patterns of 17 β -hydroxysteroid dehydrogenase 14 in human tissues. *Horm. Metab. Res.* **2012**, *44* (13), 949-956.
207. Sivik, T.; Gunnarsson, C.; Fornander, T.; Nordenskjöld, B.; Skoog, L.; Stål, O.; Jansson, A., 17 β -Hydroxysteroid dehydrogenase type 14 is a predictive marker for tamoxifen response in oestrogen receptor positive breast cancer. *PLoS One* **2012**, *7* (7), e40568.
208. Lukacik, P.; Keller, B.; Bunkoczi, G.; Kavanagh, K.; Hwa Lee, W.; Adamski, J.; Oppermann, U., Structural and biochemical characterization of human orphan DHRS10 reveals a novel cytosolic enzyme with steroid dehydrogenase activity. *Biochem. J.* **2007**, *402* (3), 419-427.
209. Luu-The, V.; Bélanger, A.; Labrie, F., Androgen biosynthetic pathways in the human prostate. *Best Pract. Res. Clin. Endocrinol. Metab.* **2008**, *22* (2), 207-221.
210. Peltoketo, H.; Isomaa, V.; Mäentausta, O.; Vihko, R., Complete amino acid sequence of human placental 17 β -hydroxysteroid dehydrogenase deduced from cDNA. *FEBS Lett.* **1988**, *239* (1), 73-77.
211. Zhu, D.-W.; Lee, X.; Breton, R.; Ghosh, D.; Pangborn, W.; Duax, W.; Lin, S.-X., Crystallization and preliminary X-ray diffraction analysis of the complex of human placental 17 β -hydroxysteroid dehydrogenase with NADP⁺. *J. Mol. Biol.* **1993**, *234* (1), 242-244.

212. Ghosh, D.; Pletnev, V. Z.; Zhu, D.-W.; Wawrzak, Z.; Duax, W. L.; Pangborn, W.; Labrie, F.; Lin, S.-X., Structure of human estrogenic 17 β -hydroxysteroid dehydrogenase at 2.20 Å resolution. *Structure* **1995**, *3* (5), 503-513.
213. Berman, H. M.; Westbrook, J.; Feng, Z.; Gilliland, G.; Bhat, T. N.; Weissig, H.; Shindyalov, I. N.; Bourne, P. E., The protein data bank. *Nucleic Acids Res.* **2000**, *28* (1), 235-242.
214. Spadaro, A.; Negri, M.; Marchais-Oberwinkler, S.; Bey, E.; Frotscher, M., Hydroxybenzothiazoles as new nonsteroidal inhibitors of 17 β -Hydroxysteroid dehydrogenase type 1 (17 β -HSD1). *PLoS One* **2012**, *7* (1), e29252.
215. Mazza, C.; Breton, R.; Housset, D.; Fontecilla-Camps, J. C., Unusual charge stabilization of NADP⁺ in 17 β -hydroxysteroid dehydrogenase. *J. Biol. Chem.* **1998**, *273* (14), 8145-8152.
216. Breton, R.; Housset, D.; Mazza, C.; Fontecilla-Camps, J. C., The structure of a complex of human 17 β -hydroxysteroid dehydrogenase with estradiol and NADP⁺ identifies two principal targets for the design of inhibitors. *Structure* **1996**, *4* (8), 905-915.
217. Azzi, A.; Rehse, P. H.; Zhu, D. W.; Campbell, R. L.; Labrie, F.; Lin, S.-X., Crystal structure of human estrogenic 17 β -hydroxysteroid dehydrogenase complexed with 17 β -estradiol. *Nat. Struct. Biol.* **1996**, *3* (8), 665-668.
218. Li, T.; Stephen, P.; Zhu, D. W.; Shi, R.; Lin, S. X., Crystal structures of human 17 β -hydroxysteroid dehydrogenase type 1 complexed with estrone and NADP⁺ reveal the mechanism of substrate inhibition. *FEBS J.* **2019**, *286* (11), 2155-2166.
219. Han, Q.; Campbell, R. L.; Gangloff, A.; Huang, Y.-W.; Lin, S.-X., dehydroepiandrosterone and dihydrotestosterone recognition by human estrogenic 17 β -hydroxysteroid dehydrogenase c-18/c-19 steroid discrimination and enzyme-induced strain. *J. Biol. Chem.* **2000**, *275* (2), 1105-1111.
220. Gangloff, A.; Shi, R.; Nahoum, V.; Lin, S. X., Pseudo-symmetry of C19-steroids, alternative binding orientations and multispecificity in human estrogenic 17 β -hydroxysteroid dehydrogenase. *FASEB J.* **2003**, *17* (2), 274-276.
221. Shi, R.; Lin, S.-X., Cofactor hydrogen bonding onto the protein main chain is conserved in the short chain dehydrogenase/reductase family and contributes to nicotinamide orientation. *J. Biol. Chem.* **2004**, *279* (16), 16778-16785.
222. Sawicki, M. W.; Erman, M.; Puranen, T.; Vihko, P.; Ghosh, D., Structure of the ternary complex of human 17 β -hydroxysteroid dehydrogenase type 1 with 3-hydroxyestra-1, 3, 5, 7-tetraen-17-one (equilin) and NADP⁺. *Proc. Natl. Acad. Sci.* **1999**, *96* (3), 840-845.
223. Qiu, W.; Campbell, R. L.; Gangloff, A.; Dupuis, P.; Boivin, R. P.; Tremblay, M. R.; Poirier, D.; Lin, S.-X., A concerted, rational design of type 1 17 β -hydroxysteroid dehydrogenase inhibitors: estradiol-adenosine hybrids with high affinity. *FASEB J.* **2002**, *16* (13), 1-26.
224. Nahoum, V.; Gangloff, A.; Shi, R.; Lin, S.-X., How estrogen-specific proteins discriminate estrogens from androgens: A common steroid-binding site architecture. *FASEB J.* **2003**, *17* (10), 1334-1336.
225. Day, J. M.; Tutill, H. J.; Purohit, A.; Reed, M. J., Design and validation of specific inhibitors of 17 β -hydroxysteroid dehydrogenases for therapeutic application in breast and prostate cancer, and in endometriosis. *Endocr. Relat. Cancer* **2008**, *15* (3), 665-692.
226. The, V. L.; Labrie, C.; Zhao, H. F.; Couët, J.; Lachance, Y.; Simard, J.; Leblanc, G.; Côté, J.; Bérubé, D.; Gagné, R., Characterization of cDNAs for human estradiol 17 β -dehydrogenase and assignment of the gene to chromosome 17: Evidence of two mRNA species with distinct 5'-termini in human placenta. *Mol. Endocrinol.* **1989**, *3* (8), 1301-1309.

227. Dumont, M.; Luu-The, V.; De Launoit, Y.; Labrie, F., Expression of human 17 β -hydroxysteroid dehydrogenase in mammalian cells. *J. Steroid Biochem. Mol. Biol.* **1992**, *41* (3), 605-608.
228. Lin, S.-X.; Chen, J.; Mazumdar, M.; Poirier, D.; Wang, C.; Azzi, A.; Zhou, M., Molecular therapy of breast cancer: progress and future directions. *Nat. Rev. Endocrinol.* **2010**, *6* (9), 485-493.
229. Aka, J. A.; Mazumdar, M.; Chen, C.-Q.; Poirier, D.; Lin, S.-X., 17 β -hydroxysteroid dehydrogenase Type 1 stimulates breast cancer by dihydrotestosterone inactivation in addition to estradiol production. *Mol. Endocrinol.* **2010**, *24* (4), 832-845.
230. Hanamura, T.; Niwa, T.; Gohno, T.; Kurosumi, M.; Takei, H.; Yamaguchi, Y.; Ito, K.-i.; Hayashi, S.-I., Possible role of the aromatase-independent steroid metabolism pathways in hormone responsive primary breast cancers. *Breast Cancer Res. Treat.* **2014**, *143* (1), 69-80.
231. Blomquist, C. H.; Lindemann, N. J.; Hakanson, E. Y., Steroid modulation of 17 beta-hydroxysteroid oxidoreductase activities in human placental villi in vitro. *J. Clin. Endocrinol. Metab.* **1987**, *65* (4), 647-652.
232. Luu-The, V.; Zhang, Y.; Poirier, D.; Labrie, F., Characteristics of human types 1, 2 and 3 17 β -hydroxysteroid dehydrogenase activities: Oxidation/reduction and inhibition. *J. Steroid Biochem. Mol. Biol.* **1995**, *55* (5-6), 581-587.
233. Miyoshi, Y.; Ando, A.; Shiba, E.; Taguchi, T.; Tamaki, Y.; Noguchi, S., Involvement of up-regulation of 17 β -hydroxysteroid dehydrogenase type 1 in maintenance of intratumoral high estradiol levels in postmenopausal breast cancers. *Int. J. Cancer* **2001**, *94* (5), 685-689.
234. Mori, T.; Ito, F.; Matsushima, H.; Takaoka, O.; Koshiba, A.; Tanaka, Y.; Kusuki, I.; Kitawaki, J., Dienogest reduces HSD17b1 expression and activity in endometriosis. *J. Endocrinol.* **2015**, *225* (2), 69-76.
235. Oduwole, O. O.; Li, Y.; Isomaa, V. V.; Mäntyniemi, A.; Pulkka, A. E.; Soini, Y.; Vihko, P. T., 17 β -Hydroxysteroid dehydrogenase type 1 is an independent prognostic marker in breast cancer. *Cancer Res.* **2004**, *64* (20), 7604-7609.
236. Cornel, K. M.; Kruitwagen, R. F.; Delvoux, B.; Visconti, L.; Van de Vijver, K. K.; Day, J. M.; Van Gorp, T.; Hermans, R. J.; Dunselman, G. A.; Romano, A., Overexpression of 17 β -hydroxysteroid dehydrogenase type 1 increases the exposure of endometrial cancer to 17 β -estradiol. *J. Clin. Endocrinol. Metab.* **2012**, *97* (4), E591-E601.
237. Konings, G. F.; Cornel, K. M.; Xanthoulea, S.; Delvoux, B.; Skowron, M. A.; Kooreman, L.; Koskimies, P.; Krakstad, C.; Salvesen, H. B.; van Kuijk, K., Blocking 17 β -hydroxysteroid dehydrogenase type 1 in endometrial cancer: a potential novel endocrine therapeutic approach. *J. Pathol.* **2018**, *244* (2), 203-214.
238. Blomquist, C. H.; Bonenfant, M.; McGinley, D. M.; Posalaky, Z.; Lakatua, D. J.; Tuli-Puri, S.; Bealka, D. G.; Tremblay, Y., Androgenic and estrogenic 17 β -hydroxysteroid dehydrogenase/17-ketosteroid reductase in human ovarian epithelial tumors: Evidence for the type 1, 2 and 5 isoforms. *J. Steroid Biochem. Mol. Biol.* **2002**, *81* (4), 343-351.
239. Shah, R.; Singh, J.; Singh, D.; Jaggi, A. S.; Singh, N., Sulfatase inhibitors for recidivist breast cancer treatment: A chemical review. *Eur. J. Med. Chem.* **2016**, *114*, 170-190.
240. Foster, P. A.; Reed, M. J.; Purohit, A., Recent developments of steroid sulfatase inhibitors as anti-cancer agents. *Anticancer Agents Med. Chem.* **2008**, *8* (7), 732-738.
241. Reed, M. J.; Purohit, A.; Woo, L. W.; Newman, S. P.; Potter, B. V., Steroid sulfatase: molecular biology, regulation, and inhibition. *Endocr. Rev.* **2005**, *26* (2), 171-202.
242. Purohit, A.; Foster, P. A., Steroid sulfatase inhibitors for estrogen- and androgen-dependent cancers. *J. Endocrinol.* **2012**, *212* (2), 99-110.
243. Maltais, R.; Poirier, D., Steroid sulfatase inhibitors: A review covering the promising 2000–2010 decade. *Steroids* **2011**, *76* (10-11), 929-948.

244. Woo, L. L.; Purohit, A.; Potter, B. V., Development of steroid sulfatase inhibitors. *Mol. Cell. Endocrinol.* **2011**, *340* (2), 175-185.
245. Geisler, J.; Sasano, H.; Chen, S.; Purohit, A., Steroid sulfatase inhibitors: promising new tools for breast cancer therapy? *J. Steroid Biochem. Mol. Biol.* **2011**, *125* (1-2), 39-45.
246. Daško, M.; Demkowicz, S.; Biernacki, K.; Ciupak, O.; Kozak, W.; Masłyk, M.; Rachon, J., Recent progress in the development of steroid sulphatase inhibitors – examples of the novel and most promising compounds from the last decade. *J. Enzyme Inhib. Med. Chem.* **2020**, *35* (1), 1163-1184.
247. Foster, P. A., Steroid sulphatase and its inhibitors: Past, present, and future. *Molecules* **2021**, *26* (10), 2852.
248. Anbar, H. S.; Isa, Z.; Elounais, J. J.; Jameel, M. A.; Hussam, J.; Samer, A. M.; Jawad, A. F.; El-Gamal, M. I., Steroid sulfatase inhibitors: the current landscape. *Expert Opin. Ther. Pat.* **2021**, *31*, 453 - 472.
249. Nussbaumer, P.; Billich, A., Steroid sulfatase inhibitors. *Med. Res. Rev.* **2004**, *24* (4), 529-576.
250. Purohit, A.; Williams, G. J.; Howarth, N. M.; Potter, B. V.; Reed, M. J., Inactivation of steroid sulfatase by an active site-directed inhibitor, estrone-3-O-sulfamate. *Biochemistry* **1995**, *34* (36), 11508-11514.
251. Howarth, N. M.; Purohit, A.; Reed, M. J.; Potter, B. V. L., Estrone sulfamates: potent inhibitors of estrone sulfatase with therapeutic potential. *J. Med. Chem.* **1994**, *37* (2), 219-221.
252. Purohit, A.; Williams, G. J.; Roberts, C. J.; Potter, B. V. L.; Reed, M. J., In vivo inhibition of oestrone sulphatase and dehydroepiandrosterone sulphatase by oestrone-3-O-sulphamate. *Int. J. Cancer* **1995**, *63* (1), 106-111.
253. Elger, W.; Schwarz, S.; Hedden, A.; Reddersen, G.; Schneider, B., Sulfamates of various estrogens are prodrugs with increased systemic and reduced hepatic estrogenicity at oral application. *J. Steroid Biochem. Mol. Biol.* **1995**, *55* (3-4), 395-403.
254. Woo, L. L.; Howarth, N. M.; Purohit, A.; Hejaz, H. A.; Reed, M. J.; Potter, B. V., Steroidal and nonsteroidal sulfamates as potent inhibitors of steroid sulfatase. *J. Med. Chem.* **1998**, *41* (7), 1068-1083.
255. Woo, L. L.; Purohit, A.; Malini, B.; Reed, M. J.; Potter, B. V., Potent active site-directed inhibition of steroid sulphatase by tricyclic coumarin-based sulphamates. *Chem. Biol.* **2000**, *7* (10), 773-791.
256. Nussbaumer, P.; Lehr, P.; Billich, A., 2-Substituted 4-(thio) chromenone 6-O-sulfamates: potent inhibitors of human steroid sulfatase. *J. Med. Chem.* **2002**, *45* (19), 4310-4320.
257. Stanway, S. J.; Purohit, A.; Woo, L. L.; Sufi, S.; Vigushin, D.; Ward, R.; Wilson, R. H.; Stanczyk, F. Z.; Dobbs, N.; Kulinskaya, E., Phase I study of STX 64 (667 Coumate) in breast cancer patients: the first study of a steroid sulfatase inhibitor. *Clin. Cancer Res.* **2006**, *12* (5), 1585-1592.
258. Poirier, D., Inhibitors of 17 β -hydroxysteroid dehydrogenases. *Curr. Med. Chem.* **2003**, *10* (6), 453-477.
259. Poirier, D., 17 β -Hydroxysteroid dehydrogenase inhibitors: A patent review. *Expert Opin. Ther. Pat.* **2010**, *20* (9), 1123-1145.
260. Deluca, D.; Krazeisen, A.; Breitling, R.; Prehn, C.; Möller, G.; Adamski, J., Inhibition of 17 β -hydroxysteroid dehydrogenases by phytoestrogens: Comparison with other steroid metabolizing enzymes. *J. Steroid Biochem. Mol. Biol.* **2005**, *93* (2), 285-292.
261. Salah, M.; Abdelsamie, A. S.; Frotscher, M., Inhibitors of 17 β -hydroxysteroid dehydrogenase type 1, 2 and 14: Structures, biological activities and future challenges. *Mol. Cell. Endocrinol.* **2019**, *489*, 66-81.
262. Gobec, S.; Brozic, P.; Rizner, T., Inhibitors of 17 β -hydroxysteroid dehydrogenase type 1. *Curr. Med. Chem.* **2008**, *15* (2), 137-150.

263. Day, J. M.; Tutill, H. J.; Purohit, A., 17 β -hydroxysteroid dehydrogenase inhibitors. *Minerva Endocrinol.* **2010**, *35* (2), 87-108.
264. Vicker, N.; Lawrence, H. R.; Allan, G. M.; Bubert, C.; Smith, A.; Tutill, H. J.; Purohit, A.; Day, J. M.; Mahon, M. F.; Reed, M. J., Focused libraries of 16-substituted estrone derivatives and modified E-ring steroids: Inhibitors of 17 β -hydroxysteroid dehydrogenase type 1. *ChemMedChem* **2006**, *1* (4), 464-481.
265. Allan, G. M.; Bubert, C.; Vicker, N.; Smith, A.; Tutill, H. J.; Purohit, A.; Reed, M. J.; Potter, B. V., Novel, potent inhibitors of 17 β -hydroxysteroid dehydrogenase type 1. *Mol. Cell. Endocrinol.* **2006**, *248* (1-2), 204-207.
266. Allan, G. M.; Lawrence, H. R.; Cornet, J.; Bubert, C.; Fischer, D. S.; Vicker, N.; Smith, A.; Tutill, H. J.; Purohit, A.; Day, J. M., Modification of estrone at the 6, 16, and 17 positions: novel potent inhibitors of 17 β -hydroxysteroid dehydrogenase type 1. *J. Med. Chem.* **2006**, *49* (4), 1325-1345.
267. Cushman, M.; He, H.-M.; Katzenellenbogen, J. A.; Lin, C. M.; Hamel, E., Synthesis, antitubulin and antimetabolic activity, and cytotoxicity of analogs of 2-methoxyestradiol, an endogenous mammalian metabolite of estradiol that inhibits tubulin polymerization by binding to the colchicine binding site. *J. Med. Chem.* **1995**, *38* (12), 2041-2049.
268. Leese, M. P.; Leblond, B.; Newman, S. P.; Purohit, A.; Reed, M. J.; Potter, B. V., Anti-cancer activities of novel D-ring modified 2-substituted estrogen-3-O-sulfamates. *J. Steroid Biochem. Mol. Biol.* **2005**, *94* (1-3), 239-251.
269. Messinger, J.; Husen, B.; Koskimies, P.; Hirvelä, L.; Kallio, L.; Saarenketo, P.; Thole, H., Estrone C15 derivatives-A new class of 17 β -hydroxysteroid dehydrogenase type 1 inhibitors. *Mol. Cell. Endocrinol.* **2009**, *301* (1-2), 216-224.
270. Messinger, J.; Schoen, U.; Thole, H.H.; Husen, B.; Koskimies, P.; nee Pirkkala, L. K., Therapeutically active triazoles and their use. U.S. Patent 8,080,540: **2011**. Abbott Products GmbH
271. Messinger, J.; Schoen, U.; Thole, H.H.; Husen, B.; Koskimies, P.; Unkila, M., Substituted estratriene derivatives as 17BETA HSD inhibitors. U.S. Patent 8,288,367: **2012**. Solvay Pharmaceuticals GmbH
272. Sam, K.-M.; Boivin, R.; Tremblay, M.; Auger, S.; Poirier, D., C16 and C17 derivatives of estradiol as inhibitors of 17 beta-hydroxysteroid dehydrogenase type 1: Chemical synthesis and structure-activity relationships. *Drug Des. Discov.* **1998**, *15* (3), 157-180.
273. Rouillard, F.; Lefebvre, J.; Fournier, M.-A.; Poirier, D., Chemical synthesis, 17 β -hydroxysteroid dehydrogenase type 1 inhibitory activity and assessment of in vitro and in vivo estrogenic activities of estradiol derivatives. *Open Enzym. Inhib. J.* **2008**, *1*, 61-71.
274. Pelletier, J. D.; Poirier, D., Synthesis and evaluation of estradiol derivatives with 16 α -(bromoalkylamide), 16 α -(bromoalkyl) or 16 α -(bromoalkynyl) side chain as inhibitors of 17 β -hydroxysteroid dehydrogenase type 1 without estrogenic activity. *Biorg. Med. Chem.* **1996**, *4* (10), 1617-1628.
275. Allan, G. M.; Vicker, N.; Lawrence, H. R.; Tutill, H. J.; Day, J. M.; Huchet, M.; Ferrandis, E.; Reed, M. J.; Purohit, A.; Potter, B. V., Novel inhibitors of 17 β -hydroxysteroid dehydrogenase type 1: Templates for design. *Biorg. Med. Chem.* **2008**, *16* (8), 4438-4456.
276. Messinger, J.; Hirvelä, L.; Husen, B.; Kangas, L.; Koskimies, P.; Pentikäinen, O.; Saarenketo, P.; Thole, H., New inhibitors of 17 β -hydroxysteroid dehydrogenase type 1. *Mol. Cell. Endocrinol.* **2006**, *248* (1-2), 192-198.
277. Karkola, S.; Alho-Richmond, S.; Wahala, K., Pharmacophore modelling of 17 β -HSD1 enzyme based on active inhibitors and enzyme structure. *Mol. Cell. Endocrinol.* **2009**, *301* (1-2), 225-228.
278. Lilienkampf, A.; Karkola, S.; Alho-Richmond, S.; Koskimies, P.; Johansson, N.; Huhtinen, K.; Vihko, K.; Wähälä, K., Synthesis and biological evaluation of 17 β -

- hydroxysteroid dehydrogenase type 1 (17 β -HSD1) inhibitors based on a Thieno[2,3- d]pyrimidin-4(3 H)-one core. *J. Med. Chem.* **2009**, *52*, 6660-6671.
279. Bey, E.; Marchais-Oberwinkler, S.; Kruchten, P.; Frotscher, M.; Werth, R.; Oster, A.; Algül, O.; Neugebauer, A.; Hartmann, R. W., Design, synthesis and biological evaluation of bis(hydroxyphenyl) azoles as potent and selective non-steroidal inhibitors of 17 β -hydroxysteroid dehydrogenase type 1 (17 β -HSD1) for the treatment of estrogen-dependent diseases. *Biorg. Med. Chem.* **2008**, *16* (12), 6423-6435.
280. Bey, E.; Marchais-Oberwinkler, S.; Werth, R.; Negri, M.; Al-Soud, Y. A.; Kruchten, P.; Oster, A.; Frotscher, M.; Birk, B.; Hartmann, R. W., Design, synthesis, biological evaluation and pharmacokinetics of bis(hydroxyphenyl) substituted azoles, thiophenes, benzenes, and aza-benzenes as potent and selective nonsteroidal inhibitors of 17 β -hydroxysteroid dehydrogenase type 1 (17 β -HSD1). *J. Med. Chem.* **2008**, *51* (21), 6725-6739.
281. Al-Soud, Y. A.; Bey, E.; Oster, A.; Marchais-Oberwinkler, S.; Werth, R.; Kruchten, P.; Frotscher, M.; Hartmann, R. W., The role of the heterocycle in bis (hydroxyphenyl) triazoles for inhibition of 17 β -hydroxysteroid dehydrogenase (17 β -HSD) type 1 and type 2. *Mol. Cell. Endocrinol.* **2009**, *301* (1-2), 212-215.
282. Bey, E.; Marchais-Oberwinkler, S.; Negri, M.; Kruchten, P.; Oster, A.; Klein, T.; Spadaro, A.; Werth, R.; Frotscher, M.; Birk, B.; Hartmann, R. W., New insights into the SAR and binding modes of Bis(hydroxyphenyl)thiophenes and -benzenes: Influence of additional substituents on 17 β -Hydroxysteroid dehydrogenase type 1 (17 β -HSD1) inhibitory activity and selectivity. *J. Med. Chem.* **2009**, *52* (21), 6724-6743.
283. Marchais-Oberwinkler, S.; Frotscher, M.; Ziegler, E.; Werth, R.; Kruchten, P.; Messinger, J.; Thole, H.; Hartmann, R. W., Structure-activity study in the class of 6-(3'-hydroxyphenyl)naphthalenes leading to an optimization of a pharmacophore model for 17 β -hydroxysteroid dehydrogenase type 1 (17 β -HSD1) inhibitors. *Mol. Cell. Endocrinol.* **2009**, *301* (1), 205-211.
284. Marchais-Oberwinkler, S.; Kruchten, P.; Frotscher, M.; Ziegler, E.; Neugebauer, A.; Bhoga, U.; Bey, E.; Müller-Vieira, U.; Messinger, J.; Thole, H.; Hartmann, R. W., Substituted 6-Phenyl-2-naphthols. Potent and selective nonsteroidal inhibitors of 17 β -hydroxysteroid dehydrogenase Type 1 (17 β -HSD1): Design, synthesis, biological evaluation, and pharmacokinetics. *J. Med. Chem.* **2008**, *51* (15), 4685-4698.
285. Frotscher, M.; Ziegler, E.; Marchais-Oberwinkler, S.; Kruchten, P.; Neugebauer, A.; Fetzer, L.; Scherer, C.; Müller-Vieira, U.; Messinger, J.; Thole, H.; Hartmann, R. W., Design, synthesis, and biological evaluation of (hydroxyphenyl)naphthalene and -quinoline derivatives: potent and selective nonsteroidal inhibitors of 17beta-hydroxysteroid dehydrogenase type 1 (17beta-HSD1) for the treatment of estrogen-dependent diseases. *J. Med. Chem.* **2008**, *51* (7), 2158-2169.
286. Oster, A.; Hinsberger, S.; Werth, R.; Marchais-Oberwinkler, S.; Frotscher, M.; Hartmann, R. W., Bicyclic substituted hydroxyphenylmethanones as novel inhibitors of 17 β -Hydroxysteroid dehydrogenase Type 1 (17 β -HSD1) for the treatment of estrogen-dependent diseases. *J. Med. Chem.* **2010**, *53* (22), 8176-8186.
287. Abdelsamie, A. S.; Bey, E.; Gargano, E. M.; van Koppen, C. J.; Empting, M.; Frotscher, M., Towards the evaluation in an animal disease model: Fluorinated 17 β -HSD1 inhibitors showing strong activity towards both the human and the rat enzyme. *Eur. J. Med. Chem.* **2015**, *103*, 56-68.
288. Abdelsamie, A. S.; van Koppen, C. J.; Bey, E.; Salah, M.; Börger, C.; Siebenbürger, L.; Laschke, M. W.; Menger, M. D.; Frotscher, M., Treatment of estrogen-dependent diseases: Design, synthesis and profiling of a selective 17 β -HSD1 inhibitor with subnanomolar IC₅₀ for a proof-of-principle study. *Eur. J. Med. Chem.* **2017**, *127*, 944-957.

289. Delvoux, B.; D'Hooghe, T.; Kyama, C.; Koskimies, P.; Hermans, R. J.; Dunselman, G. A.; Romano, A., Inhibition of type 1 17β -hydroxysteroid dehydrogenase impairs the synthesis of 17β -estradiol in endometriosis lesions. *J. Clin. Endocrinol. Metab.* **2014**, *99* (1), 276-284.
290. Barra, F.; Grandi, G.; Tantari, M.; Scala, C.; Facchinetti, F.; Ferrero, S., A comprehensive review of hormonal and biological therapies for endometriosis: Latest developments. *Expert Opin. Biol. Ther.* **2019**, *19* (4), 343-360.
291. Barra, F.; Romano, A.; Grandi, G.; Facchinetti, F.; Ferrero, S., Future directions in endometriosis treatment: discovery and development of novel inhibitors of estrogen biosynthesis. *Expert Opin. Investig. Drugs* **2019**, *28* (6), 501-504.
292. Maltais, R.; Trottier, A.; Roy, J.; Ayan, D.; Bertrand, N.; Poirier, D., Pharmacokinetic profile of PBRM in rodents, a first selective covalent inhibitor of 17β -HSD1 for breast cancer and endometriosis treatments. *J. Steroid Biochem. Mol. Biol.* **2018**, *178*, 167-176.
293. Poirier, D.; Roy, J.; Maltais, R., A Targeted-covalent inhibitor of 17β -HSD1 blocks two estrogen-biosynthesis pathways: In vitro (metabolism) and in vivo (xenograft) studies in T-47D breast cancer models. *Cancers (Basel)* **2021**, *13* (8), 1841.
294. Morphy, R.; Rankovic, Z., Designed multiple ligands. An emerging drug discovery paradigm. *J. Med. Chem.* **2005**, *48* (21), 6523-6543.
295. Espinoza-Fonseca, L. M., The benefits of the multi-target approach in drug design and discovery. *Biorg. Med. Chem.* **2006**, *14* (4), 896-897.
296. Baraldi, P. G.; Preti, D.; Fruttarolo, F.; Tabrizi, M. A.; Romagnoli, R., Hybrid molecules between distamycin A and active moieties of antitumor agents. *Biorg. Med. Chem.* **2007**, *15* (1), 17-35.
297. Chen, L.; Wilson, D.; Jayaram, H. N.; Pankiewicz, K. W., Dual inhibitors of inosine monophosphate dehydrogenase and histone deacetylases for cancer treatment. *J. Med. Chem.* **2007**, *50* (26), 6685-6691.
298. Apsel, B.; Blair, J. A.; Gonzalez, B.; Nazif, T. M.; Feldman, M. E.; Aizenstein, B.; Hoffman, R.; Williams, R. L.; Shokat, K. M.; Knight, Z. A., Targeted polypharmacology: discovery of dual inhibitors of tyrosine and phosphoinositide kinases. *Nat. Chem. Biol.* **2008**, *4* (11), 691-699.
299. Meunier, B., Hybrid molecules with a dual mode of action: dream or reality ? *Acc. Chem. Res.* **2008**, *41* (1), 69-77.
300. Wei, D.; Jiang, X.; Zhou, L.; Chen, J.; Chen, Z.; He, C.; Yang, K.; Liu, Y.; Pei, J.; Lai, L., Discovery of multitarget inhibitors by combining molecular docking with common pharmacophore matching. *J. Med. Chem.* **2008**, *51* (24), 7882-7888.
301. Gangjee, A.; Li, W.; Yang, J.; Kisliuk, R. L., Design, synthesis, and biological evaluation of classical and nonclassical 2-amino-4-oxo-5-substituted-6-methylpyrrolo [3, 2-d] pyrimidines as dual thymidylate synthase and dihydrofolate reductase inhibitors. *J. Med. Chem.* **2008**, *51* (1), 68-76.
302. Woo, L. L.; Bubert, C.; Purohit, A.; Potter, B. V., Hybrid dual aromatase-steroid sulfatase inhibitors with exquisite picomolar inhibitory activity. *ACS Med. Chem. Lett.* **2011**, *2* (3), 243-247.
303. Gediya, L. K.; Njar, V. C., Promise and challenges in drug discovery and development of hybrid anticancer drugs. *Expert Opin. Drug Discov.* **2009**, *4* (11), 1099-1111.
304. Chanplakorn, N.; Chanplakorn, P.; Suzuki, T.; Ono, K.; Chan, M. S.; Miki, Y.; Saji, S.; Ueno, T.; Toi, M.; Sasano, H., Increased estrogen sulfatase (STS) and 17β -hydroxysteroid dehydrogenase type 1 (17β -HSD1) following neoadjuvant aromatase inhibitor therapy in breast cancer patients. *Breast Cancer Res. Treat.* **2010**, *120* (3), 639-648.

305. Le Bail, J.; Laroche, T.; Marre-Fournier, F.; Habrioux, G., Aromatase and 17 β -hydroxysteroid dehydrogenase inhibition by flavonoids. *Cancer Lett.* **1998**, *133* (1), 101-106.
306. Le Bail, J.-C.; Pouget, C.; Fagnere, C.; Basly, J.-P.; Chulia, A.-J.; Habrioux, G., Chalcones are potent inhibitors of aromatase and 17 β -hydroxysteroid dehydrogenase activities. *Life Sci.* **2001**, *68* (7), 751-761.
307. Woo, L. L.; Sutcliffe, O. B.; Bubert, C.; Grasso, A.; Chander, S. K.; Purohit, A.; Reed, M. J.; Potter, B. V. L., First dual aromatase-steroid sulfatase inhibitors. *J. Med. Chem.* **2003**, *46* (15), 3193-3196.
308. Woo, L. L.; Wood, P. M.; Bubert, C.; Thomas, M. P.; Purohit, A.; Potter, B. V., Synthesis and structure-activity relationship studies of derivatives of the dual aromatase-sulfatase inhibitor 4-{{(4-cyanophenyl)(4H-1, 2, 4-triazol-4-yl) amino} methyl} phenyl sulfamate. *ChemMedChem* **2013**, *8* (5), 779-799.
309. Woo, L. L.; Bubert, C.; Sutcliffe, O. B.; Smith, A.; Chander, S. K.; Mahon, M. F.; Purohit, A.; Reed, M. J.; Potter, B. V., Dual aromatase-steroid sulfatase inhibitors. *J. Med. Chem.* **2007**, *50* (15), 3540-3560.
310. Wood, P. M.; Woo, L. L.; Labrosse, J.-R.; Trusselle, M. N.; Abbate, S.; Longhi, G.; Castiglioni, E.; Lebon, F.; Purohit, A.; Reed, M. J.; Potter, B. V., Chiral aromatase and dual aromatase-steroid sulfatase inhibitors from the letrozole template: synthesis, absolute configuration, and in vitro activity. *J. Med. Chem.* **2008**, *51* (14), 4226-4238.
311. Wood, P. M.; Woo, L. L.; Labrosse, J. R.; Thomas, M. P.; Mahon, M. F.; Chander, S. K.; Purohit, A.; Reed, M. J.; Potter, B. V., Bicyclic derivatives of the potent dual aromatase-steroid sulfatase inhibitor 2-Bromo-4-{{(4-cyanophenyl)(4H-1, 2, 4-triazol-4-yl) amino} methyl} phenylsulfamate: synthesis, SAR, crystal structure, and in vitro and in vivo activities. *ChemMedChem* **2010**, *5* (9), 1577-1593.
312. Wood, P. M.; Woo, L. L.; Thomas, M. P.; Mahon, M. F.; Purohit, A.; Potter, B. V., Aromatase and dual aromatase-steroid sulfatase inhibitors from the letrozole and vorozole templates. **2011**, *6* (8), 1423-1438.
313. Jackson, T.; Woo, L. L.; Trusselle, M. N.; Chander, S. K.; Purohit, A.; Reed, M. J.; Potter, B. V., Dual aromatase-sulfatase inhibitors based on the anastrozole template: synthesis, in vitro SAR, molecular modelling and in vivo activity. *Org. Biomol. Chem.* **2007**, *5* (18), 2940-2952.
314. Rausch, L.; Green, C.; Steinmetz, K.; LeValley, S.; Catz, P.; Zaveri, N.; Schweikart, K.; Tomaszewski, J.; Mirsalis, J., Preclinical pharmacokinetic, toxicological and biomarker evaluation of SR16157, a novel dual-acting steroid sulfatase inhibitor and selective estrogen receptor modulator. *Cancer Chemother. Pharmacol.* **2011**, *67* (6), 1341-1352.
315. Ouellet, C.; Ouellet, É.; Poirier, D., In vitro evaluation of a tetrahydroisoquinoline derivative as a steroid sulfatase inhibitor and a selective estrogen receptor modulator. *Invest. New Drugs* **2015**, *33* (1), 95-103.
316. Ouellet, C.; Maltais, R.; Ouellet, É.; Barbeau, X.; Lagüe, P.; Poirier, D., Discovery of a sulfamate-based steroid sulfatase inhibitor with intrinsic selective estrogen receptor modulator properties. *Eur. J. Med. Chem.* **2016**, *119*, 169-182.
317. Ouellet, É.; Maltais, R.; Ouellet, C.; Poirier, D., Investigation of a tetrahydroisoquinoline scaffold as dual-action steroid sulfatase inhibitors generated by parallel solid-phase synthesis. *MedChemComm* **2013**, *4* (4), 681-692.
318. Lespérance, M.; Roy, J.; Ngueta, A. D.; Maltais, R.; Poirier, D., Synthesis of 16 β -derivatives of 3-(2-bromoethyl)-estra-1, 3, 5 (10)-trien-17 β -ol as inhibitors of 17 β -HSD1 and/or steroid sulfatase for the treatment of estrogen-dependent diseases. *Steroids* **2021**, *172*, 108856.

-
319. Bacsa, I.; Herman, B. E.; Jójárt, R.; Herman, K. S.; Wölfling, J.; Schneider, G.; Varga, M.; Tömböly, C.; Rižner, T. L.; Szécsi, M., Synthesis and structure-activity relationships of 2-and/or 4-halogenated 13 β -and 13 α -estrone derivatives as enzyme inhibitors of estrogen biosynthesis. *J. Enzyme Inhib. Med. Chem.* **2018**, *33* (1), 1271-1282.